National Library of Canada
Canadian Theses Service
Ottawa, Canada
K1A 0N4

Bibliothèque nationale du Canada
Services des thèses canadiennes

# CANADIAN THESES

# THÈSES CANADIENNES

## NOTICE

The quality of this microfiche is heavily dependent upon the quality of the original thesis submitted for microfilming. Every effort has been made to ensure the highest quality of reproduction possible.

If pages are missing, contact the university which granted the degree.

Some pages may have indistinct print especially if the original pages were typed with a poor typewriter ribbon or if the university sent us an inferior photocopy.

Previously copyrighted materials (journal articles, published tests, etc.) are not filmed.

Reproduction in full or in part of this film is governed by the Canadian Copyright Act, R.S.C. 1970, c. C-30. Please read the authorization forms which accompany this thesis.

## AVIS

La qualité de cette microfiche dépend grandement de la qualité de la thèse soumise au microfilmage. Nous avons tout fait pour assurer une qualité supérieure de reproduction.

S'il manque des pages, veuillez communiquer avec l'université qui a conféré le grade.

La qualité d'impression de certaines pages peut laisser à désirer, surtout si les pages originales ont été dactylographiées à l'aide d'un ruban usé ou si l'université nous a fait parvenir une photocopie de qualité inférieure.

Les documents qui font déjà l'objet d'un droit d'auteur (articles de revue, examens publiés, etc.) ne sont pas microfilmés.

La reproduction, même partielle, de ce microfilm est soumise à la Loi canadienne sur le droit d'auteur, SRC 1970, c. C-30. Veuillez prendre connaissance des formules d'autorisation qui accompagnent cette thèse.

THIS DISSERTATION
HAS BEEN MICROFILMED
EXACTLY AS RECEIVED

LA THÈSE A ÉTÉ
MICROFILMÉE TELLE QUE
NOUS L'AVONS REÇUE

Canada

NL 339 (r. 86/01)

National Library of Canada / Bibliothèque nationale du Canada

63

Ottawa, Canada
K1A 0N4

TC –

ISB 0-315-23261-7

CANADIAN THESES ON MICROFICHE SERVICE – SERVICE DES THÈSES CANADIENNES SUR MICROFICHE

**PERMISION TO MICROFILM – AUTORISATION DE MICROFILMER**

• Please print or type – Écrire en lettres moulées ou dactylographier

**AUTHOR – AUTEUR**

Full Name of Author – Nom complet de l'auteur

ALI ALPEL TURAK

Date of Birth – Date de naissance
May 3rd 1947

Canadian Citizen – Citoyen canadien
☐ Yes / Oui ☑ No / Non

Country of Birth – Lieu de naissance
TURKEY

Permanent Address – Résidence fixe
3125 - 109 Street.
Edmonton, AB. T6J 4W6

**THESIS – THÈSE**

Title of Thesis – Titre de la thèse

Mathematical Modelling of Automedium Cyclones

Degree for which thesis was presented
Grade pour lequel cette thèse fut présentée
M Sc.

Year this degree conferred
Année d'obtention de ce grade
1985

University – Université
University of Alberta

Name of Supervisor – Nom du directeur de thèse
Prof. L. R. Plitt

**AUTHORIZATION – AUTORISATION**

Permission is hereby granted to the NATIONAL LIBRARY OF CANADA to **microfilm** this thesis and to **lend** or **sell copies of the film.**

The author reserves other publication rights, and neither the thesis nor extensive extracts from it may be printed or otherwise reproduced without the author's written permission.

L'autorisation est, par la présente, accordée à la BIBLIOTHÈQUE NATIONALE DU CANADA de **microfilmer** cette thèse et de **prêter** ou de **vendre des exemplaires du film.**

L'auteur se réserve les autres droits de publication; ni la thèse ni de longs extraits de celle-ci ne doivent être imprimés ou autrement reproduits sans l'autorisation écrite de l'auteur.

ATTACH FORM TO THESIS – VEUILLEZ JOINDRE CE FORMULAIRE À LA THÈSE

Signature

Date
Oct. 15, 1985

NL-91 (r. 84/03)

Canada

THE UNIVERSITY OF ALBERTA

# MATHEMATICAL MODELLING OF AUTOMEDIUM CYCLONES

by

Ali Alpel TURAK

A THESIS

SUBMITTED TO THE FACULTY OF GRADUATE STUDIES AND RESEARCH

IN PARTIAL FULFILMENT OF THE REQUIREMENTS FOR THE DEGREE

OF Master of Science

Department of Mineral Engineering

Edmonton, Alberta

Fall 1985

THE UNIVERSITY OF ALBERTA

**RELEASE FORM**

NAME OF AUTHOR Ali Alpel TURAK

TITLE OF THESIS MATHEMATICAL MODELLING OF AUTOMEDIUM CYCLONES

DEGREE FOR WHICH THESIS WAS PRESENTED Master of Science

YEAR THIS DEGREE GRANTED Fall 1985

Permission is hereby granted to THE UNIVERSITY OF ALBERTA LIBRARY to reproduce single copies of this thesis and to lend or sell such copies for private, scholarly or scientific research purposes only.

The author reserves other publication rights, and neither the thesis nor extensive extracts from it may be printed or otherwise reproduced without the author's written permission.

(SIGNED) Alialpel Turak

PERMANENT ADDRESS:

3125-109 street

Edmonton Alberta

CANADA T6J 4N6

DATED October 11, 1985

THE UNIVERSITY OF ALBERTA

FACULTY OF GRADUATE STUDIES AND RESEARCH

The undersigned certify that they have read, and recommend to the Faculty of Graduate Studies and Research, for acceptance, a thesis entitled MATHEMATICAL MODELLING OF AUTOMEDIUM CYCLONES submitted by Ali Alpel TURAK in partial fulfilment of the requirements for the degree of Master of Science.

.....

Supervisor

.....

.....

.....

Date..October 11, 1985.....

## ABSTRACT

Empirical model equations were developed for the automedium hydrocyclone used in fine coal cleaning. The automedium cyclone is typically utilized in the beneficiation of the -0.6 mm size fraction of plant feed in coal preparation plants. The model equations were based on data obtained from pilot scale testing on an 8 inch Visman (tricone) cyclone. The conceptual model resulted from studies of automedium cyclones in coal preparation plants, and from simulated rotating-bed experiments and cyclone bed capture tests. The developed model introduces the concept of three stage separation in the cyclone, namely the primary classification in the cylindrical section, the autogeneous partitioning by rotating bed in the conical section and secondary classification at the air core interface. The separation is modelled in terms of the well known partition functions. Modelling of pressure drop and water split for the cyclone is also introduced through empirical equations relating these macro-variables to operating conditions and the cyclone geometry.

## ACKNOWLEDGEMENTS

The author wishes to thank Professor L. R. Plitt for his invaluable guidance and input, and to Professor B. Flintoff for his enormous contribution throughout the project that made it possible to finalize the task.

The author wishes to acknowledge the generous funding provided by the Alberta/Canada Energy Resources Research Fund through the Hydrocarbon Research Centre Inc. of the University of Alberta. In particular the assistance and advice provided by Dr. D. S. Montgomery, Program Director of HRC was invaluable to this project. The cooperation of Fording River Coal Ltd. for allowing access to their plant and the cooperation of their proccess engineering staff is also very much appreciated.

The author also wishes to acknowledge the contributions of Mr. B. Mohammedbhai who participated in the analytical stages of the project, of Mr.R. Chissotti who helped in preparation of figures and of Mr. D. Margel who wrote the computer code for the semi-visual curve fitting.

Finally the author feels indebted to Ayse and Devrim who had to sacrifice a great deal, and to Nilufer Turak without whose support and help this work could not be completed.

## Table of Contents


| Chapter | | Page |
|---|---|---|
| 1. | PROJECT DESCRIPTION | 1 |
| | 1.1 Project Objectives | 1 |
| | 1.2 Project History and Funding | 2 |
| | 1.3 Report Organization | 2 |
| 2. | EMPIRICAL MODELLING OF CYCLONES | 4 |
| | 2.1 Introduction | 4 |
| | 2.2 An Overview of Cyclone Modelling Technology | 6 |
| | 2.3 What is a Hydrocyclone? | 9 |
| | 2.4 The Empirical Model of the Cyclone | 11 |
| | 2.4.1 Modelling Bypass | 14 |
| | 2.4.2 Modelling Classification | 18 |
| | 2.4.3 Characteristic Size | 20 |
| | 2.5 Parameter Estimation | 22 |
| | 2.5.1 Objective Function Formulation | 22 |
| | 2.5.2 Solution Techniques | 27 |
| | 2.5.3 Model Selection | 28 |
| | 2.6 Confidence Limits | 29 |
| | 2.7 Cyclone Modelling for Heterogeneous Ores | 30 |
| | 2.8 Peculiar Partition Curves | 35 |
| | 2.9 Operating Constraints | 40 |
| | 2.10 A General Cyclone Model: The Plitt Model | 45 |
| | 2.11 Applications of Cyclone Models | 48 |
| | 2.12 A New Conceptual Model of Cyclone Operation | 49 |
| 3. | SILICA TESTWORK | 58 |
| | 3.1 Introduction | 58 |

3.2 Experimental Design and Test Procedure .....58
3.2.1 Experimental Design .....58
3.2.2 Test Procedure .....60
3.3 Test Results .....66
3.3.1 Results of Silica Test Series A & B .....67
3.3.2 Results for Silica Test Series C .....74
3.4 Bed Capture Experiments .....78
3.5 Summary .....81
4. COAL TESTWORK: PLANT SAMPLING .....82
4.1 Introduction .....82
4.2 Fording Coal Preparation Plant .....82
4.3 Test Procedure .....83
4.4 Test Results .....85
4.5 Summary of Plant Tests .....91
5. COAL TESTWORK: LABORATORY EXPERIMENTS .....93
5.1 Test Procedure .....93
5.2 Experimental Design .....96
5.3 Results of Testwork .....100
5.4 Bed Capture Tests with Coal .....101
5.5 Bed-Simulation Tests .....103
6. MACRO VARIABLE MODELLING STUDIES .....107
6.1 Pressure - Flow Rate Modelling .....107
6.2 Underflow-Overflow Split .....111
7. MICRO-VARIABLE MODELLING .....115
7.1 General Model Form .....115
7.1.1 The Classification Behavior of the Automedium Cyclone .....115

7.1.2 Density Separation in the Automedium Cyclone .....116

7.1.3 Formulation of a Comprehensive Model ....118

7.2 Modelling the Separation in the Three Zones of AMC .....119

7.3 Parameter Estimation for the Cyclone Model ....121

8. ASSESSMENT OF INDUSTRIAL IMPACT .....132

9. CONCLUSIONS AND RECOMMENDATIONS .....134

REFERENCES .....136

NOMENCLATURE .....140

APPENDIX-1: Theoretical Computations of Flow and Separation in Hydrocyclones .....148

APPENDIX-2: Results of Silica Tests Series A and B .....195

APPENDIX-3: Results of Silica Tests Series C .....198

APPENDIX-4: Results of Plant Tests .....206

APPENDIX-5.1: Operating Conditions for Coal Tests .....208

APPENDIX-5.2: Results of Coal Tests .....210

APPENDIX-6: Results of Stepwise-linear-regression for Macro Variable Modelling .....250

APPENDIX-7.1: Table A-7.1; Parameters for Classification Model .....252

APPENDIX-7.2: Derivation of the AMC Model .....254

APPENDIX-7.3: The Semi-Visual Curve Fitting Program CPLOT .....258

APPENDIX-7.4: The Fitted Curve Parameters .....262

APPENDIX-7.5: The Predicted Parameters .....272

APPENDIX-7.6: Predicted and Observed Ash and Yield .....282

## List of Tables


| Table | | Page |
|---|---|---|
| 3.1 | Partition Function Data for Series A & B | 68 |
| 3.2 | Partition Function Data for Silica Series C | 75 |
| 5.1 | Stratification of Particles in Simulated Bed | 105 |

## List of Figures


| Figure | | Page |
|---|---|---|
| 2.1 | Principal Dimensional Variables in a Cyclone Classifier | 10 |
| 2.2 | Distribution of the Vertical and Radial Velocity Components in a Hydrocyclone Classifier | 12 |
| 2.3 | Conceptual Models of Cyclone Operation | 13 |
| 2.4 | An Illustration of the Partition Curve for an Industrial Classifying Cyclone | 15 |
| 2.5 | Partition Curves for Coal in a Classifying Cyclone | 32 |
| 2.6 | Variation of Corrected Cut Size with Solids Specific Gravity in a Classifying Cyclone | 33 |
| 2.7 | Detail on the Origin of Peculiar Partition Curves | 36 |
| 2.8 | Peculiar Partition Curves | 39 |
| 2.9 | Cyclone Underflow Flow Regimes | 41 |
| 2.10 | Flow Regime Regions for a 15cm Classifying Cyclone | 44 |
| 2.11 | Comparison af a Classifying and an Automedium Cyclone | 51 |
| 2.12 | The Separation Mechanisms in the Automedium Cyclone | 52 |
| 2.13 | The Non-Tangential Velocity Components for Solids and Water in a Cyclone with a Large Cone Angle | 54 |
| 2.14 | A Conceptual Model of Automedium Cyclone Operation | 55 |
| 3.1 | Solids Feed Size Distributions for the Silica Tests | 61 |
| 3.2 | Schematic Flowsheet of the Closed Loop Cyclone Pilot Plant | 62 |
| 3.3 | Partition Curves for Silica Series A | 69 |

| Figure | | Page |
|---|---|---|
| 3.4 | Partition Curves for Silica Series B | 70 |
| 3.5 | Partition Curves for Silca Series C | 76 |
| 3.6 | Selected Partition Curves from Silica Series C | 77 |
| 3.7 | Size Distribution of the Underflow and Bed Samples | 80 |
| 4.1 | Fines Circuit at Fording River | 84 |
| 4.2 | Fording Coal's Primary Automedium Cyclone No.37S | 86 |
| 4.3 | Change of Composition of Cyclone Feed During plant Tests | 88 |
| 4.4 | Change of Composition of Cyclone Underflow During plant Tests | 89 |
| 4.5 | Change of Composition of Cyclone Overflow During plant Tests | 90 |
| 5.1 | Comparison of Actual and Calculated Feed | 95 |
| 5.2 | Comparison of the Results Obtained from Standard and Cummulative Float-sink Analysis | 97 |
| 5.3 | The Size Distribution of Captured Bed and the Steady-State Stream | 102 |
| 5.4 | Cummulative Partition of Simulated Bed by Slicing at Various Depths | 106 |
| 6.1 | Variation of Flowrate of Water with Pressure | 109 |
| 6.2 | Predicted vs Observed Pressure Drop | 110 |
| 6.3 | Variation of Split Ratio of Water with Pressure | 112 |
| 6.4 | Predicted vs Observed Water Splits in the AMC | 114 |
| 7.1 | Partitioning Data and the Predicted Separation for Test #12112 | 125 |

Figure Page

7.2 Partitioning Data and the Predicted Separation for Test #11123 .....126

7.3 Partitioning Data and the Predicted Separation for Test #22212 .....127

7.4 Predicted and Observed Ash in the Cyclone Overflow Product .....130

7.5 Predicted and Observed Yields .....131

## List of Plates


| Plate | | Page |
|---|---|---|
| 3.1 | The Closed Loop Cyclone Pilot Plant | 63 |
| 3.2 | General View of Cyclone pilot Plant | 64 |

# 1. PROJECT DESCRIPTION

## 1.1 Project Objectives

The purpose of this project was to quantify the operating characteristics of the *auto*medium *c*yclones (AMC) in the form of an empirical model. The general aim of the project was to increase the understanding of the behaviour of the AMC.

The very complex hydrodynamics of the cyclone together with the heterogeneous character of coal and the general complexity of two-phase flow were the reasons for the empirical approach. A thorough study of the literature for the theoretical computations of the flow and separation in hydrocyclones has revealed this complexity.

The important parameters for the operation of classifying hydrocyclones have been well established by various authors. Empirical models for classifying cyclones have been derived through laboratory and plant testing. The automedium cyclone, however, was not studied by others to any appreciable extent and in spite of the wide usage, models for optimization of design, control and simulation of these units were not available.

The plant sampling campaign and pilot plant tests conducted in this project were designed to generate sufficient data for the development of an empirical model of the AMC.

## 1.2 Project History and Funding

The project was totally funded by Alberta/Canada Energy Resources Research Fund, through a research contract administered by the Hydrocarbon Research Center in the University of Alberta. The laboratory and pilot tests were conducted in the laboratories of Department of Mineral Engineering. The project cost over the years 1981-1984 totalled $ 102,000.

The principal investigator was Prof.L.R. Plitt although the project was jointly supervised by Prof.B. Flintoff.

The project was monitored by the funding agency through quarterly status reports and annual technical progress reports. This thesis forms part of the final report for the project.

## 1.3 Report Organization

In Chapter 2 an introduction is provided to the current technology in empirical modelling of cyclones and parameter estimation techniques are discussed. Applications of cyclone models and their limitations are described. The postulated mechanism of separation in automedium cyclones and a conceptual model for the separation are also introduced.

In Chapter 3, the test work with a homogenous solid phase (silica) is described and the classification characteristics of the automedium cyclone are explored.

Chapter 4 and 5 summarize the plant and laboratory test work respectively. Laboratory test work is described in

detail emphasizing experimental design and procedures.

The modelling work on macro variables such as pressure-flow relations and flow splits are described in Chapter 6.

Chapter 7 is devoted to micro variable modelling, that is description of particle partitioning in the cyclone. Model parameter estimation is also described in this chapter.

A brief assessment of the industrial impact of the model is given in Chapter 8, and the conclusions and recommendations are discussed in Chapter 9.

The extensive literature survey on theoretical computation of flow and separation in cyclones, and models derived from the fundamentals of hydrodynamics resulted in a comprehensive bibliographical study. This document is attached to this report as Appendix 1. The data from both the plant and laboratory test work is also presented in Appendices 2 through 5.

Appendices 6 and 7 include the results of modelling studies that encompass a wide range of computational effort and parameter estimation studies. A derivation of the model from the conceptual form is given in Appendix 7.2, and the novel method of semi-visual curve fitting for parameter estimation is described in Appendix 7.3.

# 2. EMPIRICAL MODELLING OF CYCLONES

## 2.1 Introduction

Mathematical modelling of coal preparation separation operations has been restricted to the the description of partition curves by simple mathematical functional forms, i.e. empirical modelling. In all cases the partition curves are obtained from curve fitting exercises on experimental data. There exist no general correlations which the operator can use to speculate, even in a semi-quantitative manner, on the expected impact of changes in operating conditions. The lack of these correlations, i.e. a general unit model, is largely the result of the tremendous amount of difficult analytical work involved to obtain the raw data (sink and float analysis on fine particle assemblies). In the mineral processing industry, the construction of general empirical models of the cyclone classifier has represented a substantial and valuable contribution to the technology. It was argued that a similar project in the coal industry would be of comparable benefit. The automedium cyclone is a logical candidate for study since it bears some obvious similarities to its classification counterpart, and it is likely that some of the technology can be easily transferred. Futhermore, the automedium cyclone is a widely used device in the preparation of fine coal in western Canada. The relatively large quantities of fine coal in the plant feed place significant importance on the role of the

automedium cyclone in coal preparation. In order that operators be able to optimize plant operation they must have a quantitative understanding of the unit operations, preferrably in the form of a reliable mathematical model. Thusfar, this type of process technology has been lacking in the coal sector. Such a model could be used in process analysis (data reduction), process simulation and process design. To facililate the transfer of technology a review of the relevant mineral processing literature was undertaken and is summarized in this chapter. This presentation is designed to consolidate the methodology into a form which would permit a coal or mineral processing engineer to bring himself "up-to-speed" in this area very quickly.

Since the publication of empirical cyclone models by Lynch and Rao in 1975 and by Plitt in 1976, the technical literature on this subject has consisted primarily of reports of applications, with only a few articles discussing basic modifications or enhancements in model form. In fact, most of the modelling effort in this period has been concerned with theoretical models based on the hydrodynamics of multiphase flow. (Preliminary results have been encouraging, however, it will be some time before this approach reaches the practical application stage.) This chapter presents a review of empirical cyclone modelling technology, with an emphasis on developments since the mid 1970's. The topics addressed include homogeneous and

heterogeneous ores, parameter estimation techniques, parameter confidence intervals, and the introduction of a new conceptual model of cyclone operation.

## 2.2 An Overview of Cyclone Modelling Technology

Since their first reported application in the mineral industry in 1938(1), cyclones have become a common unit operation in all of the process industries. The widespread use of the cyclone stems from its relative low cost and its versatility. It can be employed to carry out liquid-liquid, solid-liquid and solid-solid separations. It is the area of solid-solid separation which is of greatest interest to a mineral processing engineer. Historically, this area was divided into two application categories: (i) Separation according to density, the **cyclone washer**,and, (ii) Classification according to particle size, the **cyclone classifier**'. Classification is the principal application in mineral processing circuits. Within this category, the cyclone is most commonly employed to provide some positive control over the size distribution of product from a grinding circuit. Other uses include sand-slime separation prior to froth flotation and mill tailings treatment, either for dam construction or in backfill preparation.

Despite its geometric and operational simplicity, the separating mechanisms within a cyclone are complex and not

---

'When water is the carrier fluid, the cyclone is more often called the **hydrocyclone**. In this work the two names are used interchangably.

well understood. Efforts to mathematically quantify cyclone operation have evolved along both theoretical and empirical lines. Access to high speed computers has facilitated the numerical solution of the equations for fluid flow and thus rekindled an interest in theoretical modelling (e.g. (2),(3),(4)[2]. While there can be no question regarding the potential of theoretical models, these studies are essentially in their infancy and it is expected that it will be some time before they have a significant impact on the practical application of cyclone modelling technology. On the other hand, empirical mathematical models of the cyclone have received considerable attention in the literature. These models have been developed to the point where they are generally accepted (i.e. they are useful provided one recognizes the potential limitations). These models have been widely applied in process analysis (i.e. the reduction of experimental data), digital simulation, engineering design and as the basis for on-line size prediction.

Empirical cyclone models are based on the observation that the probability of a particle reporting to one of the product streams is dependent upon the particle settling characteristics, or size for a relatively homogeneous ore. The functional forms that are frequently adopted to characterize this relationship contain 2 or 3 unknown

---

[2]A more detailed discussion on theoretical modelling is presented in Appendix 1. This was completed in an attempt to shed some light on the expected flow patterns, separation mechanisms etc. to permit speculation on possible fundamental operational differences between the automedium cyclone and the cyclone classifier.

parameters, which, in the first instance, can be derived from experimental data by curve fitting methods. It is also common to interpret these parameters within the framework of a simple conceptual model of cyclone operation, thus giving them a physical sense. Some researchers, notably Plitt(5) and Lynch and Rao(6), have used rather extensive experimental data bases to derive correlations between the basic (2 or 3) model parameters and the independent operating variables including cyclone geometry and operating conditions as well as the characteristics of the feed slurry.

References to the empirical models of Plitt and Lynch and Rao are quite common, particularly in connection with the digital simulation of closed grinding circuits. While these models have often proved successful there have been a number of modifications reported over the last few years. The purpose of this chapter is to provide a review of empirical cyclone modelling technology including some documentation on those modifications to procedures and model form which have been recently reported. It is intended primarily for those operators who have an interest, but little experience, in cyclone modelling, especially as it relates to process analysis.

**2.3 What is a Hydrocyclone?**

Before discussing empirical modelling practice it is useful to briefly *define* a cyclone.

Although there are a number of variants, Figure 2.1 is an illustration of a typical cyclone classifier showing the principal dimensional variables.

As shown in the plan view on Figure 2.1, the feed slurry is introduced in the volute section of the cyclone whereupon the fluid pressure creates rotational fluid motion and, as a consequence, vortex flow (i.e. an air core is formed in the centre of the cyclone). This rotational motion results in the imposition of a centrifugal force which acts on the particles in the slurry. The *settling* characteristics of the partcles under this force are generally assumed to follow Stokes' law. In any case, the settling velocity is dependent upon particle mass (and shape) and, as a result, one would expect both particle size and density to influence the settling behaviour. In the absence of any other forces all particles would therefore migrate, at different rates, to the outer wall of the cyclone and subsequently flow down the wall, through the apex, reporting to the underflow product.

The nature of the cyclone geometry and the relative sizes of the orifice openings are such that most of the water which enters the cyclone leaves through the vortex finder, reporting to the overflow product. The *counter-current* movement of the water toward the centre of

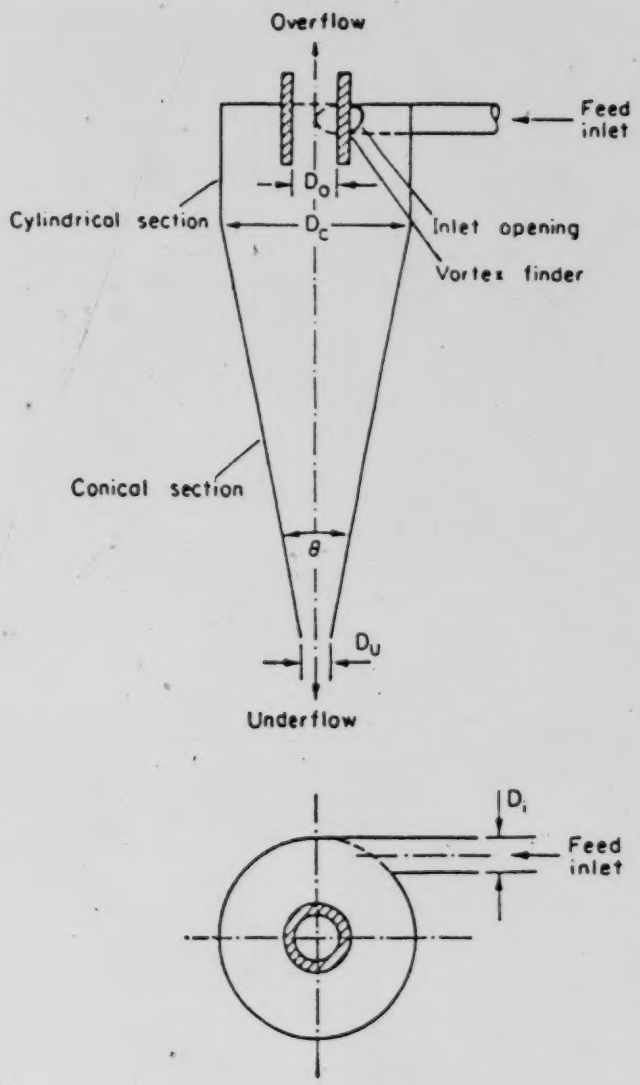


Figure 2.1 Principal Dimensional Variables in a Cyclone Classifier (after(7))

the cyclone results in the mechanical entrainment of those particles whose slip velocity is insufficient to result in a net outward motion.

For a homogeneous ore[3] the result of these competing forces is that the fine particles report with the bulk of the water to overflow product while a relatively high density (% solids) product containing the coarser particles is discharged as cyclone underflow. The vertical and radial flow components in a hydrocyclone, under normal operating conditions, are illustrated in Figure 2.2.

## 2.4 The Empirical Model of the Cyclone

The basic assumptions in empirical cyclone modelling are; (i) a certain portion of the feed solids are bypassed (or short circuited) to the underflow stream, and, (ii) the remainder of the feed solids undergo *true* classification, i.e. separation is dependent upon particle settling characteristics. Restricting this discussion to relatively homogeneous ores, the conceptual model of cyclone operation is shown if Figure 2.3a. It has been suggested that it is more reasonable to assume that the cyclone overflow solids are bypassed, rather than the feed solids. The conceptual model for this scenario is presented in Figure 2.3b, and, from the material balance equations, it is clear that there

---

[3] A homogeneous ore is one in which all particles have a substantially uniform density implying that separation is based on size alone (shape similarity is always assumed). Heterogeneous ores contain significant quantities of particles with different densities and thus density effects in separation can not be ignored.

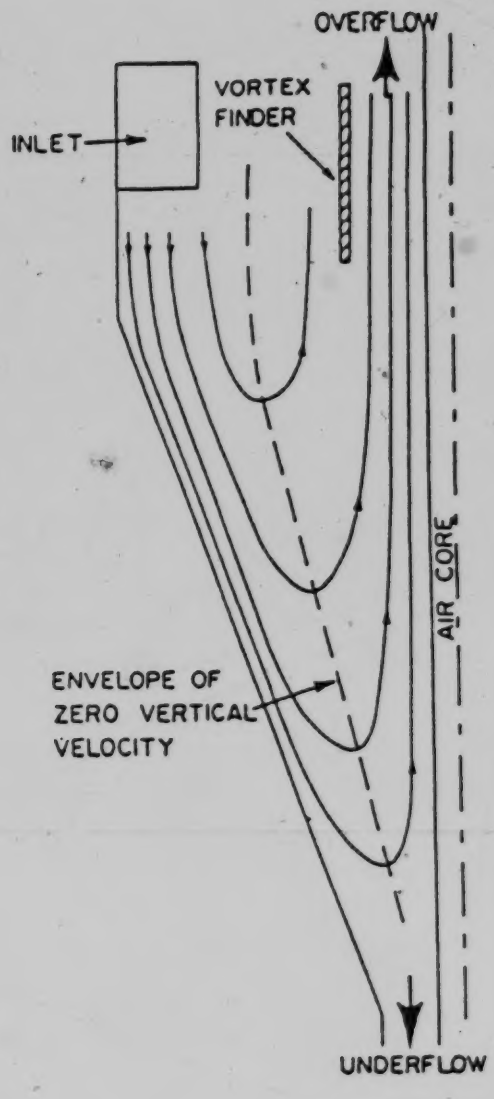


Figure 2.2 Distribution of the Vertical and Radial Velocity Components in a Hydrocyclone (after(5))

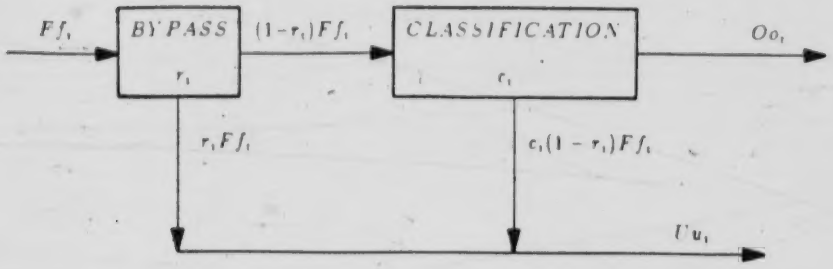


$$Uu_i = \left[r_i + (1 - r_i)c_i\right]Ff_i$$

$$Uu_i = p_iFf_i \Rightarrow p_i = \frac{Uu_i}{Ff_i}$$

$$p_i = r_i + (1 - r_i)c_i$$

(a) BYPASS FEED SOLIDS

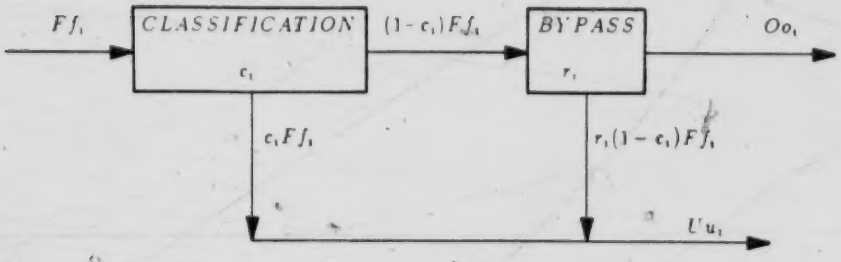


$$Uu_i = \left[c_i + (1 - c_i)r_i\right]Ff_i$$

$$Uu_i = \left[r_i + (1 - r_i)c_i\right]Ff_i$$

$$Uu_i = p_iFf_i \Rightarrow p_i = \frac{Uu_i}{Ff_i}$$

$$p_i = r_i + (1 - r_i)c_i$$

(b) BYPASS OVERFLOW SOLIDS

Figure 2.3 Conceptual Models of Cyclone Operation

is no difference in the mathematical structure of the empirical model which is given by Equation (2.1).

$$\frac{Uu_i}{Ff_i} = p_i = r_i + (1 - r_i)c_i \qquad (2.1)$$

Equation (2.1) has been found to adequately describe most *partition* (a.k.a. *selectivity*, *Tromp*, etc.) curves derived from sampling experiments around a cyclone. An example of an experimental partition curve for an industrial cyclone is presented in Figure 2.4.

In order to use Equation (2.1) it is necessary to specify the bypass ($r_i$) and classification ($c_i$) functions. Since this specification involves the selection of simple mathematical functional forms which will accurately represent the experimental data, without regard for process phenomenology, such models are empirical in nature.

### 2.4.1 Modelling Bypass

In 1953 Kelsall(8) suggested that the bypass of feed solids to the underflow was directly proportional to the fraction of water in the cyclone feed which is recovered in the underflow product, Rf. From a hydrodynamic viewpoint this is sensible since one would expect the very fine particles to "follow" the water. For mathematical convenience Kelsall simply assumed that an equivalent fraction of all particle size classes in the feed would

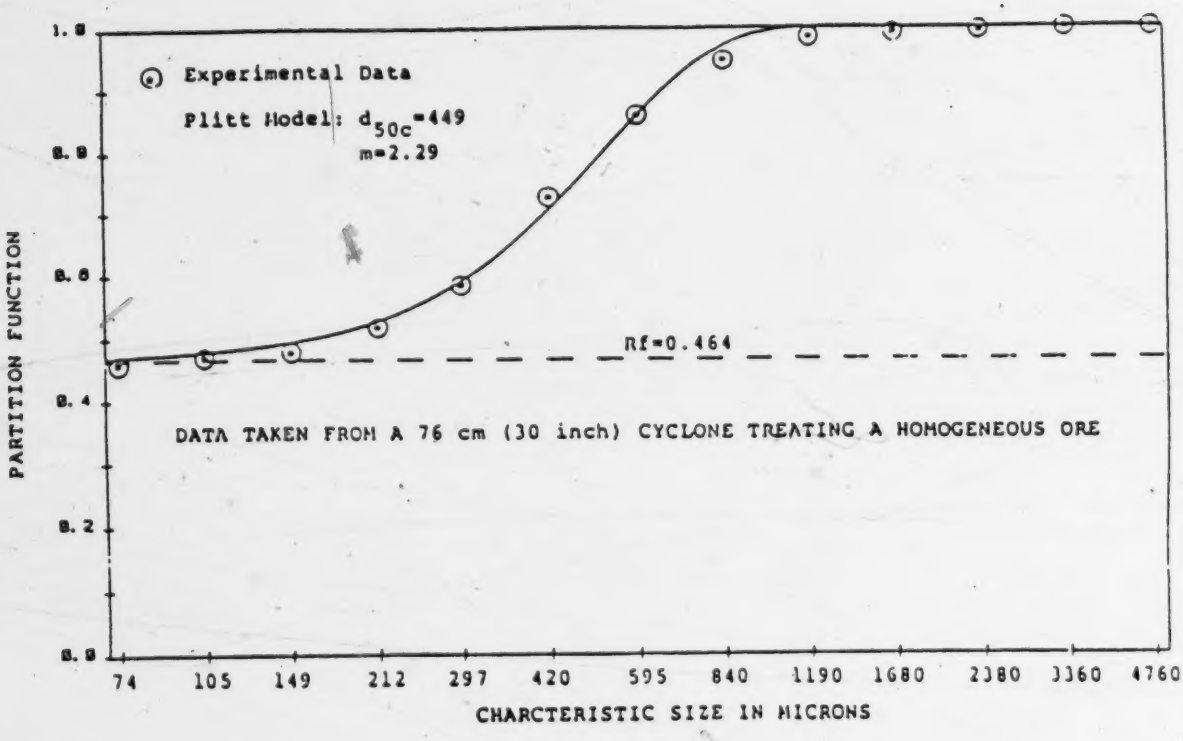


Figure 2.4 An Illustration of the Partition Curve for an Industrial Classifying Cyclone

report to the underflow with,

$$r_i = R_f \tag{2.2}$$

This is still the most widely adopted assumption regarding bypass. Of course, one of the major benefits of such a simple bypass model is that, if the water split is known or can be predicted, then the calculation of $r_i$ is trivial.

Recently, this aspect of cyclone modelling has received increasing attention. For example, Austin and Klimpel(9) argue that the thickened slurry near the cyclone wall can act as a filter for particles which are moving inward with the water. Thus they conclude that "it is not surprising that some fraction of all sizes in the slurry become locked in this layer and leave in the underflow. There is no logical reason why this fraction should equal the water split to the underflow in all circumstances(9)." In mathematical terms they assume,

$$r_i = a \tag{2.3}$$

In support of this statement they provide some experimental evidence where the constant in Equation (2.3), a, was estimated by curve fitting methods and is apparently not equal to the water split, Rf. In fairness, it should be observed that there was substantial scatter in the experimental partition function, $p_i$, data which may have

contributed to the differences. No statistical tests were performed to test the hypothesis Ho: a=Rf.

In terms of a general model of cyclone operation Equation (2.3) complicates matters since it becomes necessary to develop an additional correlation which permits the prediction of *a* as a function of the independent operating variables.

Finch(10,11) has also suggested an alternative bypass model. His model results from an effort to explain the *fishhook* which is infrequently observed in partition curves. (He rejects the claim that this phenomenon is the result of poor experimental procedures and/or fines agglomeration onto the coarse particles.) By analogy with the gangue entrainment models in froth flotation (see (12) section 3.4.4 for example), Finch postulated that the bypass was a decreasing function with increasing particle size. Retaining Kelsall's argument for the very fine particles, he assumed that in the limit as particle size tends toward zero, the bypass function approaches Rf. In the absence of any direct experimental data to define model structure and to provide a functional form that is parsimonious in parameters, Finch adopted the linear bypass model given by Equation (2.4),

$$r_i = \begin{cases} R_f(1 - \frac{d_i}{d_o}) & d_i < d_o \\ 0 & d_i \geq d_o \end{cases} \qquad (2.4)$$

Interestingly, one of the arguments advanced by Finch to

explain the fishhook phenomenon is contradictory to the mechanism suggested by Austin and Klimpel. "One possibility is that consolidated trickling occurs through the coarse particle bed rotating near the cyclone wall. The hydraulic entrainment of the particles in the 10μ to 40μ range could then be hindered. The finest particles would percolate more easily through the *network* of coarse particles, and be recovered in the same proportion as the water."(10)

To summarize, it seems clear that the origins of the bypass mechanism are not well understood. To date, efforts to modify the original model of Kelsall have been driven by a desire to more accurately "fit" the experimental data, rather than on the basis of fundamental studies. One point of general agreement is that such studies should be undertaken. Thusfar, the Kelsall model has been the most widely applied to the analysis of data derived from homogeneous ores. This is a particularly convenient form since the bypass function is easily evaluated from the water split. However, as cyclone models are increasingly applied to the classification of heterogeneous ores, where density effects often manifest themselves in the fine particle bypass, an improved model of this phenomenon is necessary. This will discussed in more detail in section 2-7.

### 2.4.2 Modelling Classification

Separation by classification occurs because of differences in particle settling behaviour, i.e. particle

size for homogeneous ores. Much experience has shown that the complex classification mechanisms can be conveniently represented by simple functional forms, all of which exhibit a characteristic shape. (They are of the general nonlinear model class known as sigmoidal growth functions.) The most common of these are summarized below (see also (13), Chap. 13).

a) Exponential Sum(6)

$$c_i = \frac{e^{mx_i} - 1}{e^{mx_i} + e^m - 2} \tag{2.5}$$

b) Rosin Rammler(5,16)

$$c_i = 1 - e^{-0.693 x_i{}^m} \tag{2.6}$$

c) Logistic(9,15)

$$c_i = \frac{1}{1 + \left(\frac{1}{x_i}\right)^m} \tag{2.7}$$

with

$$x_i = \frac{d_i}{d_{50c}} \tag{2.8}$$

All of these functional forms are monotonic increasing in $c_i$ with increasing $d_i$ and are characterized by two parameters; $d_{50_C}$ = the corrected cut size, and, (ii) m = the sharpness of separation. The classification model one selects seems to

be dependent on whose approach (Plitt, Lynch or Austin) is being followed. A preferred selection criterion would be the relative accuracy of the different models in characterizing experimental data.

To illustrate the construction of an empirical cyclone (or partition curve) model, suppose Equation (2.2) is selected as the bypass model and Equation (2.6) is selected as the classification model then the corresponding form of Equation (2.1) is,

$$p_i = R_f + (1 - R_f)(1 - e^{-0.693\left[\frac{d_i}{d_{50c}}\right]^m}) \qquad (2.9)$$

This is the standard form of the Plitt model. The solid line on Figure 2.4 illustrates how the model represents the discrete experimental data.

It should be noted that when Equation (2.2) is adopted as the bypass model, it has been the author's experience that, Equation (2.7) is better than Equation (2.6) which is better than Equation (2.5) for classification. In most cases the differences are not significant (as measured by an F-test), however the consistency of this trend is rather remarkable.

### 2.4.3 Characteristic Size

The characteristic size of a particular particle size class may be defined in a number of ways and the reader is cautioned to beware since this definition may prove to be

important. Since the screen analysis on the cyclone feed and product streams is done on a regular geometric sieve series (e.g. $\sqrt{2}$), the choice of the characteristic size is somewhat arbitrary. Again, it may depend on the convention adopted by the person whose work is followed and/or the paramater estimation technique. Probably the three most common choices for calculating $d_i$ are:

a) Geomean Size

$$d_i = \sqrt{s_i \times s_{i+1}} \tag{2.10}$$

b) Arithmetic Mean Size

$$d_i = \frac{(s_i + s_{i+1})}{2} \tag{2.11}$$

c) Size Class Boundary

$$d_i = s_i \tag{2.12}$$

Of the three, the arithmetic mean size is the closest to the *true* characteristic size (see (14) Appendix A), however, all preserve the sieve size ratio, and, apart from the expected differences in the numeric value of the estimated $d_{50_c}$, they are essentially equivalent.

## 2.5 Parameter Estimation

Once an experimental data set has been obtained through careful sampling and analysis and the raw data adjusted using some material balance technique, the next step is to fit a partition curve model to the experimental partition function data. Equation (2.1) attempted to convey this thought by simultaneously showing,

$$p_i(meas.) = \frac{Uu_i}{Ff_i}$$

$$p_i(pred.) = r_i + (1 - r_i)c_i$$

The experimental data, in this case U, F, $u_i$, and $f_i$ are used to calculate the measured partition function while functional forms are adopted for $r_i$ and $c_i$ to permit calculation of the predicted partition function. The parameters in these functional forms must then be selected in such a manner that the two partition functions are essentially equal. This curve fitting exercise is called parameter estimation.

It is convenient to think of this as a two step procedure involving both the formulation of an objective function as well as the selection of a solution technique.

### 2.5.1 Objective Function Formulation

The lack of information regarding the error variance of the measured $p_i$ data generally means that the unweighted least squares objective function, J, is minimized by the appropriate choice of the model parameters $d_{50_c}$, m, etc.

$$J(d_{50c}, m, ..) = \sum_{i=1}^{n-1} \left[ p_i(pred.) - p_i(meas.) \right]^2 \qquad (2.13)$$

Since a characteristic size can not be assigned to the pan fraction, the experimental information contained in this data ($u_n$,$f_n$) is ignored, hence the termination of the sum at the (n-1)th size class. Intuitively, one would expect to get reasonable estimates of the model parameters if a reasonable range of measured $p_i$ data is available (see Figure 2.4 for example). This reasonable range must be considered in the design of the cyclone sampling experiment and it may be useful to use Plitt's general model(5) to get some indication of the expected $p_i$ vs. $d_i$ relationship for this purpose. For situations where a reasonable range of experimental $p_i$ is not available, especially for the situation where the cut size is in the pan fraction size range, i.e. $d_{50} \leq s_n$, the parameter estimates obtained from minimizing Equation (13) can be quite poor. Austin and Klimpel(9) have developed a method which permits one to utilize the pan fraction information. This technique requires a greater amount of mathematical manipulation by the user, however, it is potentially quite useful and a summary of the approach is given below.

A cumulative partition function, $\gamma_i$, is defined as,

$$\gamma_i = \frac{U}{F}\left(\frac{U_i}{F_i}\right) \tag{2.14}$$

and,

$$U_i = \sum_{j=n}^{i} u_j \tag{2.15}$$

$$F_i = \sum_{j=n}^{i} f_j \tag{2.16}$$

Recalling from Equation (2.1) that,

$$u_i = \frac{F}{U} p_i f_i \tag{2.17}$$

and substituting Equations (2.15) and (2.17) into Equation (2.14) yields,

$$\gamma_i = \frac{\sum_{j=n}^{i} p_j f_j}{F_i} \tag{2.18}$$

Adopting a model form for $p_j$ allows one to estimate the parameters of this model by minimizing the unweighted least squares objective function,

$$J(d_{50c}, m, ..) = \sum_{i=1}^{n} \left[\gamma_i(meas.) - \gamma_i(pred.)\right]^2 \tag{2.19}$$

where $\gamma_i$(meas.) is derived from Equation (2.14) using

experimental data and $\gamma_i$(pred.) is derived from Equation (2.18) using both experimental data and the model.

It is clear that one remains faced with the problem of choosing a characteristic size for the pan fraction. While this problem can not ever be completely eliminated Austin and Klimpel have devised a technique to mininimze the impact. For mathematical simplicity they adopt Equation (2.12) for computing characteristic size. They then observe that, in most cases, the cyclone feed solids size distribution exhibits a characteristic shape in the fine size region. This part of the size distribution can be mathematically described using simple distribution functions such as the Gaudin Schuhmann function,

$$F_i = \left(\frac{s_i}{K}\right)^{\alpha} \qquad (2.20)$$

Fitting this model (i.e. estimating $\alpha$ and K) to the experimental data in the fine size region then allows the extrapolation of the cumulative frequency vector to include a total of m size fractions with  > n and $s_m \leq 5\mu$. Clearly, the error of assigning a characteristic size to the pan fraction, after extrapolation, is minimized. The extrapolated feed frequency vector is computed as,

$$f_i = F_i - F_{i+1}\ ; \qquad i = n, \ldots, \ell - 1 \tag{2.21}$$
$$f_\ell = F_\ell$$

and Equation (2.18) for $\gamma_i$(pred.) is modified to include the extrapolated data,

$$\gamma_i = \frac{\sum_{j=\ell}^{i} p_j f_j}{F_i} \tag{2.22}$$

Austin and Klimpel claim this method to be superior, to that suggested by Equation (2.13), since the pan fraction information is not ignored. This claim is still open to debate since their method seems sensitive to extrapolation errors as well as the effects of data transformation. With respect to the latter, the range of $p_i$ is approximately $Rf \leq p_i \leq 1$ while for the cumulative partition function the range is somewhat smaller, $Rf \leq \gamma_i \leq Rs$, with $Rs < 1$.

Both parameter estimation techniques were examined using Monte Carlo simulation studies. In addition, a hybrid method, that uses the Austin and Klimpel method only for the pan fraction, was also tested. The preliminary conclusion is that the Austin and Klimpel method is sensitive to extrapolation error and gives less stable estimates of the parameters if a reasonable range of experimental $p_i$ are available. However, this method is generally superior when $d_{50_C}$ lies in the pan fraction size range. This becomes increasingly so as $p_n \to 1$, i.e. as the range of experimental $p_i$ decreases in size.

### 2.5.2 Solution Techniques

It is sometimes possible to obtain estimates of the model parameters by simple transformation. For example, Plitt(16) used a double logarithmic transformation to linearize Equation (2.9) and then estimated $d_{50_C}$ and m using either graphical or linear regression techniques. In this case the objective function which is minimized is also a transformed version of Equation (2.13) and is not the preferred least squares objective function. (Log - log transformations inherently weight the smaller values of $p_i$ more heavily in the calculation of J, thereby introducing bias.) When transformation provides a good fit (e.g. $r^2 \rightarrow 1$) the parameter estimates are reasonable, however, in the presence of scatter the estimates are poor. In the latter case the parameter estimates can be taken as first approximations and used with one of the solution techniques discussed below to minimize the least squares objective function (Equation (2.13) or (2.19)).

The minimization of a least squares objective function which involves a model that is nonlinear in the parameters requires an iterative solution. Two general classes of solution algorithm can be identified and an example of each is provided.

a) Methods Requiring Derivatives: Non Linear Regression with the Marquardt Algorithm (see (17) Chap. 11).

b) Derivative Free Methods: Nelder and Mead Flexible Simplex(18)

The author prefers the Marquardt alogorithm because it is robust, converges quickly and is easier to program for this application.

### 2.5.3 Model Selection

Selection of a partition curve model form from among the available alternatives is a relatively easy task if all models have the same number of unknown parameters. In this case one can look at the values of J (or a composite $\Sigma J_i$ value) for each model fit to a number of experimental data sets. However, when attempting to compare models with different numbers of parameters the task is somewhat more complex. For example, if Equation (2.3) was used in place of Equation (2.2) there would be an additional parameter, a, to be estimated from the experimental data. Blau et. al.(19) have suggested a method for determining the significance of adding a parameter to a model. The procedure requires an independent estimate of the error variance on the dependent variable. Moreover, the error variance is assumed to be homogeneous over the range of the dependent variable and derived from a normally distributed error. In partition curve modelling it is unlikely that an independent estimate of error variance is available or that either of the conditions is met. In the absence of an independent estimate of error variance one can use the following approach to test the significance of adding an additional parameter. Using a

$\chi^2$ or a Kolmogorov-Smirnov test[1] the residuals for each model can be tested for normality. If this condition is satisfied then the sum of the residuals squared can be used to calculate an unbiased estimate of the error variance for each model. These error variances can be compared with an "F-test" and if they are found to be estimates of a common error variance it can be concluded that there is no statistical justification to add the parameter in question.

**2.6 Confidence Limits**

A natural question which arises when the parameter estimation exercise has been completed is "How good are the parameter estimates?" Statistically one usually thinks of confidence intervals. This kind of information may prove useful in comparing different modes of cyclone operation or in providing weighting factors for the regression procedures used to develop general correlations of the model parameters with the independent operating variables.

The idea of a confidence interval is somewhat suspect for these nonlinear models since there is a high degree of covariance between the parameters. It is more reasonable to think of a confidence surface. There are techniques which can be used to provide estimates of confidence intervals for the parameters. It must be remembered that all of these methods make the following assumptions, which seldom hold in

---

[1]For details see "Probability Concepts in Engineering Planning and Design", Ang A.H.S. and Tang W.H, Wiley & Sons, 1965.

practice;(i) the model form is correct, i.e. there is no lack-of-fit, and, (ii) the error variance of the dependent variable is homogeneous and derived from a normally distributed error. The best method, but the most expensive in a computational sense, is described by Draper and Smith(see (20)/Chap. 10). Other methods include the "lack-of-fit" approach used by Klimpel(21) in flotation modelling, Monte Carlo estimation, or, if a nonlinear regression solution algorithm is employed, the linear asymptotic approximation analagous to multiple linear regression. In all but the last case these calculations require significant computational effort and the "value-added" is questionable in the light of the comments made earlier.

**2.7 Cyclone Modelling for Heterogeneous Ores**

When ore heterogeneity is significant the models described above require some modification. In this situtation the common practice is to perform specific gravity fractionation on the solids samples for each flowstream and then do a size analysis on each specific gravity fraction. This permits the calculation of an experimental size partition curve for each specific gravity fraction and the techniques described above can be used to estimate the model parameters. The results of such an exercise are illustrated if Figure 2.5 for a cyclone classifier treating coal.

It is observed that $d_{50_c}$ varies inversely with particle specific gravity, as would be expected from sedimentation theory. Stokes' or Newton's law may be used to derive expected relationships between $d_{50_c}$ and $\rho_s$ which are of the form,

$$d_{50c} = \frac{C}{(\rho_s - 1)^k} \qquad (2.23)$$

where, from the theories, k will have a value of 0.5(laminar regime) or 1(turbulent regime) respectively. In practice, C and k are estimated by curve fitting techniques and it is rarely the case that k falls within the theoretical range. To illustrate, Figure 2.6 was prepared from the parameter estimates made on the data in Figure 2.5.

With regard to the sharpness of separation, it is common to assume that this value is constant and therefore independent of particle specific gravity. This assumption is based on the observation that the plot of the classification function, $c_i$, against the reduced particle size ($d_i/d_{50_c}$) is essentially a single curve for all specific gravity fractions. This plot is referred to as the **reduced efficiency curve** by Lynch and Rao. It was used to demonstrate the constancy of m in their work on both homogeneous and heterogeneous ores.

The principal unresolved problem of modelling heterogeneous ores is handling the bypass of fine particles. It is evident from Figure 2.5 that the fine particle

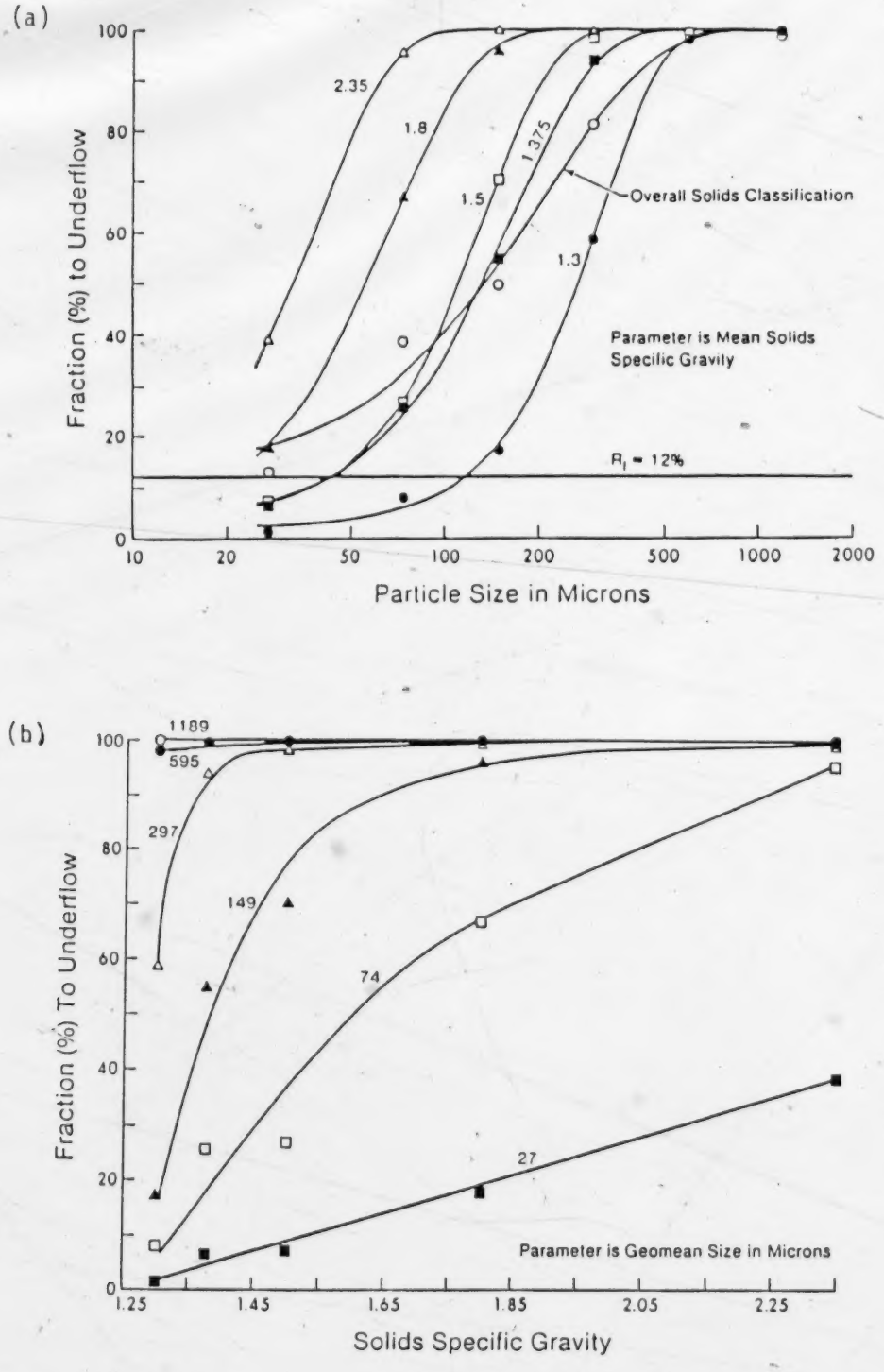


Figure 2.5 Partition Curves for Coal in a Classifying Cyclone (after(22))

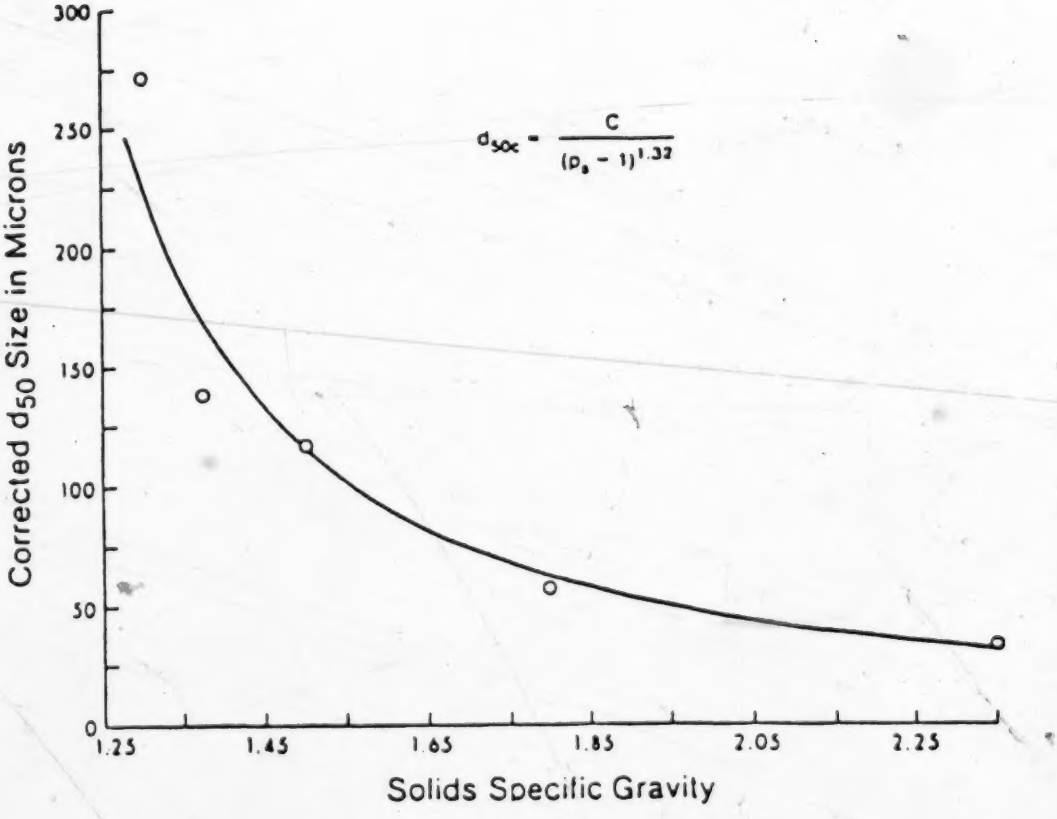


Figure 2.6 Variation of Corrected Cut Size with Solids Specific Gravity in a Classifying Cyclone (after (22))

intercepts are not equivalent to the water split. In fact they appear to exhibit a trend with the lower density components having lower bypass contributions or intercepts. This trend was also observed by Finch and Matwijenko(23). This phenomenon is thought to be due to autogeneous heavy medium separation effects which occur as the "heavier" particles move toward the apex valve. The less dense particles are likely stripped from the underflow stream by the rising fluid flow component at the air core interface. Presumably there exists a size below which specific gravity effects in the bed are negligible and ultimately the bypass is equivalent to the water split at very fine particle sizes.

The autogeneous heavy medium separation effect is exploited in coal preparation using a design variant called the **automedium cyclone.** (This unit is described in greater detail in a subsequent section - see Figure 2.11). For this reason the application of empirical cyclone models to the automedium cyclone requires that special attention be given to this separation mechanism, as will be discussed in a later section.

As a final comment, notice the low slope of the overall partition curve on Figure 2.5. This suggests poor sharpness of separation when, on a specific gravity component basis, the separation is seen to be quite respectable. Attention is drawn to this because it is possible that ore heterogeneity can give rise to very peculiar overall partition curves, as

described in the next section.

## 2.8 Peculiar Partition Curves

The overall (density composite) solids partition curve for a hetereogeneous ore such as coal does not have an unusual shape, although it is relatively "flat." This is because there is essentially a continuous distribution of particles over the specific gravity range of the coal. However, when dealing with systems where, for example, there are two identifiable solid particle species or phases with distinctly different densities and size distributions, it is possible to get overall solids partition curves which have a very peculiar form. Of course, a properly designed sink-and-float separation would permit one to solve the problem using the methods just decribed for heterogeneous ores. Laplante and Finch(24) have discussed this subject with reference to a number of plant studies.

The conditions which lead to peculiar partition curves can be deduced from a simple illustrative example, Figure 2.7a is a schematic illustration of the separation of two phases in a cyclone. (In this example it will be convenient to assume that all of the functions are continuous and differentiable.) The overall partition curve can be calculated from the two components as,

$$p = m_1 p_1 + (1 - m_1) p_2 \qquad (2.24)$$

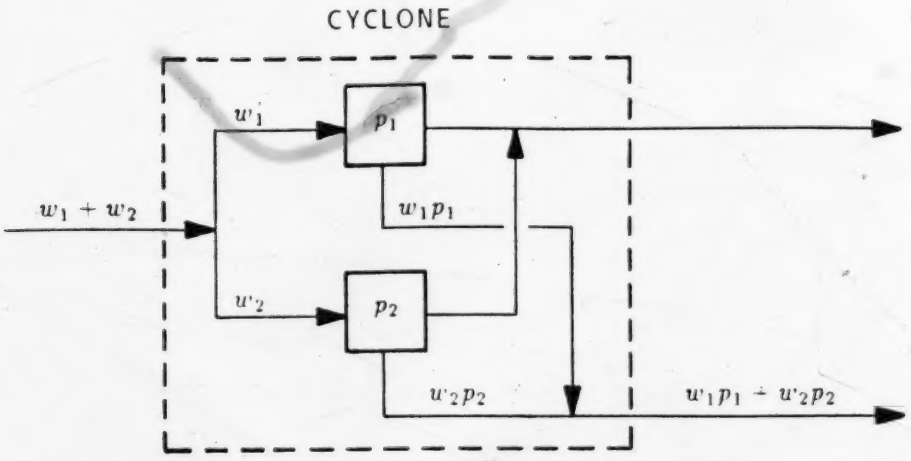


$$P = \frac{w_1 p_1 + w_2 p_2}{w_1 + w_2} = m_1 p_1 + (1 - m_1) p_1$$

$$m_1 = \frac{w_1}{w_1 + w_2}$$

(a) Classification of a two phase solid system

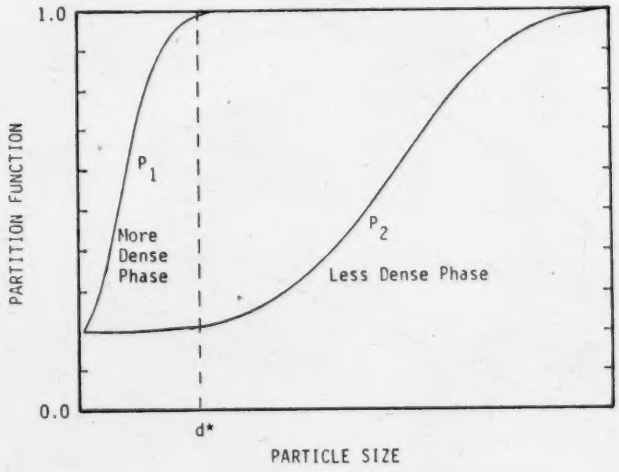


(b) Partition curves for the two solid phases

Figure 2.7 Detail on the Origin of Peculiar Partition Curves

Normally, it would be expected that p would be monotonic increasing with particle size. However, as Laplante and Finch have observed, this is not necessarily the case. This leads to the question under what conditions is p not monotonic increasing, i.e. under what conditions is,

$$\frac{\partial p}{\partial d} < 0 \tag{2.25}$$

Differentiating Equation (2.24) with respect to size and denoting this operation with the symbol, ', gives,

$$p' = (p_1 - p_2)m_1' + m_1 p_1' + (1 - m_1)p_2' \tag{2.26}$$

Since the latter two terms on the right hand side of Equation (2.26) are non-negative by definition[5], the condition defined in Equation (2.25) is most likely to be met when their contributions are essentially zero, i.e. $p_1' \simeq p_2' \simeq 0$. From Figure 2.4 it is evident that this can arise whenever $d << d_{50_c}$ or $d >> d_{50_c}$. A situation which leads to the condition just described is shown on Figure 2.7b, where it has been assumed that phase 1 is the more dense component. It is apparent from this analysis that one condition which is necessary for Equation (2.25) to be satisfied at some size, d*, is that the density difference be large enough to provide for the displacement of $p_1$ from $p_2$ shown in Figure 2.7b.

---

[5]This assumes that Equation (2.2) or (2.3) can be used to model bypass.

Given that $p_1' \simeq p_2' \simeq 0$, the first term on the right hand side of the equality in Equation (2.26) dominates the sign of p'. From Figure 2.7b it is apparent the $p_1 - p_2 > 0$ at d* and therefore $m_1'$ must be negative to satisfy Equation (2.25). Although the answer may be intuitive the conditions for which $m_1 < 0$ can be easily shown by noting that,

$$m_1 = \frac{W_1}{W_1 + W_2} \tag{2.27}$$

and,

$$m_1' = \frac{(W_1 + W_2)W_1' - W_1(W_1' + W_2')}{(W_1 + W_2)^2} \tag{2.28}$$

which can be simplified to,

$$m_1' = \frac{W_1'W_2 - W_2'W_1}{(W_1 + W_2)^2} \tag{2.29}$$

From Equation (2.29) it is clear that a condition which assures $m_1' < 0$ is $w_1' < 0$ and $w_2' > 0$, since $w_1$ and $w_2$ are non-negative. This requires that the size distributions be different for the phases, moreover it requires that the more dense phase have a finer size distribution as shown on Figure 2.8a. This is not an unreasonable expectation, particularly in closed circuit grinding.

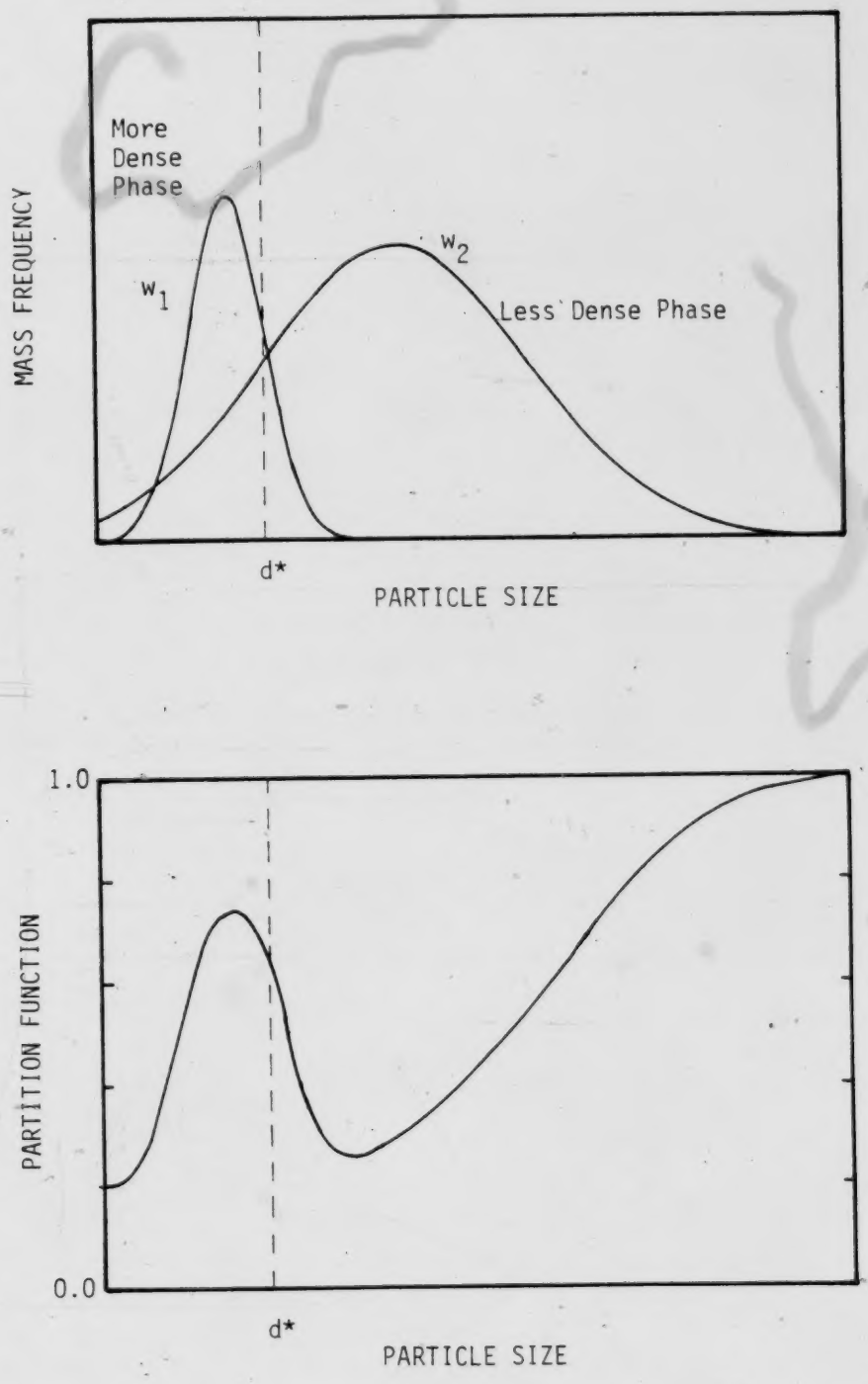


**Figure 2.8 Peculiar Partition Curves**

To summarize, two conditions which are sufficient to ensure peculiar overall solids partition curves are,

a) A significant density difference between the phases leading to the kind of situation shown on Figure 2.7b.

b) A difference in the size distributions for the phases giving rise to the kind of situation shown on Figure 2.8a.

As these conditions are relaxed the overall partition curve would be expected to become more normal in appearance. As a final illustration, Figure 2.8b was produced from the data in Figures 2.7b and 2.8a, assuming that the more dense phase accounts for 25% of the feed.

## 2.9 Operating Constraints

In developing a mathematical model of any unit operation it is important that the range of application be clearly defined, and, whenever possible, operating constraint models' should be simultaneously developed. In cyclone operation the principle operating constraint is **roping** in the cyclone underflow stream.

There are two major flow regimes which describe slurry appearance upon discharge from the apex valve. These are commonly referred to as **Spray Discharge** and **Rope Discharge** and are illustrated in Figure 2.9. Spray discharge is the most frequent operating regime and is implicit in all of the

---

'These are models which can be used to modify the basic unit model structure when unusual operating conditions are encountered.

Rope

Borderline

Spray

Figure 2.9 Cyclone Underflow Flow Regimes

published general models of cyclones. However, operators prefer to run as close as possible to the roping regime because this tends to minimize the fine particle bypass by reducing the water content of the underflow slurry. Thus, in the simulation of grinding circuits it is not unlikely that rope discharge could be obtained and it is therefore important that it be accounted for since cyclone performance is observed to change noticeably on moving from one regime to the other.

The modelling problem reduces to,

a) prediction of the onset of rope discharge,

b) modification of model parameters and/or structure to account for changes in performance.

With regard to the former, there are several options. One can adopt a manufacturer's design curve relating apex size to solids capacity.(see (25) Fig. 3) This is not advisable since this curve is averaged over many installations and is not likely to be accurate for a particular installation. The preferred approach is to assume a critical value for the underflow volumetric solids concentration, which may be corrected for operating conditions. Mular and Jull(25) have presented a graphical relationship between limiting percent solids in the underflow and the solids concentration in the overflow. Studies by Plitt and Flintoff(14) on a 15 cm cyclone has produced a correlation between underflow and cyclone feed solids concentration as shown on Figure 2.10. In the SPOC

*HCONE* simulation module, this relationship was represented mathematically by the linear empirical function,

$$L_u = L_{u20} + 0.2(\phi - 20) \tag{2.30}$$

Given $\phi$ and a user specified value for Lu20 (default is 56%), the critical volumetric solids concentration in the underflow can be determined. If the cyclone model predicts values in excess of Lu then the cyclone is said to be in rope discharge.

With regard to parameter changes, it is always observed that $d_{so_c}$ increases rapidly with increasing solids feed rate once roping has been realized. This observation is easily explained if one assumes that roping represents the limiting apex solids handling capacity. Therefore, any additional coarse product sent to the cyclone must leave via the vortex finder. On the other hand, there is no general agreement on what happens to the sharpness of separation as roping is encountered. Some have measured increases in m while others have observed m to decrease. Present practice is to have m a constant independent of the underflow regime. Based on this assumption the method which Plitt(14) has used to vary $d_{so_c}$ when the cyclone is predicted to be roping is iterative in nature and utilizes Equation (2.30). The method involves successive increase in the magnitude of $d_{so_c}$ until the model estimated solids concentration in the underflow matches the critical value predicted by Equation (2.30).

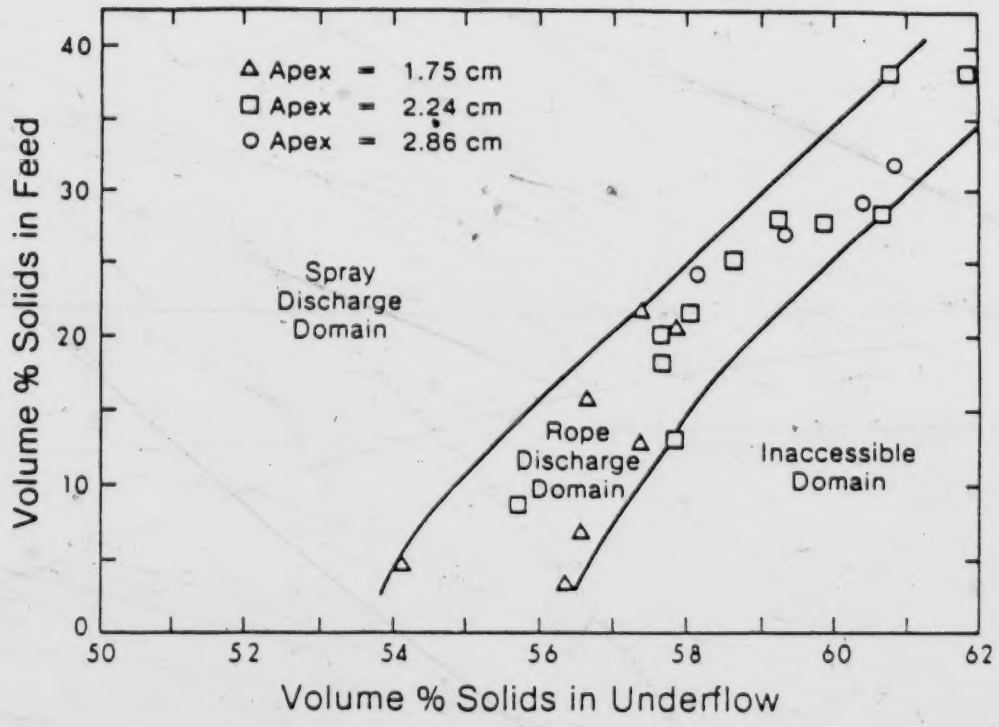


Figure 2.10 Flow Regime Regions for a 15cm Classifying Cyclone

Other constraints which can be considered, if necessary, are cyclone blockage and cyclone capacity. Of the two, the latter is probably of greatest importance in simulation calculations. Capacity constraints can be overcome by assuming maximum/minimum cyclone operating pressures and adding/subtracting a cyclone from the simulated cyclopac as the constraint conditions dictate. (Depending upon the application it might be necessary to account for the pump/sump capacity as well.)

## 2.10 A General Cyclone Model: The Plitt Model

For completeness, the general cyclone model developed by Plitt(5,14) is presented in this section. The parameter data used to derive the general correlations below were obtained by fitting Equation (2.9) to a total of 297 individual experimental data sets from tests on homogeneous ores. (This data was a composite of the work of both Plitt and Lynch and Rao and covered a wide range of operating conditions and cyclone geometry.) This model is presented since it appears to be receiving the most attention in the literature.

Before giving the set of nonlinear algebraic equations which describe cyclone operation it is necessary to make a few comments regarding model usage. First of all, and probably the main reason that the Plitt model is relatively popular, the model can be used, with reservation, without any calibration experiments. (This is the principal

difference between the Plitt and Lynch and Rao formulations where the latter requires some calibration effort.) The general correlations include default parameter values which are often observed to give reasonable predictions when compared to operating cyclone behaviour. Secondly, Plitt has designed the equations in such a fashion that it is possible to obtain a calibration using only one experimental data set. It would be expected that such a model would give improved predictions over the former. Finally, serious modelling efforts usually require the recalculation of the parameters in the Plitt model, and sometimes modification or enhancement of the model form. This is certainly not unexpected given the nature of empirical models and it is to be observed that the Plitt model provides a good basic framework for model reconstruction.

The four equations which comprise the Plitt cyclone model are,

$$d_{50c} = \frac{F_1\ 39.7\ D_c^{0.46}\ D_i^{0.6}\ D_o^{1.21}\ \mu^{0.5}\ e^{(0.063\phi)}}{D_u^{0.71}\ h^{0.38}\ Q^{0.45}\ \left[\frac{\rho_s - 1}{1.6}\right]^k} \qquad (2.31)$$

$$m = F_2\ 1.94\ e^{\left[\frac{-1.585}{1+\phi}\right]}\ \left[\frac{D_c^2 h}{Q}\right]^{0.15} \qquad (2.32)$$

$$P = \frac{F_3\ 1.88\ Q^{1.78}\ e^{(0.0055\phi)}}{D_c^{0.37}\ D_i^{0.94}\ h^{0.28}\ (D_u^2 + D_o^2)^{0.87}} \tag{2.33}$$

$$S = \frac{F_4\ 18.62\ \rho_p \left[\frac{D_u}{D_c}\right]^{3.31}\ h^{0.54}\ (D_u^2 + D_o^2)^{0.36}\ e^{(0.0054\phi)}}{D_c^{1.11}\ P} \tag{2.34}$$

with

$$R_f = \frac{\left(\frac{S}{1+S}\right) - \left(\frac{R_s \phi}{100}\right)}{1 - \left(\frac{\phi}{100}\right)} \tag{2.35}$$

Notice that in Equation (2.31) the effects of solid density have been accounted for using a form of Equation (2.23), normalized to a solids specific gravity of 2.6($SiO_2$). However, it is assumed that the bypass remains constant and equal to Rf for all specific gravity fractions, clearly an erroneous assumption.

Inspection of Equation (2.35) shows that this general cyclone model requires iterative solution since there is a dependence of Rs on Rf. Experience(14) has shown that 3 iterations are generally sufficient to stabilize the model predictions.

## 2.11 Applications of Cyclone Models

There are four major areas of application of cyclone modelling technology. These are briefly discussed below including an example of each application.

### Process Analysis

Process analysis (or data reduction) generally involves the determination of the basic (2 or 3) model parameters from experimental data gathered under different operating scenarios. The parameter values are then interpreted to reconcile changes in cyclone performance. A good example of this application is Klimpel's work with viscosity modifiers (see (13) pg. 313).

The development of general correlations (viz. Equations (2.31) → (2.34)) from such experimental data is included in process analysis.

### Simulation

The use of general cyclone models in simulation studies has received considerable attention in the literature. Suffice to say that two of the best available steady state process simulation systems (SPOC(14) and MODSIM(26)) have incorporated the Plitt cyclone model.

### Design

Design is a special case of simulation where the cyclone model is exercised (to calculate basic model

paremeters or product stream attributes) to meet some process design objective(s). In this application a set of the independent variables (e.g. cyclone diameter, etc.) is searched to find some combination which meets the design criteria and is compatible with commercial cyclone dimensions. The possibilities of implementing a design system are numerous and the reader is referred to the work of McIvor(27) for an example of one implementation.

**On-Line Size Analysis**

This is another area which has received considerable attention in the literature. While in many cases, the correlations implemented for size prediction are simpler than the equation set given in the preceeding section, these models were derived from cyclone modelling experiments. It is frequently the case that the general cyclone model can be used to suggest a structure for such a correlation. An introduction to this application which includes a summary of industrial experience is given by Seitz and Kawatra(28).

## 2.12 A New Conceptual Model of Cyclone Operation

It was mentioned earlier that autogeneous heavy medium separation effects are observed in the fine particle size range (bypass region) for a classifying cyclone treating a heterogeneous ore. It was also mentioned that this separation mechanism was exploited in coal preparation using a cyclone design variant called the automedium cyclone. It

follows that the automedium cyclone would be a logical unit to study in an effort to quantify these effects. This implies that the present project is of interest not only to coal preparation engineers, but to mineral processing engineers as well.

The basic design differences between a classifying and an automedium cyclone are illustrated in Figure 2.11. Despite their geometrical differences, both are cyclones and, as such, have basic operational similarities. It is the opinion of the author that both cyclones should be described by a general empirical model, each representing a special case. It was felt that the automedium cyclone would necessarily involve a more complex mathematical model and it could be used to develop the more general conceptual model.

According to Visman(32) the primary operational difference between the two cyclones of Figure 2.11 relates to the existence of the "bed" in the automedium cyclone. Within the bed the particles with high settling velocities are further separated according to specific gravity (buoyancy) and size (percolation). The coarse low specific gravity particles migrate to the top of this bed and are stripped by the upward flow component at the air core interface. These particles then have a chance of leaving through the vortex finder (depending on its location and the particle trajectory) or returning to the bed. Figure 2.12 is a schematic illustration of the separation mechanisms within an automedium cyclone.

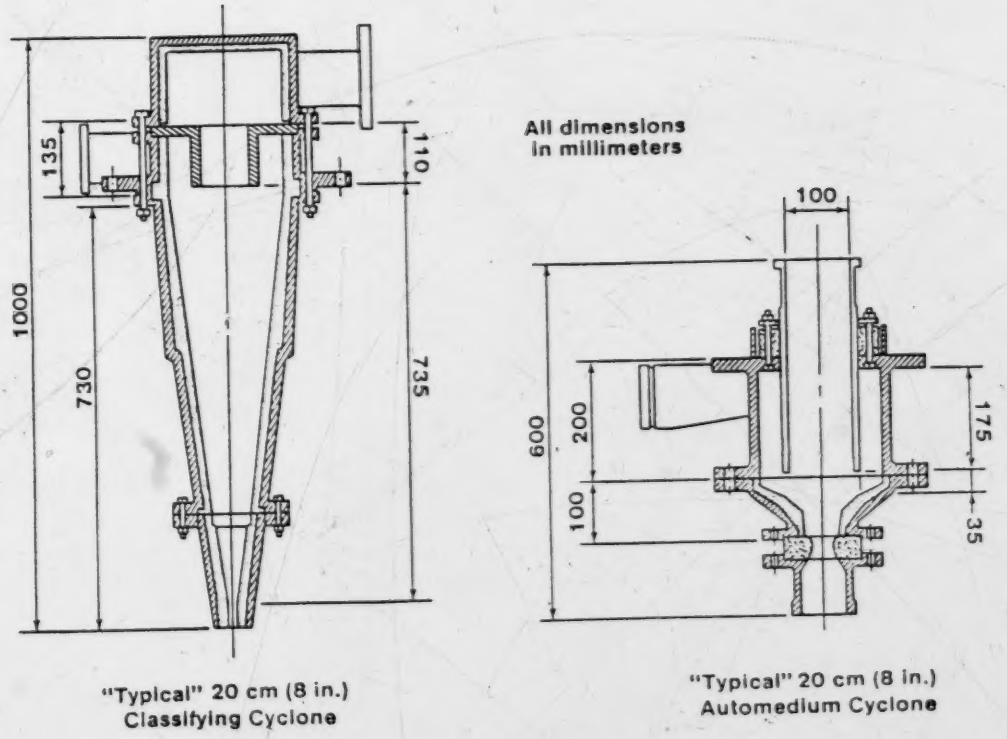


Figure 2.11 Comparison af a Classifying and an Automedium Cyclone

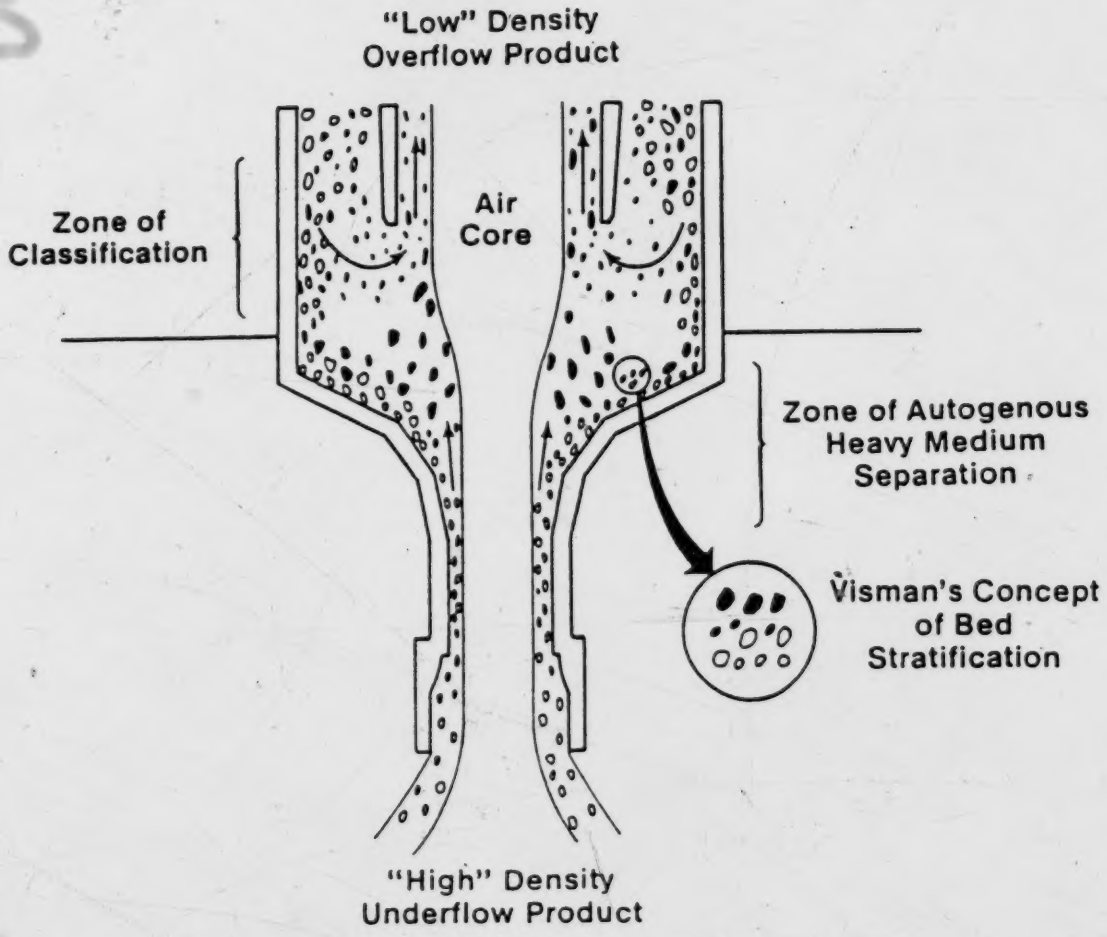


Figure 2.12 The Separation Mechanisms in the Automedium Cyclone (after (32))

Although a number of rather extensive studies have been done on the automedium cyclone(33,34), none have been entirely based on the partition curve approach that is used for classifying cyclones. However, experimental work by van Duijn et. al.(29,30,31) on a cyclone of similar design and, by Visman(32) on the automedium cyclone were very enlightening. The former was especially useful in formulating a conceptual model because of the fundamental measurements which were made.

Both van Duijn and Visman have demonstrated experimentally that a stable bed is formed in the "flat" section of cyclones with large cone angles, e.g. $\theta > 120°$. van Duijn and his coworkers also performed impulse residence time distribution studies on the solids and water components. Based on these experiments they concluded that the nontangential velocity components of the solids and water flow were as illustrated on Figure 2.13. Figure 2.14 presents a conceptual model which the author has postulated based on the work of van Duijn et. al. and Visman as well as on preliminary experiments. This is the model which is to be evaluated in this project.

From Figure 2.14 the overall partition function is now seen to depend on four separation mechanisms, rather than the traditional two shown in Figure 2.3, i.e.

$$p_{ij} = \left(r_{ij} + (1 - r_{ij})\, c_{ij}\right) \frac{(1 - a_{ij})}{(1 - a_{ij} b_{ij})} \qquad (2.36)$$

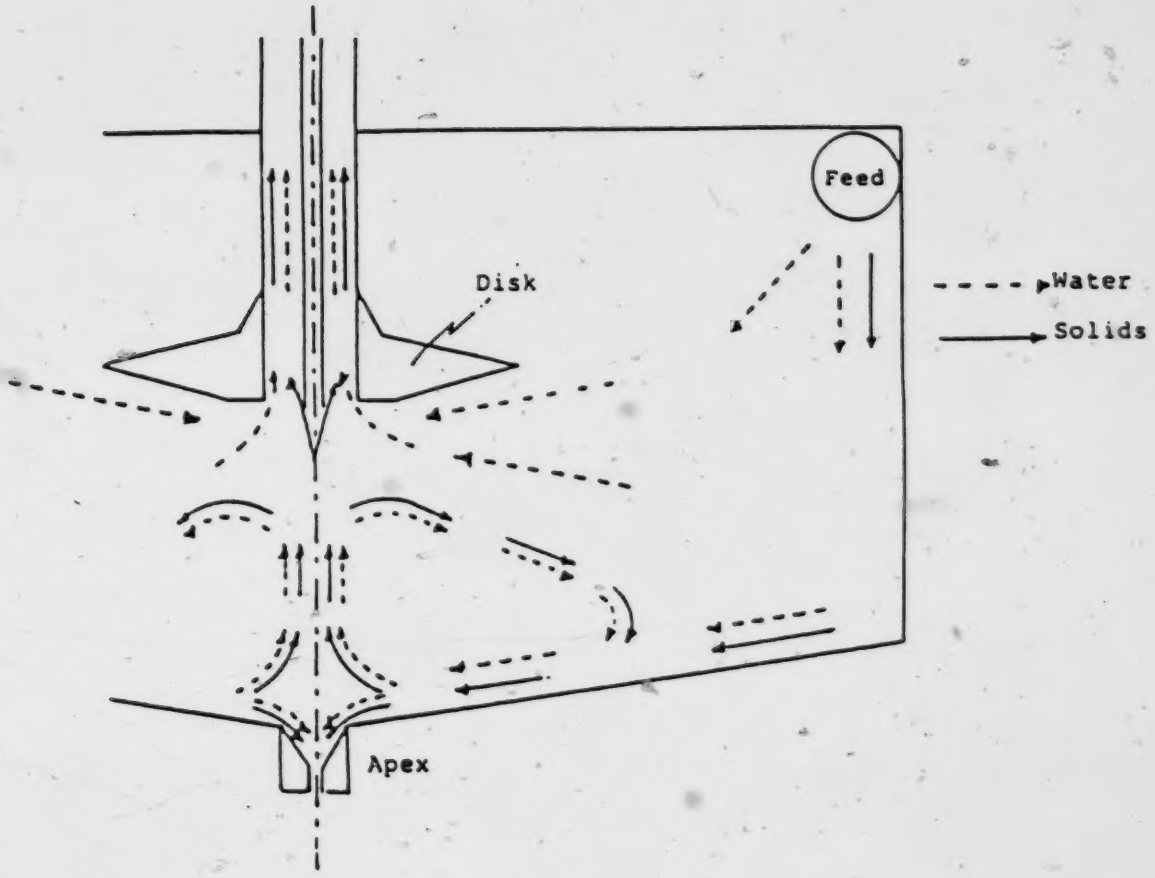


Figure 2.13 The Non-Tangential Velocity Components for Solids and Water in a Cyclone with a Large Cone Angle (after(29)

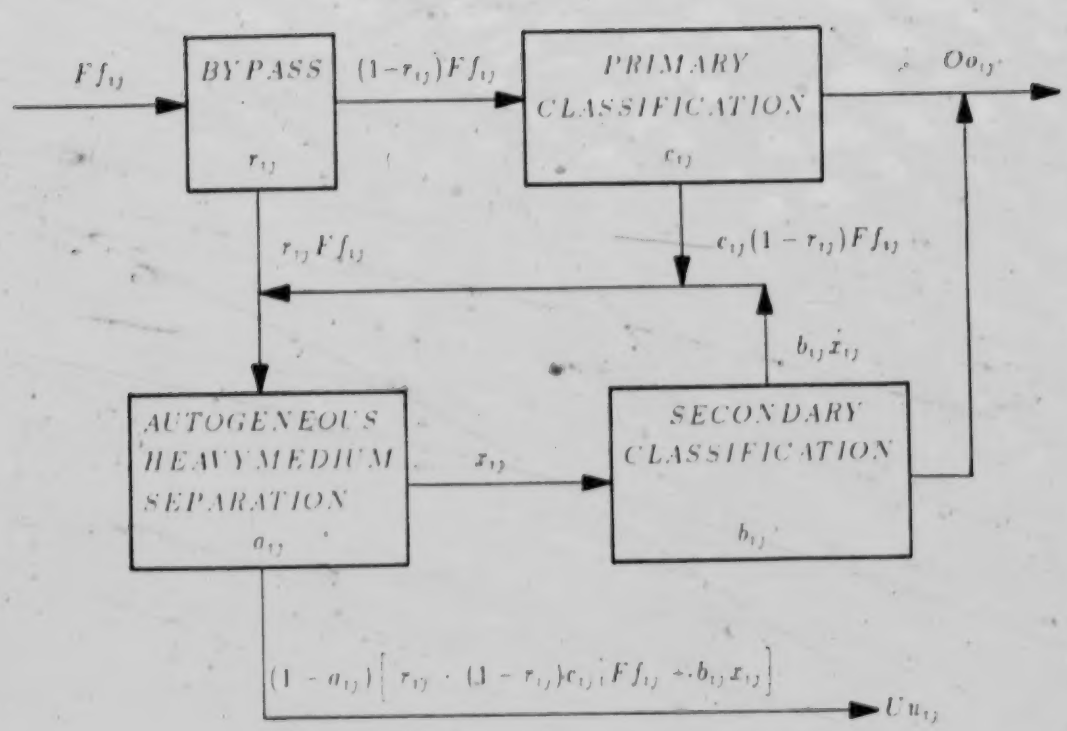


$$Uu_{ij} = P_{ij}Ff_{ij}$$

$$P_{ij} = \left[r_{ij} + (1 - r_{ij})c_{ij}\right]\left(\frac{1 - a_{ij}}{1 - a_{ij}b_{ij}}\right)$$

Figure 2.14 A Conceptual Model of Automedium Cyclone Operation

From Equation (2.36) notice that in the event that either $a_{i,j}=0$ or $b_{i,j}=1$, the model reduces to the more familiar form given by Equation (2.1).

It is readily apparent that the specification of functional forms for the four separation mechanisms could present special parameter estimation problems, particularly when the cyclone is operating as a classifier. Efforts are currently underway to develop suitable parameter estimation algorithms as well as to reduce the number of model parameters. Presently, visual (dynamic) methods are being used for parameter estimation where the parameter values are driven by a kind of interactive "joystick" control to locate a reasonable minimum in J.[7]

Much work remains to be done to determine whether the model is of general practical use. Such a model is apparently necessary to describe the complex separation mechanisms within the automedium cyclone. Moreover, the model is capable of accounting for a number of unquantified phenomena known to occur in classifying cyclones; (i) fishhook, (ii) m increases at the onset of roping, (iii) m decreases in the roping regime, (iv) peculiar partition curves for a homogeneous ore. Such occurrences are usually related to a high solids flux at the apex which is very similar to the stanard operating conditions of an automedium cyclone.

---

[7] Chapter 7 includes some documentation on this novel means of estimating parameter values.

The potential of this model is the driving force to completely explore its potential, both strengths and weaknesses!

# 3. SILICA TESTWORK

## 3.1 Introduction

It has been argued that the automedium cyclone is designed such that size classification effects are almost totally supressed in normal operation. According to Visman's theory of AMC operation, this is expected to be true for the lower specific gravity components in a multiphase solids mixture. Since most of the literature on experimental investigations of the AMC deal with coal or other multiphase solids, it was decided that an appropriate starting point would be to examine the "pure" classification behaviour of the AMC using a homogeneous solid. Silica was selected for this portion of the project because most of the published design and modelling literature is based on silaceous ores and/or pure silica.

## 3.2 Experimental Design and Test Procedure

### 3.2.1 Experimental Design

Since this was not intended to be a rigorous set of tests a simple experimental design was employed. Three series of experiments (A,B & C) were performed. In all cases the cyclone feed conditions were maintained roughly constant and the only geometrical variable was the vortex finder

clearance, h. The first two series of experiments were used to help test the system, as will be noted later. In these series the vortex finder clearance was studied at three levels: h=4.3 inches (109mm), h=2.8 inches (71mm) and h=1.3 inches (33mm). The final series of experiments involved a more detailed study of the impact of vortex finder clearance on AMC performance. In series C, a total of 7 experiments were performed with 1.125 inches (28mm) $\leq$ h $\leq$ 6 inches (152mm).

The feed solids for series A and B were produced by blending commercial coarse and fine ground silica to give a fairly natural solids size distribution. The blend proportions were calculated from the relevant size distribution data and a target size distribution for the blended product. In regard to the specification of a target, Plitt's general model (Equation 2.31) was used to compute an expected $d_{50_C}$ for the design operating conditions. The feed material was then chosen so that, under perfect classification, the solids split would be Rs=0.25. (This value compares to typical coal preparation plant yields (1-Rs) from AMC units of $\simeq$75%.) In series C the same general procedure was used, however, the feed solids size distribution was specified to be somewhat coarser. This was done in an attempt to increase the solids flux to the underflow product with the expectation that this would in turn amplify the effects of the "bed" and "secondary

classifier" on cyclone performance. The feed solids size distribution data is shown graphically in Figure 3.1.

In all of the experiments performed in this project the 8 inch (200mm) "L" type AMC was used. The unit was shown schematically in Figure 2.11.

**3.2.2 Test Procedure**

Figure 3.2 and Plates 3.1 and 3.2 show the closed loop pilot plant facility which was used throughout this project.

Briefly, the experiments were performed according to the the following procedures. The feed slurry was mixed to design specifications in the slurry reservoir. A sufficient slurry volume was prepared to allow three sets of samples to be taken in the course of a single run, i.e. from one feed slurry mixture. These three sets of samples corresponded to three different values of h, which, unlike the other operating variables, could be easily changed on-line using the electric drive mechanism. In this manner it was possible to make maximum use of the available solids material.

Once the slurry was prepared, the pumps were started, the sampling launder positioned for slurry recirculation, and the reservoir discharge valve opened. The vortex finder clearance was set to the desired design value for the first experiment in the run. Final flow rate adjustments were made

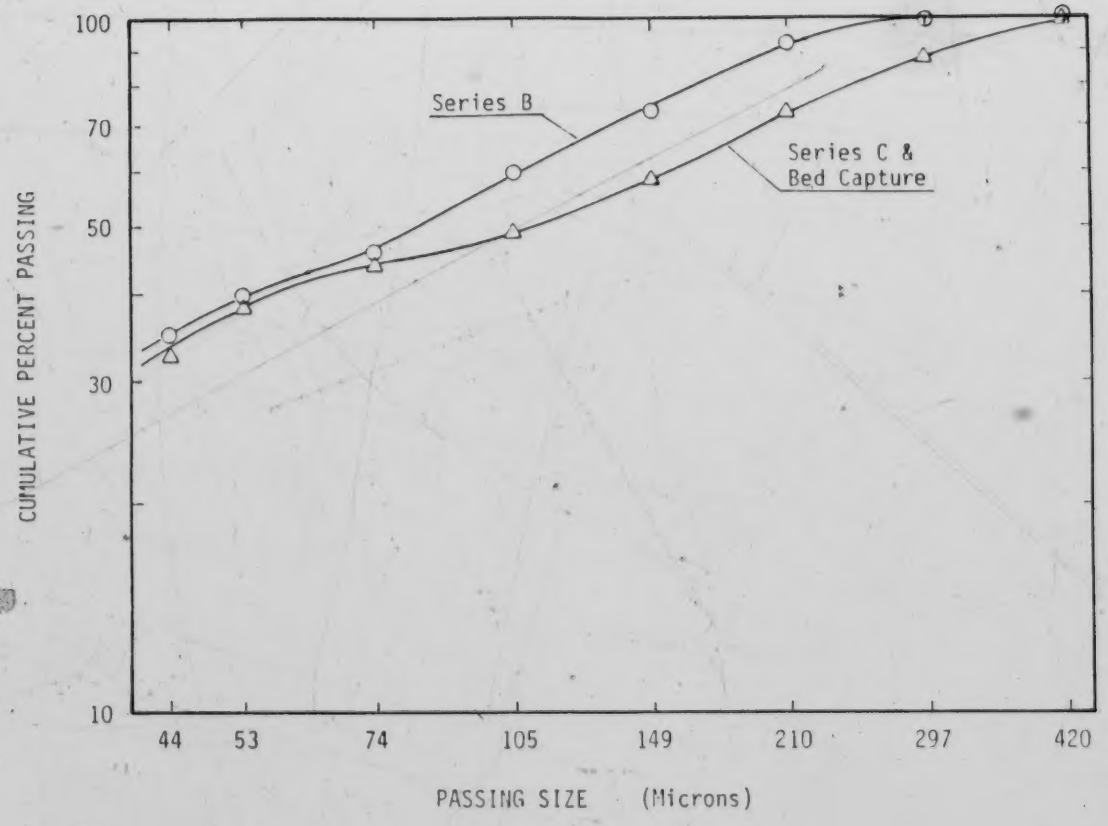


Figure 3.1 Solids Feed Size Distributions for the Silica Tests

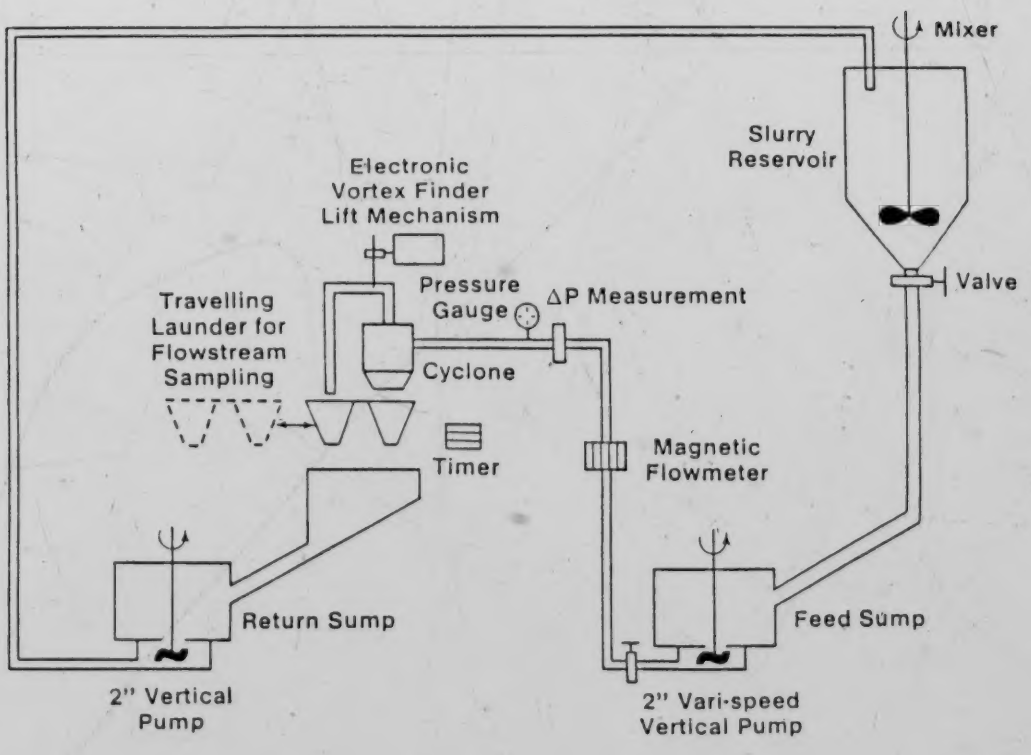


Figure 3.2 Schematic Flowsheet of the Closed Loop Cyclone Pilot Plant

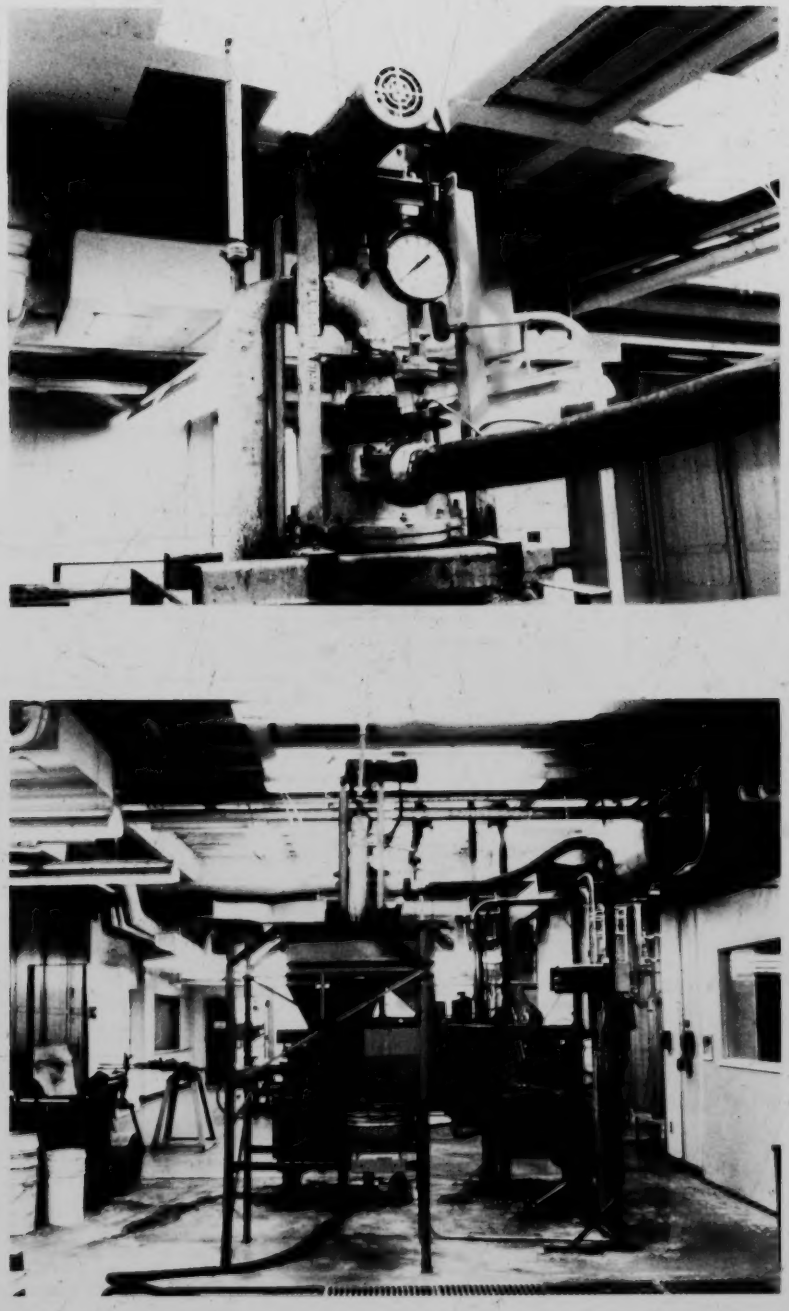

Plate 3.1 The Closed Loop Cyclone Pilot Plant

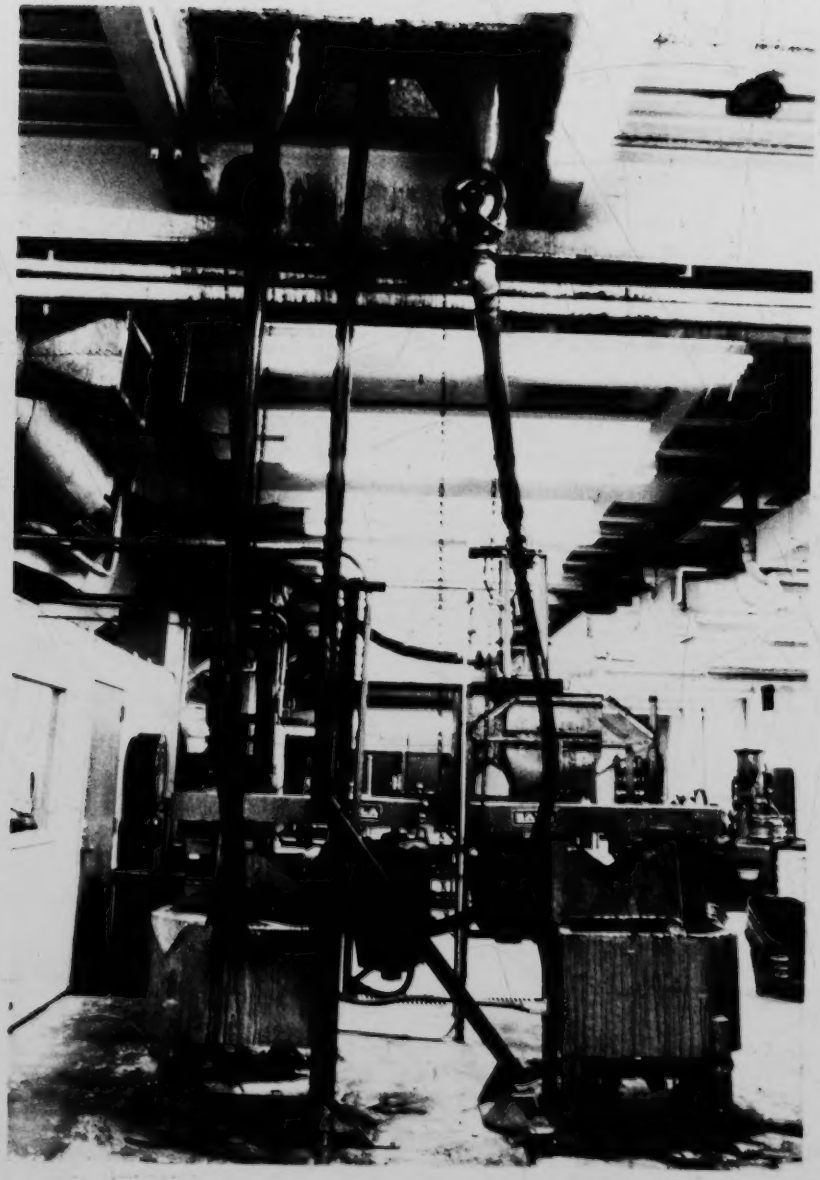

Plate 3.2 General View of Cyclone pilot Plant

using the variable speed pump drive (coarse adjustment) and the valve on the pump discharge line (fine adjustment). The reservoir discharge valve was simultaneously adjusted to ensure a reasonable level in the feed pump sump and thereby eliminate surging.

When the design specifications were satisfied and the pilot plant was operating satisfactorily, the system was allowed to run for ≥15 minutes to achieve steady state. During this time there was some unavoidable coarse particle settling in the pump sumps. (This was especially true for series A which lead to the fabrication and installation of false bottoms in the sumps for all subsequent runs. Although this action significantly reduced the problem it did not completely eliminate it.)

Once the system was judged to be at steady state samples of the underflow and overflow product streams were cut simulataneously by moving the sampling launder. When sufficient sample had been obtained the launder was repositioned for slurry recirculation and the vortex finder clearance adjusted for the subsequent experiment. After another period of ≥15 minutes, during which time the flow and feed sump level were checked, the sampling procedure was repeated. This was done once more for a total of three experiments on the inital feed slurry. (After the final samples had been taken the slurry volume in the system was

reduced to a level where pump surging was unavoidable.)

The samples were weighed, filtered, dried, and the dry weights obtained prior to sub-sampling for size analysis. For the silica tests the following ($\sqrt{2}$) sieve series was used: (Tyler Canadian Mesh) 35,48,65,100,150,200,270 and a 325 mesh screen was also included in the nest. All of the size analyses were done in a wet sieving apparatus.

### 3.3 Test Results

The detailed experimental results for all of the silica tests are presented in Appendix 3.

From this data it is apparent that the false bottoms, which were installed between series A and B to reduce coarse particle settling, were reasonably effective. For an identical feed slurry mixture, the solids concentration in the feed went from an average of 12.1% in series A to 14.8% in series B. Moreover, the reconstituted feed size distributions for the experiments in series B compare very closely to that predicted from the blending calculations. On this basis it was judged that the false bottoms were a significant corrective measure to permit close approximation to design feed solids size and feed slurry concentration specifications.

Another interesting aspect of the the silica testwork was the consistent low recovery of water to the underflow product, Rf ≤ 5%. Without similar data from a classifying cyclone it is difficult to draw any quantitative comparisons, however, the design of the lower cone section of the AMC appears to facilitate the dewatering of the underflow product stream. If this were to hold in general it would lead to a minimal misplacement of fine material by entrainment and, for example, could have potentially important implications in classification applications such as closed circuit grinding. This is an area which deserves further study as does the effect of high solids concentration and coarse feed on AMC classification performance.

From a modelling point of view the partition function data are of greatest interest and this is discussed in the following sections.

### 3.3.1 Results of Silica Test Series A & B

The partition curve data for series A and B are presented in Table 3.1 and in Figures 3.3 and 3.4. From the figures it is quite apparent that the partition curves exhibit an unusual shape, especially at lower values of h. There was some initial suspicion regarding the data and, in the case of series A, the screen analyses were repeated on some of the reject sample. However, substantially identical

Table 3.1 Partition Function Data for Series A & B

SERIES: A

| SIZE IN MICRONS | PARTITION FUNCTION h= 1.3" | 2.8" | 4.3 |
|---|---|---|---|
| 595 | 1.00 | 1.00 | 1.00 |
| 420 | 1.00 | 1.00 | 1.00 |
| 297 | 0.63 | 1.00 | 1.00 |
| 210 | 0.53 | 0.87 | 1.00 |
| 149 | 0.29 | 0.76 | 0.91 |
| 105 | 0.13 | 0.45 | 0.71 |
| 74 | 0.04 | 0.15 | 0.21 |
| 53 | 0.01 | 0.09 | 0.07 |
| Rf VALUE | 0.008 | 0.010 | 0.021 |

SERIES: B

| SIZE IN MICRONS | PARTITION FUNCTION h= 1.3" | 2.8" | 4.3" |
|---|---|---|---|
| 595 | 1.00 | 1.00 | 1.00 |
| 420 | 0.70 | 0.98 | 1.00 |
| 297 | 0.56 | 0.88 | 0.99 |
| 210 | 0.39 | 0.71 | 0.96 |
| 149 | 0.26 | 0.54 | 0.84 |
| 105 | 0.14 | 0.25 | 0.33 |
| 74 | 0.07 | 0.11 | 0.16 |
| 53 | 0.06 | 0.10 | 0.11 |
| Rf VALUE | 0.011 | 0.021 | 0.029 |

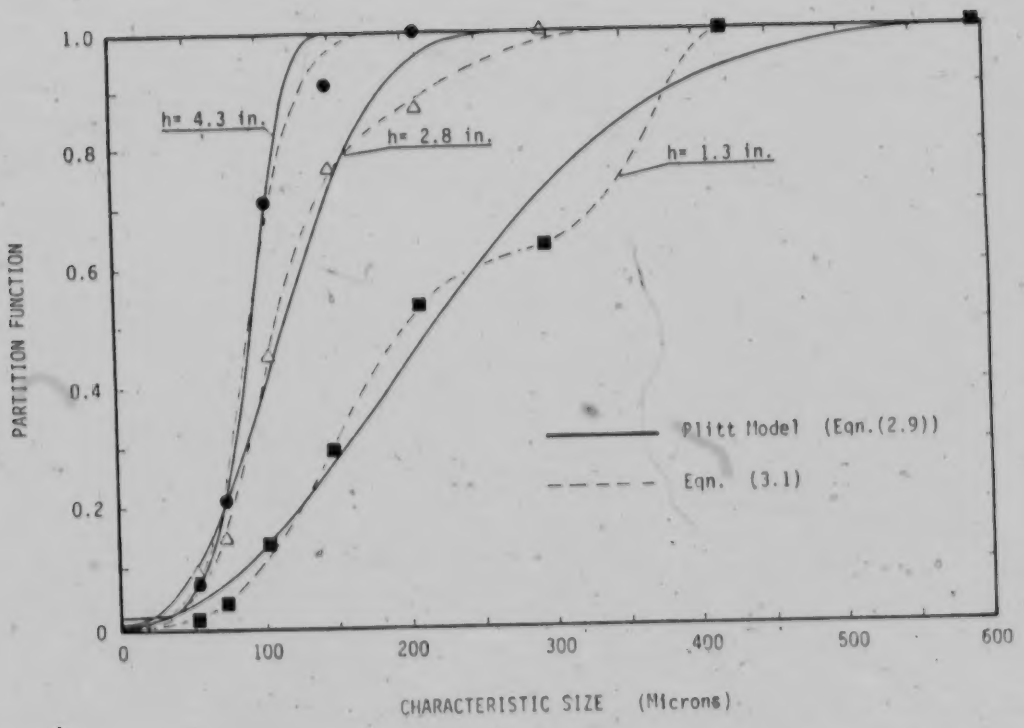


Figure 3.3 Partition Curves for Silica Series A

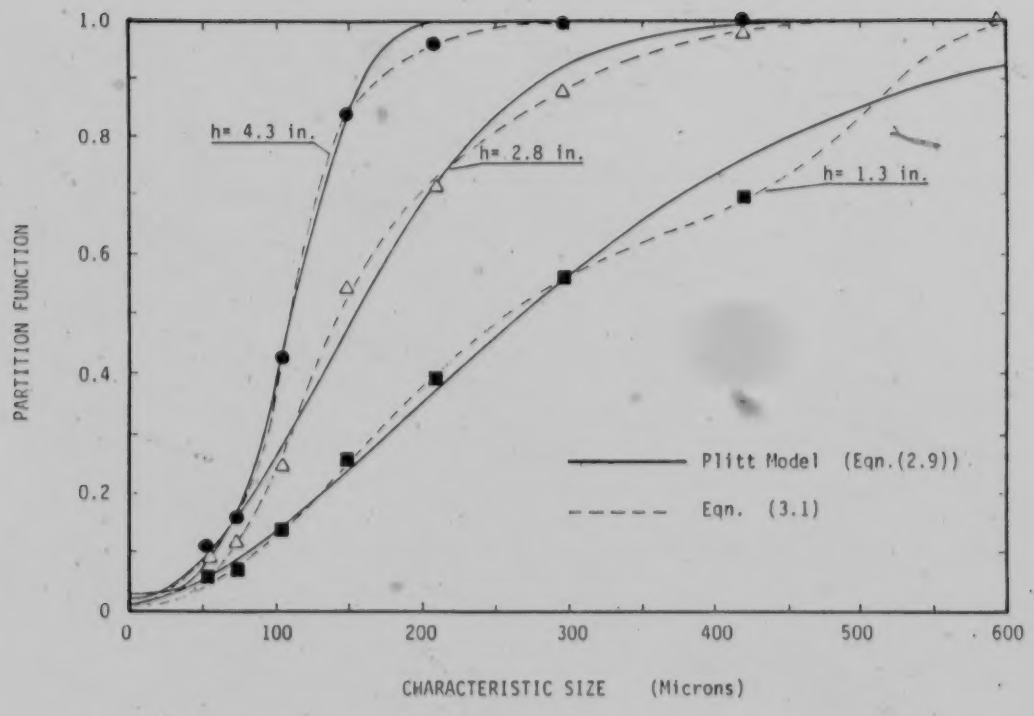


Figure 3.4 Partition Curves for Silica Series B

results were obtained. Duplicate analyses were performed for one test in an effort to estimate the error variance of the experimental partition function data. To summarize, it seems safe to conclude that for $p_i \leq 0.95$, the 95% confidence intervals are $\leq \pm 0.05$. Inspection of the data for h=1.3 inches (33mm) in Figure 3.3 would seemingly indicate that the point at d=297$\mu$, even when accounting for experimental error, is far enough removed from its "expected" position to suggest that the unusual partition curves are truly representative of cyclone performance. In this case the cyclone performance is described as unusual when compared to that expected of a cyclone classifier.

Plitt's model (Equation (2.9)) has been used throughout this project. The solid lines on Figures 3.3 and 3.4 represent the "best fits" of Equation (2.9) to the experimental data through the minimization of Equation (2.13). For the purposes of these modelling studies the characteristic size was defined by Equation (2.12). Clearly, the Plitt model is a poor representation of the experimental data and this becomes increasingly true as h decreases.

Recalling the general model form of Equation (2.36), which was based on wide angle cyclones like the AMC, a simplified model form was adopted as shown in Equation (3.1)

$$p_i = \left(R_f + (1 - R_f)\, c_i\right) \frac{(1 - a_i)}{(1 - a_i b_i)} \qquad (3.1)$$

where $c_i$ and $b_i$ were assumed to be of the form given by Equation (2.6) and $a_i$ was taken to be a constant. Equation (3.1) was fitted to each set of experimental data and the results are shown in Figures 3.3 and 3.4. Evidently the fits are much better for this model, however, from a purely statistical viewpoint (see the methodology of section 2.5.2) the 5 parameter model (Equation (3.1)) is better than the 2 parameter model (Equation (2.9)) only for the case where h=1.3 inches (33mm). Inspection of the goodness of fit, especially with respect to the slight idiosyncracies for h=2.8 inches (71mm) lead to the conclusion that AMC performance is more accurately described by Equation (3.1) than by Equation (2.9), as might have been expected based upon the work of van Duijn et al.(29,20,31)

There is one further observation of interest relative to the partition curves of Figures 3.3 and 3.4. With the installation of the false bottoms in the sump and the reduction of coarse particle settling in the system, both the feed slurry solids concentration and the coarseness of the feed size distribution were observed to increase for series B. With all other factors remaining approximately constant, it is observed that the partition curves for series B have been "shifted" to the coarser particle size range and seem "flatter" than their series A counterparts.

It would seem, therefore, that AMC operation is quite sensitive to the feed slurry solids concentration (presumably viscous effects) and/or the feed particle size distribution (presumably bed characteristics effects).

Before leaving this section it is important to make a couple of interpretive comments regarding the shape of the AMC partition curves. Without resorting to the analysis of a very limited set of parameter data, it is possible to propose a physical explanation for the unusual shape of the curve in the coarse particle size range, as h decreases. At larger values of h the particles which are stripped from the bed by the upward flow component at the air-core interface have sufficient time to recirculate to the bed under the influence of the tangential flow component and the consequent centrifugal force. Under these conditions, only the very fine particles would have a trajectory which might be intersected by the vortex finder opening and thus report to the overflow. In this situation it is postulated that $d_{50_c}$ (secondary classifier) $<<$ $d_{50_c}$ (primary classifier) and the overall partition curve can be adequatley described by a model of the form given by Equation (2.9). This is true because for all practical purposes $b_i = 1$ in Equation (3.1) which provides a default to the more traditional cyclone classifier model. However, as h decreases the $d_{50_c}$ of the secondary classifier increases as a result of the intersection of the coarser particle trajectories by the

vortex finder opening. When h is low enough that $d_{50_c}$ (secondary classifier) > $d_{50_c}$ (primary classifier), a plateau region is observed in the partition curve (at about a value of $p_i = 1-a_i$. This gives the impression of a double sigmoidal growth function as evidenced on Figures 3.3 and 3.4 for h=1.3 inches (33mm).

### 3.3.2 Results for Silica Test Series C

The experimental partition function data for series C are presented in Table 3.2 and Figure 3.5. As mentioned earlier, this series was designed to study the emergence of the influence of the bed separation and secondary classification on the AMC partition curve. This was to be accomplished by varying h over the maximum possible range (governed by mechanical design factors) using smaller increments (≤1 inch(25mm)). It was expected that by increasing the coarseness of the feed material the role of the bed and the secondary classifier would be accentuated.

The results of this series, as presented in Figure 3.5, are consistent with those given by Bradley (see (7), Fig. 39) where the vortex finder clearance was varied in a cyclone classifier. Because of the large number of curves in Figure 3.5, Figure 3.6 was prepared showing only three of these partition curves. With reference to this figure, the curve for h=6 inches (152mm) shows significant short circuiting of coarse particles to the overflow product. This

Table 3.2 Partition Function Data for Silica Series C

SERIES: C

| SIZE IN MICRONS | PARTITION FUNCTION h= 6.0" | 5.0" | 4.0" | 3.0" | 3.5" | 3.0" | 1.125" |
|---|---|---|---|---|---|---|---|
| 595 | 1.00 | 1.00 | 1.00 | 1.00 | 0.95 | 0.95 | 0.88 |
| 420 | 0.99 | 1.00 | 0.99 | 0.96 | 0.89 | 0.78 | 0.74 |
| 297 | 0.98 | 1.00 | 0.96 | 0.88 | 0.76 | 0.61 | 0.60 |
| 210 | 0.95 | 0.98 | 0.76 | 0.61 | 0.47 | 0.37 | 0.35 |
| 149 | 0.93 | 0.94 | 0.44 | 0.38 | 0.30 | 0.25 | 0.25 |
| 105 | 0.79 | 0.60 | 0.22 | 0.19 | 0.17 | 0.13 | 0.15 |
| 74 | 0.36 | 0.15 | 0.12 | 0.10 | 0.06 | 0.06 | 0.08 |
| 53 | 0.13 | 0.04 | 0.06 | 0.06 | 0.03 | 0.03 | 0.04 |
| Rf VALUE | 0.044 | 0.029 | 0.036 | 0.032 | 0.019 | 0.017 | 0.020 |

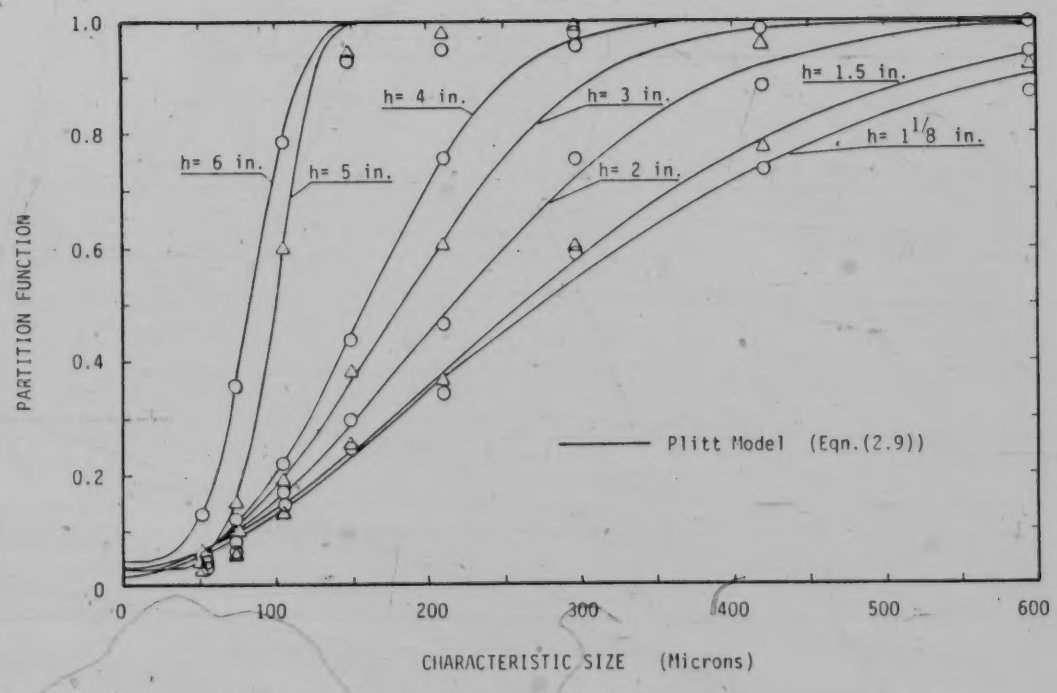


Figure 3.5 Partition Curves for Silca Series C

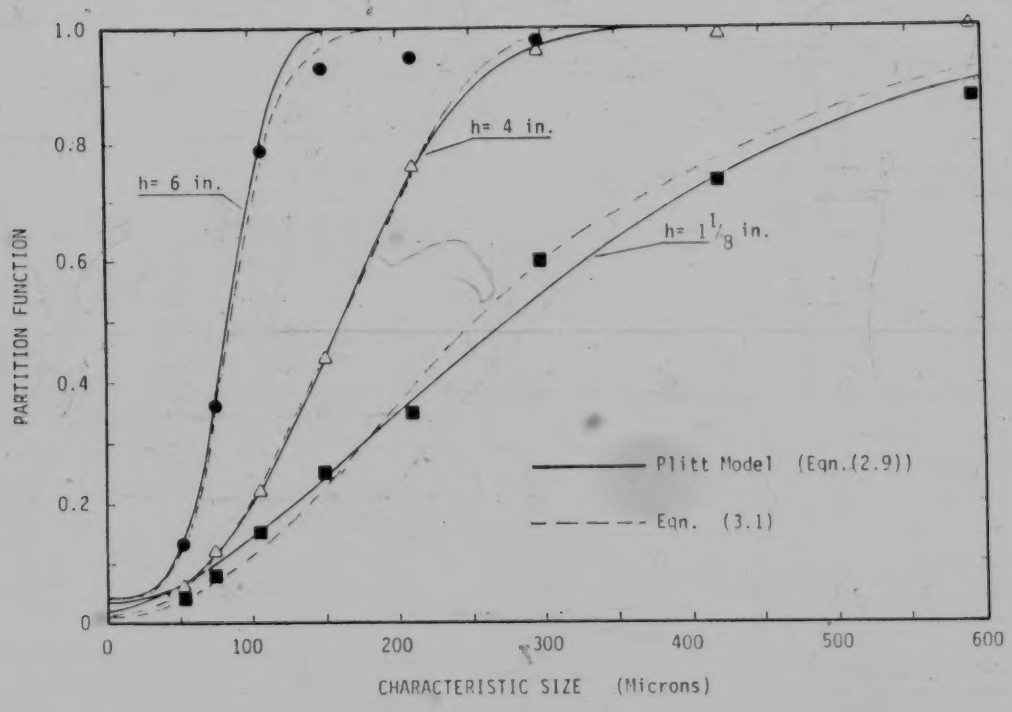


Figure 3.6 Selected Partition Curves from Silica Series C

arises because the vortex finder inlet is at about the same elevation as the bottom of the feed inlet. Bradley observed the same type of effect.

From a modelling point of view, Equation (2.9) seems to adequately describe the data as shown by the solid lines in Figures 3.5 and 3.6. Fitting Equation (3.1) to the data in Figure 3.6 produced no improvement in the fit. The inconsistency in results, for small values of h, between series A & B and series C is quite disturbing. It can only be concluded that the coarser size distribution (see Figure 3.1) and/or the higher feed solids concentration has had a dominant effect on determining the overall shape of the partition curve. This is likely a further manifestation of the effect noted earlier between series A and series B. More work is required on this aspect of AMC performance since the variation in the feed solids concentration as well as the feed sizing is typical of what might be expected in operating practice.

**3.4 Bed Capture Experiments**

Van Duijn et al. and Visman have both demonstrated that a stable bed was formed in the lower cone section of a wide angle cyclone like the AMC. In an effort to demonstrate that this was also true for the present work a bed capture experiment was performed.

The experimental procedure was essentially the same as described in an earlier section. The operating conditions were essentially equivalent to those for series C, with h=2.8 inches (71mm). Using a second reservoir (not shown in Figure 3.2), it was possible to replace the slurry entering the feed pump sump with water. Immediately when this action was taken the return pump discharge was redirected to a waste disposal system which allowed for the AMC to operate in open circuit with a clear water purge to "wash" out the AMC contents. With the available reservoir capacity, about 50 seconds of open circuit operation was possible before the water supply was exhausted. Shortly before this condition was encountered the feed pump was stopped and, simultaneously, the sampling launder was moved into position to capture the material which drained from the AMC. It was argued that the duration of water feed to the AMC would be sufficient to remove most of the solids except the bed. The results of this experiment are also included in Appendix 3. The size distributions for the steady state underflow material and the bed are shown in Figure 3.7.

It had been expected that the bed would be somewhat coarser than the underflow product reflecting the recirculation of coarse particles. If the sample data is accurate, the opposite was true as shown in Figure 3.7. Correcting the bed size distribution for contamination by the AMC holdup, using the captured overflow sample as a

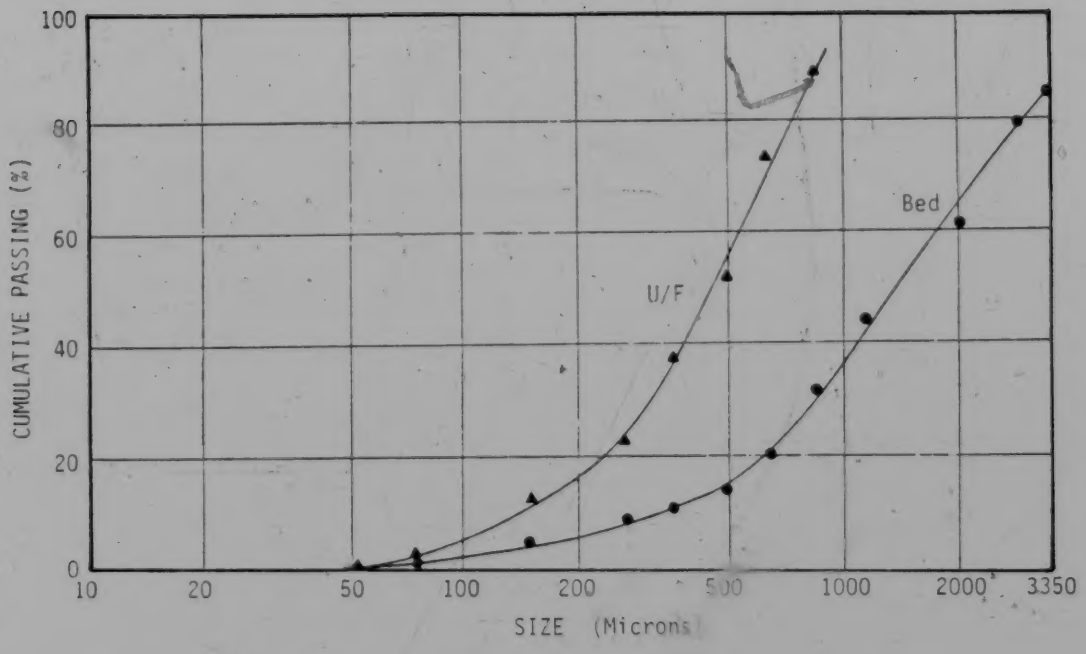


Figure 3.7 Size Distribution of the Underflow and Bed Samples

measure of the holdup attributes, yields a size distribution which is essentially the same as that for the steady state underflow. This similarity was observed in a number of preliminary bed sampling experiments.

To summarize, it seems clear that a stable bed does form in the AMC (the evidence of this was much more convincing in the case of the coal experiment, as will be seen later). The similarity of the bed and the underflow samples is not what had been intuitively expected. However, it may be reasonable when one considers that in modelling series A and B results, the bed separation was considered as a simple "split", which means that the underflow and bed would have the same solids attributes.

### 3.5 Summary

The silca testwork has demonstrated a number of the behavioural characteristics of the AMC. Firstly, the conceptual model of the AMC given in Figure 2.14 was substantiated by the results of series A and B. Secondly, and from series C, it appears that the AMC is senstive to nature of the feed solids material, especially in the formation and separating action of the bed. Finally, there is evidence that a stable bed is formed in the lower cone section of the AMC.

# 4. COAL TESTWORK: PLANT SAMPLING

## 4.1 Introduction

As part of the automedium cyclone modelling research project a sampling campaign was carried out on September 10 and 11th 1981 at the Fording River coal preparation plant. The purpose of the plant test was as follows:

(i) to determine the range of typical operating conditions of automedium cyclones in an industrial plant environment from which the pilot plant experiments could be designed.

(ii) collection of bulk coal samples for the modelling experiments.

(iii)to establish a preliminary estimate of the amenability of the cyclones to simple automatic control.

## 4.2 Fording Coal Preparation Plant

The Fording River preparation plant is located near Elkford, B.C. and was commissioned in 1972 to produce metallurgical coal for the Japanese steel mills. The plant feed is obtained from adjacent open pits using both dragline and truck-and-shovel methods from a multiple seam deposit.

The original plant was designed for 800 tonnes of feed per hour. Extensive modifications of the fines circuit in 1977 increased the plant capacity to 1200 tonnes per hour. These modifications included the installation of a two-stage automedium cyclone circuit. The configuration of the circuit

is shown in Figure 4.1. The circuit consists of two banks of thirty 12-inch diameter automedium cyclones. The primary cyclone overflow is directed to Derrick multifeed screens classifying at 65 mesh. The screen undersize product is sent to froth flotation cells. The primary underflow is routed to a bank of eight secondary automedium cyclones. The overflow from the secondary cyclones is recirculated to the primary feed and the underflow is routed to the refuse stream along with the flotation tailings.

The fines circuit had a nominal capacity of 400 tonnes per hour. The average target yield for the circuit is 85 % (range 35 - 90 %).

The automedium cyclones are of the Visman (tricone) design and were manufactured by Cyclone Engineering Sales of Edmonton.

The Fording plant was selected for the plant tests as it seemed to represent one of the more successful applications of automedium cyclones in western Canada. Also, the process engineering staff at Fording are progressive in their outlook and were very willing to collaborate on this project.

**4.3 Test Procedure**

A cyclone from the primary circuit (south #37) was selected for testing. The cyclone was first dismantled and checked for irregularities. The tricone lining was badly worn and was replaced. The dimensions of the cyclone were

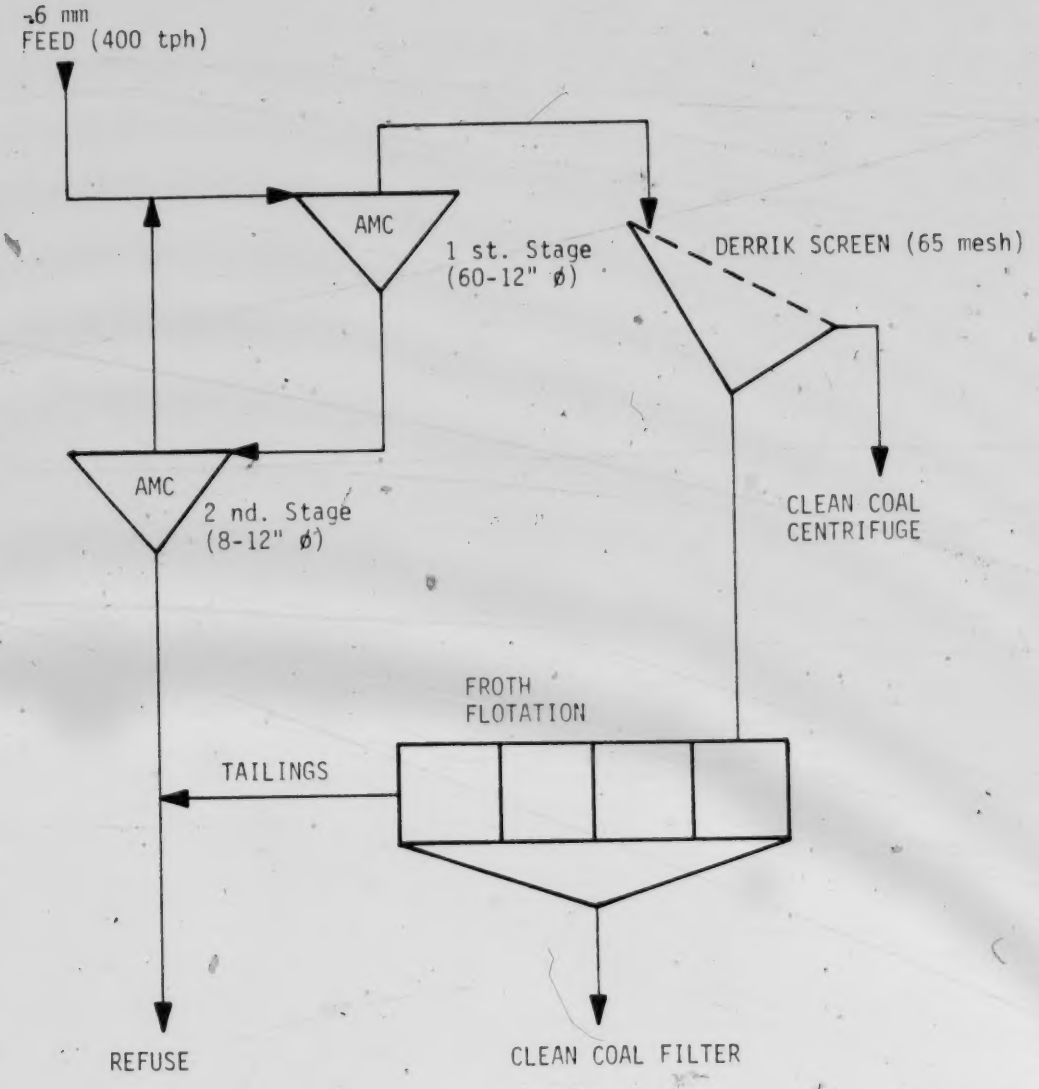


Figure 4.1 Fines Circuit at Fording River

measured and are shown in Figure 4.2.

Overflow and underflow samples were taken from the outlets of cyclone No.37S. A half-moon sampler was used for the overflow and a plastic beaker was used for the underflow. The feed was sampled from a header take-off in the No.36 position using the half-moon sampler. The valve to this line was opened for sample cutting. Wet sample weights were taken immediately. A portable vacuum filter was installed on the cyclone floor to filter all the samples. The filtered samples were transported back to the U of A laboratories for drying, weighing and ash analysis.

Samples were cut every 20 minutes from the 3 streams for 8 hours. Duplicate sampling of the feed and underflow were taken for a period of 1 hour to provide data for error estimation. During this period the overflow samples were omitted due to limitations of the filtering facilities. It was assumed that the errors associated with the half-moon sampling of the overflow would be similiar to that of the feed stream.

**4.4 Test Results**

The results of the plant sampling campaign are shown in Appendix 4. Graphical representations of the % Ash and % Solids in the three streams with respect to time are shown in Figures 4.3, 4.4, and 4.5.

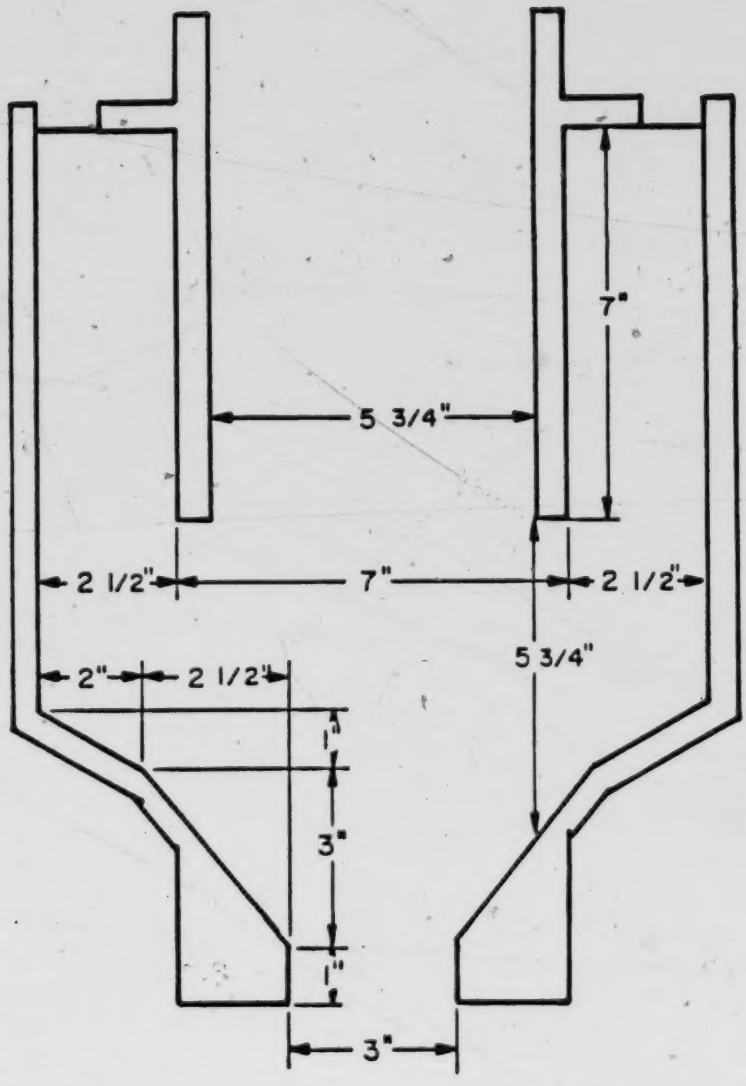


Figure 4.2 Fording Coal's Primary Automedium Cyclone No.37S

The average values for the % Solids and % Ash in the three streams together with the calculated yields were as follows:

| | % Solids | % Ash |
|---|---|---|
| Feed | 10.82 | 23.23 |
| Overflow | 9.60 | 16.19 |
| Underflow | 58.00 | 64.75 |
| Yield | 86.52 Calc. from % solids | 85.40 Calc. from % ash |

During the sampling campaign (at 15:00 h) the feed to the plant was interrupted due to a blockage in the breaker. In the period while the breaker was cleared, plant feed was obtained from a raw coal stockpile.

The variations observed on the three streams were as follows:

| | % Solids | % Ash |
|---|---|---|
| Feed | 11±6 | 23±8 |
| Overflow | 10±6 | 16±6 |
| Underflow | 58±6 | 65±8 |

These average values of the feed stream attributes were used as targets for the pilot plant modelling studies.

It was decided to test the effect of the so-called "Gagnon-valve" on the automedium cyclone. The samples cut at 18.83 h and 18.87 h represent operation with the valve open and closed respectively. The differences on the overflow and underflow stream attributes due to valve closure is profound with the yield droping from 85% to 45%. It is understood

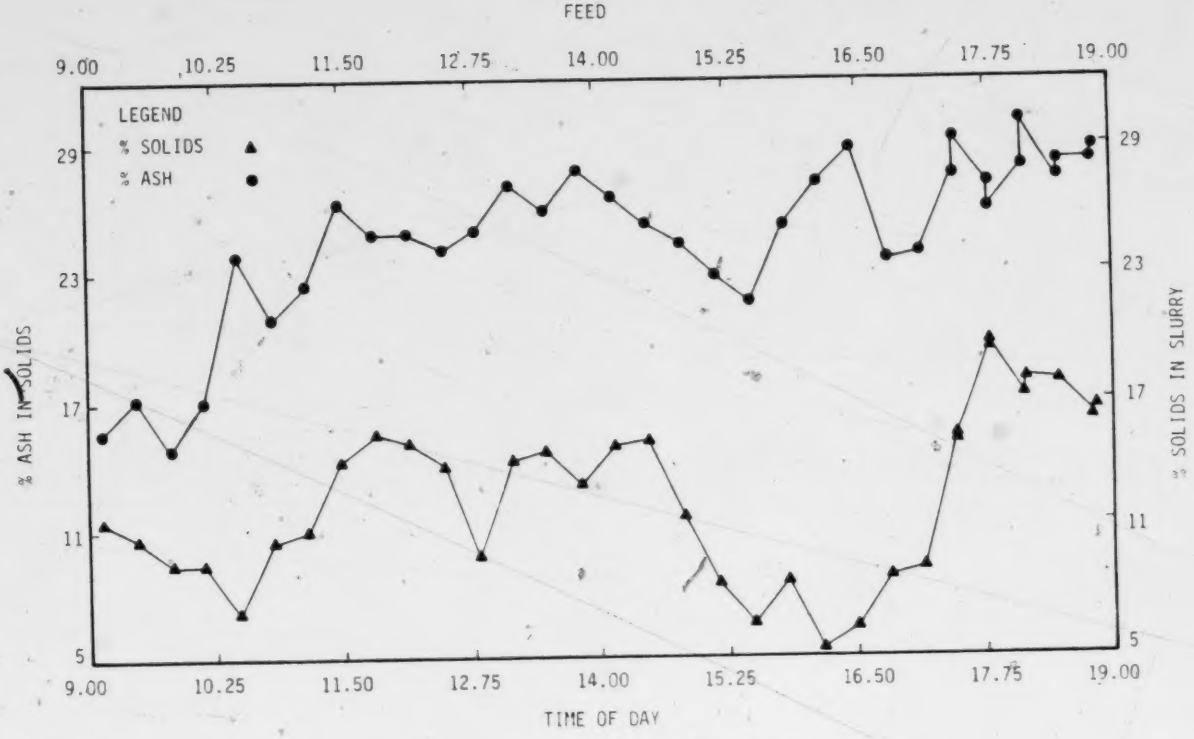


Figure 4.3 Change of Composition of Cyclone Feed During plant Tests

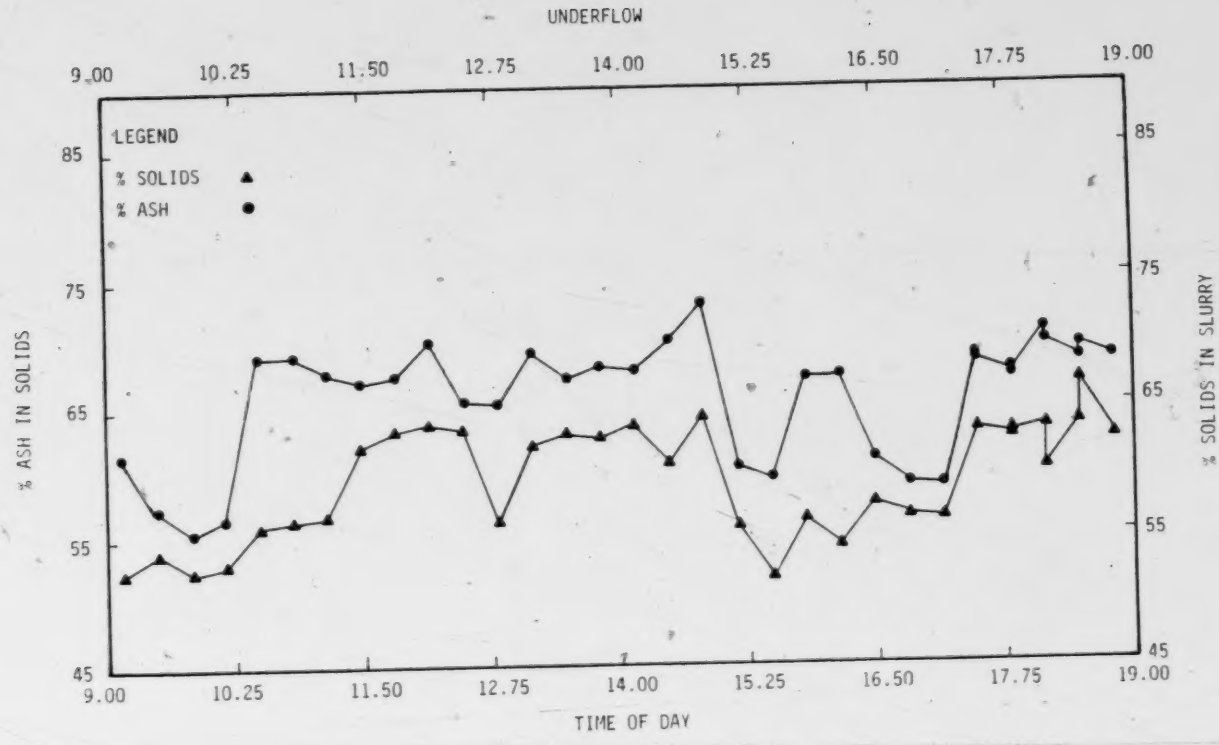


Figure 4.4 Change of Composition of Cyclone Underflow During plant Tests

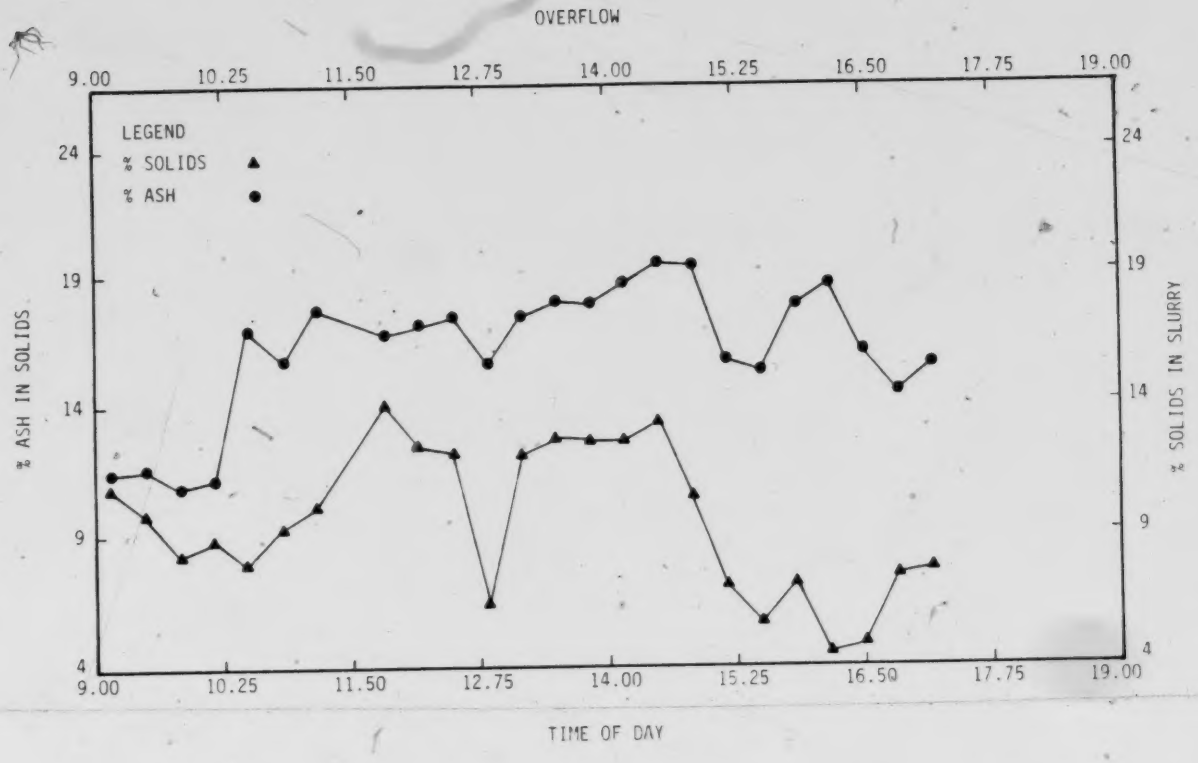


Figure 4.5 Change of Composition of Cyclone Overflow During plant Tests

from discussions with the process engineers that this device is used for process control to correct for high (valve is closed) or low (valve is opened) ash values in the Derrick screen oversize product.

The duplicate samples allowed the sampling error to be measured. The relative errors (Standard Deviation/Mean) were as follows:

| | Feed | Underflow |
|---|---|---|
| % Ash | 3.92 | 0.72 |
| % Solids | 1.53 | 2.57 |

A Monte Carlo technique to estimate the relative error of the calculated yields was carried out. The relative error of the overflow was not measured and was assumed to be identical to the feed. The results were as follows:

| Relative Error | %Solids | % Ash |
|---|---|---|
| Yield | 2.6% | 2.5% |

**4.5 Summary of Plant Tests**

The findings of the plant sampling campaign can be summarized as follows:

1. The results demonstrated that there are considerable variations in both % ash and % solids in the normal operation of an automedium cyclone circuit. These variations indicate that there is considerable potential for improved efficiency of operation from improved

control of the circuit.

2. The sampling method produced samples with a relative error less than 5 %. The relative error of the yield calculated from the measured data was 2.6 % (i.e. 2.2 yield percentage points). This demonstrates the difficulty of sampling streams with high pressure gradients.

3. It appears as if the use of the "Gagnon-valve" is an effective but very crude control device. The control problem would seem to be better answered via continuous process monitoring (e.g. on-stream ash monitor) and a more "flexible" final control element such as an adjustable vortex finder.

# 5. COAL TESTWORK: LABORATORY EXPERIMENTS

## 5.1 Test Procedure

The laboratory cyclone tests were done with the test-rig consisting of a 200 mm (8 in.) Visman-Tricone Automedium Cyclone, feed and recirculating pumps, a feed preparation tank and sampler. Details of the test-rig and the instrumentation were given in Chapter 3.

Prior to the silica testwork the basic performance of the test-rig was determined by water-only runs. Some background measurements like pressure-flow relations and flow splits were made as well as calibration of instruments and testing of the performance of the sampler and timer. The pressure-flow relations and variation o flow split with pressure for water are depicted in figures 6.1 and 6.2.

After completion of plant sampling tests as described in Chapter 4 and with the operating experience of the test-rig gained by the preliminary and silica tests an experimental procedure similar to silica testwork was adopted for coal. The procedure involved;

1. preparation of the desired slurry in the feed tank and conditioning for a certain period to insure complete mixing of solids and wetting of particles,
2. running the test-rig at the appropriate settings of the experimental variables with recirculated slurry untill steady-state conditions are reached,
3. simultaneous sampling of underflow and overflow with the

sliding sampler by which the total flow from both discharge points were collected for a certain time interval,

4. filtering and drying of the two products, after determining slurry weights, to obtain solid samples.

The procedure resulted in approximately 2-3 kg. of solid samples from the two discharge streams, that were analysed for size consist and density distribution.

Sampling of the feed stream for individual tests was found to be unnecessary since several tests conducted to compare the actual and the reconstituted feed compositions revealed close aggreements as shown in Figure 5.1. The samples thus obtained were split to approximately 250 g. These were subsequently wet-screened to obtain eight individual size fractions.

The density fractionation was done by float-sink analysis of the size fractions with heavy organic liquids. The standard procedure of succesive float-sink separation was found to be very time consuming. Since it was not necessary to obtain each density fraction separately for further analysis, a simpler approach of cumulative density distribution determination was adopted. This procedure involved splitting the sample into six portions by a rotary divider. The weight of the floats of the composite feed at each density was measured, and the distribution was calculated from the cumulative data.

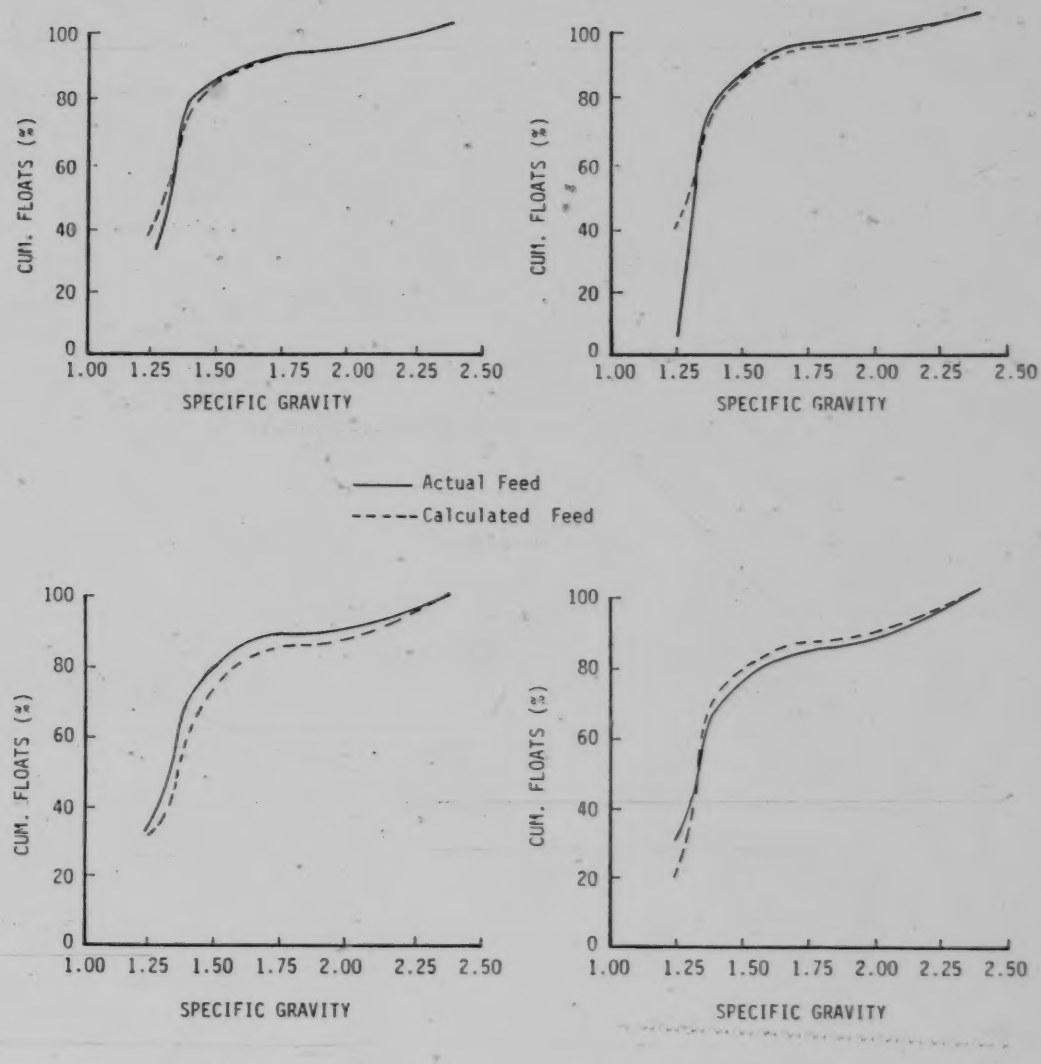


Figure 5.1 Comparison of Actual and Calculated Feed

A comparative testing of the two methods and the statistical analysis of the results showed that the errors involved were not higher than that was observed in parallel tests of the standard method. A comparison of density partition curves obtained by standard and cummulative method float-sink analysis is given in Figure 5.2.

The seven size fractions including the -200 mesh pan fraction, were analysed for density distribution at six densities ranging from 1.30 to 2.20 g/cc. The raw data on flow splits, discharge slurry densities, size and density distributions of both products were then processed by computer to calculate size partitions for individual fractions and for the composite feed.

**5.2 Experimental Design**

In the design of the laboratory experiments the following principal performance factors were considered;

1. Geometrical (design) Factors
   a. Cyclone inlet diameter
   b. Vortex finder diameter
   c. Apex Diameter
   d. Vortex finder Clearance
   e. Lower cone section options (S,L,M)
2. Operational Factors
   a. Flow rate
   b. Solids concentration
3. Feed Properties

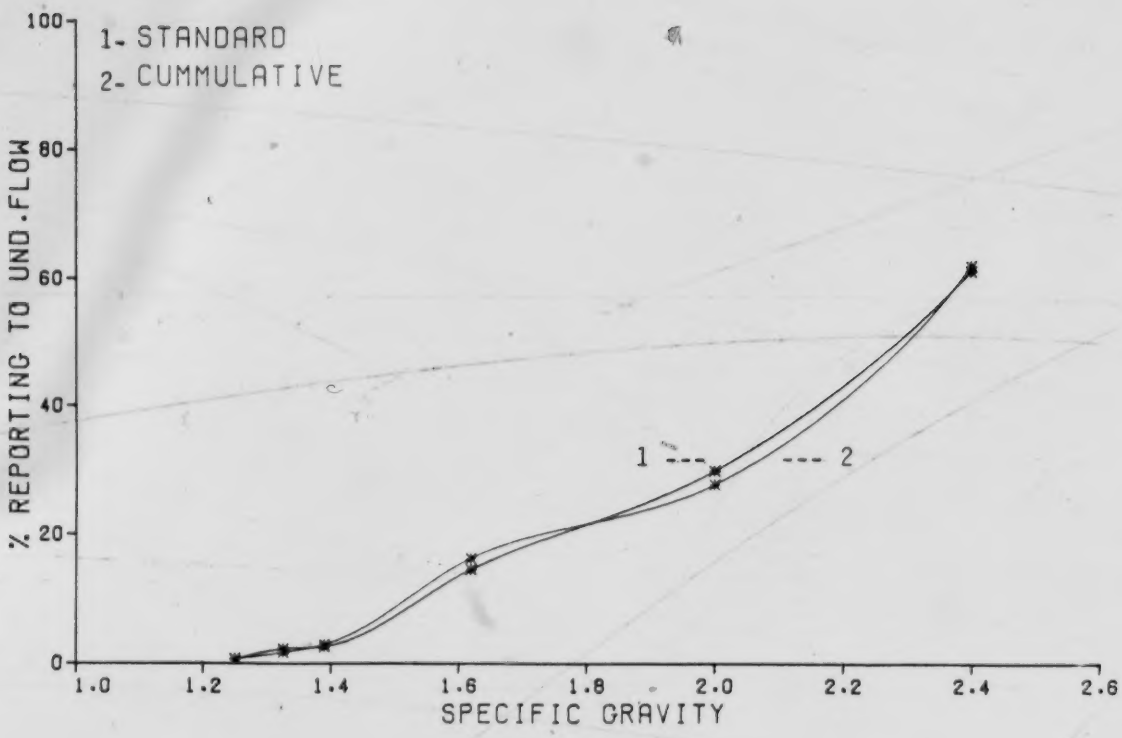


Figure 5.2 Comparison of the Results Obtained from Standard and Cummulative Float-sink Analysis

a. Size consist

b. Particle shape

c. Density distribution

The following were excluded from the study for the reasons given;

**Inlet diameter:** Was too difficult to modify for test purposes.

**Lower cone:** Weyher (33) feels that Visman (32) overstates the importance of this variable. Industrial operations favor the "L" type cone according to Bow (34).

**Size consist:** Too difficult to blend and maintain size attributes at predefined levels.

**Particle shape:** Impossible to adjust for practical purposes

**Density distribution:** As for size consist.

The main priority of this project was to increase the understanding of the behaviour of the AMC. This required a quantitative analysis of experimental data, within the framework of a proposed mathematical model. As a result of tremendous analytical overhead associated with each test the testwork planned was a compromise in achieving maximum definition in a reasonable time. To facilitate model construction, especially where non linear relationships were expected, it was desirable to run multilevel tests for each factor. However, this would reduce the number of factors

which could be studied. Since there was little quantitative knowledge of AMC operation, information on a maximum number of factors was desired. As a result of the considerations above and the evaluations of available operational data the following factors and operating levels were determined.

| FACTOR | LEVELS | COMMENTS |
|---|---|---|
| Vortex finder | 101.5 - 71.9 mm. | $[D_1^2/D_2^2=2]$ |
| Vortex Finder Clearance | 34 - 71.8 - 110 mm. | The range and median were selected after studying the operating cyclones and the design values for fixed-vortex-finder equipment. |
| Apex Diameter | 51-35 mm. | Weyher(33) observes that the flow ratio is not so strongly dependent upon orifice ratio, particularly for large values. Therefore the apex diameter was chosen as the experimental factor rather than the more common orifice ratio. |

| | | |
|---|---|---|
| % Solids | 9% - 14% | Typical of Fording's normal operating range and in line with Visman's(32) suggestions on the percent solids range. |
| Flowrate | 380 - 530 liters/min | Weyher(33) observes that pressure is important only in so far as it reflects flowrate. |

The experimental design matrix is given in Appendix 5.1. Using orthogonal design four factors were studied at two levels and one factor was varied at three levels, resulting in total of 48 tests.

## 5.3 Results of Testwork

The experimental work within the context of the test matrix described above generated considerable data on the performance of the AMC. Although certain variables like cone size and feed inlet orifice were fixed, effects of most important operating variables were studied in two or three levels. Raw data that resulted from each test comprised of;

1) water and mass splits,
2) pressure drop,
3) solids content in overflow and underflow,
4) size partition data for individual densities and for the composite feed.

Data of items 1, 2 and 3 above were used in macro-variable

modelling details of which are described in Chapter 6.

The size and density distribution data for the two cyclone products were analysed and partitions of individual fractions were calculated. A complete set of partition data is given in Appendix 5.2, with test numbers refering to the tests for which the conditions are given in Appendix 5.1.

The coal testwork results were analysed for micro-variable modelling of the hydrocyclone and the results of this work are presented in Chapter-7.

**5.4 Bed Capture Tests with Coal**

The experimental procedure for capturing the "bed" in the AMC is described in Section 3.4 for constant density material. In silica tests the bed was found to be similar to the underflow. The bed formed with coal feed consisted of *coarser* and *lighter* material than the underflow.

The thickness of the bed calculated from the captured material was approximately 17.5 mm, assuming 70% porosity. This compares favorably with the 12.1 mm bed thickness for silica which was finer in size. Assuming the flowrate through the apex to be equal to the downward flow of solids along the side walls of the cyclone, the thickness of solid bed on cylindirical section was calculated to be very small i.e. 0.6 mm.

A comparison of size distributions of the bed and the underflow for coal is given in Fig.5.3.

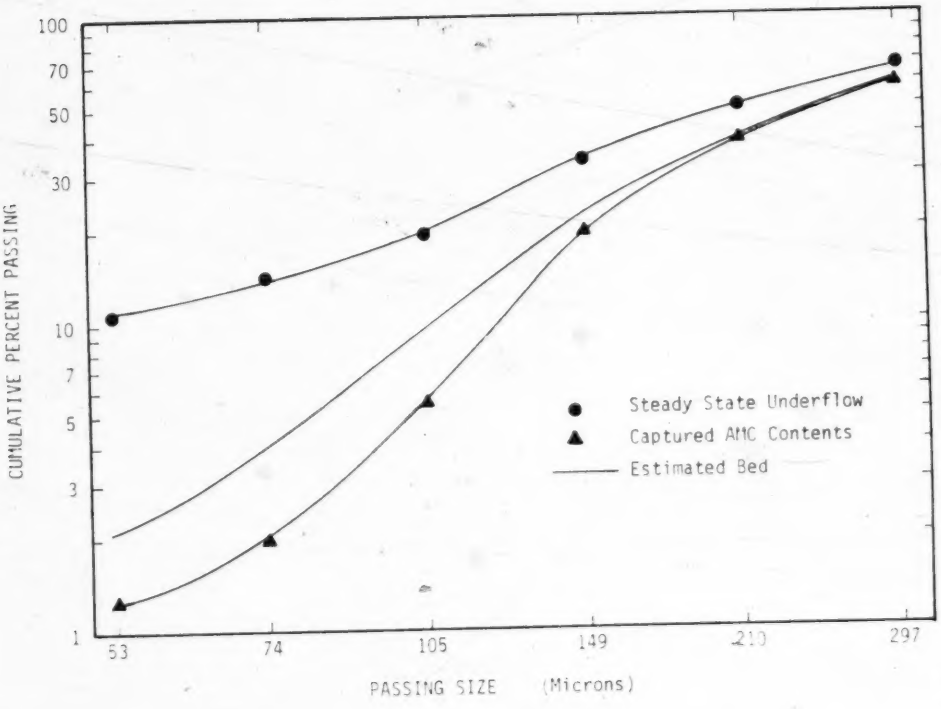


Figure 5.3 The Size Distribution of Captured Bed and the Steady-State Stream

**5.5 Bed-Simulation Tests**

The separation in the AMC was shown to be affected by the presence of a stable bed rotating at the conical section of the cyclone. This effect, although known, was not studied or described by investigators. The conceptual model presented in Section 2.12, includes partitioning resulting from a *slicing* of this bed, as one of the three separation stages. The approach to modelling this stage of separation, however, was not obvious, since the mechanism of separation was unknown.

The author postulated a *percolation* mechanism for stratification of the particles in this bed. *Erosion* of this bed by the upward flow at the air core interface results in partitioning of the species in the bed.

To study this effect, a series of simple tests were performed to simulate the rotating bed and the particle stratification in this bed was examined. The unit assembled for these tests consisted of a cylindrical vessel placed on a laboratory sieving device (RoTap ) with circular movement and tapping action. The thoroughly mixed solids containing particles of coarse coal and silica were placed in the vessel which was then filled with water to provide a slurry with 40 % solids by weight.

After rotating the bed by the circular motion of the apparatus for 15 minutes, the solids were sliced and separated at 25 mm (1 in) intervals from the top. Each section was screened to determine the size distribution, and

each size fraction was analyzed for ash content. From the feed ash and the ash content of each size fraction, the relative amounts of heavy and light (coal) fraction were determined.

By simulated bed-slicing calculations at various depths, partitioning of the light and heavy fractions are calculated. The results of bed simulation studies are given in Table 5.1 . The simulated slicing of bed was done at 12 %, 50 %, and 87.5 % of bed depth from top. The calculated partitioning of particles are given in Fig. 5.4.

As was expected, the particles were stratified in the bed with the coarsest at the top, and the size decreased with depth. The heavier fraction was stratified at a lower level with the same trend in size. The results showed that the mechanism of stratification in non-stationary beds through which there is no net upward flow is **percolation** i.e. fine particles passing through intersities of the coarser ones. The erosion of such a bed from the top in a hydrocyclone results in partitioning which is *reversed* from normal operation i.e. upward flow picks up the coarser particles, and fines *blanketted* by the coarse from this erosion effect report to the underflow. The net result of this reverse size partitioning is the inclusion of entrainment of fines in the underflow. This mechanism can be used to explain the *fish-hook* sometimes observed in partitioning data.

Table 5.1 Stratification of Particles in Simulated Bed

LIGHT FRACTION SIZE DISTRUBUTION (Mesh)

| DEPTH (IN) | +10 | -10/+20 | -20/+40 | -40 |
|---|---|---|---|---|
| 0.25 | 0.238 | 0.276 | 0.261 | 0.233 |
| 0.75 | 0.202 | 0.136 | 0.148 | 0.108 |
| 1.25 | 0.138 | 0.100 | 0.050 | 0.048 |
| 1.75 | 0.166 | 0.100 | 0.078 | 0.062 |
| 2.25 | 0.159 | 0.142 | 0.098 | 0.074 |
| 2.75 | 0.052 | 0.115 | 0.123 | 0.111 |
| 3.25 | 0.023 | 0.079 | 0.161 | 0.186 |
| 3.75 | 0.021 | 0.052 | 0.082 | 0.177 |

LIGHT FRACTION STRATIFICATION

| DEPTH (IN) | +10 | -10/+20 | -20/+40 | -40 |
|---|---|---|---|---|
| 0.25 | 0.238 | 0.276 | 0.261 | 0.233 |
| 0.75 | 0.440 | 0.412 | 0.409 | 0.342 |
| 1.25 | 0.578 | 0.512 | 0.459 | 0.390 |
| 1.75 | 0.744 | 0.612 | 0.537 | 0.452 |
| 2.25 | 0.904 | 0.754 | 0.634 | 0.526 |
| 2.75 | 0.956 | 0.869 | 0.757 | 0.637 |
| 3.25 | 0.979 | 0.948 | 0.918 | 0.823 |
| 3.75 | 1.000 | 1.000 | 1.000 | 1.000 |

HEAVY FRACTION SIZE DISTRIBUTION (Mesh)

| DEPTH (IN) | +10 | -10/+20 | -20/+40 | -40 |
|---|---|---|---|---|
| 0.25 | 0.112 | 0.131 | 0.110 | 0.086 |
| 0.75 | 0.188 | 0.134 | 0.088 | 0.067 |
| 1.25 | 0.171 | 0.120 | 0.066 | 0.045 |
| 1.75 | 0.224 | 0.146 | 0.080 | 0.051 |
| 2.25 | 0.217 | 0.196 | 0.120 | 0.074 |
| 2.75 | 0.067 | 0.160 | 0.191 | 0.143 |
| 3.25 | 0.013 | 0.075 | 0.249 | 0.239 |
| 3.75 | 0.009 | 0.009 | 0.096 | 0.295 |

HEAVY FRACTION STRATIFICATION

| DEPTH (IN) | +10 | -10/+20 | -20/+40 | -40 |
|---|---|---|---|---|
| 0.25 | 0.112 | 0.131 | 0.110 | 0.086 |
| 0.75 | 0.300 | 0.266 | 0.198 | 0.153 |
| 1.25 | 0.471 | 0.386 | 0.264 | 0.198 |
| 1.75 | 0.694 | 0.532 | 0.344 | 0.249 |
| 2.25 | 0.911 | 0.728 | 0.464 | 0.323 |
| 2.75 | 0.978 | 0.883 | 0.655 | 0.466 |
| 3.25 | 0.991 | 0.963 | 0.904 | 0.705 |
| 3.75 | 1.000 | 1.000 | 1.000 | 1.000 |

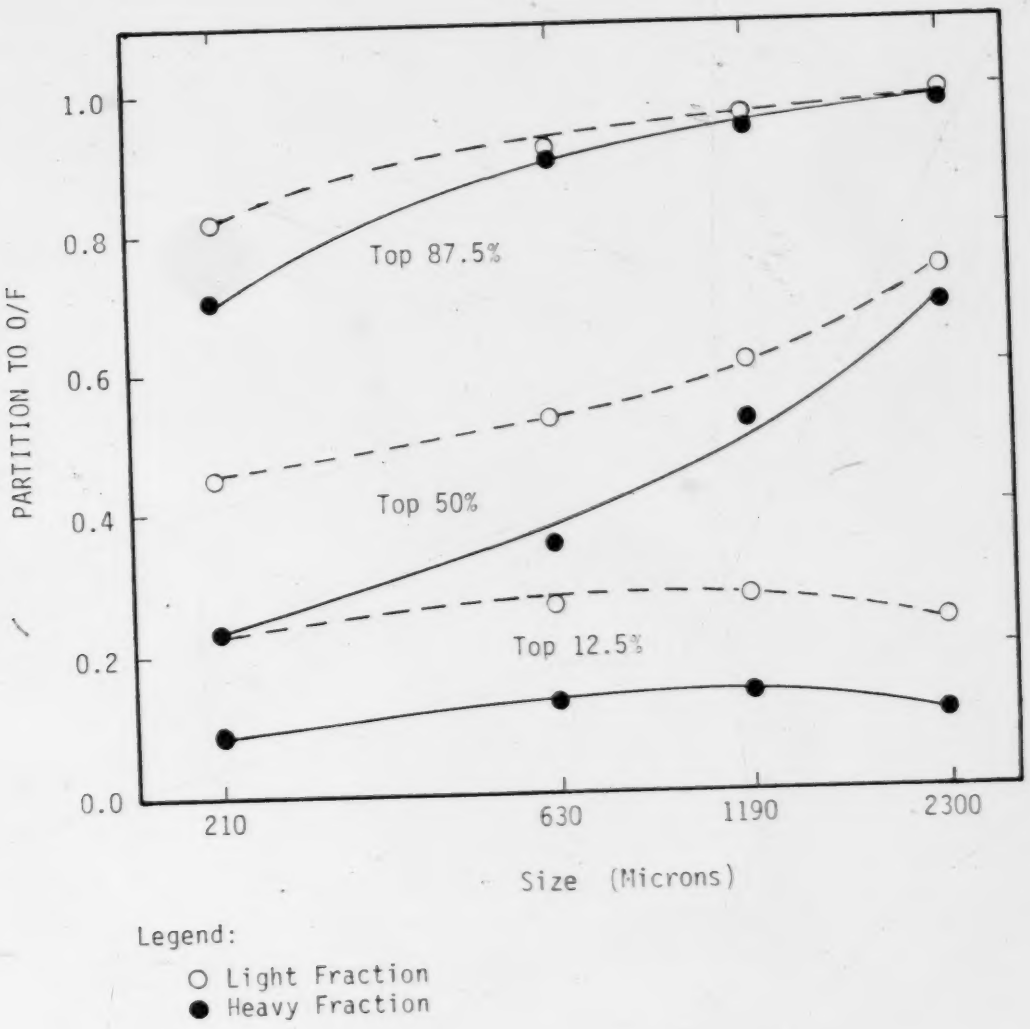


**Figure 5.4 Cummulative Partition of Simulated Bed by Slicing at Various Depths**

## 6. MACRO VARIABLE MODELLING STUDIES

In order to completely descibe the operation of the automedium cyclone one must have mathematical relationships of the macro-variables: pressure-flowrate and the flow or water split ratio*. The pressure-flowrate relationship is required to determine the processing capacity,to design the associated cyclone feed pumping system and in dynamic simulation. The split ratio is required to carry out a water balance and to establish the underflow capacity constraints.

### 6.1 Pressure - Flow Rate Modelling

There are numerous pressure drop equations for cyclones in the literature. Most of these equations express pressure drop in terms of flowrate and the inlet and overflow diameters of the cyclone. A recent pressure drop correlation based upon 300 tests including large industrial classifying cyclones was formulated (5) and is shown in equation (6.1).

$$P = \frac{4.7\, Q^{1.78}\, e^{(0.0055\phi)}}{D_c^{0.37}\, D_i^{0.94}\, h^{0.28}\, (D_u^2 + D_o^2)^{0.87}} \qquad (6.1)$$

Equation (6.1) is a more versatile equation than the others in the literature since it includes all of the variables which affect pressure drop. Variables such as underflow diameter and % solids are usually omitted from most pressure drop equations.

---

*Split ratio in cyclone terminology is defined as the ratio of volumetric underflow rate to the volumetric overflow rate i.e. S = Qu/Qo.

The literature is nearly devoid of any pressure drop correlations specifically for the wide angle cyclones (automedium). It was therefore necessary to attempt to derive a pressure drop correlation as part of this project.

The test work consisted of water only and coal slurry tests. The results of the water-only tests in the 8-inch AMC at varying vortex finder clearances are shown in Figure 6.1. Figure 6.1 reveals that the vortex finder clearance does not have a significant effect upon flowrate.

In the 48 tests using coal slurries the flowrate was varied from 125 to 155 USGPM (see Appendix 5.1). These results again confirm that the vortex finder clearance has no noticeable effect upon pressure drop. Thus this term (h) was not included in the equation. Although cyclone diameter and inlet diameter were not varied during the tests, these variables were nevertheless included in the equation on the basis of classifying cyclone modelling studies. Using stepwise linear regression of the data the following equation was formulated:

$$P = \frac{2.57\ 10^{-3}\ Q^{1.87}\ e^{(0.0089\phi)}}{D_c^{0.37}\ D_i^{0.94}\ \left(D_u^2 + D_o^2\right)^{0.804}} \qquad (6.2)$$

The coefficients determined in equation (6.2) are remarkably similar to those derived for classifying cyclones i.e. equation (6.1). A comparison of the predicted vs observed values of pressure drop for the data set is shown in Figure 6.2.

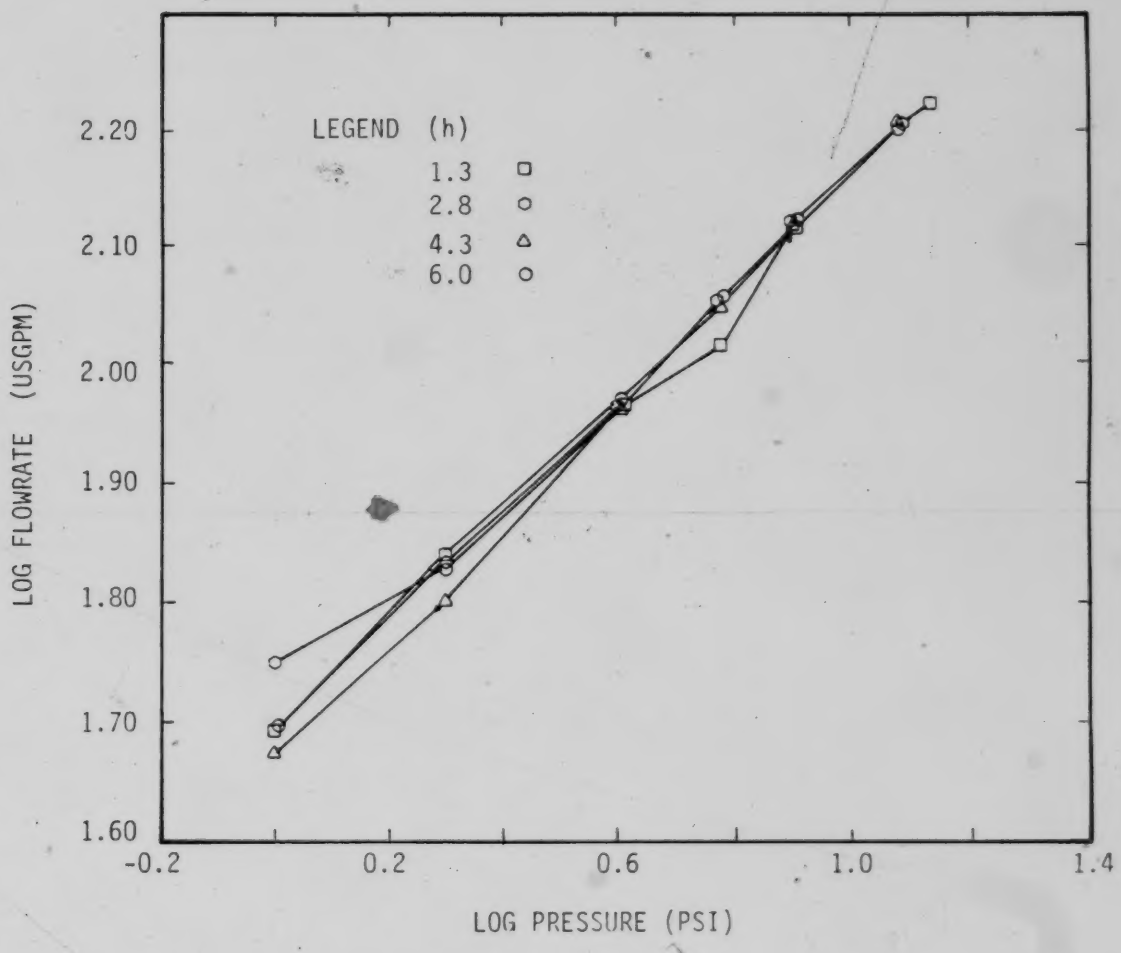


Figure 6.1 Variation of Flowrate of Water with Pressure

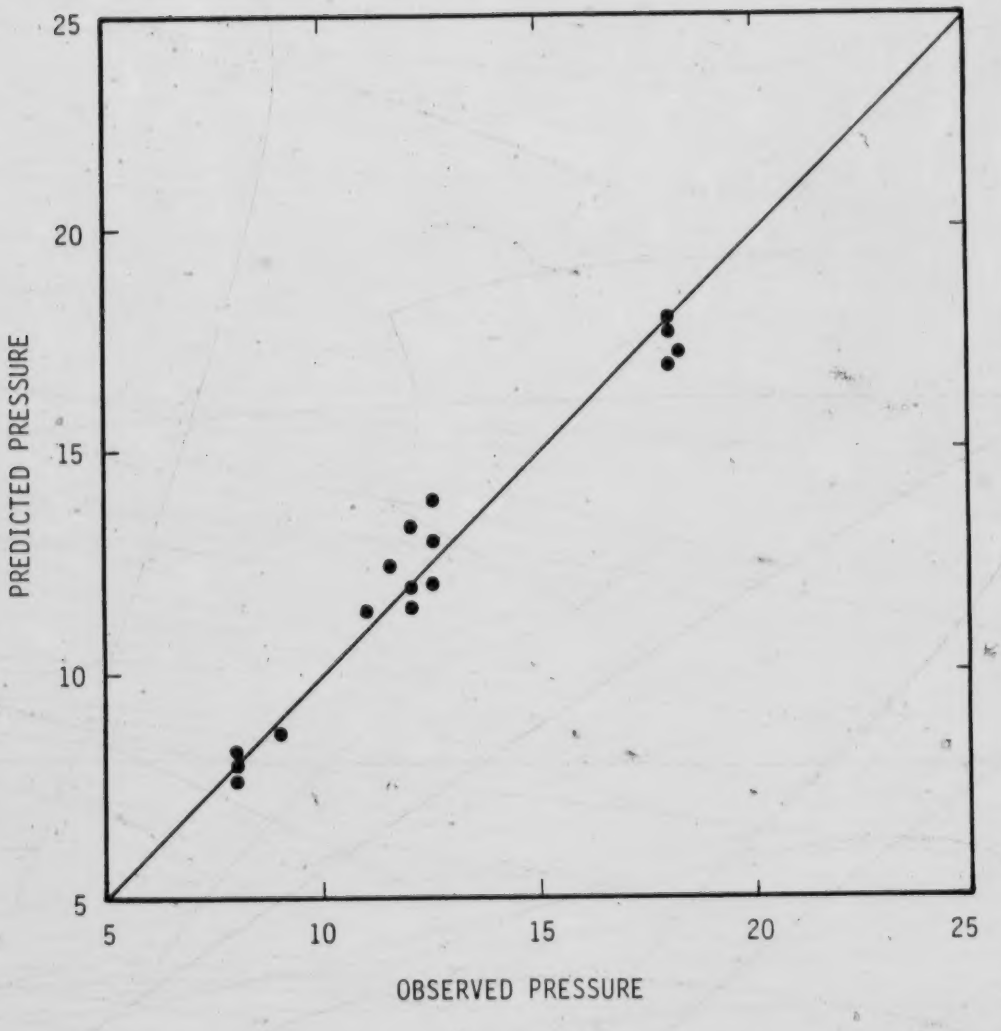


Figure 6.2 Predicted vs. Observed Pressure Drop

## 6.2 Underflow-Overflow Split

The flow split in the AMC was also studied using both water as well as the coal slurries. In the water studies the effect of feed pressure and vortex finder clearance was explored and the results are shown in Figure 6.3. It can be noted that the vortex finder clearance has very little influence on flow split. It is also noteworthy that above some minimum pressure i.e. 8 psi, there is virtually no water exiting the cyclone via the underflow. This phenomenon is generally believed to be due to the fact that the air core occupies the entire underflow orifice thereby not allowing any water to escape. This feature is much more pronounced in the wide angle cyclones than in the classifying cyclones. However, once solids are introduced to the AMC the flow appears in the underflow thus altering the flow split.

The flow split equation developed from classifying cyclone studies is:

$$S = \frac{2.9 \left(\frac{D_u}{D_o}\right)^{3.31} h^{0.54} \left(D_u^2 + D_o^2\right)^{0.36} e^{(0.0054\phi)}}{H^{0.24} D_c^{1.11}} \qquad (6.3)$$

Using stepwise linear regression on the 48-test data set new parameters were determined for the flow split expression. These are shown in equation (6.4) below:

$$S = \frac{5.22 \left(\frac{D_u}{D_o}\right)^{1.38} h^{0.25} e^{(0.005\phi)}}{\left(D_u^2 + D_o^2\right)^{1.76}} \qquad (6.4)$$

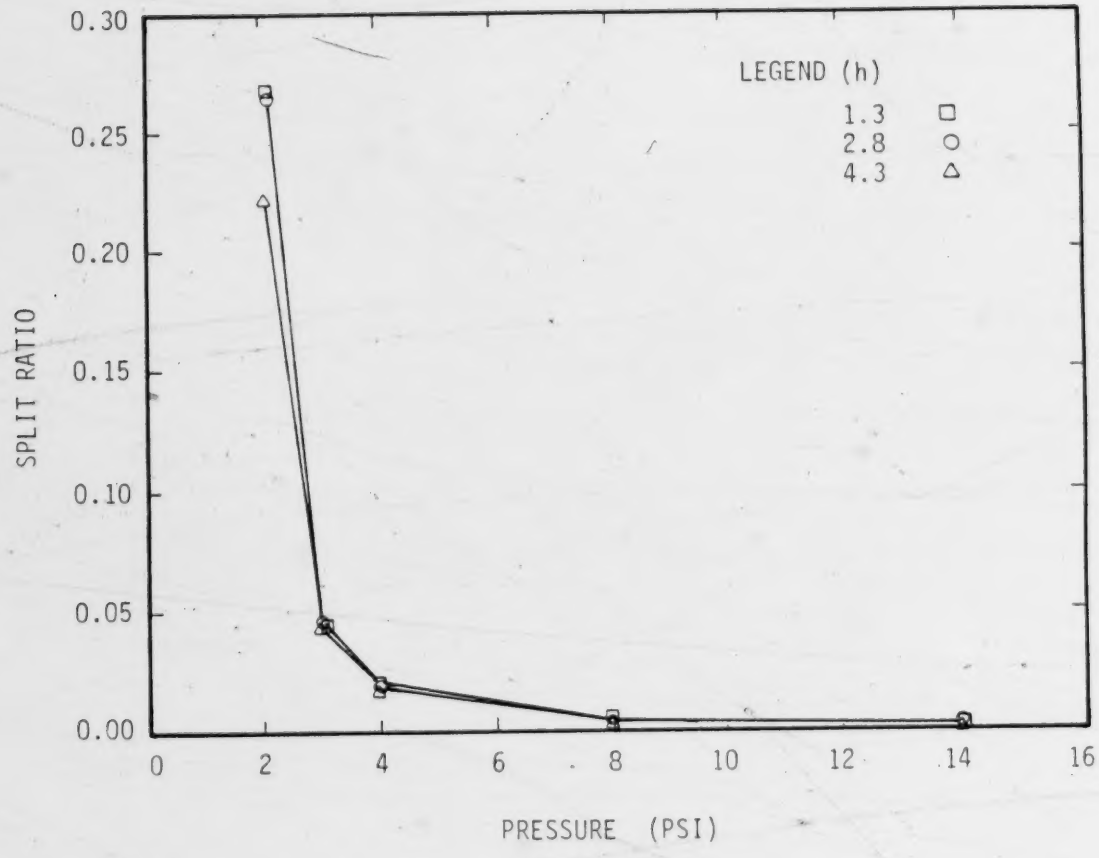


Figure 6.3 Variation of Split Ratio of Water with Pressure

In comparing equations (6.3) and (6.4) two important differnces are noted:

(i)Split is inversly proportional to the outlet area (sum of squares of the orifice diameters) for the AMC in contrast to a direct relation in classifying cyclones.

(ii) The orifice ratio (Du/Do) is less significant in controlling flow split in the AMC.

As the flow splits have relatively low values compared to classifying cyclones it is not certain whether or not these effects are really very meaningful. Therefore an alternative method of modelling the split by correlating the water split with the solids split and the orifice diameters was attempted. The resulting correlation is as follows;

$$R_f = \frac{5.08\ R_s^{1.1}}{D_o^{1.63}\left(\frac{D_o}{D_u}\right)^{0.74}} \qquad (6.5)$$

Equation (6.5) is the equation which is recommeded to predict the water split in automedium cyclones. Figure 6.4 shows the predicted vs observed splits using this equation. A bias for lower predictions at high splits is obvious but the discrepencies are very small in absolute terms. The results of stepwise linear regression analyses that resulted in formulation of the pressure-flow relation and water splits and the related statistics are presented in Appendix 6.

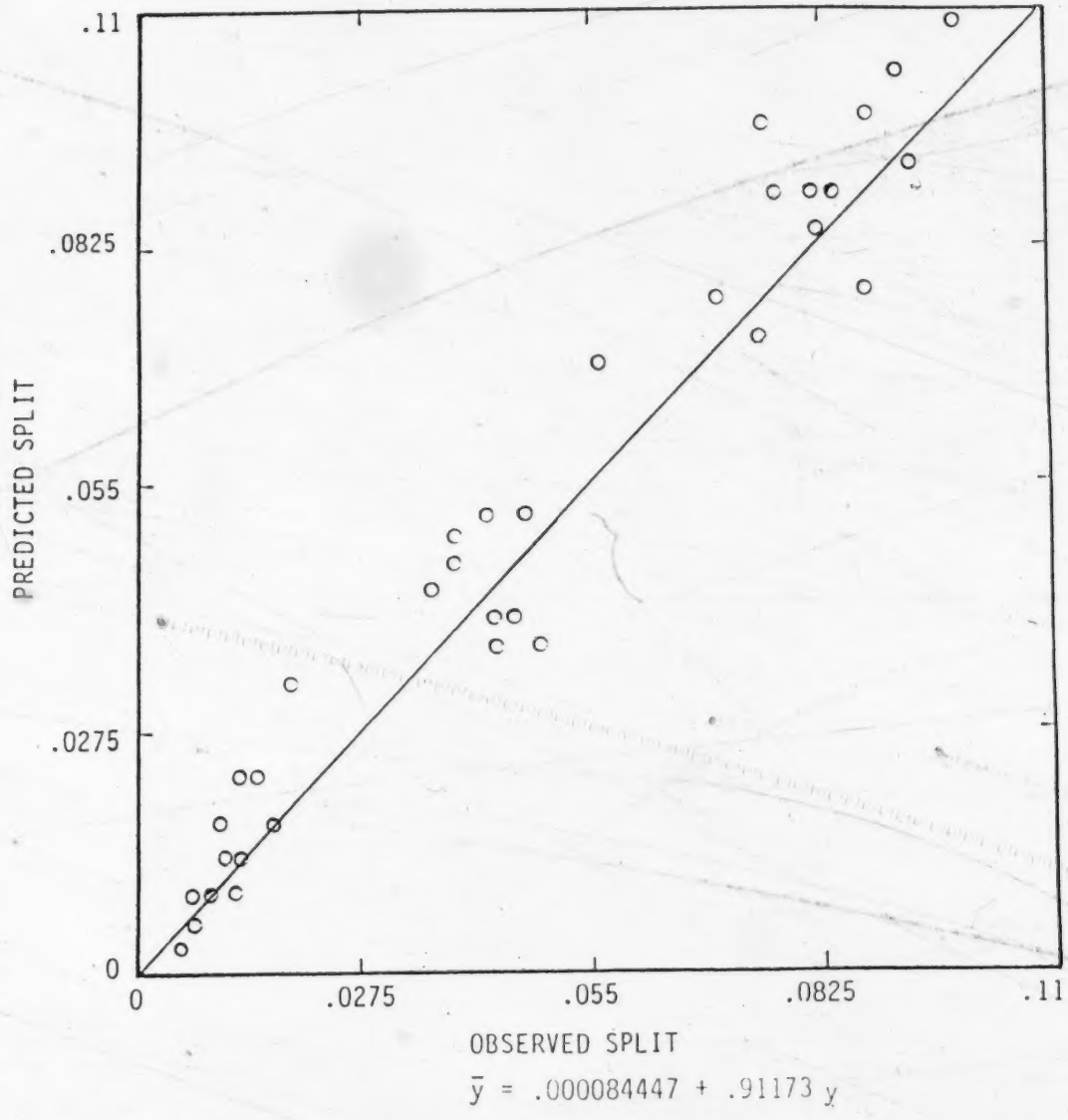


Figure 6.4 Predicted vs. Observed Water Splits in the AMC

# 7. MICRO-VARIABLE MODELLING

## 7.1 General Model Form

### 7.1.1 The Classification Behavior of the Automedium Cyclone

The classifying behavior of the AMC on a homogeneous feed was explained in Chapter 3. Partition of a composite feed in AMC can be considered to be the net result of combined size partitioning of individual density fractions. This classification, when assumed to occur as conventionally defined in classification of homogeneous ores, would result in monotonic-increasing partition curves,as described in Chapter 2, which upon combining should be *flattened* but still would be a monotonic function of particle size.

Results of test work on coal as described in Chapter 5, as well as various experimental and plant data [App. 5 and Fig. 2.7, 3.3, 3.4], revealed that partition of composite feed, both in automedium and classifying cyclones, show peculiarities that were frequently attributed to experimental error in the past. The same peculiarities are seen in the behavior of cyclones treating constant density material under certain operating conditions noted earlier.

Analysis of partition data obtained for coal in the AMC clearly indicated that the feed is classified according to size, although with varying efficiency for different density material, at all operating conditions tested. Moreover, this is consistent with the authors conceptual understanding of

the operation of this unit.

Table in Appendix-7 sumerizes the results of the parameter estimation for Plitt's classification model, given by equation (7.1) (given as eqn.(2.9) previously) for the two dense fractions of the feed.

$$P = R_f + (1 - R_f)\left[1 - e^{\left(-0.693\left[\frac{d}{d_{50}}\right]^m\right)}\right] \qquad (7.1)$$

Although the simple classification model could not define the separation in AMC satisfactorily, indications of classification behavior were obvious from the partition data obtained. The deviation from simple classification could be attributed to certain conditions in the cyclone, especially near the apex, created either by the geometry, i.e. in the AMC, or by operating conditions as in *roping* discharge from classifying cyclones.

### 7.1.2 Density Separation in the Automedium Cyclone

The goemetry and operation of the AMC, as described in Chapter 2, facilitates density partitioning of the composite feed through the rotating bed formed near the apex. The presence of this bed is responsible for partitioning of the coarse but lighter material to the overflow.

The particles that do not report to the overflow and find their way down to form a rotating bed at the bottom of the cyclone are stratified with respect to size and density and the upper layers of the bed are eroded by the rotating

fluid of the vortex.

The stratification in the bed and the extent of penetration of the erosion effect determine the amount and characteristics of the material separated from the stream that is gradually working its way to the apex.

A percolation-trickling mechanism is postulated to be responsible for the stratification. It is assumed that the smaller particles penetrate through the bed of coarser particles and are transported to the bottom. *Blanketing* of fine particles by the coarser ones hinder their elutriation by the rotating fluid.

The mechanism of stratification in the bed was not obvious, and as described in sections 5.4 and 5.5 experimental evidence was required to support the theory postulated by the author.

The partitioning, as was shown by bed simulation studies described in section 5.5, is primarily a size separation, where coarser particles are sent to the upward flow. This reverse separation is accompanied by the reversed density effects where lighter particles are positioned in the upper layers. The net result of this stratification is partitioning according to density and size. The material that is eroded from this bed is further classified in the rotating fluid before being sent up to the vortex finder or returned to the bed.

### 7.1.3 Formulation of a Comprehensive Model

The general form of the model, that is derived from the above concepts, contains terms that account for each of the three classification "zones", namely primary classification, automedium partitioning, and secondary classification. A conceptual model is presented in Figure 2.14 and in Figure 1 of Appendix 7.2.

The feed entering the cyclone is classified by the primary separator where the fine material is sent to the overflow. The coarse material and the material carried by the by-pass flow are transported downward along the cyclone wall and enter the bed. A reverse size separation, as described above, results in partitioning of the material before being discharged through the apex. The material lifted from the bed is further classified in a secondary separator, and coarse and the heavy particles are returned to the bed before this stream is discharged by the overflow.

Let A,B and C represent size partitioning in the automedium, secondary and primary separators respectively, than the overall partitioning "P" is defined by equation 7.2 (given as eqn.(2.36)). A derivation of equation 7.2 is given in Appendix 7.2.

$$P = \left(R_f + (1 - R_f)C\right) \frac{1 - A}{1 - AB} \qquad (7.2)$$

It is noteworthy to mention that under the limiting

condition :

A=0 (when bed formation is not observed) equation 7.2 is reduced to;

$$P = R_f + (1 - R_f)C \tag{7.3}$$

which characterizes size partitioning in a classifying cyclone operating at normal conditions with constant density feed material.

## 7.2 Modelling the Separation in the Three Zones of AMC

The corrected size classification in hydrocyclones was modelled successfully by Plitt's equation given as;

$$Y = 1 - e^{\left(-0.693\left[\frac{d}{d_{50}}\right]^m\right)} \tag{7.4}$$

where Y is the general partition function.

This relational form was used in the model to define partitioning in all three zones in the "AMC", with different cut sizes and sharpness of separation assigned to each relation. It was logical to adopt Plitt's relation to define separation in the primary and secondary classification zones.

A simple model form was not available for the autogeneous separation zone. A literature search on particle

stratification in non-stationary beds revealed certain modelling approaches(33,34,35) that were useful in understanding the mechanism but did not provide a simple model form that could be incorporated in the general model. It was apparent that the size of particle was the most important factor and density and geometry played some less important role in determining the stratification(34,35). It was also apparent that the segregation mechanism was *percolation* of smaller particles through the openings of the larger ones as in *sieving* and the larger particles were displaced towards the upper layers while the fines formed a closely packed bed at the bottom. The apparent packed density (or bulk density) of this bed was responsible for *floating* the larger but loosely packed particles.

Therefore, Plitt's relation for size separation was used for the autogeneous partitioning for simplicity, since, this separation was shown to be a reversed size classification.

Thus the model equations defining the partitioning in the individual zones, namely A, B and C in equation 7.2 were developed as follows;

$$A = 1 - e^{\left(-0.693\left[\frac{d}{d_{50A}}\right]^{m_A}\right)} \qquad (7.5)$$

$$B = 1 - e^{\left(-0.693\left[\frac{d}{d_{50B}}\right]^{m_B}\right)} \qquad (7.6)$$

$$C = 1 - e^{\left(-0.693\left[\frac{d}{d_{50C}}\right]^{m_C}\right)} \qquad (7.7)$$

Equations 7.2, 7.5, 7.6 and 7.7 constitute the micro-variable model for hydrocyclones in general. Classifying cyclones could be treated as a special case, and as was shown by equation 7.3 the model can be reduced to Plitt's equation describing partitioning in classifying cyclones.

The model equations contain seven parameters that should be determined by experimental or operational data; Rf, the by-pass flow, three parameters for size of separation and three parameters for sharpness of separation for the three zones in the AMC.

**7.3 Parameter Estimation for the Cyclone Model**

As described in Chapter 5, the coal test work resulted in the generation of a vast amount of partition data for individual density fractions of a composite feed at various operating conditions of the AMC. This data was used in the

parameter estimation for the model and in determining the dependence of these parameters on the operating variables.

Determination of the parameters, and fitting the model to the data was attempted using several numerical methods. A derivative free non linear regression analysis available in the statistical package BMDP[9] , and a SIMPLEX search method(18) for minimization of the objective function for a least-squares fit was found to be inadequate for regression to fit the model to the data. A derivative-free nonlinear regression method called multivariate secant that is available in the statistics package SAS[10] was also only succesful in converging only on a small fraction of the data sets.

An interactive graphics program CPLOT, developed by the author for semi-visual curve fitting[11] was used for this purpose. The method involved parameter initiation and manupulation of all seven parameters for the best visual fit, determined by minimizing the least-square fit equation by the aid of displayed values of residuals and increments. A detailed explanation of the method and the program is given in Appendix 7.3.

The parameters for the model for individual density fractions for all tests are given in Appendix 7.4. The values are for the best-fitting curve as determined

---

[9] BMDP Statistical Software, Inc.
P.O. Box 24A26, LosAngeles, California 90024

[10] SAS Institude Inc., Box 8000, Cary, North Carolina, 27511

[11] The computer program CPLOT, as given in Appendix 7.3, was developed by the author and Mr. D. Margel of Alberta Research Council, 1984.

semi-visually by the program mentioned above.

The correlations of the seven parameters with the operating variables and the cyclone geometry were analized by stepwise linear regression available in the BMDP package. The overflow and underflow orifice ratio and the sum-of-squares of orifices were also included in the analyses.

The resultant prediction equations for the seven parameters are given below:

$$d_{50A} = 1255.6 \left(\frac{D_u}{D_o}\right)^{2.36} h^{0.66} (\rho_s - \rho)^{1.14} \qquad (7.8)$$

$$d_{50B} = \frac{54.97\ {D_o}^{0.72}}{(\rho_s - \rho)^{0.24}} \qquad (7.9)$$

$$d_{50C} = \frac{7.86\ {D_o}^{2.38}}{h^{0.23} (\rho_s - \rho)^{0.945}} \qquad (7.10)$$

$$m_A = 1.032 \left(\frac{D_u}{D_o}\right)^{0.41} h^{0.945} \qquad (7.11)$$

$$m_B = \frac{0.059\, h^{0.24}\, Q^{0.52}}{D_o\, D_u{}^{0.31}} \; \frac{\rho_s^{2.54}}{(\rho_s - \rho)^{0.76}} \qquad (7.12)$$

$$m_C = \frac{0.54\, h^{0.15}}{D_o{}^{0.39}\, D_u{}^{0.34}} \; \frac{\rho_s^{3.20}}{(\rho_s - \rho)^{1.24}} \qquad (7.13)$$

$$R_f = \frac{0.0114}{D_o{}^{3.71}} \; \frac{\rho_s^{7.69}}{(\rho_s - \rho)^{3.14}} \qquad (7.14)$$

The comparison of partitioning data obtained from coal testwork and the separation predicted by the model revealed that for the cyclone operation range given in Appendix 5.1, the model can predict the peculiarities in the partitioning curve reasonably well.

Figures 7.1, 7.2 and 7.3 depict examples of model fit and predicted partitioning in the AMC. The developed model can be used in the design of automedium cyclones and in the optimization and control of fine coal cleaning circuits using such units.

| CURVE | MEAN SPECIFIC GRAVITY OF SOLIDS |
|---|---|
| 1 | 1.56 |
| 2 | 1.375 |
| 3 | 1.315 |
| 4 | 1.28 |

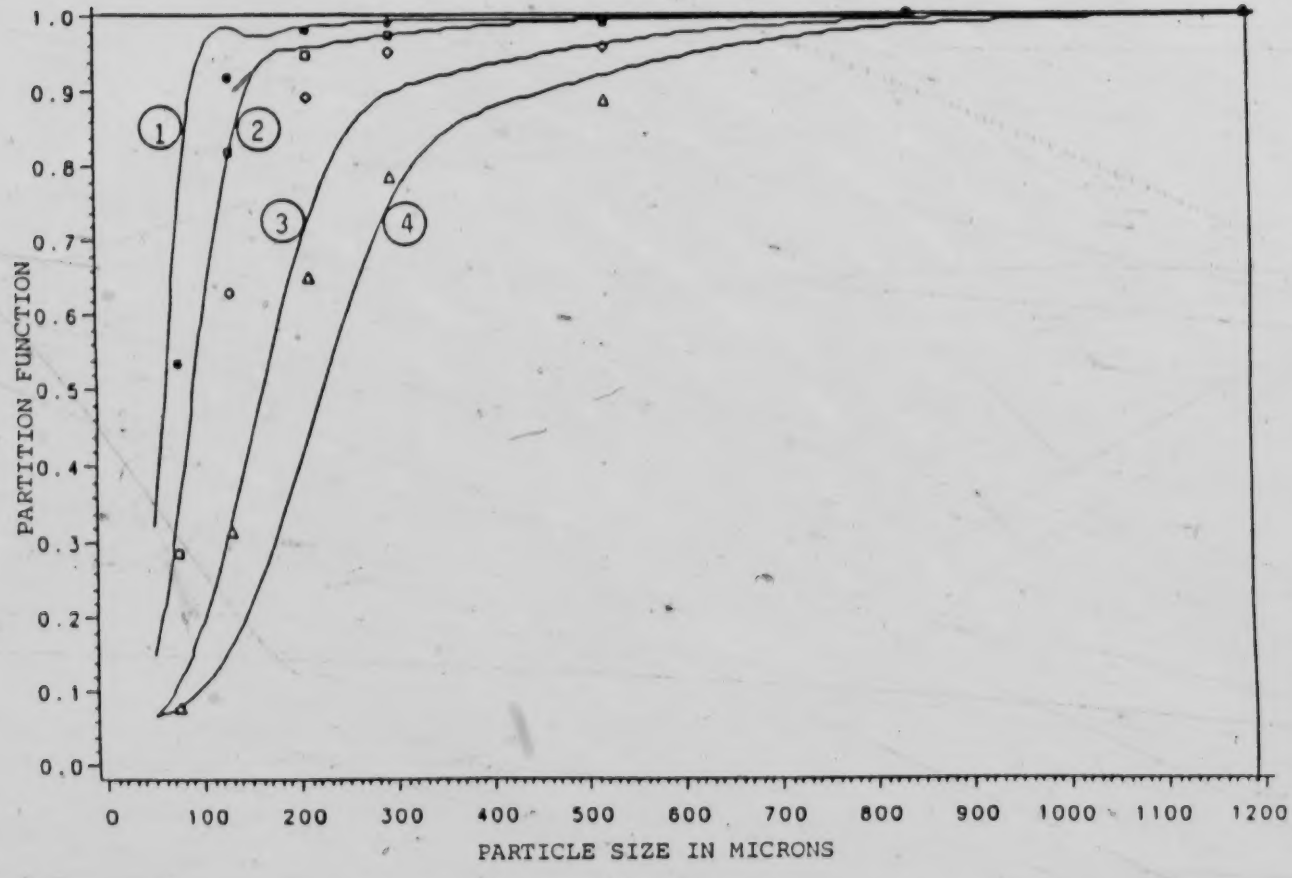


Figure 7.1 Partitioning Data and the Predicted Separation for Test #12112

| CURVE | MEAN SPECIFIC GRAVITY OF SOLIDS |
|---|---|
| (1) | 1.56 |
| (2) | 1.375 |
| (3) | 1.315 |
| (4) | 1.28 |

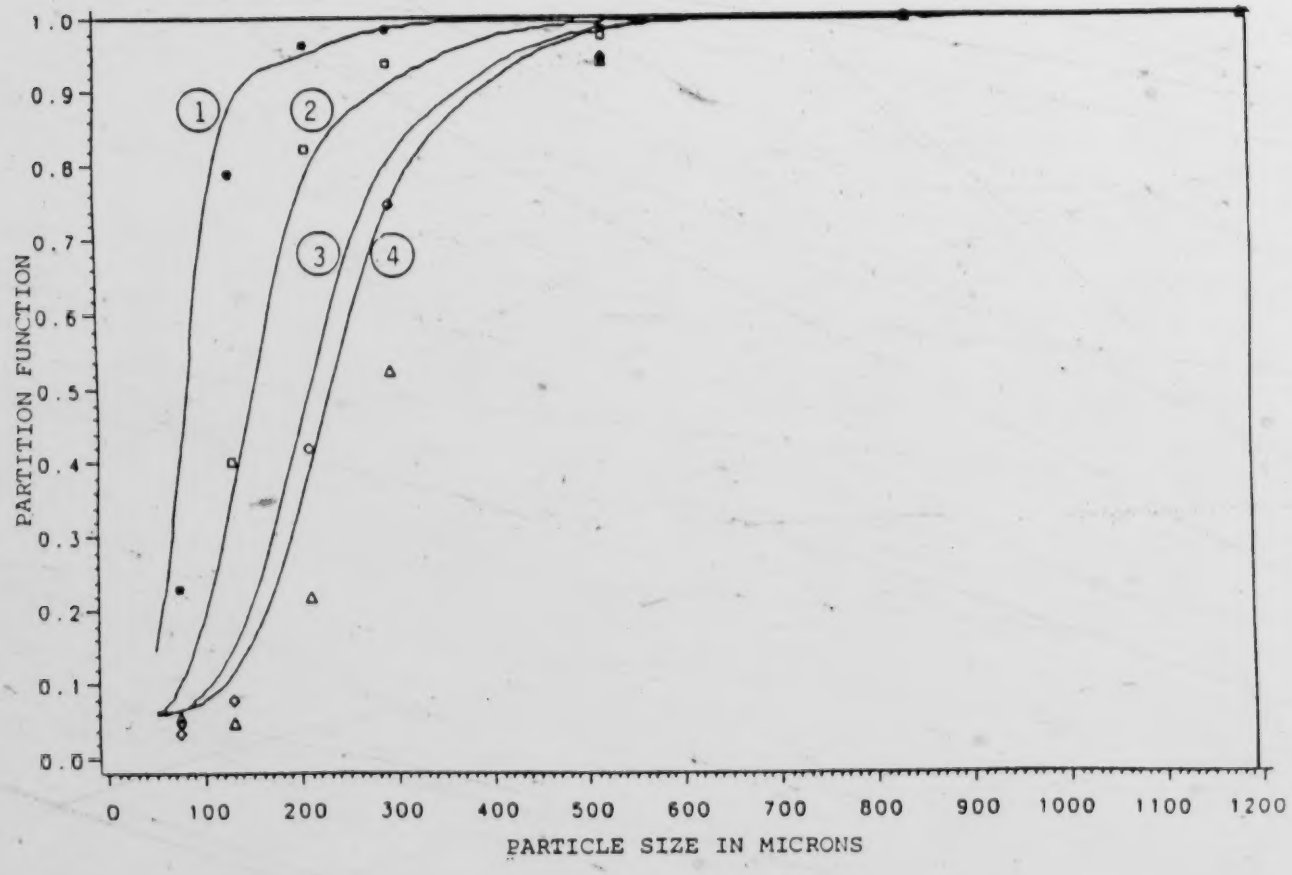


Figure 7.2 Partitioning Data and the Predicted Separation for Test #11123

| CURVE | MEAN SPECIFIC GRAVITY OF SOLIDS |
|---|---|
| (1) | 1.56 |
| (2) | 1.375 |
| (3) | 1.315 |
| (4) | 1.28 |

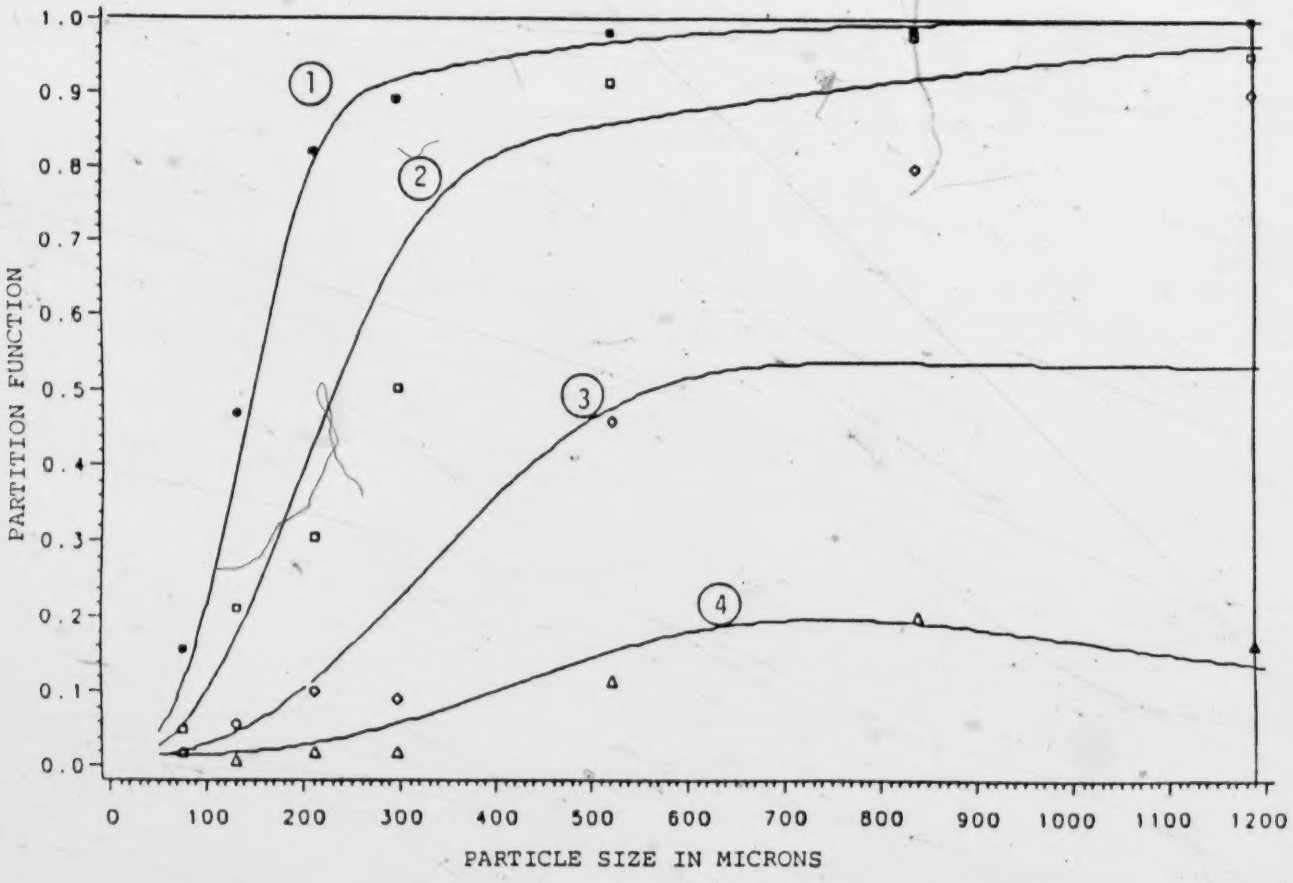


Figure 7.3 Partitioning Data and the Predicted Separation for Test #22212

The pressure flow relations will give the design engineer valuable tools in sizing the auxilliary equipment, and in estimating the optimum geometry of cyclones. Design engineers can compare performances of various configurations of multi-stage cyclone circuits through simulation, by using the model equations.

Simulation studies using the model equations can also give valuable information on the predicted changes in ash reduction and yield due to unexpected changes in the feed or planned changes in the mine production.

Possible applications of the model in predicting ash and yield in the product are demonstrated by sample calculations given below.

Assuming that a specific gravity - ash relation exists which is valid for all particle sizes for a particular coal feed, that is $A_j$ is known for all "j"s, the ash in overflow product is given by ;

$$A_o = \frac{\sum_{j=1}^{m} \left( \sum_{i=1}^{n} (1 - p_i) \times f_i \right)_j \times A_j}{\sum_{j=1}^{m} \left( \sum_{i=1}^{n} (1 - p_i) \times f_i \right)_j} \qquad (7.15)$$

Here $f_{i,j}$ and $A_j$ are known, and $P_{i,j}$ can be calculated by the model equations. Similarly, the ash in the cyclone feed can be calculated as ;

$$A_f = \sum_{j=1}^{m} \left( \sum_{i=1}^{n} f_i \right)_j \times A_j \qquad (7.16)$$

The expected ash removal efficiency can be calculated by using the above equations.

The yield is given by;

$$(1 - R_s) \times 100 \qquad (7.17)$$

and $R_s$ can be predicted by the model as follows :

$$R_s = \sum_{j=1}^{m} \sum_{i=1}^{n} p_{ij} \times f_{ij} \qquad (7.18)$$

A study of experimental results and the dependence of ash on operating variables revealed that vortex finder clearance can be used to control the ash in overflow product to some extent. The automedium cyclone model can be used to quantify this dependence and the corresponding changes in the yields can be calculated as described above.

Theoretical ash values and the yields for the 48 tests conducted on the eight inch unit were calculated from actual and predicted partitions. Ash in the cyclone products and yields for each test as calculated from the actual partitions, fitted curve and the predicted model equations are given in Appendix 7.6. Figures 7.4 and 7.5 give the comparisons of predicted and observed ash and yields. The results showed good agreement between the the experimental data and model predictions.

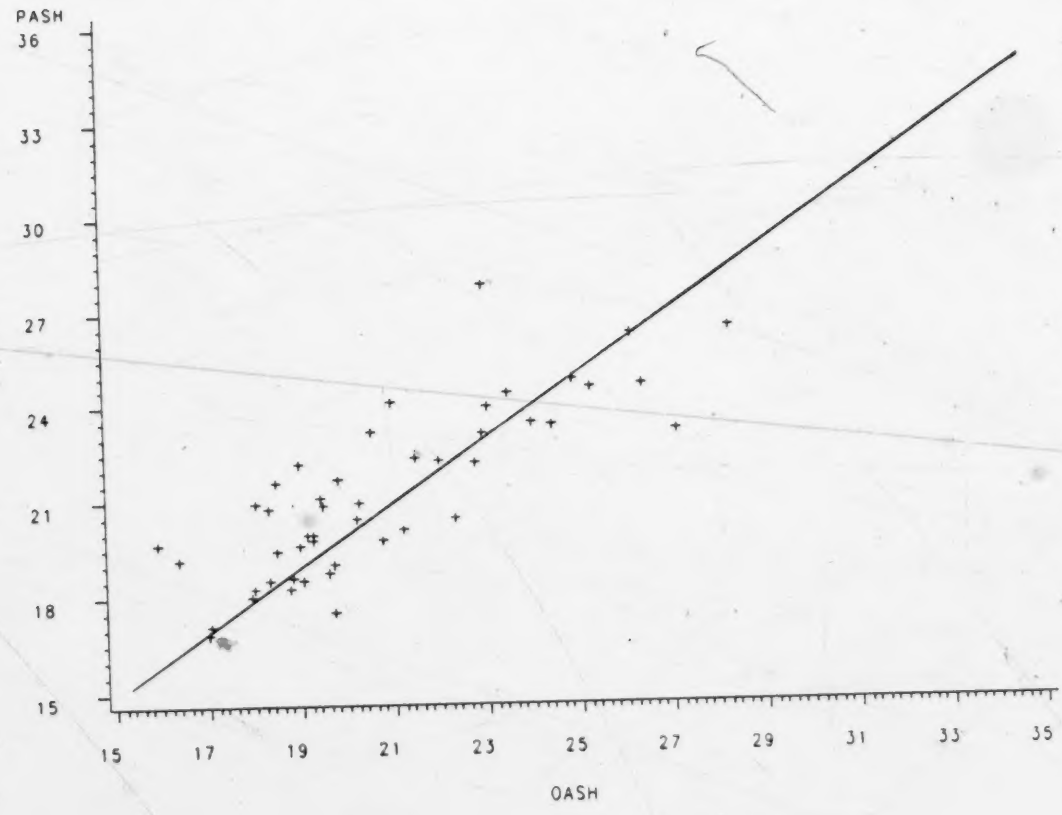


Figure 7.4 Predicted and Observed Ash in the Cyclone Overflow Product

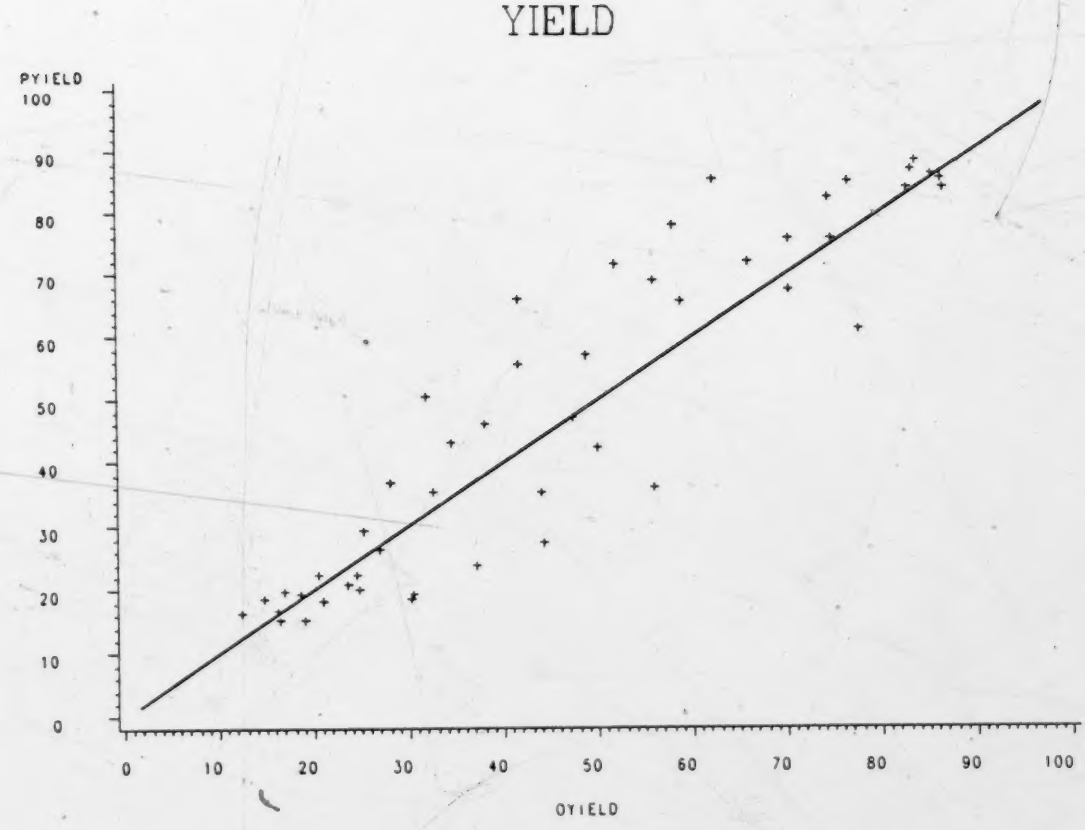


Figure 7.5 Predicted and Observed Yields

## 8. ASSESSMENT OF INDUSTRIAL IMPACT

Both bituminous and subbituminous coals mining in western Canada results in the generation of considerable quantities of fines. For metallurgical coals of the Rocky Mountains, 30 - 35 % fines (-0.6 mm) are typical as plant feed. As a consequence, fine coal cleaning has become an important part of coal preparation plants in western Canada. Most of the coal preparation plants utilize automedium cyclones in the treatment of the fines.

The necessity for better control in the coal mining industry that resulted from declining rates in the growth of demand for coal, increased the importance of mathematical models of unit operations and equipment. Moreover, the ever increasing application of computer control in the coal mining industry necessitates such models.

Although automedium cyclones have been used extensively in North America since the 1970's, the lack of process monitoring instrumentation together with the lack of a model for the separation mechanism, no feedback control for the AMC was developed, and attempts to optimize the operation by certain manual adjustments had only limited success.

An understanding of the separation mechanism, and development of empirical models that relate the performance to the operating variables will certainly improve the optimization both in the design and in the operation of AMC.

The mathematical model equations developed in this study are empirical relations that describe the well known

partition functions. These equations contain experimentally determined parameters that can be modified by plant tests for a particular operation. The present form of the model contains too many parameters. Further study in this area as recommended in the following chapter, should result in second generation models that could be utilized with more precision and ease.

The general form of model will also be useful in describing the operation of classifying cyclones that treat material with non-uniform specific gravities. Thus the general form of the model can serve as a design and simulation tool for a larger sector of the mineral processing industry.

## 9. CONCLUSIONS AND RECOMMENDATIONS

The plant tests, experimental work, and theoretical studies on the performance of the automedium cyclones resulted in :

1) Understanding of the mechanism of separation that lead to the development of a conceptual model for the AMC based on ;
   - primary classification in the upper cylindrical section
   - percolation/stratification in the non-stationary bed in the conical section, and
   - secondary classification in the upward flow of the vortex.
2) Development of a general mathematical model describing partition of coal particles of different size and density.
   (The general model simplifies to well known classifying cyclone model with elimination of bed separation and/or secondary classification effects.)
3) Development of empirical relations for prediction of parameters of the general model, from cyclone geometry and the operating conditions.
4) Generation of a high integrity data set for the AMC over a wide range of operating conditions.
5) Understanding of effects of various design and operational variables on the performance of the AMC.

It should be emphasized that the relationships developed in this study only represent a first

generation model for the AMC. Future work should be directed to simplification of the general model form by combining certain parameters. The interdependancy of the three stages of separation should be investigated. Such a study should result in a simplified model with improved accuracy in predicting the behavior of the AMC.

The operational parameters and cyclone geometry effects could also be studied in different size cyclones and by utilizing actual partition data from operating plants.

Although complicated, understanding the fundamentals of operation of the AMC, and relating the seperation to the hydrodynamics of flow should be pursued. Relating the cyclone model parameters to fundamental flow variables will result in universal relations that can be used to improve the design and performance of hydrocyclones in general.

## REFERENCES


1) Driessen M.G., "Cleaning of Coal by Heavy Liquids with Special Reference to the Staatsmijnen Process", J. Inst. Fuel, Vol. 12, No. 67, Aug. 1939, pg. 327

2) Bloor M.I.G., Ingham D.B., Laverack S.D., "An Analysis of Boundary Layer Effects in a Hydrocyclone", Proc. 1st Intl. Conf. on Hydrocyclones,BHRA Fluid Engineering, 1980

3) Boysan F., Swithenbank J.,"Numerical Prediction of Confined Vortex Flows",Proc. Conf. Num. Meth. in Lam. Turb. Flow, Venice, July, 1981

4) Pericleous K.A., Rhodes N., Cutting G.,"A Mathematical Model for Predicting the Flow Field in a Hydrocyclone Classifier", Proc. 2nd Intl. Conf. on Hydrocyclones, BHRA Fluid Engineering, 1984, pg. 27

5) Plitt L.R.,"A Mathematical Model of the Hydrocyclone Classifier", CIM Bull., Vol. 69, No. 776, Dec. 1976, pg.114

6) Lynch A.J., Rao T.C.,"Modelling and Scale Up of Hydrocyclone Classifiers", Proc. 11th Intl. Min. Proc. Cong., Cagliari,1975

7) Bradley D.,**The Hydrocyclone**,Pergamon Press, 1965

8) Kelsall D.F.,"A Further Study of the Hydraulic Cyclone", Chem. Eng. Sci., Vol. 2, pg. 254

9) Austin L.G., Klimpel R.R.,"An Improved Method of Analysing Classifier Data", Powder Tech., Vol. 29, 1981, pg. 277

10) Finch J.A,"Modelling a Fish-hook in Hydrocyclone Selectivity Curve", Powder Tech., Vol. 36, 1983, pg. 127

11) Finch J.A., Laplante A.R.,del Villar R.,"Modelling Cyclone Performance Curves with a Size Dependent Correction Factor", Unpublished, Dept. of Min. Met, McGill Univ., 1985

12) Lynch A.J.,Johnson N.W., Manalpig E.V., Thorne C.G., **Mineral and Coal Flotation Circuits**, Elsevier, 1981

13) Austin L.G., Klimpel R.R., Luckie P.T.,"Process Engineering of Size Reduction: Ball Milling", SAIME, 1984

14) Plitt L.R., Flintoff B.C.,"SPOC Manual", Chapter 5b CANMET Report MRP/MSL 83-24 (IP)

15) Lilge E.O., Plitt L.R.,"The Cone Force Equation and Hydrocyclone Design in Materials Technology - An Inter American Approach", Am. Soc. Mech. Eng., 1968, pg. 108

16) Plitt L.R.,"The Analysis of Solid-Solid Separations in Classifiers", CIM Bull., April 1971, pg. 42

17) Bevington P.R.,**Data Reduction and Error Analysis for the Physical Sciences**,McGraw-Hill, 1969

18) Nelder J., Mead N.,"A Simplex Method for Function Minimization", Comp. J., Vol. 7, 1965

19) Blau C.E., Klimpel R.R., Steiner E.C.,"Nonlinear Parameter Estimation and Model Distinguishabilityof Physicochemical Models at Chemical Equilibrium", Can. J. Chem. Engng.,Vol. 50, June 1972, pg. 399

20) Draper N.R., Smith H.,**Applied Regression Analysis**,Wiley

Sons, 1966

21) Dowling E.G., Klimpel R.R., Aplan F.F.,"Model Discrimination in the Flotation of a Porphyry Copper Ore, Paper presented at Ann. Gen. Mtg. AIME, Los Angeles, 1984

22) Plitt L.R., Finch J.A., Flintoff B.C.,"Modelling the Hydrocyclone Classifier",Proc. Eur. Symp. Part. Tech., Amsterdam, 1980, pg. 790

23) Finch J.A., Matwijenko O.,"Individual Mineral Behavior in a Closed Grinding Circuit",CIM Bull., Nov. 1977, pg. 164

24) Laplante A.R., Finch J.A.,"The Origin of Unusual Cyclone Performance Curves",Int. J. Min. Proc., Vol. 13, 1984 pg. 1

25) Mular A.L., Jull N.,"The Selection of Cyclone Classifiers, Pumps and Pump Boxes for Grinding CircuitsIn Mineral Processing Plant Design",Ed. Mular, Bhappu, AIME 1980, Chap. 17.

26) Ford M.A., King R.P.,"The Simulation of Ore Dresing Plant", Int. J. Min. Proc., Vol. 12, 1984, pg. 285

27) Mc Ivor R.E.," Material Balance Calculation Procedure for Grinding Circuit Hydrocyclone Selection, CIM Bull., Dec. 1984, pg. 50

28) Seitz R.A., Kawatra S.K.,"Further Studies on the Use of Classifiers for the Control of Wet Grinding Circuits",Int. J. Min. Proc., Vol. 12, 1984, pg 239

29) van Duijn G., Rietema K."A Hydrocyclone for the Recovery

of Heavy Minerals from Sand, Proc. Eur. Symp. Part. Tech., Amsterdam, 1980, pg. 873

30) van Duijn G., Rietema K.,"Performance of a Large Cone Angle Hydrocyclone - I", Chem. Eng. Sci., Vol. 50, No. 10, pg. 1651

31) van Duijn G., Rietema K.,"Performance of a Large Cone Angle Hydrocyclone - II, Chem. Eng. Sci., Vol. 50, No. 10, pg. 1663

32) Visman J.,"Bulk Processing of Fine Material by Compound Water Cyclone", CIM Bull., March 1966, pg. 333

33) Weyher,L.H.,Lovell,H.L.,Investigation of the Cyclone Washing of fine coal in Water,Special Report SR-61,Penn.St.U.,1966

34) Bow,R.,Personal Communication,Cyclone Engineering Sales,Edmonton, Alberta,1981

35) Tanaka,T.,Segregation Models of Solid Mixtures Composed of Different Densities and Particle Sizes,Ind.Eng.Chem.,Proc.Des.Dev.,V10,n.3, p333-340,1971

36) Cooke,M.H., Bridgwater,J,Interparticle Percolation: a Statistical Mechanical Interpretation,Ind.Eng.Chem.Fund.,V14,n1,p25-27,1979

37) Scott,A.M.,Bridgwater,J.,Interparticle Percolation: a Fundamental Solids Mixing Mechanism, Ind.Eng.Chem.,Fund.,V14,n1,p23-26,1975

38) Bridgwater,J.,Sharpe,N.W.,Stocker,D.C.,Particle Mixing by Percolation Trans.Inst.Chem.Engrs.,V47,pT114-T119,1969

## NOMENCLATURE

**Upper Case**

$A$ = the autogeneous partition function, i.e. the fraction of certain species of particles in the flow entering the bed which is sent to the secondary classification.

$B$ = partition function for the secondary classification, i.e. the fraction of certain species of particles in the material which is returned to the bed.

$C$ = the partition function for the primary classification, i.e. the fraction of certain species of particles in the feed which is sent to the bed.

$C$ = corrected cut size for particles with a specific gravity $\rho_s=2$.

$D_c$ = the diameter of the cyclindrical section of the cyclone, in cm.

$D_i$ = the diameter of a the cyclone inlet orifice (or the diameter of a circle with equal area), in cm.

$D_o$ = the diameter of the vortex finder orifice, in cm.

$D_u$ =
the diameter of the apex orifice, in cm.

F =
solids mass flow rate in the cyclone feed.

$F_i$ =
cumulative mass fraction passing size $s_i$ in the cyclone feed solids.

$F_1$ =
calibration parameter for Plitt cyclone model, default value is $F_1=1.$

$F_2$ =
calibration parameter for Plitt cyclone model, default value is $F_2=1$.

$F_3$ =
calibration parameter for Plitt cyclone model, default value is $F_3=1$.

$F_4$ =
calibration parameter for Plitt cyclone model, default value is $F_4=1$.

J =
the least squares objective function.

K =
size modulus in the Gaudin-Schuhman distribution function.

Lu =
limiting volumetric solids concentration in the underflow stream, i.e. the concetration at which

roping begins, in %.

Lu20 =
the value of Lu corresponding to $\phi$=20%, a calibration parameter with a default value of 56%.

O =
solids mass flow rate in the cyclone overflow.

P =
cyclone inlet pressure, in Kpa.

Q =
volumetric flow rate of cyclone feed slurry, in litres/min.

Rf =
mass recovery of water in the cyclone feed to the underflow product.

Rs =
mass recovery of cyclone feed solids to the underflow product, Rs = U/F.

S =
the volumetric flow split, ie. (volumetric flow rate in underflow)/(volumetric flow rate in overflow).

U =
solids mass flow rate in the cyclone underflow.

$U_i$ =
cumulative mass fraction passing size $s_i$ in the cyclone underflow solids.

$Y$ =
general partition function.

**Lower Case**

$a$ =
the bypass constant(9).

$a_{ij}$ =
the partition function for the autogeneous heavy medium separator, i.e. the fraction of the *i*th size class by *j*th specific gravity class which reports to the *underflow* stream.

$b_{ij}$ =
the partition function for the secondary classification separator, i.e. the fraction of the *i*th size class by *j*th specific gravity class which reports to the *underflow* stream.

$c_i$ =
the classification function, i.e. the fraction of size class *i* in the cyclone feed which reports to the cyclone underflow product by classification.

$c_{ij}$ =
the partition function for the primary classification separation, i.e. the fraction of the *i*th size class by *j*th specific gravity class which reports to the *underflow* stream.

$d_i$ =
the characteristic size of particle size class *i*.

$d_o$ =
the size beyond which entrainment is no longer considered significant (Finch bypass model(10)).

$d_{50_c}$ =
the corrected cut size, i.e. the particle size which has an equiprobable chance of reporting to either of the cyclone product streams, under the influence of classification alone.

$f_i$ =
mass frequency in particle size class $i$ in the cyclone feed.

$f_{ij}$ =
mass frequency in particle size class $i$ by specific gravity class $j$ in the cyclone feed, $\Sigma\Sigma f_{ij}=1$ or 100%.

h =
free vortex height in cyclone, in cm.

k =
exponent for the effect of solids density on the corrected cut size.

m =
sharpness of separation coefficient in the classification model with $m\to\infty$ implying perfect separation.

$m_1$ =
mass fraction of phase 1 in the cyclone feed, where this function is taken to be continuous with particle size.

n =
number of particle size classes in the size

analysis.

$o_i$ =
Mass frequency in particle size class *i* in the cyclone overflow.

$o_{ij}$ =
mass frequency in particle size class *i* by specific gravity class *j* in the cyclone overflow, $\Sigma\Sigma o_{ij}=1$ or 100%.

$p_i$ =
partition function for particle size class *i*, i.e. the fraction of solids in size class *i* in the cyclone feed which reports to the cyclone underflow product.

$p_{ij}$ =
the overall partition function for the cyclone i.e. the fraction of the *i*th size class by *j*th specific gravity class which reports to the yclone underflow product.

$p_1$ =
the partition function for phase 1. For the purposes of the illustrative calculation this function is assumed to be monotonic increasing and continuous with particle size.

$p_2$ =
the partition function for phase 2. See $p_1$ above.

$r^2$ =
the square of the multiple correlation coefficient.

$r_i$ =

the bypass function, i.e. the fraction of particle *i* in the cyclone feed which reports to the underflow product by short circuit.

$r_{i,j}$ =
the bypass function for the *i*th size class by *j*th specific gravity class which reports to the autogeneous separator by short circuiting.

$s_i$ =
the upper size boundary for the *i*th particle size class.

$u_i$ =
mass frequency in particle size class *i* in the cyclone underflow.

$u_{i,j}$ =
mass frequency in particle size class *i* by specific gravity class *j* in the cyclone underflow, $\Sigma\Sigma u_{i,j}=1$ or 100%.

$w_1$ =
the mass distribution of phase 1 with particle size. It is a mass frequency function which is continuous with particle size.

**Greek**

$a$ =
the distribution modulus for the Gaudin-Schuhmann distribution function.

$\gamma_i$ =
cumulative partition function, i.e. the fraction of material finer than size $s_i$ in the cyclone

feed which reports to the underflow product.

$\eta$ = viscosity of the carrier fluid, in centipoise.

$\rho_p$ = density of the cyclone feed slurry, in $g/cm^3$.

$\rho_s$ = density of the solid phase, in $g/cm^3$.

$\theta$ = cone angle in degrees.

$\mu$ = microns, $10^{-6}$ cm.

$\phi$ = volumetric concentration of solids in the cyclone feed slurry, in %.

# APPENDIX-1: Theoretical Computations of Flow and Separation in Hydrocyclones

# THEORETICAL COMPUTATIONS OF FLOW AND SEPARATION IN HYDROCYCLONES

A Bibliographical Study

A. Alpel TURAK

August 1985

UNIVERSITY OF ALBERTA

Department of Mineral Engineering

# 1. INTRODUCTION

Mechanism of separation in hydrocyclones is a settling process in centrifugal field created by the swirl of fluid due to tangential inlet at high pressures. The complex geometry and vortex flow conditions together with restricted flow through at least one outlet creates conditions that resist simple fundamental analysis, especially of micro-structure of particle and fluid flows. The complexity is further increased when turbulence is taken into account and boundary layer flows along chamber walls are considered. This complexity is reflected in the mathematical treatments of the flow and separation. The derived equations were not readily solved until modern computers were involved.

In spite of all this, in recent years many authors reported development of mathematical methods to define flow fields and separation in hydrocyclones, giving results consistent with experimental findings.

This bibliographical study is an attempt to summarize the fundamental studies on hydrocyclones, emphasizing different methodologies used. Particular attention was given to those methods that could be utilized in defining separation mechanism in auto-

medium cyclones, with appropriate modifications and additions. Some experimental studies of fundamentals of cyclones and studies on swirl flow in general were also included.

## 2. FUNDAMENTAL STUDIES ON VORTEX AND SWIRL FLOWS

The pioneering experimental work of Kelsall[12] revealed the magnitudes of axial, radial and tangential components of the main flow and confirmed the existence of axially symmetric vortex flow in a hydrocyclone. Thus, in all the following studies of hydrocyclone, authors have made the major assumption of axially symmetric vortex flow. Similar flow conditions are also ecountered in cylindrical cyclone chambers or cyclone combusters and many authors reported theoretical studies of turbulent swirl flow in these chambers[4,6,13,14,19,32].

In treatment of turbulent vortex flow in a cyclone chamber Boysan and Swithenbank[4] make some assumptions, that are common to many others, to simplify this type of flow. They assume two dimensional flow and neglect the tangential component of momentum and mass balances, and use cylindrical co-ordinates for mathematical simplicity.

Authors define the flow in vortex chambers using mass and momentum balance and including an algebraic Reynolds Stress Closure for modelling the pressure strain term in these equations to account for turbulence. According to the authors, the numeric solution was possible by setting boundary conditions such as; wall functions in the form of Plane Sheer Flow near wall regions, zero normal gradient type of relation for all variables at the axis of symmetry and fixed conditions at the inlet. The computations are

carried out on a non-uniform finite grid pattern in the axial and radial directions. The predicted flow profile is compared by measurements made by inserted probes and small discrepencies were attributed to the intrusive character of measurements.

Busnaina and Lilley[6] used the same mass and momentum balance equations and laminar flow simulation with "free slip" wall boundary conditions to predict flow profiles in confined vortex flows.

Khalil[13] also uses discrete nodes on finite difference grids to solve the turbulent case by including algebraic expressions for kinematic energy of turbulence and time average dissipation rate of turbulent energy together with the momentum and continuity equations.

Martynov[19] studied the flow in cylindrical hydrocyclones at moderate Reynolds numbers ( 2000 - 4000) assuming inviscid incompressible fluid. His method employs dimensionless flow equations of axisymmetric vortex flow in cylindrical co-ordinates and includes flow functions at cyclone inlet, apex and overflow discharge, and solves the Bernoulli integral to determine the diameter of the air core. By series approximation for the solution of flow functions and linear approximation for the Bernoulli integral, Martynov derives algebraic solutions which predict the flow pattern in the cyclone. The author claims only qualitative agreement with experimental findings.

All the above mentioned studies attempt to define the flow pat-

terns in cyclones or confined vortex flows in general. In the following sections some more ellaborate and specific studies of flow and separation in hydrocyclones are presented.

## 3. THEORETICAL STUDIES OF FLOW IN HYDROCYCLONES

Many authors studied the flow in hydrocyclones assuming both laminar[1-a,2,5] and turbulent[1-b,3,5,10,16,18,26,28] vortex flows and some authors approached the problem of defining the boundary layers on the inner surface of the cyclone walls[1,15,17] while others attempted to model hydrocyclones through bulk flow relations[9,11,33] or particle flux calculations. In the following sections these different approaches are given in some detail.

### 3.1 Laminar Flow Models of Hydrocyclones

Defining the flow in conical hydrocyclones assuming laminar conditions was attempted by Bloor and Ingham[2], and they reported development of an inviscid model which was solved by approximation by truncated series, and claimed good agreement with Kelsall's experimental findings.

They construct the equations of motion in spherical co-ordinates where $u$, $v$ and $w$ are components of velocity in the r, $\theta$ and $\lambda$ directions respectively according to the co-ordinate system shown in Figure-1 as follows:

$$u\frac{\partial u}{\partial r} + \frac{v}{r}\frac{\partial u}{\partial \theta} - \frac{v^2 - w^2}{r} = -\frac{1}{\rho}\frac{\partial P}{\partial r} \qquad (1)$$

$$u\frac{\partial v}{\partial r} + \frac{v}{r}\frac{\partial v}{\partial \theta} + \frac{uv}{r} - \frac{w^2 Cot\theta}{r} = -\frac{1}{\rho r}\frac{\partial P}{\partial \theta} \qquad (2)$$

$$u\frac{\partial w}{\partial r} + \frac{v}{r}\frac{\partial w}{\partial \theta} - \frac{uw}{r} - \frac{vw Cot\theta}{r} = 0 \qquad (3)$$

where $P$ is pressure and $\rho$ is the desity of fluid. In addition, the equation of continiuty is defined as;

$$\frac{\partial}{\partial r}(r^2 \sin\theta\, u) - \frac{\partial}{\partial r}(r \sin\theta\, v) = 0 \tag{4}$$

Now the authors assume free vortex flow and thus set;

$$u = \frac{A}{r \sin\theta} \tag{5}$$

to satisfy equation (3). This is true in the regions outside the boundary layers on the walls and the solid body rotation near the axis. Using equation (5) and defining $P'$ as;

$$P' = P - \frac{1}{2}\frac{\rho A^2}{(r^2 \sin^2\theta)} \tag{6}$$

and eliminating $P$ between equations (1) and (2) yields;

$$\left(u\frac{\partial}{\partial r} - \frac{v\partial}{r\partial\theta}\right)\left(\frac{w_\lambda}{r\sin\theta}\right) = 0 \tag{7}$$

where $w_\lambda = \frac{1}{r}\frac{\partial}{\partial r}(rv) - \frac{1}{r}\frac{\partial u}{\partial\theta}$ giving the $\lambda$ component of vorticity.

A stream function $\psi$ is introduced to satisfy the continuity so that;

$$\frac{\partial\psi}{\partial r} = -vr\sin\theta \qquad \frac{\partial\psi}{\partial\theta} = ur^2\sin\theta \tag{8}$$

Integrating equation (8) gives;

$$\frac{1}{r^2\sin\theta}\left[\frac{1}{\sin\theta}\frac{\partial^2\psi}{\partial r^2} - \frac{\partial}{\partial\theta}\left(\frac{1}{r^2\sin\theta}\frac{\partial\psi}{\partial\theta}\right)\right] = f(\psi) \tag{9}$$

Here the authors make one more assumption that is true for classifying cyclones but cannot be readily accepted for the auto-medium cyclone. The assumption is that since $\theta$, the semi-angle of cone, is small $sin\ \theta$ is equal to $\theta$. equation (9) becomes;

$$\frac{\partial}{\partial\theta}\left(\frac{1}{\theta}\frac{\partial v}{\partial\theta}\right) = -r^4\ \theta\ f(v) \qquad (10)$$

and an approximate solution was sought with the relation

$$v = \beta r^{\gamma}\theta^{\gamma}(\alpha - \theta) \qquad (11)$$

for the streamline function.

The term $(\alpha - \theta)$ is linear thus the velocity at the wall is tangential, finite and non-zero (this is actually the velocity just outside the boundary layer at the wall). Substituting the streamline function in equation (10) and including the first two terms of expansion of $(\alpha - \theta)$ constants $\beta$ and $\gamma$ can be calculated. The velocity components $u$ and $v$ are then given by;

$$u = \frac{1}{2}\beta(r\theta)^{-\frac{1}{2}}(3\alpha - \theta) \qquad (12a)$$

$$v = -\frac{3}{2}\beta r^{-\frac{1}{2}}\theta^{-\frac{1}{2}}(\alpha - \theta) \qquad (12b)$$

The volumetric flux through the cyclone can be used to determine the constant $\beta$, using equation (11) and setting;

$$2\pi\beta a^{\frac{1}{2}}\left(\alpha - \frac{a}{\ell}\right) \quad Q \qquad (13)$$

*where* $\ell$ = *vortex finder clearance*

$a$ = *vortex finder diameter*

$Q$ = *total flux through cyclone*

The cylindrical velocity terms $u$ and $v$ can be resolved into horizontal and vertical components as;

$$q_v = u = \frac{1}{2} 3(r\theta)^{-\frac{1}{2}} (3\alpha - \theta) \qquad (14a)$$

$$q_h = -3r^{\frac{1}{2}}\theta^{\frac{1}{2}} \qquad (14b)$$

The constant $A$ in equation (5) is still needs to be determined for the cyclone geometry.

If the area of inlet to cyclone is $A_1$ then $w$ at entry is equal to $\frac{Q}{A_1}$, and setting $r \cdot \sin\theta = b$ the radius of cyclone, and taking into account the energy losses upon entry to cyclone chamber by introducing a factor $\alpha$, $A$ can be calculated from $A = \frac{\alpha b Q}{A_1}$. thus;

$$w = \frac{\left(\alpha b \frac{Q}{A_1}\right)}{r \sin\theta} \qquad (15)$$

Equations (14a), (14b) and (15) together with equation (13) define the flow conditions in a hydrocyclone in terms of geometric and operational parameters.

The authors extend their study to include models for particle motions. They first show that time required for acceleration of particles to fluid velocities is negligible when compared with the time scale of the main flow, then they calculate particle "drift" velocity.

For particle Reynolds numbers less than unity the drag force on a spherical particle with diameter $d$ can be stated as $3\pi\mu lld$ where

$\mu$ is viscosity of fluid and $\mathrm{II}$ is velocity of particle relative to fluid. Then the force balance on a single particle is;

$$\rho_s \frac{\pi d^3}{6} \frac{d\mathrm{II}}{dt} = F - 3\pi\mu\,\mathrm{II}\,d \tag{16}$$

where $\rho_s$ is solid density and $F$ is force due to rotation of fluid, and for equilibrium, $F - 3\pi\mu\,\mathrm{II}\,d = 0$ where $F = (\rho_s - \rho)\frac{\pi d^3}{6}\frac{w^2}{r\cdot\sin\theta} I_r$ and $I_r$ is unit vector in $r$ direction. Then the drift velocity is;

$$\mathrm{II} = \frac{(\rho_s - \rho)\,d^2}{18\mu}\frac{w^2}{r\times\sin\theta} I_r \tag{17}$$

Using equations (13), (14), (15) and (17) equilibrium orbit diameters for a given size (and density) of particle can be determined. The equation for the radius is given by;

$$r^{\frac{5}{2}}\theta^{\frac{2}{2}} = \frac{2\pi\,(\rho_s - \rho)\,d^2 b^2 \omega^2 Q a^{\frac{5}{2}}\,(\alpha - \frac{a}{i})}{18\,\mu\,A_1^2} \tag{18}$$

The authors compare their findings with Kelsall's[12] experimental data and they claim good agreement except the over estimation of horizontal velocities, which they attribute to the fact that the model does not take short-circuit flow into account. The theory does predict general behavior of flow accurately. The zero vertical velocity is predicted to be at $0.60 \times \alpha$ which coincides with Bradley's experimental results. Kelsall's finding at $0.57 \times \alpha$ is attributed to the extra long vortex finder used in his experiments.

The general model developed for classifying hydrocyclones can be used to predict behaviour in auto-medium cyclones by taking the particle densities into account in equation (18). The viscosity term can be replaced by $\mu_s = (1 + 2.5\theta)^{\dagger}$ where $\theta$ is volumetric fraction of solids assumed to be perfect spheres[30,p212]. Kutepov and Nepomnyashchii[16] also studied laminar flow fields in hydrocyclones and derived dimensionless operational parameters $\bar{\alpha}$ and $\bar{\gamma}$ characterizing the correlation of intensity of centrifugal separation and random mixing respectively.

$$\bar{\alpha} = \frac{5\pi^2 \left(\frac{\rho}{\rho_l} - 1\right) \rho_l^2 C^2 W_{in}^3 h^{\frac{3}{2}} d^4}{4b' R^{\frac{7}{2}}} \tag{19a}$$

$$\bar{\gamma} = \frac{112.5\, A_1\, C^4}{\left(\frac{\rho}{\rho_l} - 1\right)} \left(\frac{R}{d}\right)^2 \tag{19b}$$

where;

$\rho$ = *particle density*
$\rho_l$ = *liquid density*
$C$ = *constant to account for turbulence*
$w_{in}$ = *average velocity at inlet*
$h$ = *distance from axis to inlet*
$d$ = *effective size of solid particle*
$b'$ = *intensity of delta - correlated random function*
$R$ = *radius of hydrocyclone*
$A_1$ = *constant giving the geometry of cyclone*

---

† **Author's note:** Normally higher order terms are needed in the viscosity expression $\mu_s = (1 + a\theta + b\theta^2 + \cdots)$, for Brownian motion the coefficient $a$ is taken as 2.5 and higher terms are dropped.

and if;

$r$ = *radial co - ordinate*

$r_o$ = *radius at counter - current flow interface*

the fractional removal of a certain particle through apex $S$ is given as a function of residence time as follows;

$$S_p(\bar{t}) = \frac{1}{2\bar{\alpha}} \int_o^{\bar{t}} \bar{G}\,|_{\bar{r}=\bar{r}_o}\, d\bar{t} \qquad (20a)$$

where

$$\frac{\partial \bar{G}}{\partial \bar{t}} = -\left( \frac{1}{(\bar{r})^{\frac{3}{2}}} - \frac{\bar{\gamma}}{(\bar{r})^{\frac{3}{2}}} - \frac{1}{2\bar{\alpha}} \right) \frac{\partial \bar{G}}{\partial \bar{r}} + \frac{1}{2\bar{\alpha}} \frac{\partial^2 \bar{G}}{\partial (\bar{r})^2} \qquad (20b)$$

and with boundary conditions ;

$$\frac{\partial \bar{G}}{\partial \bar{r}}\,|_{\bar{r}=\bar{r}_o} = \frac{\partial \bar{G}}{\partial \bar{r}}\,|_{\bar{r}=\bar{r}_i} = 0 \qquad (20c)$$

and initial condition;

$$\bar{G}(o, \bar{r}) = -\left( \frac{1}{(\bar{t})^{\frac{3}{2}}} - \frac{\bar{\gamma}}{(\bar{r})^{\frac{3}{2}}} - \frac{1}{2\bar{\alpha}} \right) w_o(\bar{r}) + \frac{1}{2\bar{\alpha}} \frac{\partial \bar{w}_o(\bar{r})}{\partial \bar{r}} \qquad (20d)$$

The numeric solution of the above equations give the particle removal (partition) through the apex as a function of average residence time, provided that $\bar{\alpha}$ and $\bar{\gamma}$ are calculated.

3.1. Turbulent Flow Models of Hydrocyclone

Bloor and Ingham [3] have modified the simple laminar approach of modelling the flow in hydrocyclones presented earlier. In this new study of turbulent spin in hydrocyclones the authors introduce a modified pressure term $P_1$ into equations (1) and (2) given previously for the momentum balance in the $R$ and $\theta$ directions defined as;

$$P_1 = \rho - \int^r \rho \frac{v^2(R)}{R}\, dR \tag{21}$$

and assume variation of viscosity with $R$ as follows ;

$$\mu = \frac{f(R)}{Z^2} \tag{22}$$

thus the spin velocity equation given below for axially symmetric flow;

$$\rho \frac{u}{R}\frac{\partial}{\partial R}(vR) - \rho w \frac{\partial v}{\partial Z} = \frac{\partial}{\partial R}\left[\mu\left(\frac{\partial v}{\partial R} - \frac{v}{R}\right)\right] + \frac{2\mu}{R}\left(\frac{\partial v}{\partial R} - \frac{v}{R}\right) + \frac{\partial}{\partial Z}\left(\mu \frac{\partial v}{\partial Z}\right) \tag{23}$$

(here $R$ is the radius in cylindrical co-ordinates) reduces to an ordinary differential equation when the following relations are introduced;

$$u = -\frac{BR^2}{Z^2} \tag{24a}$$

$$w = \frac{1}{2}BR^2\left(3\alpha - 5\frac{R}{Z}\right) \tag{24b}$$

(equations (14a) and (14b) expressed in cylindrical co-ordinates).

The resultant equation takes the form;

$$-\rho B R^{\frac{1}{2}} \frac{d}{dR}(vR) = \frac{d}{dR}\left[f(R)\left(\frac{dv}{dR} - \frac{v}{r}\right)\right] + \frac{2f(R)}{R}\left(\frac{dv}{dR} - \frac{v}{r}\right) \tag{25}$$

Introducing non-dimensional variables $R'$ and $v'$ as;

$R' = \frac{R}{R_c}$ and $v' = \frac{v}{v_o}$ and the boundary condition $v' = v_o$ at $R' = R_c$ and introducing a non-dimensional parameter $L$ as;

$$L = \frac{\rho B R_c^{\frac{3}{2}}}{\mu_t}$$

$\mu_t$ being the average viscosity in the cyclone and by setting $f(R) = \mu_t g(R')$ equation (25) becomes;

$$-LR'^{\frac{1}{2}} \frac{d}{dR'}(v'R') = \frac{d}{dR'}\left[g(R')\left(\frac{dv'}{dR'} - \frac{v'}{r'}\right)\right] + \frac{2g(R')}{R'}\left(\frac{dv'}{dR'} - \frac{v'}{r'}\right) \tag{26}$$

Equation (26) has to be solved with the boundary conditions

$$v' = 0 \quad at \quad R' = 0$$

$$v' = 1 \quad at \quad R' = 1$$

The authors have two distinct solutions to this problem. A simplistic approach assumes $g(R') = 1$ and equation (26) reduces to;

$$-LR'^{\frac{1}{2}} \frac{d}{dR'}(v'R') = \frac{d}{dR'}\left[\frac{1}{R'}\frac{d}{dR'}(v'R')\right] \tag{27}$$

and can be integrated twice to give;

$$v' = \frac{\frac{1}{R'}\gamma\left(\frac{4}{5}, \frac{2}{5}LR'^{\frac{5}{2}}\right)}{\gamma\left(\frac{4}{5}, \frac{2}{5}L\right)} \tag{28}$$

where $\gamma = \int_o^x t^{n-1} e^t \, dt$ which is the incomplete Gamma Function. The resultant solution from equation (28) gives the turbulent spin velocity profile in the cyclone with parameter $L$ experimentally determined. Authors claim that when $L$ is in the order of 100, which corresponds to a viscosity of about 0.4 poise, good agreement is observed with Kelsall's experiments.

A more elaborate solution involves a viscosity model developed from Prandtl mixing length model;

$$\mu = \rho \lambda^2 \left| \frac{\partial v}{\partial R} - \frac{v}{R} \right| + K$$

where $K$ is introduced to augment the model corresponding to swirling flow to account for the fact that turbulence does not vanish at points of zero rates of strain. Taking $\lambda = \frac{l}{2}$ so that $v$ is a function of $R$ only, simplifies the solution, thus;

$$\mu = \frac{M}{Z^2} \left| \frac{dv}{dR} - \frac{v}{R} \right| + K \tag{29}$$

substituting the dimensionless variables and refering to equation (22) and remembering that $f(R) = \mu_t \, g(R')$ ;

$$M = \frac{\mu_t}{v_o \, R_o}$$

$$g(R') = \left| \frac{dv}{dR} - \frac{v}{R} \right| + K \tag{30}$$

where $Q = R_o \frac{K}{v_o}$ .

Here $Q$ is another parameter and governs the size of eddies and eddy viscosity in the region near the axis of the cyclone.

Substituting $g(R')$ in equation (26) gives a non-linear second order ordinary differential equation for $v'$ subject to previous boundary conditions. The authors solved the problem by Runge-Kutta-Merson method. Given a problem where $L$ and $Q$ are known or fixed the initial velocity gradient can be determined and equation (26) can be integrated directly to give the velocity distribution.

In spite of Rietema's work[26] which was an attempt to prove the insignificance of turbulence in well-designed hydrocyclones, many investigators[1b,3,5,10,16,18,28] sought turbulent models to define flow and separation in hydrocyclones.

Boysan and Swithenbank extended their finite difference method of solving confined vortex flows (presented in Section-1) to define gas flow in cyclones and developed models for both laminar and turbulent flow and for dust collection[5]. As a result of this study the authors claim to have developed an interactive computer program modelling particle paths and thus predicting grade efficiency (partition) curves. According to the authors the program converges with approximately 2 hours of CPU time and requires an additional 2-3 hours to construct a smooth efficiency curve (for a single density).

Driessen[10] also studied turbulence in gas cyclones and hydro-

cyclones and solved the Navier-Stokes equations assuming the following relations for the radial component of flow;

$$ur = constant \quad \Rightarrow \quad \frac{d(ur)}{dr} = 0$$

$$\frac{\partial u}{\partial z} = \frac{\partial v}{\partial z} = \frac{\partial w}{\partial z} = 0$$

Schubert and Neesse[28] and Muller, Shubert and Neesse[18] approached the turbulent modelling of wet classification in cyclones by introducing diffusivity terms and assuming independent individual particle diffusivities to be independent. They propose a turbulent particle transport model in a mono-dispersed suspension as the simple mechanism and speculate on two main conceptual models for classification ,namely; pulp-partition (Figure-2a) and pulp-tapping (Figure-2b) models.

They employ a modified pulp-partition model for hydrocyclones. The particle transport equation through a unit area perpendi- cular to y co-ordinate can be written as;

$$q_i = -D_{ty}\frac{\partial n_i}{\partial y} \quad v_{im}n_i \qquad (31)$$

*where* $n$ = *particle concentration*

$v$ = *settling velocity of particle*

and subscript $i$ refers to a particular size of particle. In a closed system with homogeneous force field, for statistic equilibrium, equation (31) can be solved for $q_i = 0$ as;

$$n'_i = \frac{n_i}{n_{io}} = \exp\left[-\frac{v_{im}}{D_{ty}}\,y\right] \qquad (32)$$

where $n_{io}$ is the concentration at inlet.

For the pulp-partition model of Figure-2b, where the distribution formed by diffusion is simply divided by a separating cut at a given height, partition numbers $P_i$ of individual fractions can be stated as;

$$\frac{P_i}{100} = \frac{1 - \exp\left[-\frac{\bar{v}_i m}{D_t} H_G\right]}{1 - \exp\left[-\frac{\bar{v}_i m}{D_t} H\right]} \tag{33}$$

The authors modify this general relation for hydrocyclones where they assume highly turbulent flow exists and calculate diffusivity as;

$$\bar{D}_t = 8\bar{u}_t D \times 10^{-4}$$

(after Meesse)

where;

$\bar{D}_t$ = *the mean medium transport coefficient*

$\bar{u}_t$ = *mean tangential velocity*

$D$ = *diameter of the cyclone*

They also assume that $d << \Lambda << D$ where $\Lambda$ is the size of eddies. The calculations are also based on other assumptions regarding the separation of pulp and diameter of air core; referring to Figures 3 and 4, they take values given by Bradley for air core diameter as $0.12 \times D$ and zero vertical velocity at $0.43 \times D$. The model for partition then becomes;

$$\frac{P_i}{100} = \frac{1 - e^{-x}}{1 - e^{-x} - 0.87\frac{Q_u}{Q_u}(e^{-x} - e^{-y})} \tag{34}$$

where

$$x = 0.135 \frac{\bar{v}_i m}{\bar{D}_t} D$$

$$y = 0.29 \frac{\bar{v}_i m}{\bar{D}_t} D$$

and $\frac{Q_o}{Q_u}$ = *split ratio of pulp* and the subscripts, $u$ = *underflow* and $o$ = *overflow*.

They also give the relation;

$$\frac{Q_o}{Q'} = \frac{1}{1 - 1.13\left(\frac{D_u}{D}\right)^3} \tag{35}$$

where $Q'$ is the water flowrate, and calculate partition from split as;

$$P = 1 - \frac{\left(\frac{Q'}{Q'} - \frac{Q_o}{Q_u}\right)}{\left(\frac{\left(\frac{Q_o}{Q_u}\right)}{\left(\frac{Q'}{Q'}\right)} - 1\right)\left(\frac{d}{d_{50}} - 1\right)^2} \tag{36}$$

This model (equation (34)) can be used to evaluate performance of automedium cyclones by incorporating particle densities into the terminal velocity term together with particle size.

## 3.3 Boundary Layer Theory as Applied to Flow in Hydrocyclones

The main stream of flow in hydrocyclones that carries particles down to apex is along the cone wall. This flow was evaluated theoretically by several authors[1a,1b,15,17]. This boundary layer swirling flow through conical hydrocyclones was studied by Bhattacharyya for both cases where laminar[1a] and turbulent[1b] flow is assumed to exist outside the boundary layer. He calculated the axi-symmetric boundary layers both on the conical surface and under the cyclone roof by Pohlhausen method assuming that the tangential velocity outside boundary layers varies as $r$ up to the point where solid body rotating column is encountered, and there after it varies as $r^{-n}$, where $r$ is the distance from the axis of cone and $n$ is flow pattern constant.

His theoretical study resulted in models for flow for both laminar and turbulent cases and he was able to calculate flow through the boundary layers, as well as change in boundary layer thickness on the conical wall and under the cyclone roof. From this theoretical analysis he finds that boundary layer thickness increases up to a distance and then starts decreasing gradually until up to the point where it meets the solid body rotating liquid, and just after this point the decrease is very rapid and towards the apex flow through the boundary layer is highly accelerated. Calculating the flux through the boundary layer on the conical surface he finds that in spite of the rapid increase in velocity

towards the apex, the total flux starts decreasing before entering forced vortex region due to decreasing thickness. After entering the solid body rotation the decrease in flux is very rapid. As a result some amount of liquid is thrown out of the boundary layer. This liquid maintains the upward flowing solid body rotating column. Since most of the space in the vortex finder is filled with the air core, (and some short circuit flow) the total upward flow cannot escape through the vortex finder. Portion of this flow, together with liquid thrown out of the boundary layer under the roof in the same manner, comes down along the outer surface of the solid body rotating column. Thus the double-mantle flow pattern as shown in Figure-5 is formed.

Kumari and Nath[15] also studied theoretically the boundary layer swirling flow through a conical hydrocyclone and solved the boundary layer equations by several numeric methods to define the velocity profiles. The results showed that the effect of swirl was more pronounced on the longitudinal skin friction and the authors found good agreement between local non-symmilarity method and momentum integral methods of solution.

All the boundary layer studies mentioned above neglect the effect of particles on flow. Laverack[17] studied the effect of particle concentration on the boundary layer flow in a hydrocyclone. Two co-ordinate systems were set-up; one for side wall boundary layer flow ($S$ measured along the generator of cone and $n$ per-

pendicular to it) and one for the main body of flow in the cyclone ($R, \phi$ *and* $Z$ as given in Figure-6).

He solves the momentum and continuity equations to define the main flow and neglects the effect of solids in viscosity in this portion of calculations. For flow in boundary layer he assumes that viscosity is a function of concentration expressed as $v = v_L \times f(c)$ where $c$ is the solids concentration and $v_L$ is the viscosity of liquid

He assumes exponential relation between $v$ and $c$ and relates mass concentration $c$ to solids fraction $\eta$ and solid particle density $\rho_s$ as;

$$c = \frac{\eta}{\eta + \rho\left[1 - \frac{\eta}{\rho_s}\right]} \tag{37}$$

He also defines the Reynolds number for the cyclone as;

$$L = \frac{-\rho R_c^2 u_c}{S_c \mu_m}$$

and two non-dimensional cyclone parameters as;

$$K = \frac{v_c}{U_c}$$

$$H = \frac{1}{R_c}\left(\frac{1}{-u_c v_L S_c}\right)^{\frac{1}{2}} \frac{Q_c m^{\frac{1}{2}}}{2\pi(m \quad 1)}$$

A dimensional parameter $\lambda$ is defined as;

$$\lambda^2 = \frac{18\mu(\alpha)^{\frac{2}{3}}\ell^{\frac{2}{3}}}{(\rho_s - \rho)A^2}$$

relating to cyclone operation and geometry. Here

$U$ and $V$ are velocity components in the $S$ and *azimuthal* directions, $Q_0$ is total flux through cyclone, $\mu_m$ is typical viscosity, $\alpha$ is semi-angle of cone and $A, B$ and $m$ are constants and subscript "$_0$" denotes initial conditions.

Thus the author relates the particle concentration in the boundary layer to the operating parameters $L, K, H, \frac{d}{\lambda}$ and feed concentration $c$, and calculates the flux $Q$ through this boundary layer, thus enabling the prediction of particle flux to the apex.

## 3.4 Bulk-Flow Approach to Hydrocyclone Modelling

Much of the fundamental work on cyclones have been devoted to analyzing the microstructure of fluid flow and occasionally of particle behavior in order to obtain dynamic models.

Some authors on the other hand[9,11,33] approached to separation in cyclones as a residence time distribution or bulk flow problem.

Holland-Bratt[11] analysed separation in three stages: calculation of the bulk retention time and angular motion, solution of continuity equation to find the radial particle velocity, and determination of the particle size (and possibly particle density for the automedium cyclone) that corresponds to this radial velocity.

According to the author the average tangential velocity $V$ of the slurry entering the cyclone is;

$$v = \sqrt{2gH}$$

and acceleration is;

$$a = \frac{2v^2}{D} = \frac{4gH}{d}$$

*where* $H$ = *pressure drop in fluid head*

$D$ = *is cyclone diameter*

Then the bulk retention time is given by;

$$t \frac{V_c}{Q}$$

where $Q$ is volumetric flow rate.

Cone volume $V$ can be estimated by;

$$V_c = \frac{\pi D^3}{4}\left(n_1 - \frac{n_2}{3}\right) \tag{38}$$

and the angular motion equivalent to $v \times t$ for diameter D is;

$$\alpha = \frac{2vt}{D}$$

The continuity equation for the flux of particles within the cyclone defines the relation between volume concentration of solids $C_v$ and velocities $u$ $v$ and $\alpha$.

Particle fluxes $E_r$ and $E_\alpha$ can be given as;

$$E_r = uC_v \qquad and \qquad E_\alpha = vC_v$$

The continuity for two dimensional flow dictates that;

$$\frac{\partial(rE_r)}{\partial r} - \frac{\partial E_\alpha}{\partial \alpha} = 0 \tag{39}$$

Using average and bulk parameters simplifies the solution of these equations, and combining the above three equations the following is obtained;

$$uC_v - v\frac{dC_v}{d\alpha} = 0 \tag{40}$$

If the initial concentration of a certain particle is $C_{v_i}$, and integrating the above equation gives;

$$u = \frac{v}{\alpha}\ln\left(\frac{C_{v_\alpha}}{C_{v_i}}\right) \tag{41}$$

This is the resultant velocity of particle $v_p$ and fluid velocity $U$ defined as $U = \frac{Q}{A}$ where wall area $A_c$ is defined as;

$$A_c = \pi D^2 \left( n_1 + \frac{n_2}{2} \right)$$

thus the particle velocity is ;

$$u_p = \frac{Q}{A_c} + \frac{QD}{2V_c} \ln \left( \frac{C_{vo}}{C_v} \right) \tag{42}$$

Introducing the equilibrium for drag and centrifugal forces;

$$V_p(\rho_s - \rho)a = \frac{1}{2}\rho U_T^2 A_x C_T \tag{43}$$

*where* $A_x$ = *crossectional area of particle*
$C_T$ = *drag co − efficient*
$U_T$ = *terminal velocity*

$V_p$ can be related to particle diameter by a shape factor $k$;

$$V_p = kd^3 \qquad (k = \frac{\pi}{6} \; for \; spheres)$$

$C_T$ is a function of Reynolds number and is given by;

$$C_t = \frac{E}{R_t}$$

where

$$R_T = \frac{U_t d\rho}{\eta}$$

$$E = 24 \left( 1 + \frac{6}{2^{10k}} \right)$$

then the drag coefficient can be expressed as;

$$C_T = \frac{24}{R_T} \left( 1 + \frac{6}{2^{10k}} \right) \tag{44}$$

The performance model based on separation size can be established for the condition where $\frac{C_x}{C_o} = 0.5$. Inserting this value in the equation of particle radial velocity and substituting $u_p$ for terminal velocity $U_T$;

$$d_{50} = \sqrt{18\left(1 - \frac{6}{2^{10k}}\right)\left(\frac{\eta u_p}{(\rho_s - \rho)}\right)} \tag{45}$$

Introducing the crowding effect by the relation;

$$u_p = U_{p_o}(1 - \bar{C}_v)^{\beta}$$

where $\bar{C}_v$ is average concentration and $U_{p_o}$ is velocity at zero concentration, and taking $\beta = 4.4$ (actually $\beta$ is a function of Reynolds number but the author takes the average value for laminar flow) the separation size equation takes the form below;

$$d_{50} = \sqrt{\frac{18\eta}{(\rho_s - \rho)a}\frac{U_p}{(1 - \bar{C}_v)^{4.4}}} \tag{46}$$

The separation model developed by Holland-Bratt is based on simple bulk flow considerations and omits many variables like dimensions of both overflow and underflow orifices vortex finder clearance etc. but the author claims that in this time average model these effects are compensated by inclusion of pressure drop and volumetric flow rate.

Dietz[9] on the other hand has developed a three region model and incorporating turbulent mixing theory defined cyclone collection efficiency for gas cyclones which with some modifications can be

used for hydrocyclones. He has defined the three regions in a cyclone as entrance region (#1), down flow region (#2) and up flow region (#3) as shown in Figure-7.

According to Dietz, a model should include the following features;

- must include cyclone geometry
- must incorporate turbulent mixing
- must provide for distribution of fluid residence time
- must assume insufficient mixing in the up and down flow regions
- must allow exchange of particles between these two regions

He assumes that flow in the entrance region is also downward. To further simplify the analysis the conventional cyclone geometry is modified to a right circular cylinder. Some dimensions are defined as $D = S - \frac{a}{2}$ where $a$ = *diameter of inlet*, and vortex finder clearance is taken as length of cylinder below the vortex finder.

For each region the conservation of particles can be written as;

$$\frac{d}{dz} Q_{v_c} n_1 = -2\pi R_c \Gamma_w(z) \qquad (region\ \#\ 1)$$

$$\frac{d}{dz} Q_v(z) n_2 = -2\pi R_c \Gamma_w(z) - 2\pi R_v(z) \Gamma_v(z) \qquad (region\ \#\ 2)$$

$$-\frac{d}{dz} Q_v(z) n_3 = 2\pi R_v(z) \Gamma_v(z) \qquad (region\ \#\ 3)$$

$Q_v(z)$ is the axial volume flow rate in each region (in region # 1 it is constant and equals to the total volumetric flow rate through the cyclone),
$\Gamma_w(z)$ is the particle flux to the cyclone wall,
$R_v(z)$ is the radius of region # 3,
$\Gamma_v(z)$ is the particle flux from region # 2 to # 3.

From Stoke's Law the radial particle velocity $U_{p_w}$ is;

$$U_{p_w}(z) = -\frac{2\rho_p R_p^2 U_{tw}}{9\mu R_c}$$

where $\mu$ is viscosity, $\rho_p$ is particle density, and particle flux is given by $\Gamma_w = n_1 U_{p_w}$.

At the boundary between the central and annular (# 3 and # 2) regions flux is;

$$\Gamma_v = n_2 U_r - n_3 U_{Pv}$$

here

$$U_{Pv} = \frac{2\rho_p R_p^2 U_t^2 v}{9\mu R_v}$$

from Stoke's Law.

At this point the author makes the following assumptions;

a) The radial velocity into the center region is constant;

$$U_r(z) = U_{ro} = \frac{Q_v}{2\pi R_v \ell}$$

thus the axial flow rate is given by;

$$Q(z) = Q_{vo}(1 - \frac{z}{\ell})$$

b) Tangential velocity does not vary axially.

c) Radial velocity relation is in the form of free vortex flow;

$$U_t(r) = U_{tw}(\frac{R_c}{r})^m$$

where m is between 0.5 and 1.0.

d) The radius of center upflow region is equal to that of the vortex finder, ei. $R_v = R_f$

thus equations given for particle conservation become a set of coupled, non-constant coefficient ordinary differential equations.

The author solves the equations analytically and arrives at the axial concentration profiles for the three regions;

$$n_1(z) = n_o \exp\left[\frac{-2\pi R_c U_{Fw}(z+D)}{Q_v}\right] \tag{47a}$$

$$n_2 = n_1(z=0)\left[1-\frac{z}{\ell}\right]^{\beta} \tag{47b}$$

$$n_3 = n_1(z=0)\left[\frac{A-B}{C}\right]\left[1-\frac{z}{\ell}\right]^{\beta} \tag{47c}$$

where

$$\beta = \frac{1}{2}\left[A-1-C+\frac{1}{2}\left[(C-A-1)^2-4AC\right]^{\frac{1}{2}}\right]$$

$$A = \frac{2\pi R_c \ell U_{Fw}}{Q_v}$$

$$C = 1 - \frac{n_3(z=0)}{n_o}$$

then the efficiency of the cyclone (or the partition numbers) is given by;

$$\eta = 1 - \frac{n_3}{n_o}$$

$$= 1 - \left(K_o - (K_1^2 - K_2)^{\frac{1}{2}}\right)\exp\left[\frac{-2\pi R_c U_{Fw} D}{Q_v}\right] \tag{48}$$

where

$$K_o = \frac{R_c U_{Fw} - R_v U_{Fc} - R_v U_{Fv}}{2R_v U_{Fv}}$$

$$K_1 = \frac{1}{2}\left[1-\left(\frac{R_v}{R_c}\right)^{2n}\left[1-\frac{p\mu Q_v}{4\pi\ell\rho_p R_i^2 U_{tw}}\right]\right]$$

$$K_2 = \left(\frac{R_v}{R_c}\right)^{2n}$$

as a function of particle diameter (and density) depending on the chosen value of $n$.

The model developed is for gas cyclones and assumes the upflow region diameter equal to vortex finder diameter which is not true for hydrocyclones. In spite of these, the model can be modified to predict separation in hydrocyclones by inserting a value as a fraction of cyclone diameter for this region and including the fluid density in calculation of radial particle velocity.

## 3.5 Experimental Studies of Fundamental Parameters in Cyclones

Determination of micro structure of flow in hydrocyclones has been a challenge for investigators. In addition to the complexity of flow, conventional flow and pressure measurements in cyclone chambers were known to effect the flow substantially. The development of non-intrusive measurement techniques[12,20,25] recently made it possible to study the micro structure of flow in cyclones more accurately.

The pioneering work was done by Kelsall[12] using an optical method involving ultramicroscope illumination and microscopes fitted with rotating objectives. He measured the tangential velocity components of fine aluminum particles directly in a transparent hydrocyclone, and contoured the particle traces to obtain the vertical component of velocity. He also observed secondary flows like short-circuit flow and recirculation of particles under cyclone roof. By applying Stoke's Law of settling he derived equilibrium envelopes for particles of different sizes.

Another important area of fundamental investigation in hydrocyclones is the measurement of residence time and accumulation ratio of different size fractions (or densities) in hydrocyclones. It is evident that if components of a slurry fed into a hydrocyclone have different residence times many properties like pulp density, size distribution and mineral composition of the contents of cyclone should differ from that of the feed.

Cohen et.al.[7] conducted a series of experiments to study the residence time of particles in hydrocyclones. They used two different methods, one involves direct measurement of time by tracer method, the other involves determination of difference in cyclone contents at steady state conditions.

The direct measurement was carried out by detection of small plugs of magnetite particles injected into the cyclone during operation with quartz slurries by an electromagnetic presence detector. Analysis of contents of cyclone at steady state was made possible by stopping feed to cyclone very rapidly by turning the three way valve right at the entrance of cyclone to a by-pass line and simultaneously collecting the entire contents of the cyclone from discharge. According to the authors these tests were carried out to confirm the results of residence time studies.

The authors claim that results showed that the mean residence time of solids could be smaller or greater than that of fluid depending on their properties as well as operating conditions. Different size particles show systematic variations in their mean residence times, and a peak residence time is observed for particles near $d_{60}$ for operating conditions resulting in good classification, while poor classification is associated generally with uniform or randomly scattered residence times for particles of different sizes. They also add that the longest relative residence times were observed for particles of $d_{60}$ or $d_{70}$ rather than $d_{50}$. They

attribute this to the fact that those particles seemed to teeter near the apex opening being too light to pass down easily and too heavy to be lifted to the vortex finder.

Through extensive experiments involving probing and sampling of various locations of cyclone, Renner and Cohen[25] tried to explain flow and separation in hydrocyclones. The authors claim that most of the classifying action in hydrocyclones occurs in a restricted toroidal zone as shown in Figure-8.

They have observed four distinctly different zones in the cyclone containing different size distributions.

Referring to Figure-8 these regions are;

A - A narrow region comprising of material that is identical in size distribution to feed.

B - A large portion of the cyclone throughout which the size distribution resembles that of coarse product.

C - Another narrow region arround vortex finder with size distributi very close to overflow.

D - The troid shaped region which is overal richer in intermediate si fractions than the feed or overal cyclone contents as a whole and show distribution with fines closest to the axis.

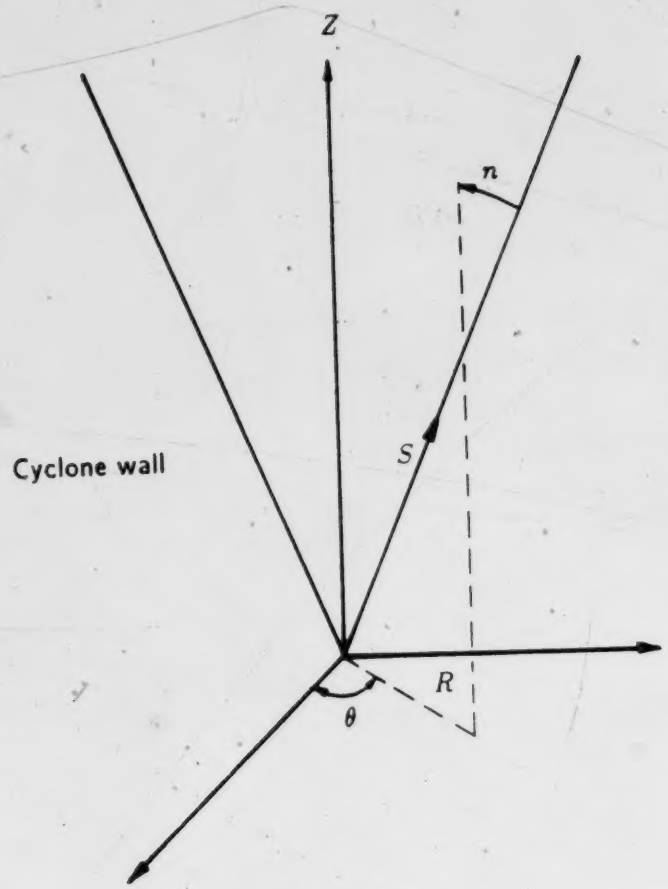


**Figure 1:** The Cyclone co-ordinate system (after [2])

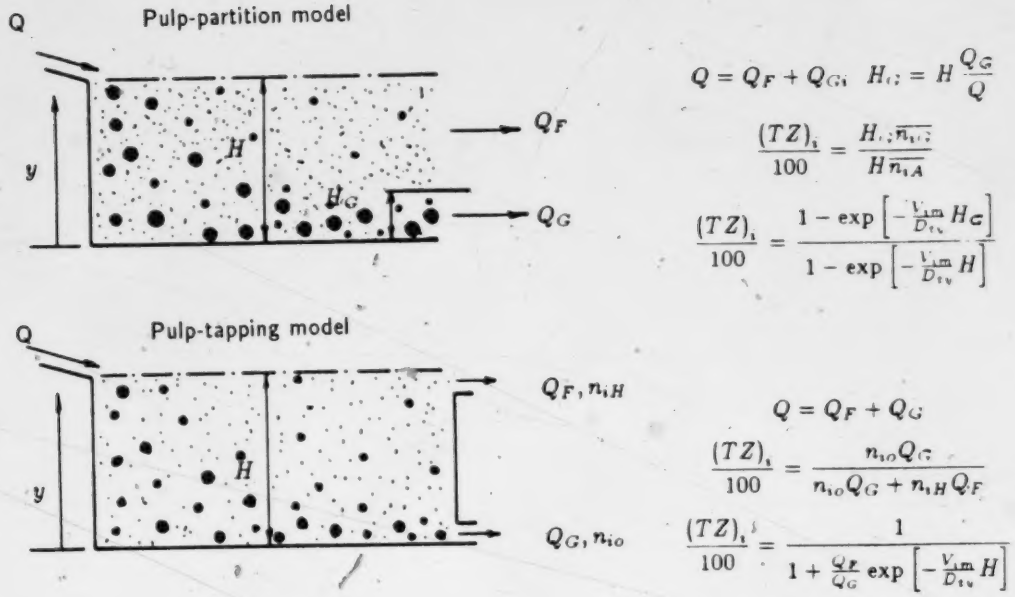


**Figure 2**: Basic models for wet turbulence classification (after [18] and [28])

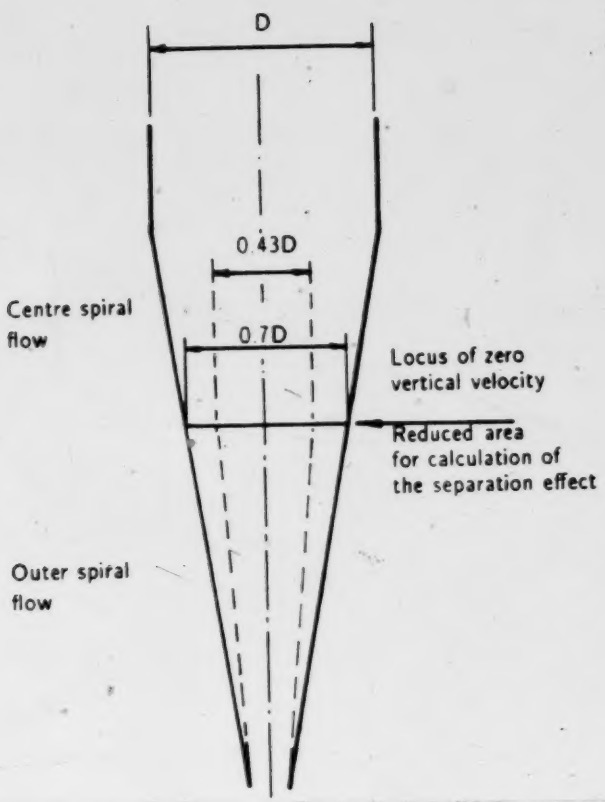


**Figure 3:** Locus of $U_v = 0$ in hydrocyclone (after [18])

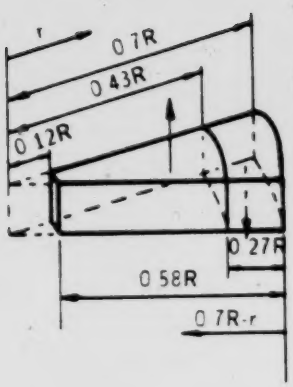


**Figure 4:** Locus of separation cut in hydrocyclone (after [18])

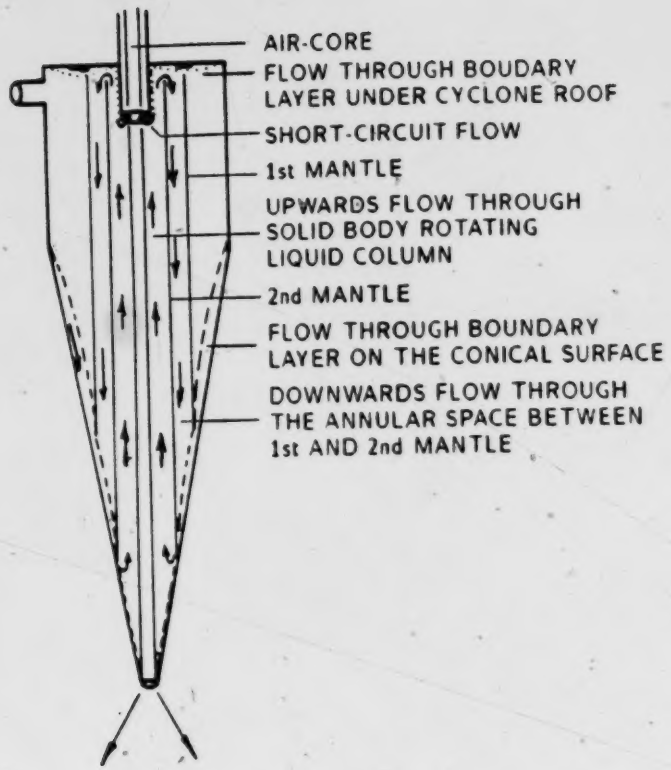
AIR-CORE
FLOW THROUGH BOUDARY LAYER UNDER CYCLONE ROOF
SHORT-CIRCUIT FLOW
1st MANTLE
UPWARDS FLOW THROUGH SOLID BODY ROTATING LIQUID COLUMN
2nd MANTLE
FLOW THROUGH BOUNDARY LAYER ON THE CONICAL SURFACE
DOWNWARDS FLOW THROUGH THE ANNULAR SPACE BETWEEN 1st AND 2nd MANTLE

Figure 5: Mathematical model of the flow field inside the cyclone (after [1])

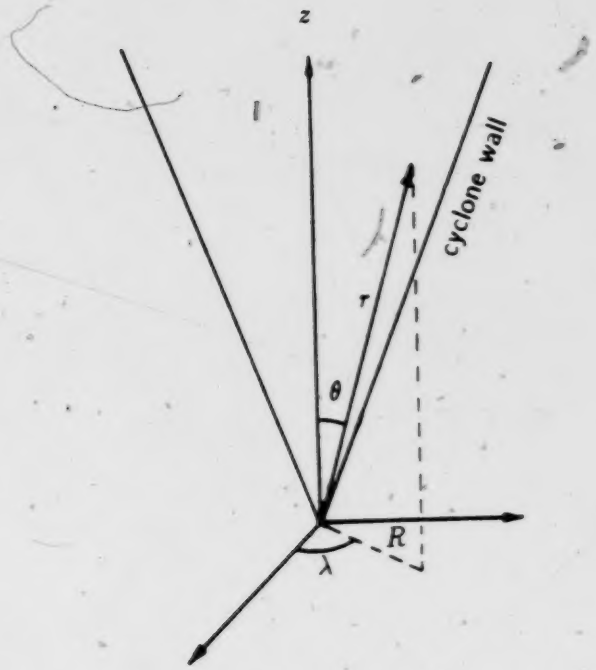


**Figure 6:** The cyclone co-ordinate system (after [17])

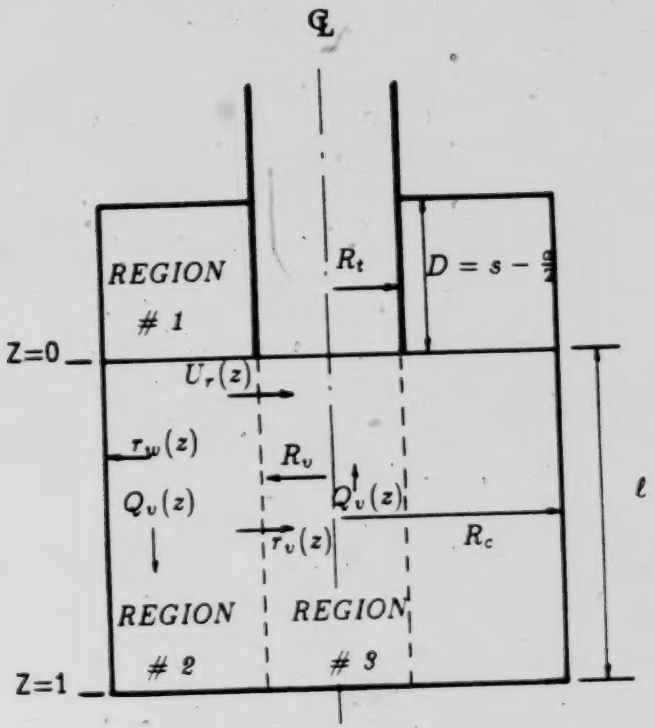


**Figure 7**: Modified cyclone geometry for analysis (after [9])

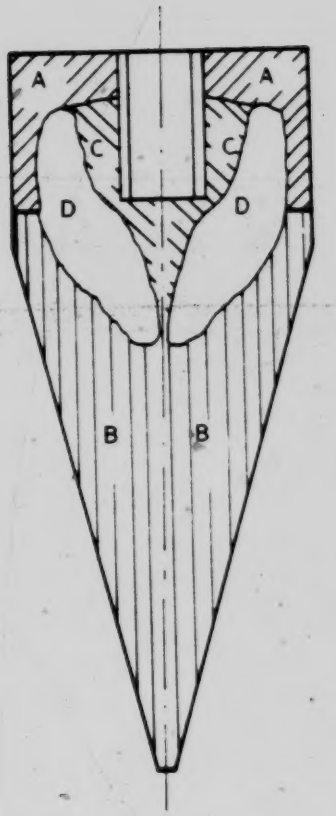


Figure 8: Regions of similar size distribution (after [25])

## REFERENCES


1. BHATTACHARYYA, P., "Theoretical Study of the Flow Field Inside a Hydrocyclone with Vortex Finder Diameter Greater than that of Apex Opening - 1. Laminar Case, 2. Turbulent Case", Appl.Sci.Res.(The Hague), V36, n.3,1980,p.197-212 and 213-225
2. BLOOR, M.I.G.,and INGHAM, D.B.,"Theoretical Investigation of the Flow in a Conical Hydrocyclone", Trans. Instn. Chem.Engrs., V.51, pp.36-41 (1973).
3. BLOOR,M.I.G.,and INGHAM,D.B.,"Turbulent Spin in a Cyclone", Tran.Instn.Chem.Engrs., V.53, pp.1-6 (1975)
4. BOYSAN, F.,SWITHENBANK,J.,"Numerical Prediction of Confined Vortex Flows", Dept. of Chem. Engrg and Fuel Techn.,Univ.of Sheffield, U.K. Rep. No. H1C370, 1981
5. BOYSAN,F.,AYERS,W.H.,SWITHENBANK, J.,"A Fundamental Mathematical Modelling Approach to Cyclone Design", Trans.Inst.Chem.Engrs., Vol.60 (1982), pp.222-230
6. BUSNAINA,A.A.,LILLEX,D.G.,"Numerical Simulation of Swirling Flow in a Cyclone Chamber", ASME - Fluids Engrg.Conf.,Boulder, Col.,June 22-23,1981, Fluid Mechanics of Combustion Systems, pp. 169 - 178
7. COHEN,H.E.,MIZRAHI,J.et al, "The Residence Time of Mineral Particles in Hydrocyclone", Tran.Inst. Min. and Met.,V.75 1978, pp. 129 - 138
8. COLLINS,D.N.,et al., "Separation Efficiency in Dense Media Cyclones", Trans. Inst. Min. and Met., V. 92 (Sec.C) March 1983 pp. C 38 - C 51
9. DIETZ, P.W., "Collection efficiency of Cyclone Separators",A.I. Ch.E. Journal, V. 27, n.6 (Nov.1981), pp.888-892
10. DRIESSEN,M.G.,"Theorie de l'ecoulement dans un Cyclone. Influence de la Turbulence et son Interpretation Mathematique",Rev.l'Ind. Minerale, V. 31 (1951), pp. 482 -495
11. HOLLAND-BATT, A.B., "Bulk Model for Separation in Hydrocyclones", Trans.Inst.Min. and Met.Sec.C.V.91, March 1982, pp.21 - 25
12. KELSALL, D.F.,"A Study of the Motion of Solid Particles in a Hydraulic Cyclone", Trans.Inst.Chem.Engrs., V.30,pp.87-108,(1952)
13. KHALIL,E.E.,"Numerical Computation of Turbulent Flow Structure in a Cyclone Chamber", Paper Submitted to ASME Meeting, Aug.6-8 1979, n.79-HT-31
14. KOTAS, T.J.,"Experimental Study of Three Dimensional Boundary Layers on the End Wall of a Vortex Chamber", Proc.R.Soc.Land V.352, pp.169 - 187 (1976)

15. KUMARI,M.,NATH.G.,"Boundary Layer Swirling Flow Through a Conical Hydrocyclone", Acta Mech.,V. 33, pp.11 - 20, ( 1979)

16. KUPETOV,A.M., NEPOMNYASHCHII,E.A.,"Kinetics of a Separation process in a Hydrolic Cyclone Based on the Hydrodynamics of Turbulent Flow" Theor.Found.of Chem.Engrg. V.14 (1980),pp. 570 - 573

17. LAVERACK, S.D., " The Effect of Particle Concentration on the Boundary Layer in a Hydrocyclone", Trans.Inst.Chem.Engrs. V.58, pp. 33 - 42 (1980)

18. MULLER,B.,NEESSE, Th. and SCHUBERT, H., "Berechnung von Hydrozyklonen nach dem Turbulenzmodell", Freiberger Forschunghefte (1975) A 544, pp. 31 - 43

19. MARTYNOV,Y.V.,"Velocity Field in a Cylindrical Hydrocyclone", Fluid Dynamics, V. 15 (1980), pp. 804 - 810

20. MOTHES, H.,SIEVERT,J.,LOFFLER,F.,"Investigation of the Cyclone Grade Efficiency Curves using a Light-Scattering Particle Size Analyzer", I.Chem.Engrg.Symposium Series, n.63, pp.D2/Q/1 - 13

21. LOPACHONOK,L.V.,et al.,"Density and Size of Shale Grains on their Distribution in Hydrocyclone", Solid Fuel Chemistry, V. 13 (1979) pp. 124 -127

22. LOPACHONOK,L.V.,et al.,"The Main Laws of the Distribution of Shale Grains in a Hydrocyclone", solid Fuel Chamistry, V. 13 (1979) n.5 pp. 100 - 103

23. PARIDA, A.,"Turbulent Swirl with Gas-Solid Flow in Cyclone", Chemical Engineering Science, V. 35, pp. 949 - 954

24. RAMIREZ-CASTRO,J.,PILLAI,K.J.,SPOTTISWOOD,D.J.,"Introduction of Individual Mineral Behavior to Hydrocyclone Models", SME - AIME 17 th Appl.of Computers and Op.Rsch. in the Min. Industry, 1982

25. REMMER,V.G.,COHEN, H.E.,"Measurement and Interpretation of Size Distribution of Particles in a Hydrocyclone", Trans.Inst.Min. and Met., V. 87, 1978, pp. C-139 - C 145

26. RIETEMA,K.," Liquid - Solids Separation in a Cyclone - the Effect of Turbulence on Separation", Proc.Symp.Interaction between Fluids and Particles, London, June 1962, pp.275 - 281

27. SCHLICTING, H, BOUNDARY LAYER THEORY, 4 th Edition, 1960, McGraw-Hill, New-York,N.Y. p.107,506,538

28. SCHUBERT,H., NEESSE,Th.,"The Role of Turbulence in Wet Classification", Proc.Tenth Int.Min. Process. Congr. London 1973, pp. 213 - 239

29. SCHUBERT,H., NEESSE,Th.," A Hydrocyclone Separation Model in Consideration of the Turbulent Multi-phase Flow", Int.Conf.

on Hydrocyclones, 1 - 3 Oct.1980, Cambridge, U.K.

30. SOO,S.L.,FLUID DYNAMICS OF MULTIPHASE SYSTEMS,Blaisdell Publ.Co. Waltham,Massach.USA,1967; pp. 317 - 322

31. TARJAN,G., MINERAL PROCESSING, V.I, Akademiai Kiado, Budapest, 1981, pp. 531 - 573

32. TAYLOR,G.I., "The Boundary Layer in the Converging Nozzle of a Swirl Atomizer" Quarterly Jour.Mech.appl.Math.,V.3(1950),pp.129-139

33. TRAWINSKI,H., "The Mathematical Simulation of Tromp Curve", Interceram. n.1.1978,pp 21-23 and 52

34. TRAWINSKI,H., "Theory, Application and Practical Operation of Hydrocyclones", E/MJ , September 1976, pp.115-127

# APPENDIX-2: Results of Silica Tests Series A and B

PARTITION VALUES FOR TEST NUMBER S-1

TEST = 1 ; VF Clearance = 33 mm.

| | % WT. UNDER | % WT. OVER | FEED | PARTITION % UNDER | PARTITION % OVER |
|---|---|---|---|---|---|
| SLURRY | 756.40 | 28300.00 | 29056.40 | 0.0260 | 0.9740 |
| DRY WT. | 561.60 | 2920.70 | 3482.30 | 0.1613 | 0.8387 |
| % SOLIDS | 74.25 | 10.32 | 11.98 | 0.1613 | 0.8387 |
| 356.0 mic. | 5.20 | 0.0 | 0.84 | 100.0000 | 0.0 |
| 251.6 mic. | 20.53 | 2.20 | 5.16 | 64.2135 | 35.7865 |
| 179.5 mic. | 41.58 | 6.21 | 11.91 | 56.2834 | 43.7166 |
| 127.0 mic. | 23.63 | 8.67 | 11.08 | 34.3860 | 65.6140 |
| 89.5 mic. | 4.95 | 5.30 | 5.24 | 15.2244 | 84.7756 |
| 63.5 mic. | 0.65 | 2.98 | 2.60 | 4.0253 | 95.9747 |
| 48.5 mic. | 0.27 | 3.36 | 2.86 | 1.5216 | 98.4784 |
| 20.0 mic. | 3.21 | 71.28 | 60.30 | 0.8585 | 99.1415 |

TEST = 2 ; VF Clearance = 71 mm.

| | % WT. UNDER | % WT. OVER | FEED | PARTITION % UNDER | PARTITION % OVER |
|---|---|---|---|---|---|
| SLURRY | 1139.00 | 31580.00 | 32719.00 | 0.0348 | 0.9652 |
| DRY WT. | 840.70 | 2831.10 | 3671.80 | 0.2290 | 0.7710 |
| % SOLIDS | 73.81 | 8.96 | 11.22 | 0.2290 | 0.7710 |
| 356.0 mic. | 3.83 | 0.0 | 0.88 | 100.0000 | 0.0 |
| 251.6 mic. | 12.98 | 0.0 | 2.97 | 100.0000 | 0.0 |
| 179.5 mic. | 37.65 | 3.19 | 11.08 | 77.8013 | 22.1987 |
| 127.0 mic. | 32.11 | 4.18 | 10.57 | 69.5227 | 30.4773 |
| 89.5 mic. | 9.67 | 4.67 | 5.81 | 38.0762 | 61.9238 |
| 63.5 mic. | 1.60 | 4.67 | 3.97 | 9.2344 | 90.7655 |
| 48.5 mic. | 1.31 | 4.91 | 4.09 | 7.3411 | 92.6589 |
| 20.0 mic. | 5.54 | 78.38 | 61.70 | 2.0557 | 97.9442 |

TEST = 3 ; VF Clearance = 105 mm.

| | % WT. UNDER | % WT. OVER | FEED | PARTITION % UNDER | PARTITION % OVER |
|---|---|---|---|---|---|
| SLURRY | 2264.50 | 28180.00 | 30444.50 | 0.0744 | 0.9256 |
| DRY WT. | 1699.50 | 2249.60 | 3949.10 | 0.4304 | 0.5696 |
| % SOLIDS | 75.05 | 7.98 | 12.97 | 0.4304 | 0.5696 |
| 356.0 mic. | 3.58 | 0.0 | 1.54 | 100.0000 | 0.0 |
| 251.6 mic. | 16.49 | 0.0 | 7.10 | 100.0000 | 0.0 |
| 179.5 mic. | 37.20 | 0.0 | 16.01 | 100.0000 | 0.0 |
| 127.0 mic. | 28.10 | 3.84 | 14.28 | 84.6821 | 15.3179 |
| 89.5 mic. | 9.90 | 4.05 | 6.57 | 64.8716 | 35.1284 |
| 63.5 mic. | 1.07 | 5.12 | 3.38 | 13.6353 | 86.3646 |
| 48.5 mic. | 0.45 | 5.33 | 3.23 | 5.9958 | 94.0042 |
| 20.0 mic. | 3.21 | 81.66 | 47.90 | 2.8840 | 97.1159 |

PARTITION VALUES FOR TEST NUMBER S-2

TEST = 1 : VF Clearance = 33 mm.

| | % WT. UNDER | % WT. OVER | FEED | PARTITION % UNDER | PARTITION % OVER |
|---|---|---|---|---|---|
| SLURRY | 1341.50 | 34791.00 | 36132.50 | 0.0371 | 0.9629 |
| DRY WT. | 1015.30 | 4340.70 | 5356.00 | 0.1896 | 0.8104 |
| % SOLIDS | 75.68 | 12.48 | 14.82 | 0.1896 | 0.8104 |
| 450.0 mic. | 0.15 | 0.0 | 0.03 | 100.0000 | 0.0 |
| 356.0 mic. | 4.32 | 0.44 | 1.18 | 69.6646 | 30.3354 |
| 251.6 mic. | 20.84 | 3.79 | 7.02 | 56.2583 | 43.7417 |
| 179.5 mic. | 39.45 | 14.33 | 19.09 | 39.1699 | 60.8301 |
| 127.0 mic. | 18.13 | 12.17 | 13.30 | 25.8407 | 74.1593 |
| 89.5 mic. | 10.10 | 14.74 | 13.86 | 13.8133 | 86.1867 |
| 63.5 mic. | 2.23 | 7.02 | 6.11 | 6.9163 | 93.0837 |
| 48.5 mic. | 1.51 | 5.27 | 4.56 | 6.2810 | 93.7190 |
| 20.0 mic. | 3.41 | 42.24 | 34.88 | 1.8533 | 98.1467 |

TEST = 2 : VF Clearance = 71 mm.

| | % WT. UNDER | % WT. OVER | FEED | PARTITION % UNDER | PARTITION % OVER |
|---|---|---|---|---|---|
| SLURRY | 2664.60 | 33743.00 | 36407.60 | 0.0732 | 0.9268 |
| DRY WT. | 2005.50 | 3450.70 | 5456.20 | 0.3676 | 0.6324 |
| % SOLIDS | 75.26 | 10.23 | 14.99 | 0.3676 | 0.6324 |
| 450.0 mic. | 0.08 | 0.0 | 0.03 | 100.0000 | 0.0 |
| 356.0 mic. | 4.19 | 0.05 | 1.57 | 97.9881 | 2.0119 |
| 251.6 mic. | 20.57 | 1.64 | 8.60 | 87.9367 | 12.0633 |
| 179.5 mic. | 39.15 | 9.08 | 20.13 | 71.4765 | 28.5235 |
| 127.0 mic. | 21.79 | 10.58 | 14.70 | 54.4829 | 45.5171 |
| 89.5 mic. | 8.73 | 15.53 | 13.03 | 24.6254 | 75.3746 |
| 63.5 mic. | 1.71 | 7.63 | 5.45 | 11.5242 | 88.4758 |
| 48.5 mic. | 1.16 | 6.34 | 4.44 | 9.6116 | 90.3884 |
| 20.0 mic. | 2.69 | 49.15 | 32.07 | 3.0828 | 96.9172 |

TEST = 3 : VF Clearance = 105 mm

| | % WT. UNDER | % WT. OVER | FEED | PARTITION % UNDER | PARTITION % OVER |
|---|---|---|---|---|---|
| SLURRY | 3258.40 | 30255.00 | 33513.40 | 0.0972 | 0.9028 |
| DRY WT. | 2416.10 | 2444.10 | 4860.20 | 0.4971 | 0.5029 |
| % SOLIDS | 74.15 | 8.08 | 14.50 | 0.4971 | 0.5029 |
| 450.0 mic. | 0.05 | 0.0 | 0.02 | 100.0000 | 0.0 |
| 356.0 mic. | 3.71 | 0.0 | 1.84 | 100.0000 | 0.0 |
| 251.6 mic. | 18.45 | 0.13 | 9.24 | 99.2922 | 0.7078 |
| 179.5 mic. | 38.07 | 1.70 | 19.78 | 95.6781 | 4.3219 |
| 127.0 mic. | 25.08 | 4.78 | 14.87 | 83.8364 | 16.1636 |
| 89.5 mic. | 9.84 | 13.13 | 11.49 | 42.5566 | 57.4434 |
| 63.5 mic. | 1.61 | 8.51 | 5.08 | 15.7555 | 84.2444 |
| 48.5 mic. | 0.84 | 6.63 | 3.75 | 11.1305 | 88.8695 |
| 20.0 mic. | 2.38 | 65.11 | 33.93 | 3.4875 | 96.5125 |

# APPENDIX-3: Results of Silica Tests Series C

h = 1.13 in

| | O/F | U/F | FEED |
|---|---|---|---|
| Slurry weights (g) | 24740 | 1739 | 26479 |
| Dry weights (g) | 3193 | 1305 | 4498 |
| % Solids | 12.91 | 75.05 | 16.99 |
| % Yields | 70.99 | 29.01 | 100.00 |
| SIZE (Micron) | | | |
| 512.50 | 0.33 | 5.93 | 1.95 |
| 362.50 | 4.04 | 28.18 | 11.04 |
| 256.00 | 8.41 | 30.39 | 14.79 |
| 181.00 | 15.55 | 20.28 | 16.92 |
| 128.00 | 11.65 | 9.43 | 11.01 |
| 90.50 | 5.56 | 2.44 | 4.65 |
| 64.00 | 4.77 | 0.97 | 0.08 |
| 49.00 | 7.08 | 0.69 | 5.23 |
| 42.00 | 42.62 | 1.70 | 30.75 |

h = 1.50 in

| | O/F | U/F | FEED |
|---|---|---|---|
| Slurry weights (g) | 31780 | 2061 | 33841 |
| Dry weights (g) | 4004 | 1578 | 5582 |
| % Solids | 12.60 | 76.57 | 16.50 |
| % Yields | 71.73 | 28.27 | 100.00 |
| SIZE (Micron) | | | |
| 512.50 | 0.18 | 6.01 | 1.83 |
| 362.50 | 3.12 | 28.24 | 10.22 |
| 256.00 | 7.41 | 29.95 | 13.78 |
| 181.00 | 14.01 | 21.18 | 16.04 |
| 128.00 | 10.93 | 9.32 | 10.47 |
| 90.50 | 5.71 | 2.26 | 4.73 |
| 64.00 | 5.09 | 0.88 | 3.90 |
| 49.00 | 7.36 | 0.66 | 5.47 |
| 42.00 | 46.18 | 1.49 | 33.55 |

h = 2.00 in

| | O/F | U/F | FEED |
|---|---|---|---|
| Slurry weights (g) | 35190 | 2648 | 37838 |
| Dry weights (g) | 4214 | 2051 | 6265 |
| % Solids | 11.98 | 77.48 | 16.56 |
| % Yields | 67.26 | 32.74 | 100.00 |
| SIZE (Micron) | | | |
| 512.50 | 0.13 | 4.96 | 1.71 |
| 362.50 | 1.62 | 26.80 | 9.86 |
| 256.00 | 4.95 | 31.64 | 13.69 |
| 181.00 | 12.84 | 23.07 | 16.19 |
| 128.00 | 9.89 | 8.74 | 9.51 |
| 90.50 | 5.12 | 2.08 | 4.12 |
| 64.00 | 6.22 | 0.81 | 4.45 |
| 49.00 | 7.93 | 0.51 | 5.50 |
| 42.00 | 51.30 | 1.40 | 34.96 |

h = 3.00 in

| | O/F | U/F | FEED |
|---|---|---|---|
| Slurry weights (g) | 35190 | 4049 | 39239 |
| Dry weights (g) | 4071 | 3019 | 39239 |
| % Solids | 11.57 | 74.55 | 18.07 |
| % Yields | 57.42 | 42.58 | 100.00 |
| SIZE (Micron) | | | |
| 512.50 | 0.00 | 0.50 | 0.21 |
| 362.50 | 0.84 | 27.45 | 12.17 |
| 256.00 | 3.42 | 33.03 | 16.03 |
| 181.00 | 12.04 | 25.32 | 17.69 |
| 128.00 | 11.24 | 9.24 | 10.39 |
| 90.50 | 5.75 | 1.85 | 4.09 |
| 64.00 | 5.10 | 0.78 | 3.26 |
| 49.00 | 8.67 | 0.56 | 5.22 |
| 42.00 | 52.94 | 1.23 | 30.92 |

h = 4.00 in

| | O/F | U/F | FEED |
|---|---|---|---|
| Slurry weights (g) | 34050 | 4484 | 38534 |
| Dry weights (g) | 3877 | 3370 | 7247 |
| % Solids | 11.39 | 75.16 | 18.81 |
| % Yields | 53.50 | 46.50 | 100.00 |
| SIZE (Micron) | | | |
| 512.50 | 0.00 | 4.08 | 1.90 |
| 362.50 | 0.17 | 23.93 | 11.22 |
| 256.00 | 1.16 | 30.89 | 14.98 |
| 181.00 | 7.22 | 25.76 | 15.84 |
| 128.00 | 11.32 | 10.42 | 10.90 |
| 90.50 | 6.59 | 2.15 | 4.53 |
| 64.00 | 5.95 | 0.89 | 3.60 |
| 49.00 | 8.09 | 0.63 | 4.62 |
| 42.00 | 59.50 | 1.26 | 32.42 |

h = 5.00 in

| | O/F | U/F | FEED |
|---|---|---|---|
| Slurry weights (g) | 28150 | 3156 | 31306 |
| Dry weights (g) | 2229 | 2377 | 4606 |
| % Solids | 7.92 | 75.31 | 14.71 |
| % Yields | 48.39 | 51.61 | 100.00 |
| SIZE (Micron) | | | |
| 512.50 | 0.00 | 2.99 | 1.54 |
| 362.50 | 0.08 | 17.08 | 8.85 |
| 256.00 | 0.08 | 24.78 | 12.83 |
| 181.00 | 0.73 | 28.08 | 14.85 |
| 128.00 | 1.06 | 16.24 | 8.89 |
| 90.50 | 4.55 | 6.39 | 5.50 |
| 64.00 | 14.54 | 2.41 | 8.28 |
| 49.00 | 19.98 | 0.84 | 10.10 |
| 42.00 | 58.98 | 1.20 | 29.16 |

h = 6.00 in

| | O/F | U/F | FEED |
|---|---|---|---|
| Slurry weights (g) | 25420 | 3862 | 29282 |
| Dry weights (g) | 2097 | 2776 | 4873 |
| % Solids | 8.25 | 71.88 | 16.64 |
| % Yields | 43.04 | 56.96 | 100.00 |
| SIZE (Micron) | | | |
| 512.50 | 0.00 | 3.13 | 1.78 |
| 362.50 | 0.22 | 19.46 | 11.18 |
| 256.00 | 0.78 | 25.00 | 14.58 |
| 181.00 | 1.63 | 24.49 | 14.65 |
| 128.00 | 1.51 | 15.30 | 9.36 |
| 90.50 | 2.13 | 6.06 | 4.37 |
| 64.00 | 8.30 | 3.59 | 5.62 |
| 49.00 | 11.49 | 1.33 | 5.70 |
| 42.00 | 73.93 | 1.64 | 0.03 |

# APPENDIX-4: Results of Plant Tests

HIGH FREQUENCY SAMPLES FROM SOUTH PRIMARY AUTOMEDIUM CYCLONE .37

| TIME | FEED STREAM | | UNDERFLOW STREAM | | OVERFLOW STREAM | | YIELD INFORMATION | |
|---|---|---|---|---|---|---|---|---|
| (decimal) | %solids | %ash | %solids | %ash | %solids | %ash | %solids | %ash |
| 9.17 | 11.39 | 15.49 | 52.39 | 61.41 | 10.89 | 11.38 | 94.46 | 91.78 |
| 9.50 | 10.55 | 17.07 | 53.94 | 57.26 | 9.84 | 11.55 | 91.77 | 87.92 |
| 9.83 | 9.43 | 14.64 | 52.42 | 55.40 | 8.25 | 10.84 | 85.15 | 91.47 |
| 10.17 | 9.40 | 16.90 | 52.94 | 56.46 | 8.81 | 11.17 | 92.47 | 87.35 |
| 10.50 | 7.11 | 23.67 | 55.88 | 69.01 | 7.91 | 16.93 | 113.11 ? | 87.06 |
| 10.83 | 10.45 | 20.70 | 56.25 | 69.09 | 9.31 | 15.68 | 86.93 | 90.60 |
| 11.17 | 10.93 | 22.30 | 56.61 | 67.76 | 10.19 | 17.69 | 91.74 | 90.79 |
| 11.50 | 14.16 | 26.17 | 61.99 | 67.05 | N/A | N/A | N/A | N/A |
| 11.83 | 15.40 | 24.69 | 63.23 | 67.47 | 14.07 | 16.75 | 88.89 | 84.35 |
| 12.17 | 14.98 | 24.76 | 63.74 | 70.19 | 12.53 | 17.14 | 79.64 | 85.64 |
| 12.50 | 13.91 | 23.93 | 63.36 | 65.54 | 12.20 | 17.45 | 84.78 | 86.53 |
| 12.83 | 9.73 | 24.88 | 56.19 | 65.42 | 6.44 | 15.65 | 61.81 | 81.45 |
| 13.17 | 14.18 | 27.00 | 62.20 | 69.30 | 12.18 | 17.47 | 82.46 | 81.61 |
| 13.50 | 14.57 | 25.78 | 63.14 | 67.26 | 12.87 | 18.07 | 85.34 | 84.33 |
| 13.83 | 13.10 | 27.69 | 62.70 | 68.15 | 12.76 | 18.03 | 96.74 | 80.73 |
| 14.17 | 14.76 | 26.44 | 63.67 | 67.87 | 12.79 | 18.80 | 83.30 | 84.43 |
| 14.50 | 15.07 | 25.15 | 60.66 | 70.22 | 13.50 | 19.62 | 86.60 | 89.07 |
| 14.83 | 11.52 | 24.25 | 64.36 | 73.06 | 10.66 | 19.52 | 91.05 | 91.17 |
| 15.17 | 8.45 | 22.71 | 55.73 | 60.40 | 7.20 | 15.84 | 83.01 | 84.58 |
| 15.50 | 6.58 | 21.50 | 51.82 | 59.41 | 5.72 | 15.44 | 85.31 | 86.22 |
| 15.83 | 8.54 | 25.10 | 56.32 | 67.25 | 7.31 | 17.99 | 83.45 | 85.57 |
| 16.17 | 5.39 | 27.04 | 54.19 | 67.33 | 4.54 | 18.85 | 82.79 | 83.11 |
| 16.50 | 6.39 | 28.65 | 57.37 | 60.92 | 4.92 | 16.22 | 74.84 | 72.19 |
| 16.83 | 8.72 | 23.42 | 56.49 | 58.98 | 7.68 | 14.65 | 86.20 | 80.22 |
| 17.17 | 9.07 | 23.79 | 56.38 | 58.86 | 7.87 | 15.76 | 84.62 | 81.37 |
| 17.50 | 15.37 | 27.37 | 63.27 | 68.69 | N/A | N/A | N/A | N/A |
| 17.50 | 15.09 | 29.12 | 63.16 | 68.41 | N/A | N/A | N/A | N/A |
| 17.83 | 19.50 | 26.97 | 62.60 | 67.20 | N/A | N/A | N/A | N/A |
| 17.83 | 19.26 | 25.80 | 63.06 | 67.61 | N/A | N/A | N/A | N/A |
| 18.17 | 17.21 | 27.81 | 63.42 | 70.75 | N/A | N/A | N/A | N/A |
| 18.17 | 17.85 | 29.95 | 60.20 | 69.93 | N/A | N/A | N/A | N/A |
| 18.50 | 17.76 | 27.28 | 63.58 | 68.45 | N/A | N/A | N/A | N/A |
| 18.50 | 17.60 | 27.99 | 66.82 | 69.48 | N/A | N/A | N/A | N/OA |
| 18.83 | 16.10 | 28.10 | 62.66 | 68.66 | 14.30 | 19.76 | 85.51 | 82.94 |
| ** 18.87 | 16.54 | 28.69 | 22.57 | 39.71 | 12.74 | 15.56 | 47.25 | 45.63 |

** Restricted flow using "Gagnon valve"

MEANS (Computed from complete data sets)

| | | | | | | | |
|---|---|---|---|---|---|---|---|
| 10.82 | 23.23 | 58.00 | 64.75 | 9.60 | 16.19 | 86.52 | 85.40 |
| | | Calculated from attribute mean values | | | | 86.49 | 85.50 |

## APPENDIX-5.1: Operating Conditions for Coal Tests

AMC - OPERATING CONDITIONS

| Test | OFDm. | UFDm. | %Sld. | F.Rate | VFC1 |
|---|---|---|---|---|---|
| 11111 | 2.83 | 1.42 | 9.00 | 125.00 | 1.30 |
| 11112 | 2.83 | 1.42 | 9.00 | 125.00 | 2.80 |
| 11113 | 2.83 | 1.42 | 9.00 | 125.00 | 4.30 |
| 11121 | 2.83 | 1.42 | 9.00 | 142.00 | 1.30 |
| 11122 | 2.83 | 1.42 | 9.00 | 142.00 | 2.80 |
| 11123 | 2.83 | 1.42 | 9.00 | 142.00 | 4.30 |
| 11211 | 2.83 | 1.42 | 14.00 | 125.00 | 1.30 |
| 11212 | 2.83 | 1.42 | 14.00 | 125.00 | 2.80 |
| 11213 | 2.83 | 1.42 | 14.00 | 125.00 | 4.30 |
| 11221 | 2.83 | 1.42 | 14.00 | 142.00 | 1.30 |
| 11222 | 2.83 | 1.42 | 14.00 | 142.00 | 2.80 |
| 11223 | 2.83 | 1.42 | 14.00 | 142.00 | 4.30 |
| 12111 | 2.83 | 2.00 | 9.00 | 125.00 | 1.30 |
| 12112 | 2.83 | 2.00 | 9.00 | 125.00 | 2.80 |
| 12113 | 2.83 | 2.00 | 9.00 | 125.00 | 4.30 |
| 12121 | 2.83 | 2.00 | 9.00 | 155.00 | 1.30 |
| 12122 | 2.83 | 2.00 | 9.00 | 155.00 | 2.80 |
| 12123 | 2.83 | 2.00 | 9.00 | 155.00 | 4.30 |
| 12211 | 2.83 | 2.00 | 14.00 | 125.00 | 1.30 |
| 12212 | 2.83 | 2.00 | 14.00 | 125.00 | 2.80 |
| 12213 | 2.83 | 2.00 | 14.00 | 125.00 | 4.30 |
| 12221 | 2.83 | 2.00 | 14.00 | 155.00 | 1.30 |
| 12222 | 2.83 | 2.00 | 14.00 | 155.00 | 2.80 |
| 12223 | 2.83 | 2.00 | 14.00 | 155.00 | 4.30 |
| 21111 | 4.00 | 1.42 | 9.00 | 125.00 | 1.30 |
| 21112 | 4.00 | 1.42 | 9.00 | 125.00 | 2.80 |
| 21113 | 4.00 | 1.42 | 9.00 | 125.00 | 4.30 |
| 21121 | 4.00 | 1.42 | 9.00 | 155.00 | 1.30 |
| 21122 | 4.00 | 1.42 | 9.00 | 155.00 | 2.80 |
| 21123 | 4.00 | 1.42 | 9.00 | 155.00 | 4.30 |
| 21211 | 4.00 | 1.42 | 14.00 | 125.00 | 1.30 |
| 21212 | 4.00 | 1.42 | 14.00 | 125.00 | 2.80 |
| 21213 | 4.00 | 1.42 | 14.00 | 125.00 | 4.30 |
| 21221 | 4.00 | 1.42 | 14.00 | 155.00 | 1.30 |
| 21222 | 4.00 | 1.42 | 14.00 | 155.00 | 2.80 |
| 21223 | 4.00 | 1.42 | 14.00 | 155.00 | 4.30 |
| 22111 | 4.00 | 2.00 | 9.00 | 125.00 | 1.30 |
| 22112 | 4.00 | 2.00 | 9.00 | 125.00 | 2.80 |
| 22113 | 4.00 | 2.00 | 9.00 | 125.00 | 4.30 |
| 22121 | 4.00 | 2.00 | 9.00 | 155.00 | 1.30 |
| 22122 | 4.00 | 2.00 | 9.00 | 155.00 | 2.80 |
| 22123 | 4.00 | 2.00 | 9.00 | 155.00 | 4.30 |
| 22211 | 4.00 | 2.00 | 14.00 | 125.00 | 1.30 |
| 22212 | 4.00 | 2.00 | 14.00 | 125.00 | 2.80 |
| 22213 | 4.00 | 2.00 | 14.00 | 125.00 | 4.30 |
| 22221 | 4.00 | 2.00 | 14.00 | 155.00 | 1.30 |
| 22222 | 4.00 | 2.00 | 14.00 | 155.00 | 2.80 |
| 22223 | 4.00 | 2.00 | 14.00 | 155.00 | 4.30 |

## APPENDIX-5.2: Results of Coal Tests

TEST 11111

SIZE CLASSIFICATION IN AMC

| SIZE (MIC) | SPGR=1.250 | SPGR=1.325 | SPGR=1.390 | SPGR=1.620 | SPGR=2.0 | SPGR=2.4 | OVERALL |
|---|---|---|---|---|---|---|---|
| 35.0 | 37.64 | 10.35 | 4.40 | 8.99 | 25.78 | 41.02 | 4.81 |
| 100.0 | 9.53 | 3.89 | 14.40 | 23.84 | 49.27 | 82.98 | 14.19 |
| 175.0 | 10.34 | 1.45 | 18.19 | 44.63 | 80.63 | 94.49 | 19.80 |
| 250.0 | 17.03 | 19.36 | 31.79 | 69.14 | 92.84 | 97.60 | 33.78 |
| 360.0 | 34.55 | 52.85 | 59.08 | 87.52 | 97.28 | 98.90 | 57.28 |
| 625.0 | 70.10 | 84.09 | 84.88 | 96.47 | 98.61 | 100.00 | 82.82 |
| 1000.0 | 79.28 | 81.05 | 92.51 | 98.96 | 99.34 | 100.00 | 86.44 |
| D50 | 475.18 | 347.15 | 317.26 | 189.28 | 101.14 | 48.91 | 320.45 |

DENSITY PARTITION IN AMC

| DENSITY | 35.0 mic. | 100.0 mic. | 175.0 mic. | 250.0 mic. | 360.0 mic. | 625.0 mic. | 1000.0 mic. | OVERALL |
|---|---|---|---|---|---|---|---|---|
| 1.250 | 66.71 | 55.11 | 21.66 | 9.70 | 5.70 | 5.23 | 24.02 | 16.46 |
| 1.325 | 69.14 | 73.46 | 36.99 | 11.17 | 0.76 | 2.08 | 5.70 | 22.01 |
| 1.390 | 86.61 | 74.62 | 43.06 | 19.62 | 10.43 | 8.10 | 2.36 | 18.07 |
| 1.620 | 98.04 | 93.46 | 78.60 | 53.98 | 29.68 | 14.09 | 4.92 | 40.07 |
| 2.000 | 98.74 | 97.39 | 94.93 | 87.16 | 68.56 | 33.72 | 15.39 | 81.05 |
| 2.400 | 99.99 | 99.99 | 97.91 | 95.51 | 89.99 | 71.86 | 26.70 | 89.17 |
| SG. SEP. | 1.25 | 1.25 | 1.44 | 1.59 | 1.80 | 2.17 | 2.40 | 1.71 |

TEST 11112

SIZE CLASSIFICATION IN AMC

| SIZE (MIC) | SPGR=1.250 | SPGR=1.325 | SPGR=1.390 | SPGR=1.620 | SPGR=2.0 | SPGR=2.4 | OVERALL |
|---|---|---|---|---|---|---|---|
| 35.0 | 10.87 | 7.52 | 6.90 | 24.23 | 17.81 | 58.54 | 8.55 |
| 100.0 | 7.47 | 0.45 | 12.09 | 36.27 | 70.50 | 93.14 | 17.89 |
| 175.0 | 12.41 | 15.11 | 27.70 | 69.52 | 98.03 | 98.37 | 32.10 |
| 250.0 | 27.56 | 37.53 | 59.35 | 90.84 | 98.49 | 99.70 | 53.02 |
| 360.0 | 67.79 | 65.55 | 83.54 | 97.19 | 99.50 | 99.48 | 81.37 |
| 625.0 | 100.00 | 100.00 | 100.00 | 100.00 | 100.00 | 100.00 | 99.94 |
| 1000.0 | 100.00 | 100.00 | 100.00 | 100.00 | 100.00 | 100.00 | 99.89 |
| D50 | 307.49 | 292.83 | 228.56 | 139.97 | 74.71 | 35.00 | 240.28 |

DENSITY PARTITION IN AMC

| DENSITY | 35.0 mic. | 100.0 mic. | 175.0 mic. | 250.0 mic. | 360.0 mic. | 625.0 mic. | 1000.0 mic. | OVERALL |
|---|---|---|---|---|---|---|---|---|
| 1.250 | 100.00 | 100.00 | 58.46 | 20.29 | 8.66 | 5.12 | 7.54 | 27.07 |
| 1.325 | 100.00 | 100.00 | 56.00 | 28.67 | 10.64 | 0.30 | 5.16 | 23.64 |
| 1.390 | 100.00 | 100.00 | 77.24 | 49.41 | 20.40 | 8.42 | 4.72 | 19.95 |
| 1.620 | 100.00 | 100.00 | 95.86 | 86.89 | 60.41 | 27.57 | 17.62 | 47.44 |
| 2.000 | 100.00 | 100.00 | 99.26 | 97.75 | 97.08 | 61.52 | 12.66 | 84.39 |
| 2.400 | 100.00 | 100.00 | 99.23 | 99.55 | 97.58 | 90.08 | 48.57 | 95.03 |
| SG. SEP. | 1.25 | 1.25 | 1.25 | 1.39 | 1.55 | 1.87 | 2.40 | 1.62 |

TEST 11113

SIZE CLASSIFICATION IN AMC

| SIZE (MIC) | SPGR=1.250 | SPGR=1.325 | SPGR=1.390 | SPGR=1.620 | SPGR=2.0 | SPGR=2.4 | OVERALL |
|---|---|---|---|---|---|---|---|
| 35.0 | 9.28 | 5.71 | 8.45 | 15.27 | 30.13 | 63.99 | 9.01 |
| 100.0 | 9.40 | 6.17 | 21.14 | 57.06 | 84.87 | 96.08 | 23.32 |
| 175.0 | 22.20 | 24.78 | 57.51 | 87.82 | 97.67 | 99.10 | 44.35 |
| 250.0 | 51.39 | 68.34 | 83.86 | 95.75 | 99.09 | 99.52 | 70.51 |
| 360.0 | 88.13 | 94.09 | 96.21 | 99.10 | 99.32 | 100.00 | 93.58 |
| 625.0 | 100.00 | 100.00 | 100.00 | 100.00 | 100.00 | 100.00 | 99.92 |

| | | | | | | | |
|---|---|---|---|---|---|---|---|
| 1000.0 | 100.00 | 100.00 | 100.00 | 100.00 | 100.00 | 100.00 | 99.87 |
| D50 | 247.77 | 218.54 | 164.09 | 89.02 | 58.59 | 35.00 | 190.57 |

DENSITY PARTITION IN AMC

| DENSITY | 35.0 mic. | 100.0 mic. | 175.0 mic. | 250.0 mic. | 360.0 mic. | 625.0 mic. | 1000.0 mic. | OVERALL |
|---|---|---|---|---|---|---|---|---|
| 1.250 | 100.00 | 100.00 | 84.31 | 43.34 | 17.12 | 6.98 | 6.89 | 35.94 |
| 1.325 | 100.00 | 100.00 | 92.01 | 60.97 | 19.25 | 4.54 | 4.20 | 30.54 |
| 1.390 | 100.00 | 100.00 | 94.83 | 78.99 | 49.48 | 16.25 | 6.26 | 24.72 |
| 1.620 | 100.00 | 100.00 | 98.76 | 94.22 | 83.92 | 49.02 | 11.53 | 44.44 |
| 2.000 | 100.00 | 100.00 | 99.07 | 98.75 | 96.80 | 80.24 | 23.78 | 88.48 |
| 2.400 | 100.00 | 100.00 | 100.00 | 99.33 | 98.76 | 94.66 | 56.25 | 94.35 |
| SG. SEP. | 2.40 | 1.25 | 1.25 | 1.28 | 1.39 | 1.63 | 2.32 | 1.67 |

TEST 11121

SIZE CLASSIFICATION IN AMC

| SIZE (MIC) | SPGR=1.250 | SPGR=1.325 | SPGR=1.390 | SPGR=1.620 | SPGR=2.0 | SPGR=2.4 | OVERALL |
|---|---|---|---|---|---|---|---|
| 35.0 | 12.41 | 16.48 | 9.11 | 16.52 | 16.60 | 16.50 | 7.14 |
| 100.0 | 8.23 | 21.14 | 7.54 | 38.93 | 53.17 | 83.91 | 16.13 |
| 175.0 | 14.49 | 17.82 | 22.16 | 63.21 | 84.90 | 96.25 | 33.06 |
| 250.0 | 18.41 | 12.94 | 28.75 | 64.39 | 90.25 | 96.98 | 36.18 |
| 360.0 | 37.06 | 37.39 | 64.30 | 87.30 | 97.58 | 99.00 | 61.42 |
| 625.0 | 64.53 | 71.34 | 87.08 | 96.80 | 99.59 | 99.76 | 83.50 |
| 1000.0 | 74.31 | 75.45 | 90.94 | 98.84 | 99.42 | 100.00 | 86.58 |
| D50 | 396.33 | 458.41 | 330.84 | 134.20 | 94.36 | 67.30 | 310.23 |

DENSITY PARTITION IN AMC

| DENSITY | 35.0 mic. | 100.0 mic. | 175.0 mic. | 250.0 mic. | 360.0 mic. | 625.0 mic. | 1000.0 mic. | OVERALL |
|---|---|---|---|---|---|---|---|---|

| | | | | | | | | |
|---|---|---|---|---|---|---|---|---|
| 1.250 | 63.15 | 51.87 | 25.86 | 11.79 | 9.12 | 5.05 | 7.74 | 18.43 |
| 1.325 | 64.54 | 59.58 | 26.13 | 8.09 | 11.38 | 13.70 | 10.46 | 19.42 |
| 1.390 | 85.61 | 79.97 | 51.62 | 19.29 | 14.43 | 4.60 | 5.60 | 18.54 |
| 1.620 | 98.05 | 94.72 | 80.28 | 51.72 | 50.44 | 27.41 | 10.49 | 50.03 |
| 2.000 | 99.03 | 99.32 | 95.97 | 84.57 | 76.91 | 40.21 | 10.55 | 84.30 |
| 2.400 | 99.99 | 99.60 | 98.32 | 95.01 | 93.83 | 75.55 | 10.48 | 90.29 |
| SG. SEP. | 1.25 | 1.25 | 1.39 | 1.61 | 1.62 | 2.11 | 2.40 | 1.62 |

TEST 11122

SIZE CLASSIFICATION IN AMC

| SIZE (MIC) | SPGR=1.250 | SPGR=1.325 | SPGR=1.390 | SPGR=1.620 | SPGR=2.0 | SPGR=2.4 | OVERALL |
|---|---|---|---|---|---|---|---|
| 35.0 | 7.02 | 5.22 | 4.38 | 16.75 | 38.98 | 93.47 | 6.85 |
| 100.0 | 6.24 | 8.90 | 8.35 | 43.29 | 74.06 | 94.92 | 19.17 |
| 175.0 | 9.10 | 21.26 | 27.24 | 78.71 | 96.04 | 99.13 | 36.29 |
| 250.0 | 19.96 | 44.28 | 44.57 | 89.64 | 98.32 | 99.36 | 48.16 |
| 360.0 | 68.12 | 68.62 | 86.43 | 97.96 | 99.72 | 99.78 | 82.67 |
| 625.0 | 90.68 | 96.26 | 98.34 | 99.52 | 100.00 | 100.00 | 96.77 |
| 1000.0 | 100.00 | 100.00 | 100.00 | 100.00 | 100.00 | 100.00 | 99.90 |
| D50 | 303.34 | 270.11 | 264.27 | 105.76 | 55.42 | 35.00 | 254.63 |

DENSITY PARTITION IN AMC

| DENSITY | 35.0 mic. | 100.0 mic. | 175.0 mic. | 250.0 mic. | 360.0 mic. | 625.0 mic. | 1000.0 mic. | OVERALL |
|---|---|---|---|---|---|---|---|---|
| 1.250 | 100.00 | 86.95 | 59.40 | 14.59 | 6.41 | 4.36 | 4.91 | 25.74 |
| 1.325 | 100.00 | 94.63 | 59.95 | 35.24 | 15.60 | 6.27 | 3.64 | 24.70 |
| 1.390 | 100.00 | 97.60 | 81.34 | 35.51 | 20.41 | 5.87 | 3.04 | 19.11 |
| 1.620 | 100.00 | 99.31 | 97.05 | 85.55 | 71.68 | 34.33 | 12.11 | 51.43 |
| 2.000 | 100.00 | 100.00 | 99.59 | 97.56 | 94.31 | 66.16 | 30.43 | 89.23 |
| 2.400 | 100.00 | 100.00 | 99.68 | 99.07 | 98.74 | 92.75 | 90.74 | 98.24 |

| | | | | | | | | |
|---|---|---|---|---|---|---|---|---|
| SG. SEP. | 1.25 | 1.25 | 1.25 | 1.46 | 1.53 | 1.79 | 2.13 | 1.59 |

TEST 11123

SIZE CLASSIFICATION IN AMC

| SIZE (MIC) | SPGR=1.250 | SPGR=1.325 | SPGR=1.390 | SPGR=1.620 | SPGR=2.0 | SPGR=2.4 | OVERALL |
|---|---|---|---|---|---|---|---|
| 35.0 | 14.55 | 6.84 | 4.34 | 6.22 | 26.73 | 58.16 | 6.94 |
| 100.0 | 9.73 | 6.11 | 9.36 | 45.17 | 82.31 | 96.02 | 20.04 |
| 175.0 | 14.83 | 25.61 | 47.01 | 85.04 | 97.08 | 99.01 | 40.00 |
| 250.0 | 37.17 | 57.65 | 78.47 | 94.83 | 98.85 | 99.26 | 65.38 |
| 360.0 | 82.38 | 95.16 | 95.54 | 97.94 | 99.30 | 100.00 | 93.37 |
| 625.0 | 100.00 | 100.00 | 100.00 | 100.00 | 100.00 | 100.00 | 99.94 |
| 1000.0 | 100.00 | 100.00 | 100.00 | 100.00 | 100.00 | 100.00 | 99.90 |
| D50 | 250.11 | 234.07 | 178.52 | 109.09 | 62.21 | 35.00 | 205.02 |

DENSITY PARTITION IN AMC

| DENSITY | 35.0 mic. | 100.0 mic. | 175.0 mic. | 250.0 mic. | 360.0 mic. | 625.0 mic. | 1000.0 mic. | OVERALL |
|---|---|---|---|---|---|---|---|---|
| 1.250 | 100.00 | 100.00 | 79.33 | 32.69 | 12.50 | 8.13 | 12.26 | 35.73 |
| 1.325 | 100.00 | 100.00 | 94.17 | 52.78 | 22.03 | 5.07 | 5.69 | 30.23 |
| 1.390 | 100.00 | 100.00 | 94.62 | 74.95 | 42.13 | 7.82 | 3.59 | 25.01 |
| 1.620 | 100.00 | 100.00 | 97.50 | 93.77 | 82.35 | 40.34 | 5.16 | 45.96 |
| 2.000 | 100.00 | 100.00 | 99.14 | 98.60 | 96.46 | 79.25 | 23.05 | 88.97 |
| 2.400 | 100.00 | 100.00 | 100.00 | 99.10 | 98.79 | 95.20 | 53.30 | 94.88 |
| SG. SEP. | 1.25 | 1.25 | 1.25 | 1.31 | 1.39 | 1.67 | 2.36 | 1.66 |

TEST 11211

SIZE CLASSIFICATION IN AMC

| SIZE (MIC) | SPGR=1.250 | SPGR=1.325 | SPGR=1.390 | SPGR=1.620 | SPGR=2.0 | SPGR=2.4 | OVERALL |
|---|---|---|---|---|---|---|---|
| 35.0 | 2.76 | 4.06 | 11.12 | 11.43 | 16.62 | 37.90 | 5.60 |
| 100.0 | 4.39 | 13.33 | 16.40 | 33.11 | 50.94 | 80.30 | 14.74 |
| 175.0 | 12.03 | 14.85 | 20.90 | 44.12 | 76.14 | 93.46 | 24.76 |
| 250.0 | 8.39 | 26.70 | 35.93 | 60.96 | 89.57 | 97.24 | 36.50 |
| 360.0 | 16.40 | 35.99 | 52.53 | 82.13 | 97.01 | 99.07 | 53.96 |
| 625.0 | 46.34 | 56.92 | 74.25 | 94.76 | 99.05 | 99.77 | 72.91 |
| 1000.0 | 65.45 | 69.36 | 90.25 | 99.05 | 99.63 | 100.00 | 83.68 |
| D50 | 696.86 | 508.40 | 339.59 | 204.35 | 98.22 | 53.55 | 329.21 |

DENSITY PARTITION IN AMC

| DENSITY | 35.0 mic. | 100.0 mic. | 175.0 mic. | 250.0 mic. | 360.0 mic. | 625.0 mic. | 1000.0 mic. | OVERALL |
|---|---|---|---|---|---|---|---|---|
| 1.250 | 47.65 | 29.33 | 8.62 | 4.21 | 6.17 | 2.16 | 1.35 | 9.96 |
| 1.325 | 52.10 | 38.84 | 21.27 | 14.90 | 7.73 | 6.88 | 1.99 | 11.44 |
| 1.390 | 81.65 | 58.09 | 34.71 | 21.23 | 11.27 | 8.61 | 5.67 | 16.53 |
| 1.620 | 98.05 | 89.68 | 68.83 | 42.86 | 27.50 | 19.21 | 5.84 | 35.54 |
| 2.000 | 99.22 | 98.05 | 93.98 | 80.50 | 60.53 | 33.29 | 8.74 | 78.34 |
| 2.400 | 99.99 | 99.52 | 98.08 | 94.43 | 87.30 | 66.20 | 22.68 | 88.07 |
| SG. SEP. | 1.29 | 1.37 | 1.47 | 1.66 | 1.88 | 2.20 | 2.40 | 1.64 |

TEST 11212

SIZE CLASSIFICATION IN AMC

| SIZE (MIC) | SPGR=1.250 | SPGR=1.325 | SPGR=1.390 | SPGR=1.620 | SPGR=2.0 | SPGR=2.4 | OVERALL |
|---|---|---|---|---|---|---|---|
| 35.0 | 4.70 | 3.16 | 6.85 | 13.94 | 19.16 | 40.63 | 5.62 |
| 100.0 | 8.30 | 4.76 | 7.39 | 52.32 | 58.97 | 91.62 | 15.47 |
| 175.0 | 15.83 | 10.17 | 11.69 | 47.62 | 85.64 | 96.89 | 24.00 |
| 250.0 | 14.88 | 26.04 | 28.39 | 70.87 | 95.30 | 98.79 | 35.76 |
| 360.0 | 24.46 | 39.37 | 52.71 | 89.88 | 98.68 | 99.59 | 53.53 |

| | | | | | | | |
|---|---|---|---|---|---|---|---|
| 625.0 | 63.04 | 69.09 | 87.28 | 98.12 | 99.69 | 99.73 | 78.60 |
| 1000.0 | 87.38 | 94.82 | 98.14 | 99.68 | 99.70 | 100.00 | 93.11 |
| D50 | 529.95 | 445.54 | 346.14 | 96.07 | 85.36 | 46.94 | 335.89 |

DENSITY PARTITION IN AMC

| DENSITY | 35.0 mic. | 100.0 mic. | 175.0 mic. | 250.0 mic. | 360.0 mic. | 625.0 mic. | 1000.0 mic. | OVERALL |
|---|---|---|---|---|---|---|---|---|
| 1.250 | 78.79 | 47.78 | 14.80 | 8.57 | 9.16 | 4.63 | 2.58 | 19.52 |
| 1.325 | 90.76 | 54.52 | 25.83 | 15.89 | 5.73 | 2.61 | 1.72 | 17.06 |
| 1.390 | 96.59 | 78.64 | 37.42 | 17.53 | 6.63 | 4.10 | 3.79 | 21.03 |
| 1.620 | 99.41 | 96.56 | 82.65 | 56.62 | 32.78 | 37.05 | 7.99 | 44.85 |
| 2.000 | 99.44 | 99.42 | 97.56 | 91.58 | 76.19 | 43.53 | 11.28 | 81.05 |
| 2.400 | 99.99 | 99.49 | 99.24 | 97.77 | 94.35 | 85.44 | 26.85 | 89.00 |
| SG.'SEP. | 1.25 | 1.27 | 1.41 | 1.58 | 1.72 | 2.06 | 2.40 | 1.67 |

TEST 11213

SIZE CLASSIFICATION IN AMC

| SIZE (MIC) | SPGR=1.250 | SPGR=1.325 | SPGR=1.390 | SPGR=1.620 | SPGR=2.0 | SPGR=2.4 | OVERALL |
|---|---|---|---|---|---|---|---|
| 35.0 | 0.30 | 5.72 | 8.70 | 10.07 | 20.94 | 59.09 | 6.35 |
| 100.0 | 3.99 | 7.08 | 10.90 | 45.76 | 70.29 | 93.62 | 19.27 |
| 175.0 | 7.31 | 21.06 | 24.99 | 66.70 | 93.72 | 98.67 | 33.53 |
| 250.0 | 15.54 | 27.19 | 45.45 | 85.82 | 98.25 | 99.53 | 52.16 |
| 360.0 | 36.08 | 56.08 | 76.81 | 96.40 | 99.58 | 99.81 | 73.86 |
| 625.0 | 78.36 | 90.99 | 95.76 | 99.48 | 99.63 | 100.00 | 92.34 |
| 1000.0 | 100.00 | 100.00 | 100.00 | 100.00 | 100.00 | 100.00 | 99.92 |
| D50 | 415.98 | 353.02 | 257.22 | 113.82 | 73.27 | 35.00 | 241.38 |

DENSITY PARTITION IN AMC

| DENSITY | 35.0 mic. | 100.0 mic. | 175.0 mic. | 250.0 mic. | 360.0 mic. | 625.0 mic. | 1000.0 mic. | OVERALL |
|---|---|---|---|---|---|---|---|---|
| 1.250 | 100.00 | 71.61 | 28.22 | 11.36 | 5.21 | 2.81 | 0.21 | 16.41 |
| 1.325 | 100.00 | 87.56 | 47.07 | 20.64 | 15.67 | 5.04 | 4.05 | 25.63 |
| 1.390 | 100.00 | 94.02 | 69.77 | 36.72 | 18.83 | 7.85 | 6.23 | 27.59 |
| 1.620 | 100.00 | 99.26 | 94.91 | 80.82 | 58.26 | 37.02 | 7.24 | 50.52 |
| 2.000 | 100.00 | 99.47 | 99.40 | 97.51 | 91.22 | 62.24 | 15.58 | 88.05 |
| 2.400 | 100.00 | 100.00 | 99.72 | 99.33 | 98.11 | 91.09 | 50.15 | 94.85 |
| SG. SEP. | 1.25 | 1.25 | 1.33 | 1.41 | 1.61 | 1.81 | 2.40 | 1.61 |

TEST 11221

SIZE CLASSIFICATION IN AMC

| SIZE (MIC) | SPGR=1.250 | SPGR=1.325 | SPGR=1.390 | SPGR=1.620 | SPGR=2.0 | SPGR=2.4 | OVERALL |
|---|---|---|---|---|---|---|---|
| 35.0 | 8.23 | 6.68 | 9.95 | 19.18 | 20.42 | 39.71 | 7.27 |
| 100.0 | 14.01 | 5.26 | 11.54 | 31.17 | 50.65 | 84.73 | 15.72 |
| 175.0 | 13.52 | 7.71 | 12.70 | 43.49 | 72.48 | 92.62 | 22.34 |
| 250.0 | 11.55 | 25.28 | 33.72 | 55.64 | 88.08 | 97.32 | 36.50 |
| 360.0 | 19.56 | 23.42 | 42.40 | 78.31 | 96.60 | 99.18 | 55.09 |
| 625.0 | 38.16 | 53.65 | 69.81 | 93.75 | 99.42 | 99.83 | 72.43 |
| 1000.0 | 48.40 | 54.14 | 74.29 | 98.34 | 99.79 | 100.00 | 78.77 |
| D50 | 1000.00 | 593.03 | 433.47 | 215.66 | 98.60 | 49.85 | 319.41 |

DENSITY PARTITION IN AMC

| DENSITY | 35.0 mic. | 100.0 mic. | 175.0 mic. | 250.0 mic. | 360.0 mic. | 625.0 mic. | 1000.0 mic. | OVERALL |
|---|---|---|---|---|---|---|---|---|
| 1.250 | 34.56 | 25.79 | 12.04 | 6.85 | 8.09 | 8.40 | 4.81 | 12.69 |
| 1.325 | 39.93 | 39.45 | 14.69 | 16.00 | 4.49 | 3.03 | 3.88 | 10.62 |
| 1.390 | 61.93 | 56.55 | 29.30 | 22.27 | 7.57 | 6.84 | 5.86 | 16.19 |
| 1.620 | 97.08 | 89.41 | 67.03 | 41.39 | 30.23 | 20.32 | 11.79 | 46.59 |
| 2.000 | 99.63 | 98.97 | 94.11 | 80.62 | 59.72 | 36.63 | 12.62 | 83.04 |
| 2.400 | 99.99 | 99.71 | 98.56 | 95.33 | 87.60 | 75.76 | 27.05 | 91.34 |

| | | | | | | | | |
|---|---|---|---|---|---|---|---|---|
| SG. SEP. | 1.39 | 1.37 | 1.49 | 1.68 | 1.87 | 2.14 | 2.40 | 1.66 |

TEST 11222

SIZE CLASSIFICATION IN AMC

| SIZE (MIC) | SPGR=1.250 | SPGR=1.325 | SPGR=1.390 | SPGR=1.620 | SPGR=2.0 | SPGR=2.4 | OVERALL |
|---|---|---|---|---|---|---|---|
| 35.0 | 14.01 | 6.47 | 7.30 | 13.75 | 20.97 | 45.58 | 7.38 |
| 100.0 | 6.18 | 12.16 | 9.95 | 41.95 | 64.94 | 91.42 | 18.15 |
| 175.0 | 6.99 | 11.32 | 19.78 | 60.42 | 89.06 | 98.08 | 27.05 |
| 250.0 | 11.69 | 36.46 | 26.13 | 79.24 | 96.65 | 99.32 | 42.11 |
| 360.0 | 37.19 | 54.02 | 64.89 | 93.00 | 99.21 | 99.57 | 66.20 |
| 625.0 | 79.42 | 71.12 | 89.22 | 98.56 | 99.49 | 100.00 | 85.75 |
| 1000.0 | 100.00 | 100.00 | 100.00 | 100.00 | 100.00 | 100.00 | 99.92 |
| D50 | 403.11 | 323.93 | 337.88 | 131.37 | 77.91 | 41.27 | 276.56 |

DENSITY PARTITION IN AMC

| DENSITY | 35.0 mic. | 100.0 mic. | 175.0 mic. | 250.0 mic. | 360.0 mic. | 625.0 mic. | 1000.0 mic. | OVERALL |
|---|---|---|---|---|---|---|---|---|
| 1.250 | 100.00 | 72.00 | 28.30 | 8.11 | 4.77 | 4.21 | 9.79 | 18.84 |
| 1.325 | 100.00 | 62.14 | 43.92 | 27.66 | 7.84 | 8.44 | 4.40 | 24.42 |
| 1.390 | 100.00 | 84.66 | 55.20 | 19.08 | 14.12 | 6.86 | 4.98 | 21.77 |
| 1.620 | 100.00 | 97.86 | 89.85 | 71.79 | 50.43 | 32.51 | 9.61 | 52.16 |
| 2.000 | 100.00 | 99.23 | 98.81 | 95.06 | 84.44 | 55.25 | 15.03 | 85.95 |
| 2.400 | 100.00 | 99.99 | 99.36 | 98.99 | 97.14 | 87.66 | 35.82 | 92.54 |
| SG. SEP. | 1.25 | 1.25 | 1.36 | 1.52 | 1.62 | 1.91 | 2.40 | 1.56 |

TEST 11223

SIZE CLASSIFICATION IN AMC

| SIZE (MIC) | SPGR=1.250 | SPGR=1.325 | SPGR=1.390 | SPGR=1.620 | SPGR=2.0 | SPGR=2.4 | OVERALL |
|---|---|---|---|---|---|---|---|
| 35.0 | 8.04 | 6.21 | 8.66 | 11.96 | 20.58 | 52.72 | 9.08 |
| 100.0 | 8.10 | 10.37 | 13.16 | 34.73 | 77.78 | 95.14 | 20.87 |
| 175.0 | 12.74 | 17.19 | 23.95 | 64.73 | 93.79 | 98.92 | 34.12 |
| 250.0 | 21.06 | 32.13 | 49.93 | 85.14 | 98.49 | 99.65 | 52.16 |
| 360.0 | 45.72 | 61.26 | 75.97 | 96.00 | 99.65 | 99.86 | 75.69 |
| 625.0 | 84.53 | 90.49 | 96.97 | 99.56 | 99.88 | 100.00 | 94.34 |
| 1000.0 | 100.00 | 100.00 | 100.00 | 100.00 | 100.00 | 100.00 | 99.92 |
| D50 | 368.36 | 312.45 | 250.15 | 136.18 | 68.43 | 35.00 | 241.57 |

DENSITY PARTITION IN AMC

| DENSITY | 35.0 mic. | 100.0 mic. | 175.0 mic. | 250.0 mic. | 360.0 mic. | 625.0 mic. | 1000.0 mic. | OVERALL |
|---|---|---|---|---|---|---|---|---|
| 1.250 | 100.00 | 81.06 | 39.75 | 17.28 | 10.27 | 6.45 | 6.41 | 24.05 |
| 1.325 | 100.00 | 88.17 | 55.33 | 27.05 | 13.98 | 8.31 | 4.93 | 30.16 |
| 1.390 | 100.00 | 96.16 | 71.23 | 43.85 | 19.79 | 10.61 | 6.91 | 29.07 |
| 1.620 | 100.00 | 99.44 | 94.94 | 81.78 | 58.97 | 29.41 | 9.62 | 50.68 |
| 2.000 | 100.00 | 99.84 | 99.56 | 98.09 | 92.20 | 73.27 | 16.87 | 87.75 |
| 2.400 | 100.00 | 100.00 | 99.82 | 99.55 | 98.63 | 93.88 | 46.61 | 94.12 |
| SG. SEP. | 1.25 | 1.25 | 1.30 | 1.40 | 1.58 | 1.77 | 2.40 | 1.58 |

TEST 12111

SIZE CLASSIFICATION IN AMC

| SIZE (MIC) | SPGR=1.250 | SPGR=1.325 | SPGR=1.390 | SPGR=1.620 | SPGR=2.0 | SPGR=2.4 | OVERALL |
|---|---|---|---|---|---|---|---|
| 35.0 | 41.12 | 11.38 | 8.37 | 22.77 | 40.68 | 51.56 | 15.07 |
| 100.0 | 17.91 | 13.25 | 19.68 | 36.95 | 65.87 | 90.70 | 30.35 |
| 175.0 | 33.57 | 18.41 | 34.56 | 62.50 | 88.81 | 96.14 | 48.15 |
| 250.0 | 40.06 | 49.01 | 55.52 | 81.10 | 94.76 | 98.14 | 64.24 |

| | | | | | | | |
|---|---|---|---|---|---|---|---|
| 360.0 | 59.02 | 64.42 | 75.58 | 90.93 | 97.53 | 98.95 | 80.15 |
| 625.0 | 83.71 | 87.25 | 91.61 | 97.00 | 98.99 | 100.00 | 93.20 |
| 1000.0 | 94.29 | 96.48 | 98.32 | 99.49 | 100.00 | 100.00 | 97.80 |
| D50 | 317.94 | 255.50 | 229.70 | 140.01 | 59.05 | 35.00 | 182.69 |

DENSITY PARTITION IN AMC

| DENSITY | 35.0 mic. | 100.0 mic. | 175.0 mic. | 250.0 mic. | 360.0 mic. | 625.0 mic. | 1000.0 mic. | OVERALL |
|---|---|---|---|---|---|---|---|---|
| 1.250 | 94.72 | 84.80 | 60.99 | 42.05 | 35.42 | 19.15 | 43.12 | 49.17 |
| 1.325 | 96.75 | 88.13 | 66.28 | 51.06 | 19.67 | 14.22 | 12.23 | 32.92 |
| 1.390 | 98.45 | 92.22 | 77.06 | 57.54 | 36.43 | 21.02 | 9.02 | 35.07 |
| 1.620 | 99.53 | 97.23 | 91.58 | 82.33 | 64.41 | 38.88 | 24.25 | 64.14 |
| 2.000 | 100.00 | 99.07 | 97.72 | 95.15 | 89.60 | 67.69 | 42.68 | 88.62 |
| 2.400 | 100.00 | 100.00 | 99.03 | 98.29 | 96.44 | 91.37 | 53.61 | 93.39 |
| SG. SEP. | 1.25 | 1.25 | 1.25 | 1.32 | 1.48 | 1.76 | 2.27 | 1.60 |

TEST 12112

SIZE CLASSIFICATION IN AMC

| SIZE (MIC) | SPGR=1.250 | SPGR=1.325 | SPGR=1.390 | SPGR=1.620 | SPGR=2.0 | SPGR=2.4 | OVERALL |
|---|---|---|---|---|---|---|---|
| 35.0 | 7.22 | 3.82 | 6.81 | 25.27 | 25.47 | 49.42 | 12.35 |
| 100.0 | 12.63 | 6.58 | 28.20 | 59.27 | 79.50 | 90.72 | 31.83 |
| 175.0 | 28.24 | 33.40 | 61.40 | 87.62 | 94.23 | 98.21 | 58.83 |
| 250.0 | 58.07 | 65.03 | 75.52 | 94.48 | 97.23 | 99.36 | 79.81 |
| 360.0 | 69.92 | 78.19 | 87.22 | 95.49 | 99.47 | 99.50 | 88.42 |
| 625.0 | 100.00 | 100.00 | 100.00 | 100.00 | 100.00 | 100.00 | 99.97 |
| 1000.0 | 100.00 | 100.00 | 100.00 | 100.00 | 100.00 | 100.00 | 99.94 |
| D50 | 214.23 | 194.85 | 140.48 | 82.28 | 64.51 | 35.91 | 149.84 |

DENSITY PARTITION IN AMC

| DENSITY | 35.0 mic. | 100.0 mic. | 175.0 mic. | 250.0 mic. | 360.0 mic. | 625.0 mic. | 1000.0 mic. | OVERALL |
|---|---|---|---|---|---|---|---|---|
| 1.250 | 100.00 | 100.00 | 73.36 | 62.13 | 31.80 | 14.63 | 8.44 | 47.98 |
| 1.325 | 100.00 | 100.00 | 80.94 | 68.78 | 37.27 | 7.70 | 4.49 | 35.03 |
| 1.390 | 100.00 | 100.00 | 88.99 | 78.52 | 65.33 | 31.75 | 7.96 | 37.73 |
| 1.620 | 100.00 | 100.00 | 96.17 | 95.30 | 89.35 | 63.29 | 28.60 | 70.49 |
| 2.000 | 100.00 | 100.00 | 99.55 | 97.65 | 95.08 | 82.12 | 28.82 | 90.66 |
| 2.400 | 100.00 | 100.00 | 99.58 | 99.46 | 98.48 | 92.05 | 53.65 | 94.04 |
| SG. SEP. | 2.40 | 1.25 | 1.25 | 1.25 | 1.35 | 1.48 | 2.34 | 1.55 |

TEST 12113

SIZE CLASSIFICATION IN AMC

| SIZE (MIC) | SPGR=1.250 | SPGR=1.325 | SPGR=1.390 | SPGR=1.620 | SPGR=2.0 | SPGR=2.4 | OVERALL |
|---|---|---|---|---|---|---|---|
| 35.0 | 5.81 | 4.06 | 7.53 | 19.07 | 37.61 | 63.73 | 15.58 |
| 100.0 | 19.73 | 23.47 | 37.74 | 74.40 | 86.45 | 96.05 | 49.23 |
| 175.0 | 41.85 | 63.09 | 71.33 | 90.13 | 96.00 | 98.81 | 74.12 |
| 250.0 | 73.43 | 81.66 | 86.86 | 94.94 | 97.43 | 99.99 | 90.74 |
| 360.0 | 85.02 | 86.02 | 92.78 | 97.56 | 98.58 | 100.00 | 95.33 |
| 625.0 | 100.00 | 100.00 | 100.00 | 100.00 | 100.00 | 100.00 | 99.98 |
| 1000.0 | 100.00 | 100.00 | 100.00 | 100.00 | 100.00 | 100.00 | 99.94 |
| D50 | 181.69 | 146.15 | 119.82 | 71.34 | 51.49 | 35.00 | 101.82 |

DENSITY PARTITION IN AMC

| DENSITY | 35.0 mic. | 100.0 mic. | 175.0 mic. | 250.0 mic. | 360.0 mic. | 625.0 mic. | 1000.0 mic. | OVERALL |
|---|---|---|---|---|---|---|---|---|
| 1.250 | 100.00 | 100.00 | 89.61 | 80.77 | 52.23 | 27.20 | 8.57 | 63.82 |
| 1.325 | 100.00 | 100.00 | 90.34 | 87.12 | 72.20 | 31.78 | 6.05 | 47.06 |
| 1.390 | 100.00 | 100.00 | 95.13 | 90.95 | 79.08 | 47.94 | 11.00 | 41.23 |
| 1.620 | 100.00 | 100.00 | 98.38 | 96.61 | 93.27 | 81.54 | 26.36 | 66.94 |
| 2.000 | 100.00 | 100.00 | 99.06 | 98.29 | 97.33 | 90.65 | 47.80 | 94.14 |

| | | | | | | | | |
|---|---|---|---|---|---|---|---|---|
| 2.400 | 100.00 | 100.00 | 100.00 | 100.00 | 99.21 | 97.37 | 72.75 | 97.11 |
| SG. SEP. | 2.40 | 1.25 | 1.25 | 1.25 | 1.25 | 1.40 | 2.04 | 1.25 |

TEST 12121

SIZE CLASSIFICATION IN AMC

| SIZE (MIC) | SPGR=1.250 | SPGR=1.325 | SPGR=1.390 | SPGR=1.620 | SPGR=2.0 | SPGR=2.4 | OVERALL |
|---|---|---|---|---|---|---|---|
| 35.0 | 26.94 | 6.61 | 9.29 | 20.25 | 34.15 | 55.54 | 15.31 |
| 100.0 | 11.15 | 10.03 | 25.20 | 53.24 | 69.37 | 87.12 | 30.66 |
| 175.0 | 20.65 | 30.48 | 46.43 | 74.13 | 89.59 | 96.47 | 50.23 |
| 250.0 | 35.48 | 44.75 | 61.82 | 84.59 | 94.34 | 98.08 | 66.29 |
| 360.0 | 59.48 | 71.87 | 77.18 | 91.04 | 95.04 | 99.99 | 83.25 |
| 625.0 | 77.65 | 75.59 | 89.51 | 97.49 | 99.18 | 100.00 | 93.93 |
| 1000.0 | 100.00 | 100.00 | 100.00 | 100.00 | 100.00 | 100.00 | 99.94 |
| D50 | 300.53 | 271.30 | 190.10 | 93.62 | 64.25 | 35.00 | 174.06 |

DENSITY PARTITION IN AMC

| DENSITY | 35.0 mic. | 100.0 mic. | 175.0 mic. | 250.0 mic. | 360.0 mic. | 625.0 mic. | 1000.0 mic. | OVERALL |
|---|---|---|---|---|---|---|---|---|
| 1.250 | 100.00 | 80.11 | 62.99 | 38.93 | 23.18 | 12.71 | 29.95 | 42.58 |
| 1.325 | 100.00 | 78.21 | 74.76 | 48.43 | 33.70 | 11.45 | 7.59 | 32.17 |
| 1.390 | 100.00 | 90.82 | 79.68 | 65.25 | 50.12 | 28.09 | 10.61 | 36.09 |
| 1.620 | 100.00 | 97.83 | 92.17 | 86.42 | 76.86 | 56.90 | 22.75 | 63.27 |
| 2.000 | 100.00 | 99.29 | 95.69 | 95.08 | 90.89 | 72.42 | 37.56 | 91.21 |
| 2.400 | 100.00 | 100.00 | 99.99 | 98.34 | 96.94 | 88.69 | 59.16 | 94.85 |
| SG. SEP. | 2.40 | 1.25 | 1.25 | 1.33 | 1.39 | 1.52 | 2.23 | 1.54 |

TEST 12122

SIZE CLASSIFICATION IN AMC

| SIZE (MIC) | SPGR=1.250 | SPGR=1.325 | SPGR=1.390 | SPGR=1.620 | SPGR=2.0 | SPGR=2.4 | OVERALL |
|---|---|---|---|---|---|---|---|
| 35.0 | 22.70 | 6.53 | 5.59 | 12.46 | 41.65 | 65.10 | 12.22 |
| 100.0 | 8.78 | 25.13 | 23.82 | 67.52 | 83.00 | 96.27 | 35.63 |
| 175.0 | 31.39 | 45.82 | 62.30 | 89.29 | 96.29 | 99.10 | 62.74 |
| 250.0 | 54.15 | 81.85 | 85.73 | 93.51 | 97.51 | 99.99 | 83.57 |
| 360.0 | 70.68 | 85.20 | 91.77 | 96.41 | 98.25 | 100.00 | 91.77 |
| 625.0 | 100.00 | 100.00 | 100.00 | 100.00 | 100.00 | 100.00 | 99.97 |
| 1000.0 | 100.00 | 100.00 | 100.00 | 100.00 | 100.00 | 100.00 | 99.93 |
| D50 | 231.96 | 183.71 | 151.52 | 79.32 | 48.12 | 35.00 | 138.10 |

DENSITY PARTITION IN AMC

| DENSITY | 35.0 mic. | 100.0 mic. | 175.0 mic. | 250.0 mic. | 360.0 mic. | 625.0 mic. | 1000.0 mic. | OVERALL |
|---|---|---|---|---|---|---|---|---|
| 1.250 | 100.00 | 100.00 | 74.61 | 59.00 | 35.80 | 10.50 | 26.35 | 48.61 |
| 1.325 | 100.00 | 100.00 | 87.52 | 84.60 | 50.75 | 29.03 | 7.84 | 42.15 |
| 1.390 | 100.00 | 100.00 | 93.15 | 87.98 | 66.82 | 27.59 | 6.73 | 35.57 |
| 1.620 | 100.00 | 100.00 | 97.03 | 94.61 | 91.04 | 71.69 | 14.78 | 59.09 |
| 2.000 | 100.00 | 100.00 | 98.56 | 97.95 | 96.93 | 85.61 | 46.52 | 93.05 |
| 2.400 | 100.00 | 100.00 | 100.00 | 99.99 | 99.26 | 96.92 | 69.45 | 96.52 |
| SG. SEP. | 1.25 | 1.25 | 1.25 | 1.25 | 1.32 | 1.51 | 2.06 | 1.40 |

TEST 12123

SIZE CLASSIFICATION IN AMC

| SIZE (MIC) | SPGR=1.250 | SPGR=1.325 | SPGR=1.390 | SPGR=1.620 | SPGR=2.0 | SPGR=2.4 | OVERALL |
|---|---|---|---|---|---|---|---|
| 35.0 | 14.88 | 8.73 | 3.91 | 11.66 | 40.79 | 66.25 | 12.32 |
| 100.0 | 13.67 | 40.55 | 54.96 | 76.91 | 90.07 | 97.02 | 55.57 |
| 175.0 | 53.25 | 60.84 | 72.97 | 86.76 | 96.58 | 98.92 | 76.99 |

| | | | | | | | |
|---|---|---|---|---|---|---|---|
| 250.0 | 75.42 | 86.46 | 86.88 | 92.56 | 96.70 | 99.99 | 90.51 |
| 360.0 | 84.88 | 90.74 | 91.48 | 97.30 | 97.78 | 100.00 | 95.04 |
| 625.0 | 100.00 | 100.00 | 100.00 | 100.00 | 100.00 | 100.00 | 99.97 |
| 1000.0 | 100.00 | 100.00 | 100.00 | 100.00 | 100.00 | 100.00 | 99.93 |
| D50 | 168.84 | 134.33 | 93.69 | 73.20 | 47.15 | 35.00 | 91.63 |

DENSITY PARTITION IN AMC

| DENSITY | 35.0 mic. | 100.0 mic. | 175.0 mic. | 250.0 mic. | 360.0 mic. | 625.0 mic. | 1000.0 mic. | OVERALL |
|---|---|---|---|---|---|---|---|---|
| 1.250 | 100.00 | 100.00 | 89.12 | 81.74 | 62.44 | 18.78 | 20.33 | 64.83 |
| 1.325 | 100.00 | 100.00 | 93.46 | 90.31 | 69.39 | 49.89 | 12.24 | 49.92 |
| 1.390 | 100.00 | 100.00 | 94.00 | 90.62 | 79.76 | 64.04 | 5.61 | 38.12 |
| 1.620 | 100.00 | 100.00 | 98.13 | 94.78 | 90.53 | 82.94 | 16.15 | 61.23 |
| 2.000 | 100.00 | 100.00 | 98.47 | 97.72 | 97.63 | 92.97 | 50.13 | 93.80 |
| 2.400 | 100.00 | 100.00 | 100.00 | 100.00 | 99.25 | 97.94 | 74.13 | 97.08 |
| SG. SEP. | 2.40 | 1.25 | 1.25 | 1.25 | 1.25 | 1.33 | 2.00 | 1.25 |

TEST 12211

SIZE CLASSIFICATION IN AMC

| SIZE (MIC) | SPGR=1.250 | SPGR=1.325 | SPGR=1.390 | SPGR=1.620 | SPGR=2.0 | SPGR=2.4 | OVERALL |
|---|---|---|---|---|---|---|---|
| 35.0 | 13.23 | 4.97 | 10.36 | 29.90 | 29.61 | 48.52 | 12.39 |
| 100.0 | 11.98 | 14.31 | 21.96 | 34.08 | 61.97 | 84.58 | 25.59 |
| 175.0 | 20.52 | 27.84 | 35.39 | 61.97 | 86.22 | 95.47 | 39.93 |
| 250.0 | 30.45 | 28.91 | 55.40 | 67.53 | 93.87 | 97.80 | 55.97 |
| 360.0 | 44.94 | 55.48 | 66.32 | 87.77 | 96.61 | 98.71 | 70.95 |
| 625.0 | 73.07 | 84.68 | 86.20 | 97.32 | 99.00 | 100.00 | 90.88 |
| 1000.0 | 93.89 | 95.78 | 98.28 | 99.22 | 100.00 | 100.00 | 97.40 |
| D50 | 397.88 | 337.29 | 221.19 | 145.54 | 75.96 | 37.66 | 219.80 |

DENSITY PARTITION IN AMC

| DENSITY | 35.0 mic. | 100.0 mic. | 175.0 mic. | 250.0 mic. | 360.0 mic. | 625.0 mic. | 1000.0 mic. | OVERALL |
|---|---|---|---|---|---|---|---|---|
| 1.250 | 93.44 | 71.57 | 43.09 | 28.88 | 19.32 | 11.21 | 12.39 | 35.04 |
| 1.325 | 95.46 | 83.68 | 53.62 | 27.39 | 26.36 | 13.41 | 4.63 | 30.63 |
| 1.390 | 98.14 | 85.28 | 64.63 | 53.53 | 33.69 | 20.70 | 9.68 | 30.46 |
| 1.620 | 99.16 | 97.12 | 86.93 | 65.86 | 60.18 | 32.41 | 28.35 | 64.15 |
| 2.000 | 100.00 | 98.92 | 96.36 | 93.42 | 85.30 | 60.18 | 28.06 | 89.20 |
| 2.400 | 100.00 | 100.00 | 98.61 | 97.63 | 95.13 | 83.58 | 46.65 | 93.28 |
| SG. SEP. | 1.25 | 1.25 | 1.30 | 1.38 | 1.52 | 1.87 | 2.40 | 1.52 |

TEST 12212

SIZE CLASSIFICATION IN AMC

| SIZE (MIC) | SPGR=1.250 | SPGR=1.325 | SPGR=1.390 | SPGR=1.620 | SPGR=2.0 | SPGR=2.4 | OVERALL |
|---|---|---|---|---|---|---|---|
| 35.0 | 9.53 | 6.22 | 7.49 | 23.49 | 31.27 | 60.90 | 11.37 |
| 100.0 | 9.95 | 7.08 | 18.00 | 54.94 | 75.57 | 92.20 | 28.40 |
| 175.0 | 20.44 | 24.49 | 45.00 | 81.29 | 93.49 | 98.09 | 45.14 |
| 250.0 | 34.36 | 50.95 | 74.71 | 91.17 | 96.95 | 98.94 | 67.70 |
| 360.0 | 64.89 | 81.14 | 86.96 | 95.60 | 97.37 | 99.99 | 85.56 |
| 625.0 | 88.86 | 93.01 | 96.18 | 99.11 | 99.09 | 100.00 | 96.51 |
| 1000.0 | 100.00 | 100.00 | 100.00 | 100.00 | 100.00 | 100.00 | 99.94 |
| D50 | 297.89 | 247.46 | 179.11 | 89.79 | 62.48 | 35.00 | 190.45 |

DENSITY PARTITION IN AMC

| DENSITY | 35.0 mic. | 100.0 mic. | 175.0 mic. | 250.0 mic. | 360.0 mic. | 625.0 mic. | 1000.0 mic. | OVERALL |
|---|---|---|---|---|---|---|---|---|
| 1.250 | 100.00 | 88.95 | 65.11 | 34.58 | 20.59 | 10.04 | 9.62 | 38.44 |
| 1.325 | 100.00 | 93.07 | 81.29 | 51.19 | 24.67 | 7.14 | 6.28 | 31.10 |
| 1.390 | 100.00 | 96.21 | 87.07 | 74.89 | 45.24 | 18.14 | 7.56 | 33.44 |
| 1.620 | 100.00 | 99.12 | 95.64 | 91.25 | 81.43 | 55.18 | 23.67 | 70.15 |

| | | | | | | | | |
|---|---|---|---|---|---|---|---|---|
| 2.000 | 100.00 | 99.10 | 97.39 | 96.98 | 93.55 | 75.75 | 31.48 | 90.16 |
| 2.400 | 100.00 | 100.00 | 99.99 | 98.95 | 98.11 | 92.27 | 61.13 | 95.10 |
| SG. SEP. | 2.40 | 1.25 | 1.25 | 1.32 | 1.42 | 1.57 | 2.25 | 1.60 |

TEST 12213

SIZE CLASSIFICATION IN AMC

| SIZE (MIC) | SPGR=1.250 | SPGR=1.325 | SPGR=1.390 | SPGR=1.620 | SPGR=2.0 | SPGR=2.4 | OVERALL |
|---|---|---|---|---|---|---|---|
| 35.0 | 10.33 | 4.78 | 7.77 | 16.10 | 42.76 | 65.09 | 13.27 |
| 100.0 | 15.80 | 14.35 | 37.40 | 67.24 | 85.05 | 94.88 | 43.51 |
| 175.0 | 33.00 | 37.95 | 64.29 | 85.99 | 96.11 | 98.54 | 61.84 |
| 250.0 | 56.03 | 69.34 | 79.20 | 92.83 | 96.47 | 99.99 | 81.18 |
| 360.0 | 76.25 | 80.95 | 89.92 | 96.69 | 98.41 | 100.00 | 91.74 |
| 625.0 | 100.00 | 100.00 | 100.00 | 100.00 | 100.00 | 100.00 | 99.97 |
| 1000.0 | 100.00 | 100.00 | 100.00 | 100.00 | 100.00 | 100.00 | 99.94 |
| D50 | 228.65 | 184.80 | 128.66 | 78.09 | 46.12 | 35.00 | 125.38 |

DENSITY PARTITION IN AMC

| DENSITY | 35.0 mic. | 100.0 mic. | 175.0 mic. | 250.0 mic. | 360.0 mic. | 625.0 mic. | 1000.0 mic. | OVERALL |
|---|---|---|---|---|---|---|---|---|
| 1.250 | 100.00 | 100.00 | 79.98 | 61.33 | 37.99 | 18.93 | 12.54 | 53.92 |
| 1.325 | 100.00 | 100.00 | 84.10 | 73.78 | 43.21 | 17.25 | 5.88 | 37.17 |
| 1.390 | 100.00 | 100.00 | 91.73 | 82.57 | 69.14 | 42.64 | 9.49 | 38.60 |
| 1.620 | 100.00 | 100.00 | 97.32 | 94.15 | 88.43 | 71.86 | 19.28 | 62.16 |
| 2.000 | 100.00 | 100.00 | 98.72 | 97.14 | 96.85 | 87.62 | 48.18 | 92.81 |
| 2.400 | 100.00 | 100.00 | 100.00 | 99.99 | 98.83 | 95.84 | 69.88 | 96.33 |
| SG. SEP. | 2.40 | 1.25 | 1.25 | 1.25 | 1.37 | 1.41 | 2.03 | 1.25 |

TEST 12221

SIZE CLASSIFICATION IN AMC

| SIZE (MIC) | SPGR=1.250 | SPGR=1.325 | SPGR=1.390 | SPGR=1.620 | SPGR=2.0 | SPGR=2.4 | OVERALL |
|---|---|---|---|---|---|---|---|
| 35.0 | 25.48 | 4.89 | 17.33 | 17.11 | 65.00 | 82.86 | 13.59 |
| 100.0 | 8.33 | 16.40 | 22.37 | 42.69 | 63.67 | 86.94 | 25.02 |
| 175.0 | 24.24 | 23.33 | 32.03 | 70.26 | 90.84 | 96.96 | 39.63 |
| 250.0 | 41.68 | 35.87 | 63.68 | 85.00 | 95.58 | 98.50 | 59.07 |
| 360.0 | 50.48 | 63.88 | 71.49 | 90.99 | 96.48 | 99.99 | 75.17 |
| 625.0 | 76.26 | 85.84 | 88.07 | 97.26 | 99.30 | 100.00 | 90.00 |
| 1000.0 | 100.00 | 100.00 | 100.00 | 100.00 | 100.00 | 100.00 | 99.90 |
| D50 | 353.45 | 297.57 | 190.62 | 115.61 | 35.00 | 35.00 | 212.87 |

DENSITY PARTITION IN AMC

| DENSITY | 35.0 mic. | 100.0 mic. | 175.0 mic. | 250.0 mic. | 360.0 mic. | 625.0 mic. | 1000.0 mic. | OVERALL |
|---|---|---|---|---|---|---|---|---|
| 1.250 | 100.00 | 71.56 | 44.41 | 35.90 | 20.04 | 6.65 | 21.14 | 35.42 |
| 1.325 | 100.00 | 82.61 | 58.08 | 30.47 | 19.26 | 13.33 | 3.87 | 20.12 |
| 1.390 | 100.00 | 85.26 | 66.28 | 57.87 | 26.97 | 18.42 | 14.11 | 36.29 |
| 1.620 | 100.00 | 96.53 | 88.78 | 81.62 | 64.93 | 36.86 | 13.92 | 49.21 |
| 2.000 | 100.00 | 99.11 | 95.55 | 94.43 | 88.60 | 57.87 | 59.27 | 89.50 |
| 2.400 | 100.00 | 100.00 | 99.99 | 98.09 | 96.15 | 83.92 | 79.11 | 94.65 |
| SG. SEP. | 2.40 | 1.25 | 1.28 | 1.37 | 1.51 | 1.85 | 1.92 | 1.62 |

TEST 12222

SIZE CLASSIFICATION IN AMC

| SIZE (MIC) | SPGR=1.250 | SPGR=1.325 | SPGR=1.390 | SPGR=1.620 | SPGR=2.0 | SPGR=2.4 | OVERALL |
|---|---|---|---|---|---|---|---|
| 35.0 | 7.44 | 8.75 | 8.71 | 20.25 | 50.01 | 71.86 | 13.69 |
| 100.0 | 8.91 | 5.07 | 23.31 | 48.70 | 76.61 | 92.93 | 24.02 |

| | | | | | | | |
|---|---|---|---|---|---|---|---|
| 175.0 | 19.82 | 37.66 | 55.35 | 84.35 | 95.55 | 98.81 | 47.64 |
| 250.0 | 45.41 | 52.17 | 74.34 | 91.73 | 96.89 | 99.99 | 69.42 |
| 360.0 | 54.96 | 81.75 | 88.34 | 95.39 | 98.58 | 99.99 | 83.73 |
| 625.0 | 100.00 | 100.00 | 100.00 | 100.00 | 100.00 | 100.00 | 99.96 |
| 1000.0 | 100.00 | 100.00 | 100.00 | 100.00 | 100.00 | 100.00 | 99.91 |
| D50 | 300.28 | 238.61 | 162.05 | 102.74 | 35.00 | 35.00 | 180.63 |

DENSITY PARTITION IN AMC

| DENSITY | 35.0 mic. | 100.0 mic. | 175.0 mic. | 250.0 mic. | 360.0 mic. | 625.0 mic. | 1000.0 mic. | OVERALL |
|---|---|---|---|---|---|---|---|---|
| 1.250 | 100.00 | 100.00 | 52.14 | 42.62 | 18.08 | 8.03 | 6.70 | 37.24 |
| 1.325 | 100.00 | 100.00 | 80.00 | 49.34 | 35.04 | 4.55 | 7.89 | 33.93 |
| 1.390 | 100.00 | 100.00 | 87.12 | 72.12 | 52.53 | 21.35 | 7.85 | 32.53 |
| 1.620 | 100.00 | 100.00 | 94.86 | 90.83 | 82.80 | 45.87 | 18.48 | 49.68 |
| 2.000 | 100.00 | 100.00 | 98.41 | 96.53 | 95.04 | 74.52 | 47.18 | 89.63 |
| 2.400 | 100.00 | 100.00 | 99.99 | 99.98 | 98.66 | 92.15 | 69.52 | 94.83 |
| SG. SEP. | 1.25 | 1.25 | 1.25 | 1.33 | 1.38 | 1.66 | 2.05 | 1.62 |

TEST 12223

SIZE CLASSIFICATION IN AMC

| SIZE (MIC) | SPGR=1.250 | SPGR=1.325 | SPGR=1.390 | SPGR=1.620 | SPGR=2.0 | SPGR=2.4 | OVERALL |
|---|---|---|---|---|---|---|---|
| 35.0 | 10.54 | 7.24 | 14.83 | 16.83 | 10.46 | 78.42 | 18.04 |
| 100.0 | 11.80 | 13.02 | 35.81 | 61.59 | 80.90 | 94.10 | 34.03 |
| 175.0 | 30.08 | 54.64 | 70.38 | 88.73 | 95.99 | 99.00 | 64.10 |
| 250.0 | 70.22 | 81.67 | 84.22 | 94.73 | 98.02 | 99.99 | 85.38 |
| 360.0 | 80.81 | 90.36 | 91.41 | 96.58 | 97.99 | 100.00 | 92.98 |
| 625.0 | 100.00 | 100.00 | 100.00 | 100.00 | 100.00 | 100.00 | 99.97 |
| 1000.0 | 100.00 | 100.00 | 100.00 | 100.00 | 100.00 | 100.00 | 99.91 |
| D50 | 181.67 | 166.65 | 123.32 | 83.17 | 71.49 | 35.00 | 141.74 |

DENSITY PARTITION IN AMC

| DENSITY | 35.0 mic. | 100.0 mic. | 175.0 mic. | 250.0 mic. | 360.0 mic. | 625.0 mic. | 1000.0 mic. | OVERALL |
|---|---|---|---|---|---|---|---|---|
| 1.250 | 100.00 | 100.00 | 83.00 | 73.22 | 33.28 | 13.43 | 12.02 | 54.96 |
| 1.325 | 100.00 | 100.00 | 91.58 | 83.78 | 58.27 | 14.79 | 8.30 | 36.03 |
| 1.390 | 100.00 | 100.00 | 92.50 | 86.09 | 73.37 | 39.28 | 16.80 | 45.89 |
| 1.620 | 100.00 | 100.00 | 97.04 | 95.42 | 90.12 | 65.03 | 19.00 | 50.83 |
| 2.000 | 100.00 | 100.00 | 98.27 | 98.29 | 96.52 | 83.08 | 11.92 | 61.82 |
| 2.400 | 100.00 | 100.00 | 100.00 | 99.99 | 99.14 | 94.87 | 80.81 | 96.02 |
| SG. SEP. | 2.40 | 2.40 | 1.25 | 1.25 | 1.30 | 1.45 | 2.22 | 1.25 |

TEST 21111

SIZE CLASSIFICATION IN AMC

| SIZE (MIC) | SPGR=1.250 | SPGR=1.325 | SPGR=1.390 | SPGR=1.620 | SPGR=2.0 | SPGR=2.4 | OVERALL |
|---|---|---|---|---|---|---|---|
| 35.0 | 13.35 | 7.32 | 3.25 | 8.56 | 27.69 | 31.74 | 1.55 |
| 100.0 | 7.39 | 5.90 | 7.15 | 6.88 | 27.51 | 69.31 | 5.62 |
| 175.0 | 1.50 | 33.77 | 14.90 | 17.16 | 43.38 | 84.16 | 12.19 |
| 250.0 | 5.43 | 14.10 | 18.03 | 31.72 | 64.95 | 92.08 | 20.34 |
| 360.0 | 15.57 | 19.80 | 19.29 | 42.32 | 82.34 | 94.57 | 29.00 |
| 625.0 | 14.00 | 17.79 | 27.65 | 57.59 | 90.80 | 97.73 | 32.82 |
| 1000.0 | 12.10 | 18.63 | 22.32 | 68.41 | 97.17 | 99.47 | 29.75 |
| D50 | 35.00 | 1000.00 | 1000.00 | 466.09 | 197.00 | 66.59 | 1000.00 |

DENSITY PARTITION IN AMC

| DENSITY | 35.0 mic. | 100.0 mic. | 175.0 mic. | 250.0 mic. | 360.0 mic. | 625.0 mic. | 1000.0 mic. | OVERALL |
|---|---|---|---|---|---|---|---|---|
| 1.250 | 2.48 | 2.92 | 3.30 | 1.05 | 0.28 | 1.45 | 2.77 | 1.81 |
| 1.325 | 4.06 | 3.85 | 4.37 | 2.94 | 8.62 | 1.15 | 1.44 | 3.15 |
| 1.390 | 5.05 | 6.60 | 4.23 | 3.91 | 3.14 | 1.40 | 0.62 | 2.21 |

| | | | | | | | | |
|---|---|---|---|---|---|---|---|---|
| 1.620 | 28.59 | 20.07 | 11.95 | 7.91 | 3.69 | 1.35 | 1.70 | 6.50 |
| 2.000 | 86.38 | 64.60 | 46.30 | 25.52 | 12.41 | 6.56 | 6.61 | 43.52 |
| 2.400 | 97.19 | 88.85 | 76.31 | 68.27 | 49.56 | 29.46 | 7.92 | 62.77 |
| SG. SEP. | 1.76 | 1.88 | 2.05 | 2.23 | 2.40 | 2.40 | 2.40 | 2.13 |

TEST 21112

SIZE CLASSIFICATION IN AMC

| SIZE (MIC) | SPGR=1.250 | SPGR=1.325 | SPGR=1.390 | SPGR=1.620 | SPGR=2.0 | SPGR=2.4 | OVERALL |
|---|---|---|---|---|---|---|---|
| 35.0 | 11.44 | 3.45 | 1.77 | 3.83 | 23.10 | 29.86 | 1.66 |
| 100.0 | 1.44 | 1.76 | 16.61 | 14.06 | 29.07 | 84.96 | 11.82 |
| 175.0 | 0.77 | 14.96 | 13.79 | 29.54 | 50.77 | 95.02 | 24.74 |
| 250.0 | 3.45 | 3.98 | 19.16 | 37.37 | 85.24 | 98.12 | 31.31 |
| 360.0 | 7.27 | 29.59 | 21.23 | 75.95 | 95.72 | 99.53 | 43.83 |
| 625.0 | 29.73 | 44.60 | 59.90 | 92.77 | 99.70 | 99.91 | 56.55 |
| 1000.0 | 35.84 | 50.77 | 77.64 | 97.98 | 99.82 | 99.99 | 62.30 |
| D50 | 1000.00 | 953.31 | 557.17 | 293.46 | 174.96 | 58.76 | 422.30 |

DENSITY PARTITION IN AMC

| DENSITY | 35.0 mic. | 100.0 mic. | 175.0 mic. | 250.0 mic. | 360.0 mic. | 625.0 mic. | 1000.0 mic. | OVERALL |
|---|---|---|---|---|---|---|---|---|
| 1.250 | 15.40 | 12.12 | 2.49 | 1.15 | 0.25 | 0.47 | 4.04 | 3.52 |
| 1.325 | 25.15 | 20.79 | 12.04 | 1.33 | 5.42 | 0.58 | 1.15 | 5.98 |
| 1.390 | 53.08 | 32.74 | 8.07 | 7.17 | 4.95 | 6.09 | 0.58 | 6.66 |
| 1.620 | 94.05 | 80.70 | 50.72 | 16.28 | 12.02 | 5.06 | 1.28 | 16.83 |
| 2.000 | 99.44 | 99.10 | 87.93 | 65.30 | 25.16 | 11.78 | 8.92 | 69.29 |
| 2.400 | 99.98 | 99.73 | 98.59 | 94.45 | 86.15 | 64.80 | 12.18 | 84.09 |
| SG. SEP. | 1.39 | 1.43 | 1.61 | 1.94 | 2.16 | 2.29 | 2.40 | 1.82 |

TEST 21113

SIZE CLASSIFICATION IN AMC

| SIZE (MIC) | SPGR=1.250 | SPGR=1.325 | SPGR=1.390 | SPGR=1.620 | SPGR=2.0 | SPGR=2.4 | OVERALL |
|---|---|---|---|---|---|---|---|
| 35.0 | 2.84 | 6.46 | 2.87 | 3.79 | 30.18 | 35.28 | 2.51 |
| 100.0 | 1.09 | 3.63 | 2.79 | 21.01 | 53.39 | 88.42 | 14.68 |
| 175.0 | 2.09 | 16.50 | 15.80 | 32.18 | 64.59 | 98.92 | 27.58 |
| 250.0 | 4.83 | 22.58 | 15.12 | 51.11 | 95.68 | 99.56 | 33.99 |
| 360.0 | 15.69 | 33.39 | 43.90 | 89.42 | 99.40 | 99.86 | 50.05 |
| 625.0 | 39.25 | 87.81 | 88.96 | 98.89 | 99.87 | 99.94 | 77.95 |
| 1000.0 | 85.87 | 94.14 | 98.05 | 99.34 | 100.00 | 100.00 | 93.86 |
| D50 | 711.50 | 440.89 | 395.86 | 246.79 | 90.52 | 53.01 | 359.74 |

DENSITY PARTITION IN AMC

| DENSITY | 35.0 mic. | 100.0 mic. | 175.0 mic. | 250.0 mic. | 360.0 mic. | 625.0 mic. | 1000.0 mic. | OVERALL |
|---|---|---|---|---|---|---|---|---|
| 1.250 | 71.04 | 20.68 | 6.99 | 2.01 | 0.85 | 0.44 | 1.17 | 5.56 |
| 1.325 | 86.63 | 74.40 | 16.83 | 10.53 | 7.39 | 1.50 | 2.71 | 16.34 |
| 1.390 | 95.30 | 76.49 | 24.00 | 6.71 | 7.04 | 1.14 | 1.18 | 10.21 |
| 1.620 | 98.38 | 97.29 | 77.33 | 29.68 | 16.07 | 9.69 | 1.56 | 18.79 |
| 2.000 | 99.99 | 99.67 | 98.52 | 89.94 | 42.40 | 31.61 | 14.86 | 77.94 |
| 2.400 | 100.00 | 99.84 | 99.67 | 98.91 | 97.37 | 75.50 | 18.03 | 87.93 |
| SG. SEP. | 1.25 | 1.29 | 1.48 | 1.75 | 2.06 | 2.17 | 2.40 | 1.73 |

TEST 21121

SIZE CLASSIFICATION IN AMC

| SIZE (MIC) | SPGR=1.250 | SPGR=1.325 | SPGR=1.390 | SPGR=1.620 | SPGR=2.0 | SPGR=2.4 | OVERALL |
|---|---|---|---|---|---|---|---|
| 35.0 | 6.15 | 4.79 | 2.96 | 5.34 | 19.13 | 27.80 | 1.03 |

| | | | | | | | |
|---|---|---|---|---|---|---|---|
| 100.0 | 8.97 | 8.27 | 5.14 | 15.39 | 35.54 | 66.71 | 5.45 |
| 175.0 | 11.16 | 7.80 | 12.65 | 24.35 | 46.02 | 78.49 | 10.57 |
| 250.0 | 12.40 | 12.62 | 13.71 | 29.20 | 55.43 | 83.06 | 14.54 |
| 360.0 | 16.07 | 18.53 | 22.85 | 45.38 | 68.64 | 91.61 | 24.14 |
| 625.0 | 22.29 | 29.62 | 30.65 | 58.22 | 84.82 | 94.86 | 31.70 |
| 1000.0 | 14.01 | 16.10 | 24.15 | 55.92 | 88.91 | 97.76 | 27.32 |
| D50 | 1000.00 | 1000.00 | 1000.00 | 455.30 | 206.09 | 72.08 | 1000.00 |

DENSITY PARTITION IN AMC

| DENSITY | 35.0 mic. | 100.0 mic. | 175.0 mic. | 250.0 mic. | 360.0 mic. | 625.0 mic. | 1000.0 mic. | OVERALL |
|---|---|---|---|---|---|---|---|---|
| 1.250 | 2.72 | 4.69 | 3.18 | 2.37 | 2.11 | 1.66 | 1.11 | 2.60 |
| 1.325 | 3.19 | 6.74 | 3.76 | 2.42 | 1.43 | 1.52 | 0.86 | 2.72 |
| 1.390 | 5.18 | 7.05 | 4.84 | 2.65 | 2.43 | 0.92 | 0.52 | 2.07 |
| 1.620 | 17.88 | 19.30 | 12.48 | 6.61 | 5.23 | 3.03 | 0.96 | 6.50 |
| 2.000 | 57.92 | 48.95 | 27.30 | 17.59 | 12.76 | 8.64 | 3.90 | 29.92 |
| 2.400 | 88.23 | 76.00 | 65.20 | 45.69 | 38.51 | 25.59 | 6.20 | 54.59 |
| SG. SEP. | 1.94 | 2.02 | 2.24 | 2.40 | 2.40 | 2.40 | 2.40 | 2.33 |

TEST 21122

SIZE CLASSIFICATION IN AMC

| SIZE (MIC) | SPGR=1.250 | SPGR=1.325 | SPGR=1.390 | SPGR=1.620 | SPGR=2.0 | SPGR=2.4 | OVERALL |
|---|---|---|---|---|---|---|---|
| 35.0 | 8.01 | 3.67 | 2.80 | 3.80 | 20.45 | 34.48 | 1.66 |
| 100.0 | 10.05 | 4.17 | 6.65 | 17.18 | 51.57 | 80.36 | 11.91 |
| 175.0 | 12.20 | 5.43 | 8.29 | 26.64 | 57.86 | 89.54 | 19.45 |
| 250.0 | 11.26 | 9.13 | 14.45 | 33.83 | 74.18 | 95.87 | 26.57 |
| 360.0 | 15.22 | 42.75 | 16.64 | 59.90 | 93.89 | 99.30 | 41.95 |
| 625.0 | 30.60 | 27.66 | 47.02 | 86.38 | 98.57 | 99.71 | 53.70 |
| 1000.0 | 19.41 | 34.56 | 54.70 | 93.81 | 99.24 | 99.95 | 51.69 |
| D50 | 1000.00 | 1000.00 | 770.52 | 329.54 | 96.71 | 56.99 | 541.63 |

DENSITY PARTITION IN AMC

| DENSITY | 35.0 mic. | 100.0 mic. | 175.0 mic. | 250.0 mic. | 360.0 mic. | 625.0 mic. | 1000.0 mic. | OVERALL |
|---|---|---|---|---|---|---|---|---|
| 1.250 | 6.83 | 11.82 | 5.18 | 3.72 | 4.05 | 3.29 | 2.58 | 4.98 |
| 1.325 | 13.84 | 10.42 | 18.51 | 2.97 | 1.72 | 1.31 | 1.15 | 3.79 |
| 1.390 | 26.86 | 21.26 | 5.73 | 4.89 | 2.68 | 2.12 | 0.87 | 4.56 |
| 1.620 | 82.16 | 65.86 | 31.24 | 13.46 | 9.95 | 5.94 | 1.19 | 11.28 |
| 2.000 | 97.56 | 95.44 | 82.38 | 46.64 | 29.46 | 24.47 | 7.25 | 66.65 |
| 2.400 | 99.83 | 99.07 | 97.73 | 87.59 | 72.25 | 55.46 | 13.80 | 82.10 |
| SG. SEP. | 1.40 | 1.52 | 1.68 | 2.03 | 2.19 | 2.33 | 2.40 | 1.90 |

TEST 21123

SIZE CLASSIFICATION IN AMC

| SIZE (MIC) | SPGR 1.250 | SPGR=1.325 | SPGR=1.390 | SPGR=1.620 | SPGR=2.0 | SPGR=2.4 | OVERALL |
|---|---|---|---|---|---|---|---|
| 35.0 | 19.72 | 4.13 | 2.30 | 1.84 | 17.00 | 30.71 | 2.07 |
| 100.0 | 5.31 | 3.88 | 6.74 | 24.50 | 21.71 | 89.55 | 18.95 |
| 175.0 | 7.38 | 0.07 | 9.35 | 26.13 | 64.89 | 94.96 | 27.50 |
| 250.0 | 6.59 | 9.57 | 14.65 | 46.54 | 88.76 | 98.27 | 33.90 |
| 360.0 | 14.19 | 33.40 | 34.79 | 86.87 | 98.72 | 99.66 | 53.23 |
| 625.0 | 36.45 | 50.57 | 83.41 | 98.63 | 99.63 | 99.74 | 71.86 |
| 1000.0 | 62.23 | 82.90 | 92.19 | 98.45 | 99.72 | 99.91 | 84.60 |
| D50 | 822.08 | 615.54 | 442.89 | 259.45 | 149.14 | 56.31 | 341.69 |

DENSITY PARTITION IN AMC

| DENSITY | 35.0 mic. | 100.0 mic. | 175.0 mic. | 250.0 mic. | 360.0 mic. | 625.0 mic. | 1000.0 mic. | OVERALL |
|---|---|---|---|---|---|---|---|---|
| 1.250 | 43.41 | 21.08 | 7.15 | 3.18 | 3.58 | 2.55 | 10.26 | 6.75 |
| 1.325 | 69.29 | 32.26 | 18.93 | 4.69 | 0.03 | 1.85 | 1.97 | 9.43 |

| | | | | | | | | |
|---|---|---|---|---|---|---|---|---|
| 1.390 | 84.61 | 70.07 | 19.90 | 7.40 | 4.58 | 3.25 | 1.09 | 11.65 |
| 1.620 | 96.73 | 97.10 | 75.49 | 28.84 | 14.14 | 13.13 | 0.86 | 19.17 |
| 2.000 | 99.39 | 99.21 | 97.30 | 78.63 | 46.25 | 11.44 | 8.71 | 79.50 |
| 2.400 | 99.82 | 99.45 | 99.26 | 96.37 | 89.77 | 79.96 | 17.11 | 89.05 |
| SG. SEP. | 1.27 | 1.36 | 1.51 | 1.73 | 2.03 | 2.23 | 2.40 | 1.75 |

TEST 21211

SIZE CLASSIFICATION IN AMC

| SIZE (MIC) | SPGR=1.250 | SPGR-1.325 | SPGR=1.390 | SPGR=1.620 | SPGR=2.0 | SPGR=2.4 | OVERALL |
|---|---|---|---|---|---|---|---|
| 35.0 | 15.89 | 6.55 | 4.87 | 13.97 | 22.35 | 44.97 | 2.00 |
| 100.0 | 11.05 | 6.82 | 9.54 | 28.90 | 52.62 | 78.42 | 7.34 |
| 175.0 | 13.66 | 12.13 | 11.85 | 25.66 | 54.76 | 79.13 | 11.71 |
| 250.0 | 16.13 | 15.39 | 13.70 | 28.37 | 61.22 | 83.39 | 16.66 |
| 360.0 | 18.55 | 28.15 | 33.29 | 51.44 | 77.55 | 95.00 | 33.61 |
| 625.0 | 16.62 | 28.40 | 36.17 | 60.42 | 92.62 | 98.03 | 40.99 |
| 1000.0 | 16.10 | 18.59 | 31.56 | 70.41 | 96.02 | 99.20 | 35.31 |
| D50 | 1000.00 | 1000.00 | 1000.00 | 344.66 | 94.37 | 44.77 | 1000.00 |

DENSITY PARTITION IN AMC

| DENSITY | 35.0 mic. | 100.0 mic. | 175.0 mic. | 250.0 mic. | 360.0 mic. | 625.0 mic. | 1000.0 mic. | OVERALL |
|---|---|---|---|---|---|---|---|---|
| 1.250 | 3.93 | 4.07 | 4.63 | 3.94 | 3.26 | 2.58 | 3.87 | 3.63 |
| 1.325 | 4.64 | 7.79 | 7.70 | 3.73 | 2.86 | 1.54 | 1.47 | 3.37 |
| 1.390 | 8.95 | 10.77 | 9.61 | 3.27 | 2.78 | 2.20 | 1.08 | 2.86 |
| 1.620 | 33.64 | 24.55 | 18.41 | 7.78 | 6.85 | 7.97 | 3.34 | 12.23 |
| 2.000 | 83.72 | 72.78 | 42.40 | 25.17 | 20.50 | 19.14 | 5.78 | 46.15 |
| 2.400 | 96.37 | 91.40 | 80.18 | 51.69 | 44.68 | 43.65 | 14.83 | 68.37 |
| SG. SEP. | 1.65 | 1.81 | 2.08 | 2.37 | 2.40 | 2.40 | 2.40 | 2.07 |

TEST 21212

SIZE CLASSIFICATION IN AMC

| SIZE (MIC) | SPGR=1.250 | SPGR=1.325 | SPGR=1.390 | SPGR=1.620 | SPGR=2.0 | SPGR=2.4 | OVERALL |
|---|---|---|---|---|---|---|---|
| 35.0 | 16.74 | 4.27 | 5.15 | 17.73 | 30.89 | 41.20 | 2.67 |
| 100.0 | 15.25 | 6.73 | 7.01 | 24.06 | 52.73 | 77.38 | 9.52 |
| 175.0 | 14.81 | 9.19 | 13.32 | 21.24 | 62.72 | 87.83 | 15.47 |
| 250.0 | 15.65 | 10.39 | 13.51 | 35.44 | 75.83 | 94.56 | 20.84 |
| 360.0 | 21.67 | 18.49 | 26.64 | 66.44 | 95.23 | 99.46 | 36.46 |
| 625.0 | 23.62 | 33.50 | 39.14 | 86.07 | 99.12 | 99.99 | 42.42 |
| 1000.0 | 18.17 | 36.78 | 59.54 | 96.30 | 99.70 | 99.99 | 43.51 |
| D50 | 1000.00 | 1000.00 | 824.69 | 285.89 | 91.87 | 50.81 | 1000.00 |

DENSITY PARTITION IN AMC

| DENSITY | 35.0 mic. | 100.0 mic. | 175.0 mic. | 250.0 mic. | 360.0 mic. | 625.0 mic. | 1000.0 mic. | OVERALL |
|---|---|---|---|---|---|---|---|---|
| 1.250 | 5.25 | 7.16 | 6.45 | 4.42 | 4.16 | 4.29 | 4.78 | 5.35 |
| 1.325 | 12.67 | 11.16 | 5.36 | 2.81 | 2.46 | 1.77 | 1.10 | 3.71 |
| 1.390 | 26.84 | 13.82 | 8.30 | 3.75 | 3.69 | 1.85 | 1.34 | 4.22 |
| 1.620 | 86.65 | 60.64 | 33.05 | 12.04 | 6.30 | 7.32 | 5.10 | 21.95 |
| 2.000 | 98.83 | 96.58 | 83.28 | 43.89 | 29.56 | 21.77 | 10.03 | 68.41 |
| 2.400 | 99.97 | 99.97 | 97.88 | 81.25 | 64.29 | 46.04 | 14.87 | 76.31 |
| SG. SEP. | 1.48 | 1.57 | 1.67 | 2.07 | 2.24 | 2.40 | 2.40 | 1.85 |

TEST 21213

SIZE CLASSIFICATION IN AMC

| SIZE (MIC) | SPGR=1.250 | SPGR=1.325 | SPGR=1.390 | SPGR=1.620 | SPGR=2.0 | SPGR=2.4 | OVERALL |
|---|---|---|---|---|---|---|---|

| | | | | | | | |
|---|---|---|---|---|---|---|---|
| 35.0 | 9.23 | 4.43 | 4.38 | 11.63 | 26.49 | 43.62 | 3.16 |
| 100.0 | 7.06 | 5.87 | 11.78 | 21.27 | 49.03 | 87.28 | 14.10 |
| 175.0 | 8.21 | 6.52 | 13.31 | 29.31 | 69.39 | 94.92 | 21.87 |
| 250.0 | 7.87 | 8.88 | 14.81 | 41.37 | 86.13 | 98.88 | 27.93 |
| 360.0 | 15.69 | 26.55 | 35.51 | 82.91 | 98.59 | 99.99 | 49.65 |
| 625.0 | 36.35 | 62.63 | 78.16 | 98.11 | 99.86 | 99.99 | 64.34 |
| 1000.0 | 60.70 | 55.66 | 96.06 | 99.68 | 99.99 | 100.00 | 76.27 |
| D50 | 835.22 | 532.25 | 403.78 | 263.79 | 103.20 | 44.50 | 364.24 |

DENSITY PARTITION IN AMC

| DENSITY | 35.0 mic. | 100.0 mic. | 175.0 mic. | 250.0 mic. | 360.0 mic. | 625.0 mic. | 1000.0 mic. | OVERALL |
|---|---|---|---|---|---|---|---|---|
| 1.250 | 36.50 | 17.53 | 6.48 | 3.08 | 3.22 | 2.75 | 3.65 | 7.35 |
| 1.325 | 31.84 | 38.41 | 11.86 | 3.50 | 2.53 | 2.27 | 1.69 | 6.01 |
| 1.390 | 90.08 | 57.11 | 17.01 | 6.08 | 5.40 | 4.73 | 1.68 | 9.27 |
| 1.620 | 99.15 | 95.07 | 64.36 | 20.80 | 13.37 | 9.14 | 4.67 | 29.76 |
| 2.000 | 99.98 | 99.62 | 96.30 | 69.79 | 45.76 | 26.36 | 11.82 | 77.01 |
| 2.400 | 99.99 | 99.99 | 99.98 | 97.04 | 87.44 | 71.85 | 22.35 | 88.45 |
| SG. SEP. | 1.35 | 1.36 | 1.57 | 1.86 | 2.04 | 2.21 | 2.40 | 1.67 |

TEST 21221

SIZE CLASSIFICATION IN AMC

| SIZE (MIC) | SPGR=1.250 | SPGR=1.325 | SPGR=1.390 | SPGR=1.620 | SPGR=2.0 | SPGR=2.4 | OVERALL |
|---|---|---|---|---|---|---|---|
| 35.0 | 24.18 | 6.89 | 4.63 | 4.38 | 22.59 | 42.58 | 3.19 |
| 100.0 | 9.30 | 15.03 | 12.05 | 19.19 | 42.38 | 76.15 | 11.47 |
| 175.0 | 11.05 | 15.67 | 17.26 | 25.84 | 50.96 | 90.00 | 18.94 |
| 250.0 | 13.90 | 14.90 | 17.48 | 32.59 | 69.15 | 97.73 | 27.86 |
| 360.0 | 19.65 | 21.07 | 26.30 | 60.25 | 97.32 | 99.84 | 50.69 |
| 625.0 | 20.51 | 26.21 | 35.61 | 90.17 | 99.70 | 100.00 | 63.06 |
| 1000.0 | 18.23 | 31.01 | 60.93 | 98.16 | 99.99 | 100.00 | 73.18 |

| | | | | | | | |
|---|---|---|---|---|---|---|---|
| D50 | 35.00 | 1000.00 | 838.09 | 336.69 | 166.80 | 49.37 | 352.13 |

DENSITY PARTITION IN AMC

| DENSITY | 35.0 mic. | 100.0 mic. | 175.0 mic. | 250.0 mic. | 360.0 mic. | 625.0 mic. | 1000.0 mic. | OVERALL |
|---|---|---|---|---|---|---|---|---|
| 1.250 | 7.82 | 8.95 | 8.52 | 5.79 | 4.52 | 3.76 | 10.83 | 6.17 |
| 1.325 | 14.61 | 11.91 | 9.22 | 6.25 | 6.61 | 6.31 | 2.74 | 5.75 |
| 1.390 | 37.25 | 17.39 | 11.96 | 7.46 | 7.36 | 4.96 | 1.81 | 5.43 |
| 1.620 | 95.30 | 77.73 | 36.58 | 15.54 | 11.71 | 8.29 | 1.72 | 11.04 |
| 2.000 | 99.98 | 99.20 | 93.25 | 46.04 | 28.34 | 21.87 | 10.00 | 67.62 |
| 2.400 | 99.99 | 99.99 | 99.58 | 94.25 | 77.40 | 54.86 | 22.01 | 88.95 |
| SG. SEP. | 1.44 | 1.51 | 1.71 | 2.03 | 2.18 | 2.34 | 2.40 | 1.88 |

TEST 21222

SIZE CLASSIFICATION IN AMC

| SIZE (MIC) | SPGR=1.250 | SPGR=1.325 | SPGR=1.390 | SPGR=1.620 | SPGR=2.0 | SPGR=2.4 | OVERALL |
|---|---|---|---|---|---|---|---|
| 35.0 | 10.76 | 3.77 | 5.05 | 25.07 | 19.67 | 36.93 | 3.40 |
| 100.0 | 11.02 | 5.71 | 12.72 | 20.23 | 45.92 | 74.70 | 9.86 |
| 175.0 | 12.95 | 11.25 | 15.07 | 22.06 | 48.96 | 84.43 | 16.75 |
| 250.0 | 11.42 | 16.30 | 13.45 | 24.18 | 60.77 | 92.11 | 23.50 |
| 360.0 | 20.84 | 27.65 | 29.76 | 61.55 | 91.13 | 98.67 | 44.02 |
| 625.0 | 19.72 | 24.36 | 32.58 | 76.42 | 98.20 | 99.73 | 52.08 |
| 1000.0 | 17.08 | 19.69 | 41.04 | 90.43 | 99.40 | 99.99 | 46.24 |
| D50 | 1000.00 | 1000.00 | 1000.00 | 326.01 | 194.17 | 57.49 | 556.61 |

DENSITY PARTITION IN AMC

| DENSITY | 35.0 mic. | 100.0 mic. | 175.0 mic. | 250.0 mic. | 360.0 mic. | 625.0 mic. | 1000.0 mic. | OVERALL |
|---|---|---|---|---|---|---|---|---|
| 1.250 | 5.69 | 6.71 | 7.16 | 3.64 | 4.17 | 3.50 | 3.41 | 4.83 |

| | | | | | | | | |
|---|---|---|---|---|---|---|---|---|
| 1.325 | 6.70 | 8.62 | 10.07 | 5.39 | 3.58 | 1.74 | 1.13 | 3.81 |
| 1.390 | 16.93 | 12.40 | 11.04 | 4.35 | 4.94 | 4.09 | 1.53 | 4.25 |
| 1.620 | 73.46 | 48.69 | 31.91 | 8.54 | 7.65 | 6.91 | 8.92 | 18.17 |
| 2.000 | 97.99 | 94.12 | 75.06 | 31.21 | 21.93 | 19.91 | 6.69 | 60.72 |
| 2.400 | 99.98 | 99.10 | 95.61 | 77.38 | 61.35 | 46.38 | 14.64 | 79.26 |
| SG. SEP. | 1.49 | 1.63 | 1.75 | 2.16 | 2.28 | 2.40 | 2.40 | 1.88 |

TEST 21223

SIZE CLASSIFICATION IN AMC

| SIZE (MIC) | SPGR=1.250 | SPGR=1.325 | SPGR=1.390 | SPGR=1.620 | SPGR=2.0 | SPGR=2.4 | OVERALL |
|---|---|---|---|---|---|---|---|
| 35.0 | 4.96 | 2.99 | 6.85 | 37.81 | 25.06 | 41.69 | 3.60 |
| 100.0 | 7.32 | 13.67 | 11.99 | 16.74 | 57.99 | 77.50 | 11.56 |
| 175.0 | 7.41 | 25.67 | 16.24 | 21.98 | 57.71 | 81.17 | 17.73 |
| 250.0 | 10.19 | 21.18 | 20.00 | 38.49 | 70.57 | 86.58 | 22.11 |
| 360.0 | 18.49 | 22.68 | 32.01 | 63.71 | 79.09 | 88.37 | 34.95 |
| 625.0 | 29.50 | 38.50 | 57.66 | 71.30 | 83.13 | 91.70 | 39.27 |
| 1000.0 | 25.98 | 36.88 | 50.28 | 68.88 | 83.38 | 95.17 | 32.48 |
| D50 | 1000.00 | 1000.00 | 545.89 | 300.19 | 84.23 | 50.08 | 1000.00 |

DENSITY PARTITION IN AMC

| DENSITY | 35.0 mic. | 100.0 mic. | 175.0 mic. | 250.0 mic. | 360.0 mic. | 625.0 mic. | 1000.0 mic. | OVERALL |
|---|---|---|---|---|---|---|---|---|
| 1.250 | 8.30 | 9.73 | 5.52 | 2.84 | 2.02 | 1.99 | 1.33 | 4.10 |
| 1.325 | 13.09 | 13.89 | 7.03 | 6.48 | 8.17 | 3.92 | 0.79 | 6.63 |
| 1.390 | 20.68 | 25.98 | 10.82 | 6.05 | 4.76 | 3.39 | 1.86 | 5.91 |
| 1.620 | 36.33 | 39.04 | 31.15 | 13.89 | 6.77 | 4.93 | 13.55 | 20.29 |
| 2.000 | 56.38 | 55.95 | 49.36 | 38.20 | 26.02 | 26.24 | 7.94 | 44.63 |
| 2.400 | 83.56 | 74.00 | 66.19 | 62.45 | 52.62 | 47.02 | 15.56 | 61.17 |
| SG. SEP. | 1.88 | 1.86 | 2.02 | 2.19 | 2.36 | 2.40 | 2.40 | 2.13 |

TEST 22111

SIZE CLASSIFICATION IN AMC

| SIZE (MIC) | SPGR=1.250 | SPGR=1.325 | SPGR=1.390 | SPGR=1.620 | SPGR=2.0 | SPGR=2.4 | OVERALL |
|---|---|---|---|---|---|---|---|
| 35.0 | 27.37 | 8.86 | 7.17 | 10.04 | 27.26 | 39.50 | 1.68 |
| 100.0 | 10.50 | 8.46 | 10.36 | 29.71 | 50.70 | 78.58 | 6.31 |
| 175.0 | 7.60 | 13.48 | 18.06 | 41.75 | 67.86 | 90.02 | 11.24 |
| 250.0 | 15.85 | 18.05 | 20.91 | 63.06 | 84.37 | 93.65 | 19.07 |
| 360.0 | 22.00 | 25.31 | 31.68 | 76.29 | 92.47 | 97.69 | 27.76 |
| 625.0 | 34.94 | 27.47 | 52.24 | 85.35 | 96.60 | 98.52 | 31.80 |
| 1000.0 | 33.94 | 21.12 | 51.87 | 89.46 | 98.75 | 99.01 | 25.11 |
| D50 | 1000.00 | 1000.00 | 596.15 | 202.46 | 98.05 | 52.46 | 1000.00 |

DENSITY PARTITION IN AMC

| DENSITY | 35.0 mic. | 100.0 mic. | 175.0 mic. | 250.0 mic. | 360.0 mic. | 625.0 mic. | 1000.0 mic. | OVERALL |
|---|---|---|---|---|---|---|---|---|
| 1.250 | 6.66 | 6.94 | 3.77 | 2.55 | 1.13 | 1.60 | 4.98 | 3.22 |
| 1.325 | 3.59 | 5.00 | 4.50 | 2.97 | 2.12 | 1.27 | 1.33 | 2.65 |
| 1.390 | 13.02 | 13.19 | 6.05 | 3.54 | 2.97 | 1.58 | 1.06 | 2.96 |
| 1.620 | 54.12 | 44.74 | 30.89 | 19.17 | 9.06 | 5.55 | 1.53 | 8.71 |
| 2.000 | 91.64 | 79.78 | 63.04 | 42.87 | 22.68 | 12.51 | 4.95 | 46.60 |
| 2.400 | 93.29 | 90.22 | 85.43 | 67.20 | 55.63 | 33.77 | 8.32 | 59.18 |
| SG. SEP. | 1.59 | 1.63 | 1.83 | 2.12 | 2.33 | 2.40 | 2.40 | 2.11 |

TEST 22112

SIZE CLASSIFICATION IN AMC

| SIZE (MIC) | SPGR=1.250 | SPGR=1.325 | SPGR=1.390 | SPGR=1.620 | SPGR=2.0 | SPGR=2.4 | OVERALL |
|---|---|---|---|---|---|---|---|

| | | | | | | | |
|---|---|---|---|---|---|---|---|
| 35.0 | 37.05 | 6.09 | 4.20 | 3.64 | 29.57 | 49.38 | 1.53 |
| 100.0 | 4.96 | 1.64 | 5.94 | 32.95 | 48.96 | 87.44 | 8.25 |
| 175.0 | 4.97 | 7.81 | 8.70 | 45.75 | 82.74 | 97.27 | 15.66 |
| 250.0 | 9.08 | 10.02 | 17.22 | 63.99 | 93.48 | 98.68 | 21.26 |
| 360.0 | 13.21 | 22.00 | 42.25 | 85.53 | 98.49 | 99.34 | 35.73 |
| 625.0 | 35.01 | 52.92 | 77.01 | 96.69 | 99.53 | 99.53 | 51.94 |
| 1000.0 | 40.85 | 61.08 | 87.07 | 97.79 | 99.50 | 99.59 | 54.27 |
| D50 | 1000.00 | 538.91 | 419.06 | 194.24 | 101.64 | 36.06 | 404.44 |

DENSITY PARTITION IN AMC

| DENSITY | 35.0 mic. | 100.0 mic. | 175.0 mic. | 250.0 mic. | 360.0 mic. | 625.0 mic. | 1000.0 mic. | OVERALL |
|---|---|---|---|---|---|---|---|---|
| 1.250 | 11.37 | 9.10 | 2.75 | 1.82 | 0.96 | 0.96 | 9.86 | 3.48 |
| 1.325 | 22.58 | 17.28 | 4.98 | 2.03 | 1.55 | 0.31 | 1.19 | 3.29 |
| 1.390 | 55.58 | 38.36 | 11.97 | 3.72 | 1.74 | 1.16 | 0.81 | 5.40 |
| 1.620 | 89.14 | 84.43 | 52.34 | 24.82 | 13.55 | 8.37 | 0.70 | 10.82 |
| 2.000 | 97.37 | 97.51 | 92.39 | 72.69 | 47.12 | 15.13 | 7.24 | 66.12 |
| 2.400 | 97.82 | 97.53 | 96.56 | 93.28 | 86.86 | 56.39 | 15.34 | 75.43 |
| SG. SEP. | 1.38 | 1.45 | 1.61 | 1.78 | 2.03 | 2.34 | 2.40 | 1.80 |

TEST 22113

SIZE CLASSIFICATION IN AMC

| SIZE (MIC) | SPGR-1.250 | SPGR-1.325 | SPGR-1.390 | SPGR=1.620 | SPGR=2.0 | SPGR=2.4 | OVERALL |
|---|---|---|---|---|---|---|---|
| 35.0 | 26.67 | 6.56 | 2.97 | 3.43 | 28.82 | 50.23 | 2.03 |
| 100.0 | 2.40 | 4.96 | 6.34 | 34.80 | 66.21 | 94.22 | 12.67 |
| 175.0 | 5.68 | 12.62 | 22.91 | 62.27 | 92.43 | 98.82 | 23.24 |
| 250.0 | 13.25 | 19.05 | 38.59 | 82.16 | 98.36 | 99.05 | 33.93 |
| 360.0 | 35.44 | 57.89 | 80.43 | 96.40 | 99.33 | 99.43 | 57.35 |
| 625.0 | 83.73 | 80.08 | 95.85 | 99.15 | 99.64 | 99.49 | 83.80 |
| 1000.0 | 91.68 | 96.28 | 98.49 | 98.79 | 99.32 | 99.35 | 92.80 |

| | | | | | | | |
|---|---|---|---|---|---|---|---|
| D50 | 439.90 | 338.71 | 255.39 | 138.24 | 71.81 | 35.00 | 324.39 |

DENSITY PARTITION IN AMC

| DENSITY | 35.0 mic. | 100.0 mic. | 175.0 mic. | 250.0 mic. | 360.0 mic. | 625.0 mic. | 1000.0 mic. | OVERALL |
|---|---|---|---|---|---|---|---|---|
| 1.250 | 76.09 | 59.78 | 13.68 | 4.22 | 1.71 | 0.71 | 9.50 | 10.74 |
| 1.325 | 88.18 | 53.72 | 28.41 | 6.36 | 4.00 | 1.48 | 1.99 | 10.45 |
| 1.390 | 94.95 | 86.95 | 54.26 | 15.36 | 7.90 | 1.92 | 0.87 | 10.64 |
| 1.620 | 95.93 | 97.11 | 88.56 | 57.08 | 32.27 | 13.35 | 1.01 | 15.18 |
| 2.000 | 97.70 | 98.77 | 97.70 | 94.54 | 77.90 | 36.13 | 10.47 | 79.23 |
| 2.400 | 97.80 | 98.26 | 98.06 | 96.77 | 96.02 | 82.48 | 22.56 | 83.31 |
| SG. SEP. | 1.25 | 1.25 | 1.38 | 1.58 | 1.72 | 2.12 | 2.40 | 1.83 |

TEST 22121

SIZE CLASSIFICATION IN AMC

| SIZE (MIC) | SPGR=1.250 | SPGR=1.325 | SPGR=1.390 | SPGR=1.620 | SPGR=2.0 | SPGR=2.4 | OVERALL |
|---|---|---|---|---|---|---|---|
| 35.0 | 20.32 | 5.62 | 1.06 | 8.09 | 23.07 | 39.44 | 1.12 |
| 100.0 | 6.56 | 5.88 | 4.87 | 23.67 | 49.57 | 69.06 | 5.44 |
| 175.0 | 8.82 | 13.06 | 15.69 | 29.72 | 53.23 | 83.83 | 11.52 |
| 250.0 | 6.77 | 15.89 | 26.26 | 41.70 | 74.25 | 93.62 | 19.09 |
| 360.0 | 20.60 | 20.67 | 31.64 | 60.22 | 88.45 | 96.05 | 30.18 |
| 625.0 | 30.88 | 38.36 | 40.15 | 72.40 | 93.92 | 97.64 | 38.07 |
| 1000.0 | 16.89 | 18.63 | 31.82 | 82.59 | 97.02 | 99.20 | 31.41 |
| D50 | 35.00 | 1000.00 | 1000.00 | 279.01 | 108.95 | 58.18 | 1000.00 |

DENSITY PARTITION IN AMC

| DENSITY | 35.0 mic. | 100.0 mic. | 175.0 mic. | 250.0 mic. | 360.0 mic. | 625.0 mic. | 1000.0 mic. | OVERALL |
|---|---|---|---|---|---|---|---|---|

| | | | | | | | | |
|---|---|---|---|---|---|---|---|---|
| 1.250 | 3.49 | 7.38 | 4.42 | 1.28 | 1.70 | 1.23 | 4.35 | 3.18 |
| 1.325 | 3.92 | 9.98 | 4.44 | 3.26 | 2.61 | 1.10 | 1.05 | 2.90 |
| 1.390 | 7.68 | 10.68 | 7.62 | 5.97 | 3.21 | 0.90 | 0.19 | 2.55 |
| 1.620 | 45.80 | 31.85 | 21.24 | 11.30 | 7.01 | 5.24 | 1.55 | 11.83 |
| 2.000 | 85.28 | 73.36 | 57.72 | 33.95 | 16.86 | 14.90 | 5.07 | 49.15 |
| 2.400 | 95.65 | 88.05 | 81.26 | 72.34 | 48.02 | 28.46 | 10.40 | 64.15 |
| SG. SEP. | 1.66 | 1.72 | 1.92 | 2.17 | 2.40 | 2.40 | 2.40 | 2.02 |

TEST 22122

SIZE CLASSIFICATION IN AMC

| SIZE (MIC) | SPGR=1.250 | SPGR=1.325 | SPGR=1.390 | SPGR=1.620 | SPGR=2.0 | SPGR=2.4 | OVERALL |
|---|---|---|---|---|---|---|---|
| 35.0 | 10.70 | 7.17 | 3.13 | 8.75 | 27.96 | 51.43 | 2.16 |
| 100.0 | 8.01 | 2.06 | 3.66 | 28.19 | 55.77 | 87.00 | 8.83 |
| 175.0 | 10.16 | 5.89 | 9.40 | 30.90 | 74.09 | 96.13 | 15.66 |
| 250.0 | 6.75 | 5.86 | 20.13 | 66.44 | 92.60 | 99.09 | 26.26 |
| 360.0 | 15.73 | 29.06 | 39.73 | 85.72 | 98.73 | 99.65 | 42.02 |
| 625.0 | 24.82 | 38.13 | 67.61 | 96.25 | 99.77 | 99.79 | 54.26 |
| 1000.0 | 41.04 | 64.20 | 87.90 | 98.94 | 99.33 | 99.99 | 57.64 |
| D50 | 1000.00 | 795.78 | 434.50 | 215.31 | 86.52 | 35.00 | 381.42 |

DENSITY PARTITION IN AMC

| DENSITY | 35.0 mic. | 100.0 mic. | 175.0 mic. | 250.0 mic. | 360.0 mic. | 625.0 mic. | 1000.0 mic. | OVERALL |
|---|---|---|---|---|---|---|---|---|
| 1.250 | 14.43 | 7.41 | 4.33 | 1.72 | 2.67 | 2.07 | 2.82 | 4.14 |
| 1.325 | 30.29 | 12.99 | 9.03 | 1.49 | 1.49 | 0.51 | 1.84 | 3.48 |
| 1.390 | 63.78 | 33.59 | 13.77 | 5.76 | 2.45 | 0.91 | 0.78 | 4.67 |
| 1.620 | 95.75 | 86.14 | 59.27 | 32.42 | 9.78 | 8.69 | 2.27 | 19.53 |
| 2.000 | 97.29 | 99.05 | 94.94 | 75.21 | 40.93 | 23.41 | 8.60 | 67.19 |
| 2.400 | 99.98 | 99.14 | 98.56 | 96.35 | 85.76 | 61.87 | 20.43 | 84.28 |
| SG. SEP. | 1.36 | 1.46 | 1.59 | 1.74 | 2.08 | 2.28 | 2.40 | 1.82 |

TEST 22123

SIZE CLASSIFICATION IN AMC

| SIZE (MIC) | SPGR=1.250 | SPGR=1.325 | SPGR=1.390 | SPGR=1.620 | SPGR=2.0 | SPGR=2.4 | OVERALL |
|---|---|---|---|---|---|---|---|
| 35.0 | 33.47 | 5.84 | 2.61 | 2.00 | 24.65 | 59.07 | 1.97 |
| 100.0 | 0.42 | 5.53 | 5.73 | 46.24 | 83.05 | 97.09 | 14.17 |
| 175.0 | 2.74 | 9.20 | 16.26 | 65.79 | 94.06 | 98.96 | 21.96 |
| 250.0 | 5.35 | 33.91 | 27.04 | 85.45 | 98.43 | 99.45 | 32.73 |
| 360.0 | 26.52 | 57.46 | 64.28 | 95.91 | 99.69 | 99.81 | 55.74 |
| 625.0 | 69.82 | 83.54 | 95.12 | 99.26 | 99.62 | 100.00 | 82.83 |
| 1000.0 | 86.78 | 94.35 | 97.74 | 99.35 | 99.41 | 100.00 | 90.35 |
| D50 | 432.98 | 316.01 | 321.85 | 113.50 | 63.22 | 35.00 | 331.47 |

DENSITY PARTITION IN AMC

| DENSITY | 35.0 mic. | 100.0 mic. | 175.0 mic. | 250.0 mic. | 360.0 mic. | 625.0 mic. | 1000.0 mic. | OVERALL |
|---|---|---|---|---|---|---|---|---|
| 1.250 | 65.34 | 39.91 | 9.39 | 1.60 | 0.80 | 0.12 | 12.62 | 5.78 |
| 1.325 | 82.75 | 59.30 | 27.95 | 12.84 | 2.83 | 1.65 | 1.75 | 9.20 |
| 1.390 | 92.56 | 84.84 | 34.07 | 9.62 | 5.28 | 1.72 | 0.76 | 7.61 |
| 1.620 | 97.76 | 97.49 | 87.07 | 62.78 | 35.58 | 19.80 | 0.58 | 18.32 |
| 2.000 | 97.99 | 98.69 | 98.92 | 94.73 | 81.97 | 58.45 | 8.59 | 78.06 |
| 2.400 | 100.00 | 99.99 | 99.34 | 98.12 | 96.47 | 90.56 | 29.30 | 89.61 |
| SG. SEP. | 1.25 | 1.29 | 1.42 | 1.41 | 1.66 | 1.92 | 2.40 | 1.73 |

TEST 22211

SIZE CLASSIFICATION IN AMC

| SIZE (MIC) | SPGR=1.250 | SPGR=1.325 | SPGR=1.390 | SPGR=1.620 | SPGR=2.0 | SPGR=2.4 | OVERALL |
|---|---|---|---|---|---|---|---|
| 35.0 | 12.19 | 7.41 | 5.45 | 15.42 | 27.43 | 54.25 | 1.69 |
| 100.0 | 3.66 | 2.14 | 12.66 | 27.18 | 36.68 | 67.34 | 4.67 |
| 175.0 | 6.50 | 10.95 | 8.60 | 48.80 | 56.73 | 82.36 | 9.69 |
| 250.0 | 12.62 | 10.65 | 16.94 | 40.66 | 64.44 | 90.19 | 14.75 |
| 360.0 | 22.24 | 15.86 | 29.00 | 55.50 | 84.26 | 95.75 | 24.47 |
| 625.0 | 32.37 | 37.14 | 36.72 | 67.92 | 91.70 | 97.69 | 30.73 |
| 1000.0 | 20.93 | 33.98 | 42.96 | 80.49 | 97.30 | 99.37 | 27.95 |
| D50 | 1000.00 | 1000.00 | 1000.00 | 319.24 | 141.97 | 35.00 | 1000.00 |

DENSITY PARTITION IN AMC

| DENSITY | 35.0 mic. | 100.0 mic. | 175.0 mic. | 250.0 mic. | 360.0 mic. | 625.0 mic. | 1000.0 mic. | OVERALL |
|---|---|---|---|---|---|---|---|---|
| 1.250 | 3.79 | 6.66 | 4.08 | 2.11 | 1.02 | 0.56 | 2.03 | 2.81 |
| 1.325 | 7.12 | 8.09 | 2.73 | 1.74 | 1.80 | 0.32 | 1.18 | 2.21 |
| 1.390 | 10.09 | 7.95 | 5.73 | 2.95 | 1.38 | 2.11 | 0.85 | 2.62 |
| 1.620 | 38.07 | 23.98 | 15.66 | 9.26 | 12.43 | 5.27 | 2.64 | 12.05 |
| 2.000 | 84.32 | 62.19 | 44.37 | 21.26 | 16.34 | 7.94 | 5.33 | 41.13 |
| 2.400 | 95.93 | 86.29 | 77.03 | 57.78 | 41.02 | 23.50 | 15.01 | 59.15 |
| SG. SEP. | 1.63 | 1.87 | 2.07 | 2.31 | 2.40 | 2.40 | 2.40 | 2.20 |

TEST 22212

SIZE CLASSIFICATION IN AMC

| SIZE (MIC) | SPGR=1.250 | SPGR=1.325 | SPGR=1.390 | SPGR=1.620 | SPGR=2.0 | SPGR=2.4 | OVERALL |
|---|---|---|---|---|---|---|---|
| 35.0 | 6.06 | 9.22 | 3.31 | 9.49 | 20.08 | 47.23 | 1.63 |
| 100.0 | 3.22 | 3.95 | 4.13 | 22.72 | 56.83 | 81.17 | 6.97 |
| 175.0 | 3.26 | 9.35 | 10.38 | 35.00 | 67.88 | 95.73 | 12.43 |
| 250.0 | 11.96 | 9.85 | 11.04 | 32.62 | 83.10 | 97.62 | 14.93 |
| 360.0 | 17.59 | 38.81 | 34.60 | 80.56 | 98.12 | 99.67 | 39.72 |
| 625.0 | 23.25 | 55.83 | 66.71 | 95.16 | 99.60 | 99.70 | 48.42 |

| | | | | | | | |
|---|---|---|---|---|---|---|---|
| 1000.0 | 34.06 | 48.84 | 76.19 | 97.68 | 98.89 | 99.99 | 47.61 |
| D50 | 1000.00 | 534.19 | 364.50 | 289.88 | 87.92 | 40.30 | 1000.00 |

DENSITY PARTITION IN AMC

| DENSITY | 35.0 mic. | 100.0 mic. | 175.0 mic. | 250.0 mic. | 360.0 mic. | 625.0 mic. | 1000.0 mic. | OVERALL |
|---|---|---|---|---|---|---|---|---|
| 1.250 | 9.64 | 5.89 | 4.22 | 2.73 | 0.69 | 0.68 | 1.31 | 2.61 |
| 1.325 | 16.47 | 20.71 | 11.58 | 2.21 | 2.09 | 0.84 | 2.06 | 6.72 |
| 1.390 | 39.79 | 29.28 | 9.85 | 2.50 | 2.34 | 0.88 | 0.70 | 4.47 |
| 1.620 | 89.69 | 80.25 | 46.12 | 9.09 | 10.01 | 5.73 | 2.12 | 22.16 |
| 2.000 | 94.86 | 98.08 | 91.51 | 50.39 | 30.39 | 21.38 | 4.93 | 68.69 |
| 2.400 | 99.97 | 98.57 | 98.42 | 89.44 | 82.25 | 47.10 | 15.61 | 78.34 |
| SG. SEP. | 1.44 | 1.45 | 1.65 | 2.00 | 2.15 | 2.40 | 2.40 | 1.67 |

TEST 22213

SIZE CLASSIFICATION IN AMC

| SIZE (MIC) | SPGR=1.250 | SPGR=1.325 | SPGR=1.390 | SPGR=1.620 | SPGR=2.0 | SPGR=2.4 | OVERALL |
|---|---|---|---|---|---|---|---|
| 35.0 | 15.71 | 6.33 | 3.12 | 5.75 | 21.76 | 45.65 | 2.57 |
| 100.0 | 2.12 | 2.65 | 7.56 | 40.33 | 57.64 | 92.76 | 15.49 |
| 175.0 | 2.20 | 6.23 | 15.67 | 55.21 | 83.62 | 98.14 | 23.18 |
| 250.0 | 3.84 | 5.71 | 18.83 | 69.75 | 95.45 | 98.69 | 28.02 |
| 360.0 | 17.60 | 21.19 | 40.90 | 91.75 | 99.35 | 99.73 | 47.22 |
| 625.0 | 53.52 | 67.76 | 90.96 | 99.11 | 99.43 | 100.00 | 71.71 |
| 1000.0 | 86.40 | 95.41 | 97.84 | 99.23 | 100.00 | 100.00 | 91.56 |
| D50 | 595.91 | 503.04 | 408.17 | 147.60 | 86.17 | 41.00 | 381.72 |

DENSITY PARTITION IN AMC

| DENSITY | 35.0 mic. | 100.0 mic. | 175.0 mic. | 250.0 mic. | 360.0 mic. | 625.0 mic. | 1000.0 mic. | OVERALL |
|---|---|---|---|---|---|---|---|---|

| | | | | | | | | |
|---|---|---|---|---|---|---|---|---|
| 1.250 | 67.91 | 27.72 | 6.64 | 1.31 | 0.74 | 0.72 | 5.84 | 8.04 |
| 1.325 | 87.38 | 41.18 | 8.22 | 1.98 | 2.16 | 0.90 | 2.20 | 6.88 |
| 1.390 | 93.78 | 77.01 | 18.73 | 7.17 | 5.83 | 2.65 | 1.06 | 7.44 |
| 1.620 | 97.71 | 97.37 | 78.73 | 43.44 | 29.10 | 18.37 | 1.99 | 26.09 |
| 2.000 | 99.99 | 98.31 | 98.07 | 87.47 | 62.96 | 31.18 | 8.48 | 78.18 |
| 2.400 | 100.00 | 99.99 | 99.18 | 96.16 | 94.61 | 81.02 | 21.86 | 86.78 |
| SG. SEP. | 1.25 | 1.34 | 1.44 | 1.68 | 1.85 | 2.15 | 2.40 | 1.79 |

TEST 22221

SIZE CLASSIFICATION IN AMC

| SIZE (MIC) | SPGR=1.250 | SPGR=1.325 | SPGR=1.390 | SPGR=1.620 | SPGR=2.0 | SPGR=2.4 | OVERALL |
|---|---|---|---|---|---|---|---|
| 35.0 | 19.53 | 7.26 | 3.64 | 12.75 | 39.62 | 40.10 | 1.15 |
| 100.0 | 5.33 | 4.14 | 9.78 | 23.60 | 52.32 | 69.91 | 4.39 |
| 175.0 | 7.31 | 5.68 | 12.92 | 32.45 | 57.39 | 82.61 | 8.34 |
| 250.0 | 8.45 | 11.00 | 17.04 | 38.29 | 66.09 | 87.70 | 12.59 |
| 360.0 | 10.89 | 25.29 | 39.77 | 55.08 | 77.42 | 94.62 | 24.09 |
| 625.0 | 27.46 | 39.83 | 49.34 | 72.82 | 90.78 | 97.34 | 30.32 |
| 1000.0 | 26.85 | 27.04 | 33.53 | 73.93 | 94.37 | 99.14 | 25.03 |
| D50 | 1000.00 | 1000.00 | 1000.00 | 329.84 | 88.14 | 56.59 | 1000.00 |

DENSITY PARTITION IN AMC

| DENSITY | 35.0 mic. | 100.0 mic. | 175.0 mic. | 250.0 mic. | 360.0 mic. | 625.0 mic. | 1000.0 mic. | OVERALL |
|---|---|---|---|---|---|---|---|---|
| 1.250 | 4.44 | 4.58 | 1.53 | 1.16 | 0.99 | 0.71 | 2.98 | 2.22 |
| 1.325 | 4.48 | 7.74 | 4.11 | 1.54 | 0.76 | 0.54 | 0.98 | 2.38 |
| 1.390 | 6.01 | 10.98 | 7.72 | 2.54 | 1.85 | 1.35 | 0.48 | 2.01 |
| 1.620 | 26.44 | 25.34 | 13.44 | 7.29 | 5.74 | 3.77 | 1.82 | 8.15 |
| 2.000 | 67.99 | 55.52 | 30.28 | 19.80 | 14.58 | 12.20 | 7.67 | 32.71 |
| 2.400 | 93.58 | 82.29 | 69.04 | 47.47 | 37.58 | 22.74 | 7.82 | 53.72 |

| | | | | | | | | |
|---|---|---|---|---|---|---|---|---|
| SG. SEP. | 1.82 | 1.93 | 2.20 | 2.40 | 2.40 | 2.40 | 2.40 | 2.33 |

TEST 22222

SIZE CLASSIFICATION IN AMC

| SIZE (MIC) | SPGR=1.250 | SPGR=1.325 | SPGR=1.390 | SPGR=1.620 | SPGR=2.0 | SPGR=2.4 | OVERALL |
|---|---|---|---|---|---|---|---|
| 35.0 | 35.19 | 33.36 | 3.08 | 5.44 | 27.76 | 25.67 | 1.86 |
| 100.0 | 6.88 | 3.60 | 11.32 | 16.75 | 32.21 | 69.89 | 6.44 |
| 175.0 | 10.42 | 7.96 | 15.24 | 27.62 | 58.04 | 90.44 | 15.26 |
| 250.0 | 15.22 | 13.40 | 18.28 | 38.05 | 78.23 | 96.78 | 23.88 |
| 360.0 | 23.64 | 23.16 | 31.44 | 69.84 | 96.25 | 99.25 | 43.81 |
| 625.0 | 30.99 | 39.04 | 54.31 | 88.66 | 99.17 | 99.66 | 54.44 |
| 1000.0 | 29.67 | 32.03 | 63.41 | 93.88 | 97.96 | 99.97 | 50.18 |
| D50 | 35.00 | 35.00 | 520.88 | 286.35 | 151.65 | 70.76 | 514.39 |

DENSITY PARTITION IN AMC

| DENSITY | 35.0 mic. | 100.0 mic. | 175.0 mic. | 250.0 mic. | 360.0 mic. | 625.0 mic. | 1000.0 mic. | OVERALL |
|---|---|---|---|---|---|---|---|---|
| 1.250 | 10.10 | 10.69 | 7.62 | 4.56 | 3.00 | 1.93 | 12.64 | 5.16 |
| 1.325 | 11.15 | 14.57 | 7.43 | 3.96 | 2.25 | 0.99 | 11.77 | 6.65 |
| 1.390 | 31.58 | 24.05 | 10.89 | 5.62 | 4.57 | 3.29 | 0.84 | 4.52 |
| 1.620 | 80.34 | 67.55 | 38.16 | 14.07 | 9.23 | 5.09 | 1.51 | 18.96 |
| 2.000 | 92.74 | 96.94 | 87.25 | 48.91 | 26.93 | 11.24 | 9.29 | 64.97 |
| 2.400 | 99.89 | 98.74 | 97.23 | 88.91 | 71.60 | 38.21 | 8.43 | 79.85 |
| SG. SEP. | 1.48 | 1.51 | 1.71 | 2.01 | 2.21 | 2.40 | 1.25 | 1.81 |

TEST 22223

SIZE CLASSIFICATION IN AMC

| SIZE (MIC) | SPGR=1.250 | SPGR=1.325 | SPGR=1.390 | SPGR=1.620 | SPGR=2.0 | SPGR=2.4 | OVERALL |
|---|---|---|---|---|---|---|---|
| 35.0 | 16.59 | 5.71 | 8.17 | 5.54 | 26.81 | 42.27 | 3.29 |
| 100.0 | 4.90 | 6.61 | 6.70 | 33.70 | 56.23 | 91.13 | 11.96 |
| 175.0 | 7.38 | 2.04 | 14.75 | 45.76 | 89.09 | 98.60 | 20.53 |
| 250.0 | 10.19 | 0.08 | 25.85 | 64.58 | 97.16 | 98.87 | 28.66 |
| 360.0 | 23.92 | 25.48 | 59.39 | 93.53 | 99.49 | 99.60 | 51.24 |
| 625.0 | 58.85 | 68.97 | 93.43 | 99.30 | 99.66 | 99.88 | 81.63 |
| 1000.0 | 84.13 | 95.48 | 99.21 | 99.73 | 100.00 | 100.00 | 91.47 |
| D50 | 543.82 | 475.76 | 332.17 | 195.22 | 86.23 | 45.28 | 354.97 |

DENSITY PARTITION IN AMC

| DENSITY | 35.0 mic. | 100.0 mic. | 175.0 mic. | 250.0 mic. | 360.0 mic. | 625.0 mic. | 1000.0 mic. | OVERALL |
|---|---|---|---|---|---|---|---|---|
| 1.250 | 64.65 | 33.04 | 9.79 | 3.77 | 2.67 | 1.75 | 6.42 | 8.40 |
| 1.325 | 87.93 | 43.40 | 10.55 | 0.03 | 0.71 | 2.39 | 2.05 | 7.92 |
| 1.390 | 97.73 | 83.07 | 33.54 | 10.74 | 5.63 | 2.42 | 2.98 | 11.29 |
| 1.620 | 99.23 | 98.00 | 83.29 | 38.61 | 22.55 | 14.92 | 1.98 | 19.60 |
| 2.000 | 99.99 | 99.02 | 98.53 | 92.19 | 73.81 | 30.71 | 11.22 | 80.53 |
| 2.400 | 100.00 | 99.64 | 98.84 | 96.78 | 96.04 | 77.99 | 20.17 | 87.97 |
| SG. SEP. | 1.25 | 1.34 | 1.47 | 1.70 | 1.81 | 2.16 | 2.40 | 1.63 |

# APPENDIX-6: Results of Stepwise-linear-regression for Macro Variable Modelling

SUMMARY OF REGRESSION RESULTS

| DEPENDENT VARIABLE | INDEPENDENT VARIABLES | PLITT'S RESULTS Coeff. | F Ratio | Mult.Corr. | AMC Coeff. | F Ratio | Mult.Corr. |
|---|---|---|---|---|---|---|---|
| ln S | Constant | 1.065 | - | 0.9026 | 1.652 | - | 0.9227 |
| | ln(Du/Do) | 3.31 | 1060 | | 1.376 | 36 | |
| | ln h | 0.544 | 67 | | 0.253 | 7 | |
| | ln Dc | -1.11 | 56 | | - | - | |
| | ln (Do2+Du2) | 0.357 | 33 | | -1.756 | 81 | |
| | ln H | -0.236 | 24 | | - | - | |
| | Ø | 0.00539 | 4 | | 0.050 | 7 | |
| ln P | Constant | 1.556 | - | 0.9009 | -4.68209 | - | 0.9814 |
| | ln Q | 1.78 | 923 | | 1.872 | 524 | |
| | ln(Du2+Do2) | -0.870 | 348 | | -0.804 | 775 | |
| | Ø | 0.00546 | 120 | | 0.0089 | 8 | |
| | ln Di | -0.938 | 46 | | - | - | |
| | ln h | -0.281 | 46 | | - | < 4 | |
| | ln Dc | -0.365 | 6 | | - | - | |
| ln Rf | Constant | - | - | | 1.62440 | - | 0.9577 |
| | ln Rs | - | - | | 1.0968 | 278 | |
| | ln (Do/Du) | - | - | | -0.7399 | 19 | |
| | ln Do | - | - | | -1.6333 | 9 | |
| | ln Du | - | - | | - | < 4 | |

## APPENDIX-7.1: Table A-7.1; Parameters for Classification Model

HIGH FREQUENCY SAMPLES FROM SOUTH PRIMARY AUTOMEDIUM CYCLONE .37

| TIME | FEED STREAM | | UNDERFLOW STREAM | | OVERFLOW STREAM | | YIELD INFORMATION | |
|---|---|---|---|---|---|---|---|---|
| (decimal) | %solids | %ash | %solids | %ash | %solids | %ash | %solids | %ash |
| 9 17 | 11 39 | 15.49 | 52 39 | 61 41 | 10.89 | 11 38 | 94 46 | 91.78 |
| 9.50 | 10 55 | 17 07 | 53.94 | 57 26 | 9 84 | 11.55 | 91.77 | 87.92 |
| 9 83 | 9 43 | 14.64 | 52.42 | 55 40 | 8 25 | 10.84 | 85.15 | 91.47 |
| 10 17 | 9.40 | 16.90 | 52 94 | 56 46 | 8 81 | 11 17 | 92 47 | 87.35 |
| 10.50 | 7 11 | 23 67 | 55.88 | 69.01 | 7.91 | 16 93 | 113.11 ? | 87.06 |
| 10 83 | 10 45 | 20 70 | 56.25 | 69.09 | 9.31 | 15 68 | 86.93 | 90.60 |
| 11 17 | 10 93 | 22 30 | 56.61 | 67.76 | 10.19 | 17 69 | 91.74 | 90.79 |
| 11 50 | 14 16 | 26 17 | 61.99 | 67 05 | N/A | N/A | N/A | N/A |
| 11 83 | 15 40 | 24.69 | 63 23 | 67.47 | 14 07 | 16.75 | 88.89 | 84.35 |
| 12 17 | 14.98 | 24.76 | 63.74 | 70.19 | 12.53 | 17.14 | 79.64 | 85.64 |
| 12.50 | 13 91 | 23 93 | 63.36 | 65 54 | 12.20 | 17 45 | 84 78 | 86.53 |
| 12 83 | 9 73 | 24 88 | 56 19 | 65.42 | 6 44 | 15 65 | 61 81 | 81.45 |
| 13 17 | 14 18 | 27.00 | 62.20 | 69.30 | 12 18 | 17.47 | 82.46 | 81.61 |
| 13 50 | 14 57 | 25.78 | 63.14 | 67.26 | 12 87 | 18 07 | 85.34 | 84.33 |
| 13 83 | 13 10 | 27.69 | 62.70 | 68 15 | 12.76 | 18.03 | 96.74 | 80.73 |
| 14 17 | 14 76 | 26 44 | 63 67 | 67.87 | 12 79 | 18.80 | 83 30 | 84.43 |
| 14 50 | 15 07 | 25 15 | 60 66 | 70 22 | 13 50 | 19 62 | 86 60 | 89.07 |
| 14 83 | 11 52 | 24 25 | 64 36 | 73.06 | 10.66 | 19.52 | 91.05 | 91.17 |
| 15 17 | 8.45 | 22 71 | 55.73 | 60.40 | 7.20 | 15 84 | 83.01 | 84.58 |
| 15 50 | 6 58 | 21.50 | 51.82 | 59.41 | 5.72 | 15 44 | 85.31 | 86.22 |
| 15.83 | 8 54 | 25 10 | 56.32 | 67.25 | 7.31 | 17.99 | 83.45 | 85.57 |
| 16 17 | 5.39 | 27.04 | 54 19 | 67.33 | 4.54 | 18 85 | 82.79 | 83.11 |
| 16 50 | 6 39 | 28 65 | 57 37 | 60.92 | 4 92 | 16 22 | 74.84 | 72.19 |
| 16 83 | 8.72 | 23 42 | 56 49 | 58 98 | 7 68 | 14 65 | 86 20 | 80.22 |
| 17 17 | 9 07 | 23 79 | 56 38 | 58 86 | 7 87 | 15.76 | 84.62 | 81 37 |
| 17 50 | 15 37 | 27 37 | 63.27 | 68 69 | N/A | N/A | N/A | N/A |
| 17 50 | 15 09 | 29 12 | 63 16 | 68 41 | N/A | N/A | N/A | N/A |
| 17 83 | 19 50 | 26 97 | 62 60 | 67 20 | N/A | N/A | N/A | N/A |
| 17 83 | 19.26 | 25 80 | 63.06 | 67.61 | N/A | N/A | N/A | N/A |
| 18 17 | 17 21 | 27 81 | 63 42 | 70 75 | N/A | N/A | N/A | N/A |
| 18 17 | 17 85 | 29.95 | 60 20 | 69 93 | N/A | N/A | N/A | N/A |
| 18 50 | 17 76 | 27 28 | 63.58 | 68 45 | N/A | N/A | N/A | N/A |
| 18 50 | 17 60 | 27.99 | 66 82 | 69 48 | N/A | N/A | N/A | N/OA |
| 18 83 | 16 10 | 28.10 | 62.66 | 68 66 | 14.30 | 19 76 | 85.51 | 82.94 |
| ** 18 87 | 16 54 | 28.69 | 22 57 | 39 71 | 12.74 | 15.56 | 47.25 | 45 63 |

** Restricted flow using "Gagnon valve"

MEANS (Computed from complete data sets)

| | | | | | | | |
|---|---|---|---|---|---|---|---|
| 10 82 | 23.23 | 58.00 | 64.75 | 9.60 | 16.19 | 86.52 | 85 40 |
| Calculated from attribute mean values | | | | | | 86.49 | 85.50 |

# APPENDIX-7.2: Derivation of the AMC Model

Derivation of the Comprehensive Model for the AMC

Let $C, A$ and $B$ represent the primary classification, bed separation and secondary classification respectively, according to Figure-1.

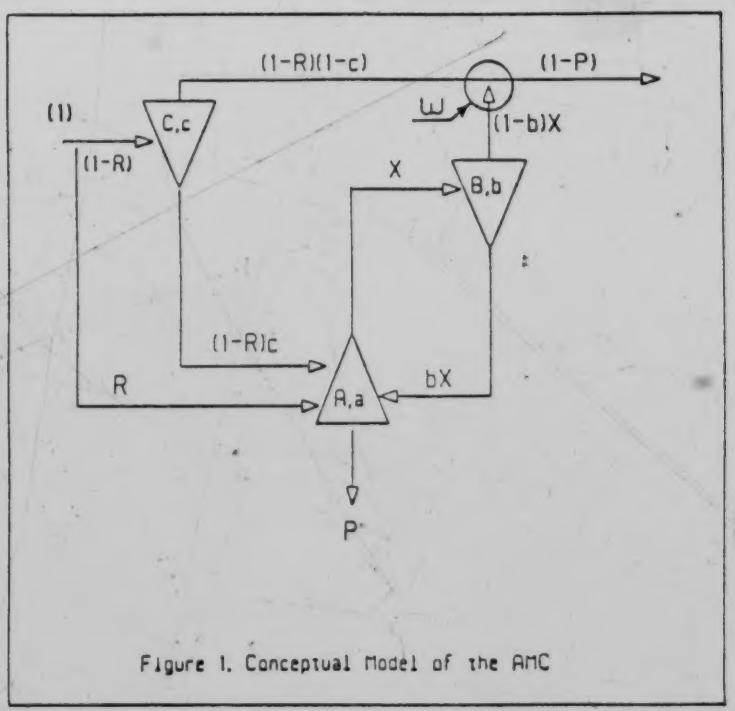


Figure 1. Conceptual Model of the AMC

Also let fraction of any species (certain size fraction of a given density in the stream entering these separators) that is sent to *underflow* be represented by $c, a$ and $b$ respectively for the same regions (here *underflow* denotes the stream richer in the coarser size fractions, in case of $C$ and $B$ the streams sent to the bed

are coarser, while in case of separation in $A$ the stream that is sent to the second classifier, $B$, is coarser and this stream, designated as X, is the *underflow*).

Taking the feed stream as unity and calling the by-pass flow from feed to the apex R, and total apex flow $P$, a mass balance arround separator $A$ gives;

$$P = [(1 - R)c + R + bX](1 - a) \qquad (A7.1)$$

A second balance at the mixing point "w" of vortex flow gives;

$$(1 - P) = (1 - R)(1 - c) + X(1 - b) \qquad (A7.2)$$

rearranging equation $(A7.2)$;

$$X = \frac{(1 - P) - (1 - R)(1 - c)}{(1 - b)} \qquad (A7.3)$$

Substituting equation $(A7.3)$ in equation $(A7.1)$ yields;

$$P = \left[(1 - R)c + R + b\left[\frac{(1 - P) - (1 - R)(1 - c)}{(1 - b)}\right]\right](1 - a) \qquad (A7.4)$$

Simplifying equation $(A7.4)$;

$$(1 - b)P = [c(1 - R) + R - Pb](1 - a)$$

and solving for $P$;

$$P = \frac{c(1 - R)(1 - a) + R(1 - a)}{1 - ab}$$

rearranging;

$$P = R + (1 - R)c\left[\frac{1 - a}{1 - ab}\right] \qquad (A7.5)$$

Equation (A7.5) represents the partition value for any particular species in the feed that reports to the apex of AMC.

**Note that** : when $a = 0$ (e.i. there is no significant bed formation) equation (A7.5) reduces to;

$$P = R - (1 - R)c$$

which is the simple classification partition model.

## APPENDIX-7.3: The Semi-Visual Curve Fitting Program CPLOT

CPLOT - An Interactive Graphics Program for Fitting
Non-linear Models to Experimental Data

1. Background.

The CPLOT program was written in direct response to a problem encountered when trying to fit a non-linear model with seven parameters to observed data. None of the available statistical analysis programs were able to solve for the parameters with reasonable convergence time. It was decided to write a customized graphics program that would prompt for changes in parameters, plot the equation against experimental data, and give an error metric. Because the program was written specifically for this purpose, and specifically for a VT125 terminal, the above process could be completed in a few seconds; the speed limitation being the users typing speed, and the baud rate of the terminal.

The procedure involves "grabing" data set either from the file containing partition data or from terminal, entering first approximations for the parameters, plotting the experimental data and the curve given by the model, adjusting the parameters interactively to improve the fit. Since the resultant value for the minimization function for least-square-fit and it's change is displayed at each step the process is not subjective to human error as would be for a visual curve-fitting procedure.

In using the program, several advantages to this approach became apparent. We found that as sets of data were fitted, one acquired a feel for the behavior of the model, and was able to find the best fit with increasing speed. Because this was a custom written program, we were also able to change it as desired to streamline the runs.

A pseudo-code for the semi-visual curve fitting program is given in the following sections.

2. The Program

```
BEGIN
Initialize memory;
Initialize output file control;
Ask whether manual data entry or data file input is used;
Initialize input file control or manual input control;
LOOP

        Ask if input is from file
        if YES then LOOP

                Display record number;
                Prompt for input
                if input=OK leave loop;
                if input=PREVIOUS decrement record number;
                if input=NEXT increment record number;
                if input=STOP leave program;
                if input=<value> set record number to value;

        If not first run ask if old parameter values are to be used
        if NO then LOOP

                Prompt for paramater values one at a time;
                Ask if parameter values are ok
                if YES then leave loop;

        If input is from a file
                Open input file;
                Locate the record corresponding to record number;
                Load the input data;
                Close input file;

        If input is not from a file
                Prompt for X and Y values until non <value> is typed;

        Initialize error and last_error to something very big;
        LOOP
                Scale and plot input values;
                If last input was not PAGE
                        Last_error = error;
                        Calculate error;
                        If error is less than last_error
                                Best parameters = current parameters;

                If plotting is not inhibited or locked
                        Solve model for given parameters;
                        Plot data from model;
```

```
                Uninhibit plotting;
                Print menu and prompt for input;
                If input=BEST copy best parameters to current ones;
                If input=COLOUR
                        Prompt for colour;
                        Set colour;
                        Inhibit plotting;
                If input=LOCK
                        If plotting is not locked then lock plotting;
                        If plotting is locked then unlock plotting;
                If input=HARDCOPY
                        Turn on hardcopy;
                        Print the parameter values;
                        Print the error;
                        Print escape sequences to hardcopy plot;

                If input=NEXT leave loop;
                If input=PAGE goto beginning of loop;
                If input=STOP leave loop;
                If input=<parameter name>
                        Prompt for parameter value;
                        Set parameter to value;

                If input=<blank>
                        Prompt for parameter value;
                        Set last named parameter to value;

        Ask if results are to be saved
        if YES write parameters and run id to output file;
        If input=STOP (from idem menu prompt) leave loop;

Finish off and tidy up;
END.
```

## APPENDIX-7.4: The Fitted Curve Parameters

MODEL PARAMETERS FOR THE BEST-FIT DETERMINED BY "CPLOT" ON VAX

| TEST | RHO | d50A | d50B | d50C | mA | mB | mC | Rf |
|---|---|---|---|---|---|---|---|---|
| 11111 | | | | | | | | |
| | 2.40 | 650.00 | 108.00 | 92.00 | 0.35 | 1.30 | 3.60 | 0.041 |
| | 2.00 | 500.00 | 125.00 | 150.00 | 0.80 | 1.00 | 2.50 | 0.041 |
| | 1.62 | 165.00 | 135.00 | 232.00 | 1.02 | 1.20 | 2.80 | 0.041 |
| | 1.39 | 82.00 | 73.00 | 415.00 | 1.10 | 1.10 | 2.20 | 0.041 |
| | 1.33 | 370.00 | 60.00 | 530.00 | 1.10 | 0.52 | 3.00 | 0.005 |
| | 1.25 | 85.00 | 225.00 | 1120.00 | 1.15 | 2.50 | 1.80 | 0.330 |
| 11112 | | | | | | | | |
| | 2.40 | 800.00 | 74.00 | 74.00 | 0.80 | 1.20 | 3.30 | 0.036 |
| | 2.00 | 850.00 | 115.00 | 120.00 | 1.35 | 1.20 | 3.80 | 0.036 |
| | 1.62 | 500.00 | 130.00 | 185.00 | 3.50 | 1.50 | 1.85 | 0.036 |
| | 1.39 | 400.00 | 350.00 | 265.00 | 1.50 | 2.50 | 3.80 | 0.036 |
| | 1.33 | 5.00 | 62.00 | 175.00 | 0.54 | 1.25 | 3.00 | 0.420 |
| | 1.25 | 8.20 | 57.00 | 232.00 | 0.62 | 1.20 | 3.50 | 0.500 |
| 11113 | | | | | | | | |
| | 2.40 | 1200.00 | 85.00 | 70.00 | 0.80 | 1.40 | 3.50 | 0.036 |
| | 2.00 | 1050.00 | 137.00 | 95.00 | 1.00 | 1.80 | 4.50 | 0.036 |
| | 1.62 | 210.00 | 128.00 | 126.00 | 1.60 | 1.95 | 3.60 | 0.036 |
| | 1.39 | 202.00 | 144.00 | 188.00 | 1.50 | 1.66 | 4.10 | 0.052 |
| | 1.33 | 185.00 | 125.00 | 260.00 | 1.66 | 1.57 | 4.80 | 0.036 |
| | 1.25 | 350.00 | 278.00 | 299.00 | 1.60 | 2.10 | 4.20 | 0.067 |
| 11121 | | | | | | | | |
| | 2.40 | 575.00 | 154.00 | 110.00 | 1.28 | 1.50 | 5.60 | 0.047 |
| | 2.00 | 265.00 | 155.00 | 140.00 | 1.40 | 1.60 | 3.50 | 0.047 |
| | 1.62 | 113.00 | 128.00 | 142.00 | 1.33 | 1.59 | 3.50 | 0.082 |
| | 1.39 | 85.00 | 56.00 | 452.00 | 1.11 | 1.00 | 2.20 | 0.060 |
| | 1.33 | 350.00 | 33.00 | 680.00 | 0.80 | 0.33 | 3.50 | 0.110 |
| | 1.25 | 38.00 | 92.00 | 990.00 | 0.90 | 1.40 | 0.95 | 0.180 |
| 11122 | | | | | | | | |
| | 2.40 | 650.00 | 110.00 | 31.50 | 0.78 | 2.40 | 2.30 | 0.036 |
| | 2.00 | 642.00 | 150.00 | 102.00 | 1.60 | 1.80 | 2.30 | 0.036 |
| | 1.62 | 325.00 | 180.00 | 155.00 | 2.00 | 1.85 | 2.60 | 0.036 |
| | 1.39 | 310.00 | 265.00 | 285.00 | 1.40 | 1.98 | 3.80 | 0.036 |
| | 1.33 | 220.00 | 265.00 | 275.00 | 1.55 | 2.15 | 3.80 | 0.036 |
| | 1.25 | 263.00 | 295.00 | 375.00 | 1.55 | 2.08 | 4.50 | 0.051 |
| 11123 | | | | | | | | |
| | 2.40 | 1550.00 | 105.00 | 71.50 | 0.80 | 2.20 | 3.80 | 0.033 |

| | | | | | | | |
|---|---|---|---|---|---|---|---|
| 2.00 | 850.00 | 120.00 | 97.00 | 0.75 | 1.95 | 3.80 | 0.030 |
| 1.62 | 775.00 | 135.00 | 138.00 | 0.25 | 1.50 | 4.50 | 0.033 |
| 1.39 | 330.00 | 265.00 | 204.00 | 1.20 | 2.50 | 6.00 | 0.033 |
| 1.33 | 265.00 | 265.00 | 250.00 | 1.20 | 2.65 | 4.80 | 0.033 |
| 1.25 | 102.00 | 202.00 | 250.00 | 1.10 | 2.15 | 6.00 | 0.190 |

11211

| | | | | | | | |
|---|---|---|---|---|---|---|---|
| 2.40 | 350.00 | 115.00 | 104.00 | 0.80 | 1.40 | 3.00 | 0.039 |
| 2.00 | 165.00 | 116.00 | 152.00 | 0.92 | 1.26 | 2.85 | 0.039 |
| 1.62 | 1.20 | 25.00 | 88.00 | 0.35 | 0.75 | 4.00 | 0.039 |
| 1.39 | 150.00 | 160.00 | 450.00 | 1.00 | 1.15 | 1.80 | 0.039 |
| 1.33 | 130.00 | 151.00 | 585.00 | 1.00 | 1.09 | 1.80 | 0.039 |
| 1.25 | 16.00 | 82.00 | 166.00 | 0.70 | 1.12 | 7.00 | 0.080 |

11212

| | | | | | | | |
|---|---|---|---|---|---|---|---|
| 2.40 | 450.00 | 90.00 | 88.00 | 0.80 | 1.35 | 4.50 | 0.045 |
| 2.00 | 375.00 | 118.00 | 141.00 | 1.05 | 1.20 | 3.05 | 0.045 |
| 1.62 | 31.00 | 51.00 | 95.00 | 0.85 | 1.08 | 6.65 | 0.045 |
| 1.39 | 28.00 | 81.50 | 275.00 | 0.74 | 1.11 | 4.40 | 0.099 |
| 1.33 | 31.00 | 81.50 | 275.00 | 0.80 | 1.12 | 4.80 | 0.060 |
| 1.25 | 20.00 | 76.00 | 185.00 | 0.73 | 1.12 | 3.00 | 0.045 |

11213

| | | | | | | | |
|---|---|---|---|---|---|---|---|
| 2.40 | 800.00 | 81.00 | 72.00 | 0.80 | 1.50 | 3.00 | 0.045 |
| 2.00 | 375.00 | 120.00 | 110.00 | 0.80 | 1.80 | 3.80 | 0.045 |
| 1.62 | 19.00 | 112.00 | 118.00 | 0.28 | 1.30 | 3.80 | 0.045 |
| 1.39 | 204.00 | 275.00 | 280.00 | 0.68 | 1.62 | 3.40 | 0.075 |
| 1.33 | 48.00 | 96.00 | 239.00 | 0.91 | 1.28 | 3.60 | 0.066 |
| 1.25 | 42.00 | 91.00 | 305.00 | 0.94 | 1.28 | 3.60 | 0.025 |

11221

| | | | | | | | |
|---|---|---|---|---|---|---|---|
| 2.40 | 410.00 | 155.00 | 87.00 | 0.75 | 2.00 | 5.20 | 0.048 |
| 2.00 | 256.00 | 188.00 | 136.00 | 0.40 | 1.60 | 2.55 | 0.048 |
| 1.62 | 80.00 | 242.00 | 165.00 | 0.42 | 1.35 | 1.63 | 0.048 |
| 1.39 | 55.00 | 94.00 | 276.00 | 0.94 | 1.15 | 5.60 | 0.110 |
| 1.33 | 130.00 | 435.00 | 285.00 | 1.00 | 2.20 | 6.00 | 0.050 |
| 1.25 | 18.50 | 73.00 | 120.00 | 0.76 | 1.13 | 2.80 | 0.048 |

11222

| | | | | | | | |
|---|---|---|---|---|---|---|---|
| 2.40 | 990.00 | 155.00 | 85.00 | 0.98 | 3.00 | 3.60 | 0.048 |
| 2.00 | 350.00 | 155.00 | 126.00 | 1.35 | 1.95 | 3.30 | 0.048 |
| 1.62 | 60.00 | 70.00 | 130.00 | 1.02 | 1.27 | 2.94 | 0.048 |
| 1.39 | 56.00 | 93.00 | 282.00 | 1.02 | 1.33 | 2.38 | 0.048 |
| 1.33 | 30.00 | 66.00 | 250.00 | 0.80 | 1.08 | 6.00 | 0.110 |
| 1.25 | 8.00 | 60.00 | 300.00 | 0.60 | 1.10 | 5.50 | 0.430 |

11223

| | | | | | | | |
|---|---|---|---|---|---|---|---|
| 2.40 | 1000.00 | 100.00 | 77.00 | 1.10 | 1.80 | 4.20 | 0.058 |
| 2.00 | 770.00 | 185.00 | 108.00 | 1.10 | 3.50 | 4.00 | 0.085 |
| 1.62 | 270.00 | 175.00 | 158.00 | 0.80 | 1.55 | 2.80 | 0.058 |
| 1.39 | 95.00 | 104.00 | 255.00 | 1.05 | 1.24 | 4.00 | 0.090 |
| 1.33 | 85.00 | 170.00 | 285.00 | 0.80 | 1.38 | 2.85 | 0.058 |
| 1.25 | 85.00 | 170.00 | 366.00 | 0.88 | 1.42 | 2.40 | 0.100 |

12111

| | | | | | | | |
|---|---|---|---|---|---|---|---|
| 2.40 | 1000.00 | 125.00 | 71.00 | 0.80 | 1.85 | 3.50 | 0.080 |
| 2.00 | 920.00 | 122.00 | 88.00 | 0.80 | 1.15 | 1.60 | 0.080 |
| 1.62 | 822.00 | 160.00 | 148.00 | 0.80 | 1.02 | 1.55 | 0.080 |
| 1.39 | 300.00 | 209.00 | 218.00 | 1.25 | 1.38 | 2.24 | 0.040 |
| 1.33 | 75.00 | 99.00 | 240.00 | 0.91 | 1.16 | 6.00 | 0.200 |
| 1.25 | 60.00 | 142.00 | 860.00 | 0.98 | 1.85 | 3.00 | 0.720 |

12112

| | | | | | | | |
|---|---|---|---|---|---|---|---|
| 2.40 | 1000.00 | 120.00 | 72.00 | 1.00 | 2.00 | 3.30 | 0.078 |
| 2.00 | 920.00 | 175.00 | 96.00 | 1.12 | 2.20 | 3.45 | 0.078 |
| 1.62 | 810.00 | 205.00 | 112.00 | 1.50 | 1.44 | 2.20 | 0.078 |
| 1.39 | 366.00 | 226.00 | 156.00 | 0.88 | 1.65 | 3.80 | 0.078 |
| 1.33 | 232.00 | 213.00 | 214.00 | 1.10 | 1.60 | 5.50 | 0.055 |
| 1.25 | 216.00 | 213.00 | 214.00 | 1.44 | 1.80 | 4.80 | 0.092 |

12113

| | | | | | | | |
|---|---|---|---|---|---|---|---|
| 2.40 | 1000.00 | 82.00 | 56.00 | 1.00 | 2.30 | 2.45 | 0.078 |
| 2.00 | 750.00 | 108.00 | 77.00 | 1.10 | 1.38 | 3.30 | 0.099 |
| 1.62 | 380.00 | 75.00 | 88.00 | 0.59 | 1.16 | 5.40 | 0.099 |
| 1.39 | 210.00 | 100.00 | 140.00 | 1.22 | 1.25 | 4.00 | 0.099 |
| 1.33 | 314.00 | 150.00 | 158.00 | 1.66 | 1.38 | 4.00 | 0.040 |
| 1.25 | 210.00 | 128.00 | 166.00 | 1.65 | 1.45 | 3.35 | 0.040 |

12121

| | | | | | | | |
|---|---|---|---|---|---|---|---|
| 2.40 | 1000.00 | 125.00 | 68.00 | 0.80 | 1.80 | 3.00 | 0.082 |
| 2.00 | 792.00 | 176.00 | 94.00 | 1.20 | 1.25 | 2.20 | 0.082 |
| 1.62 | 350.00 | 132.00 | 111.00 | 0.68 | 1.10 | 2.32 | 0.082 |
| 1.39 | 160.00 | 225.00 | 152.00 | 0.25 | 1.15 | 2.32 | 0.082 |
| 1.33 | 365.00 | 280.00 | 249.00 | 1.26 | 1.42 | 3.80 | 0.075 |
| 1.25 | 18.00 | 110.00 | 249.00 | 0.55 | 1.20 | 3.80 | 0.750 |

12122

| | | | | | | | |
|---|---|---|---|---|---|---|---|
| 2.40 | 1200.00 | 112.00 | 62.00 | 1.20 | 1.85 | 2.80 | 0.066 |
| 2.00 | 1200.00 | 112.00 | 79.00 | 1.20 | 1.22 | 2.20 | 0.066 |
| 1.62 | 850.00 | 150.00 | 110.00 | 0.83 | 1.26 | 4.50 | 0.066 |
| 1.39 | 520.00 | 166.00 | 174.00 | 1.12 | 1.20 | 3.22 | 0.042 |
| 1.33 | 455.00 | 320.00 | 176.00 | 2.35 | 2.90 | 3.30 | 0.042 |
| 1.25 | 503.00 | 420.00 | 260.00 | 2.40 | 3.00 | 3.30 | 0.045 |

12123

| | | | | | | | |
|---|---|---|---|---|---|---|---|
| 2.40 | 1000.00 | 85.00 | 60.00 | 1.20 | 1.80 | 3.00 | 0.085 |
| 2.00 | 975.00 | 175.00 | 76.00 | 1.65 | 1.38 | 2.80 | 0.085 |
| 1.62 | 680.00 | 166.00 | 94.00 | 0.95 | 1.45 | 5.00 | 0.020 |
| 1.39 | 420.00 | 120.00 | 115.00 | 0.20 | 1.10 | 5.00 | 0.020 |
| 1.33 | 1250.00 | 500.00 | 145.00 | 1.44 | 4.00 | 2.60 | 0.020 |
| 1.25 | 1300.00 | 530.00 | 220.00 | 1.10 | 4.20 | 4.00 | 0.180 |

12211

| | | | | | | | |
|---|---|---|---|---|---|---|---|
| 2.40 | 1000.00 | 132.00 | 78.00 | 0.80 | 1.55 | 3.00 | 0.087 |
| 2.00 | 685.00 | 158.00 | 116.00 | 1.28 | 1.15 | 2.20 | 0.087 |
| 1.62 | 155.00 | 150.00 | 153.00 | 1.40 | 1.62 | 4.50 | 0.300 |
| 1.39 | 155.00 | 153.00 | 196.00 | 1.53 | 1.62 | 2.85 | 0.087 |
| 1.33 | 55.00 | 97.00 | 153.00 | 1.02 | 1.32 | 3.50 | 0.040 |
| 1.25 | 77.00 | 136.00 | 238.00 | 0.99 | 1.36 | 4.00 | 0.200 |

12212

| | | | | | | | |
|---|---|---|---|---|---|---|---|
| 2.40 | 1000.00 | 116.00 | 65.00 | 0.80 | 1.95 | 3.00 | 0.080 |
| 2.00 | 950.00 | 151.00 | 96.00 | 1.10 | 1.20 | 3.00 | 0.080 |
| 1.62 | 710.00 | 152.00 | 121.00 | 0.80 | 1.20 | 2.20 | 0.080 |
| 1.39 | 355.00 | 176.00 | 201.00 | 1.00 | 1.20 | 2.90 | 0.050 |
| 1.33 | 202.00 | 146.00 | 265.00 | 1.10 | 1.22 | 3.60 | 0.060 |
| 1.25 | 175.00 | 175.00 | 315.00 | 1.00 | 1.30 | 2.30 | 0.100 |

12213

| | | | | | | | |
|---|---|---|---|---|---|---|---|
| 2.40 | 1000.00 | 95.00 | 60.00 | 0.80 | 2.00 | 3.00 | 0.094 |
| 2.00 | 1600.00 | 175.00 | 78.00 | 1.00 | 1.60 | 2.65 | 0.094 |
| 1.62 | 480.00 | 126.00 | 102.00 | 0.80 | 1.30 | 3.25 | 0.022 |
| 1.39 | 225.00 | 142.00 | 135.00 | 1.10 | 1.39 | 3.00 | 0.018 |
| 1.33 | 225.00 | 166.00 | 192.00 | 1.40 | 1.52 | 3.60 | 0.042 |
| 1.25 | 225.00 | 208.00 | 211.00 | 1.40 | 1.75 | 3.50 | 0.130 |

12221

| | | | | | | | |
|---|---|---|---|---|---|---|---|
| 2.40 | 403.00 | 130.00 | 45.00 | 0.60 | 2.60 | 3.85 | 0.066 |
| 2.00 | 1000.00 | 166.00 | 185.00 | 0.80 | 1.10 | 8.00 | 0.620 |
| 1.62 | 560.00 | 205.00 | 152.00 | 0.60 | 1.15 | 2.60 | 0.075 |
| 1.39 | 206.00 | 200.00 | 230.00 | 1.30 | 1.50 | 5.00 | 0.160 |
| 1.33 | 195.00 | 185.00 | 300.00 | 1.30 | 1.45 | 2.10 | 0.020 |
| 1.25 | 15.00 | 90.00 | 55.00 | 0.65 | 1.25 | 5.00 | 0.100 |

12222

| | | | | | | | |
|---|---|---|---|---|---|---|---|
| 2.40 | 1200.00 | 125.00 | 61.00 | 1.00 | 2.00 | 2.40 | 0.061 |
| 2.00 | 915.00 | 150.00 | 82.00 | 1.60 | 1.30 | 1.72 | 0.061 |
| 1.62 | 485.00 | 186.00 | 136.00 | 1.60 | 1.50 | 2.60 | 0.061 |
| 1.39 | 235.00 | 210.00 | 170.00 | 0.80 | 1.60 | 3.60 | 0.072 |
| 1.33 | 95.00 | 175.00 | 185.00 | 0.86 | 1.65 | 6.60 | 0.110 |
| 1.25 | 185.00 | 365.00 | 230.00 | 0.90 | 2.75 | 6.50 | 0.100 |

12223

| | | | | | | | |
|---|---|---|---|---|---|---|---|
| 2.40 | 1000.00 | 125.00 | 44.00 | 1.10 | 2.50 | 1.75 | 0.088 |
| 2.00 | 1200.00 | 135.00 | 105.00 | 1.10 | 1.20 | 7.50 | 0.088 |
| 1.62 | 796.00 | 135.00 | 120.00 | 0.80 | 1.20 | 3.30 | 0.088 |
| 1.39 | 580.00 | 235.00 | 151.00 | 1.00 | 1.60 | 3.00 | 0.120 |
| 1.33 | 580.00 | 260.00 | 195.00 | 1.00 | 1.66 | 5.00 | 0.080 |
| 1.25 | 395.00 | 296.00 | 238.00 | 2.60 | 2.50 | 5.00 | 0.120 |

21111

| | | | | | | | |
|---|---|---|---|---|---|---|---|
| 2.40 | 395.00 | 285.00 | 174.00 | 1.10 | 1.45 | 2.20 | 0.005 |
| 2.00 | 205.00 | 314.00 | 310.00 | 1.10 | 1.70 | 3.50 | 0.070 |
| 1.62 | 205.00 | 425.00 | 810.00 | 0.80 | 1.20 | 1.70 | 0.010 |
| 1.39 | 300.00 | 1200.00 | 1200.00 | 1.05 | 0.60 | 1.80 | 0.010 |
| 1.33 | 18.00 | 600.00 | 180.00 | 0.55 | 0.50 | 8.00 | 0.035 |
| 1.25 | 62.00 | 800.00 | 510.00 | 0.69 | 2.00 | 6.00 | 0.060 |

21112

| | | | | | | | |
|---|---|---|---|---|---|---|---|
| 2.40 | 225.00 | 132.00 | 108.00 | 1.50 | 2.00 | 4.00 | 0.005 |
| 2.00 | 485.00 | 295.00 | 245.00 | 0.80 | 1.96 | 4.80 | 0.104 |
| 1.62 | 16.00 | 75.00 | 155.00 | 0.69 | 1.20 | 4.00 | 0.025 |
| 1.39 | 20.00 | 96.00 | 135.00 | 0.77 | 1.28 | 4.00 | 0.025 |
| 1.33 | 250.00 | 125.00 | 1350.00 | 1.00 | 0.75 | 1.80 | 0.010 |
| 1.25 | 9.00 | 95.00 | 600.00 | 0.51 | 0.90 | 9.00 | 0.150 |

21113

| | | | | | | | |
|---|---|---|---|---|---|---|---|
| 2.40 | 1000.00 | 125.00 | 100.00 | 0.80 | 2.00 | 3.75 | 0.011 |
| 2.00 | 45.00 | 110.00 | 105.00 | 0.80 | 1.65 | 4.50 | 0.180 |
| 1.62 | 95.00 | 150.00 | 300.00 | 0.85 | 1.50 | 2.00 | 0.005 |
| 1.39 | 35.00 | 150.00 | 200.00 | 0.84 | 1.55 | 5.80 | 0.020 |
| 1.33 | 30.00 | 110.00 | 230.00 | 0.79 | 1.28 | 6.40 | 0.050 |
| 1.25 | 30.00 | 120.00 | 500.00 | 0.82 | 1.35 | 4.20 | 0.040 |

21121

| | | | | | | | |
|---|---|---|---|---|---|---|---|
| 2.40 | 32.00 | 285.00 | 140.00 | 0.20 | 1.10 | 2.00 | 0.001 |
| 2.00 | 32.00 | 265.00 | 285.00 | 0.40 | 1.06 | 1.40 | 0.001 |
| 1.62 | 50.00 | 100.00 | 455.00 | 0.80 | 0.95 | 2.10 | 0.011 |
| 1.39 | 50.00 | 110.00 | 645.00 | 0.80 | 0.90 | 2.10 | 0.011 |
| 1.33 | 50.00 | 110.00 | 650.00 | 0.80 | 0.88 | 3.10 | 0.020 |
| 1.25 | 50.00 | 95.00 | 800.00 | 0.80 | 0.82 | 3.00 | 0.025 |

21122

| | | | | | | | |
|---|---|---|---|---|---|---|---|
| 2.40 | 125.00 | 106.00 | 105.00 | 1.30 | 1.62 | 3.50 | 0.008 |
| 2.00 | 35.00 | 80.00 | 102.00 | 0.82 | 1.25 | 3.00 | 0.008 |
| 1.62 | 85.00 | 135.00 | 425.00 | 0.80 | 1.10 | 1.80 | 0.008 |
| 1.39 | 80.00 | 84.00 | 810.00 | 0.80 | 0.75 | 3.50 | 0.030 |
| 1.33 | 51.00 | 93.00 | 370.00 | 1.03 | 1.23 | 8.00 | 0.010 |
| 1.25 | 160.00 | 610.00 | 590.00 | 0.95 | 1.50 | 6.00 | 0.045 |

21123

| | | | | | | | |
|---|---|---|---|---|---|---|---|
| 2.40 | 485.00 | 135.00 | 88.00 | 0.55 | 2.00 | 7.00 | 0.020 |
| 2.00 | 485.00 | 200.00 | 210.00 | 0.55 | 1.80 | 4.00 | 0.095 |
| 1.62 | 5.00 | 200.00 | 100.00 | 0.35 | 1.75 | 7.50 | 0.010 |
| 1.39 | 250.00 | 200.00 | 600.00 | 0.80 | 1.00 | 3.00 | 0.025 |
| 1.33 | 250.00 | 200.00 | 820.00 | 0.80 | 1.00 | 2.00 | 0.010 |
| 1.25 | 55.00 | 159.00 | 1250.00 | 0.98 | 1.72 | 5.00 | 0.220 |

21211

| | | | | | | | |
|---|---|---|---|---|---|---|---|
| 2.40 | 62.00 | 245.00 | 86.00 | 0.39 | 1.45 | 4.80 | 0.010 |
| 2.00 | 6.00 | 101.00 | 95.00 | 0.38 | 0.92 | 5.00 | 0.040 |
| 1.62 | 3.50 | 26.00 | 85.00 | 0.53 | 0.80 | 6.00 | 0.020 |
| 1.39 | 45.00 | 400.00 | 490.00 | 0.53 | 0.78 | 3.30 | 0.020 |
| 1.33 | 45.00 | 650.00 | 485.00 | 0.53 | 0.70 | 2.80 | 0.020 |
| 1.25 | 45.00 | 600.00 | 485.00 | 0.60 | 1.20 | 2.80 | 0.090 |

21212

| | | | | | | | |
|---|---|---|---|---|---|---|---|
| 2.40 | 155.00 | 165.00 | 110.00 | 1.10 | 2.00 | 3.20 | 0.011 |
| 2.00 | 70.00 | 110.00 | 165.00 | 1.00 | 1.40 | 2.00 | 0.060 |
| 1.62 | 70.00 | 116.00 | 390.00 | 1.00 | 1.28 | 2.40 | 0.080 |
| 1.39 | 80.00 | 175.00 | 615.00 | 1.00 | 1.36 | 2.40 | 0.030 |
| 1.33 | 80.00 | 190.00 | 580.00 | 1.00 | 1.36 | 3.50 | 0.025 |
| 1.25 | 75.00 | 260.00 | 520.00 | 0.87 | 1.28 | 3.30 | 0.090 |

21213

| | | | | | | | |
|---|---|---|---|---|---|---|---|
| 2.40 | 750.00 | 210.00 | 95.00 | 0.80 | 4.00 | 3.50 | 0.016 |
| 2.00 | 750.00 | 285.00 | 185.00 | 0.80 | 2.40 | 1.85 | 0.016 |
| 1.62 | 880.00 | 120.00 | 485.00 | 1.60 | 2.20 | 2.60 | 0.050 |
| 1.39 | 625.00 | 120.00 | 825.00 | 1.15 | 2.20 | 3.10 | 0.025 |
| 1.33 | 29.00 | 32.00 | 585.00 | 0.45 | 0.40 | 4.50 | 0.038 |
| 1.25 | 29.00 | 30.00 | 985.00 | 0.45 | 0.45 | 3.50 | 0.050 |

2.221

| | | | | | | | |
|---|---|---|---|---|---|---|---|
| 2.40 | 320.00 | 200.00 | 106.00 | 0.90 | 3.30 | 2.75 | 0.050 |
| 2.00 | 55.00 | 125.00 | 110.00 | 1.02 | 1.82 | 3.00 | 0.012 |
| 1.62 | 16.00 | 118.00 | 165.00 | 0.56 | 1.21 | 2.20 | 0.010 |
| 1.39 | 15.00 | 96.00 | 165.00 | 0.64 | 1.10 | 2.50 | 0.010 |
| 1.33 | 350.00 | 950.00 | 1120.00 | 0.85 | 0.60 | 2.00 | 0.050 |
| 1.25 | 22.00 | 50.00 | 520.00 | 0.68 | 0.77 | 3.00 | 0.200 |

21222

| | | | | | | | |
|---|---|---|---|---|---|---|---|
| 2.40 | 100.00 | 125.00 | 102.00 | 0.90 | 1.60 | 3.30 | 0.010 |
| 2.00 | 30.00 | 78.00 | 104.00 | 0.85 | 1.28 | 3.30 | 0.010 |
| 1.62 | 87.00 | 202.00 | 425.00 | 0.81 | 1.28 | 5.50 | 0.150 |
| 1.39 | 87.00 | 220.00 | 450.00 | 0.93 | 1.30 | 3.30 | 0.040 |
| 1.33 | 87.00 | 230.00 | 450.00 | 0.93 | 1.23 | 3.00 | 0.020 |
| 1.25 | 87.00 | 245.00 | 525.00 | 0.93 | 1.25 | 3.00 | 0.050 |

21223

| | | | | | | | |
|---|---|---|---|---|---|---|---|
| 2.40 | 85.00 | 132.00 | 100.00 | 0.50 | 0.83 | 3.00 | 0.016 |
| 2.00 | 200.00 | 185.00 | 245.00 | 1.00 | 0.99 | 1.52 | 0.016 |
| 1.62 | 480.00 | 650.00 | 520.00 | 1.20 | 1.10 | 2.20 | 0.016 |
| 1.39 | 400.00 | 750.00 | 680.00 | 1.20 | 1.10 | 3.30 | 0.035 |
| 1.33 | 400.00 | 850.00 | 950.00 | 1.20 | 1.10 | 2.20 | 0.035 |
| 1.25 | 51.00 | 94.00 | 685.00 | 0.80 | 0.87 | 2.85 | 0.030 |

22111

| | | | | | | | |
|---|---|---|---|---|---|---|---|
| 2.40 | 84.00 | 58.00 | 142.00 | 0.40 | 0.62 | 2.00 | 0.010 |
| 2.00 | 90.00 | 45.00 | 310.00 | 0.45 | 0.56 | 1.60 | 0.010 |
| 1.62 | 350.00 | 18.00 | 710.00 | 0.32 | 0.18 | 1.30 | 0.001 |
| 1.39 | 450.00 | 1000.00 | 1100.00 | 1.00 | 0.20 | 2.60 | 0.015 |
| 1.33 | 280.00 | 1850.00 | 1180.00 | 1.00 | 0.60 | 2.20 | 0.015 |
| 1.25 | 250.00 | 1300.00 | 950.00 | 0.99 | 0.40 | 3.50 | 0.030 |

22112

| | | | | | | | |
|---|---|---|---|---|---|---|---|
| 2.40 | 275.00 | 48.00 | 120.00 | 0.95 | 0.75 | 2.80 | 0.008 |
| 2.00 | 275.00 | 78.00 | 215.00 | 0.95 | 0.84 | 2.80 | 0.040 |
| 1.62 | 275.00 | 78.00 | 420.00 | 0.95 | 0.72 | 1.95 | 0.008 |
| 1.39 | 275.00 | 78.00 | 995.00 | 0.95 | 0.72 | 2.20 | 0.005 |
| 1.33 | 275.00 | 250.00 | 1000.00 | 0.95 | 0.72 | 2.70 | 0.005 |
| 1.25 | 400.00 | 850.00 | 1100.00 | 1.20 | 1.60 | 3.00 | 0.010 |

22113

| | | | | | | | |
|---|---|---|---|---|---|---|---|
| 2.40 | 950.00 | 28.00 | 92.00 | 0.55 | 0.53 | 3.60 | 0.011 |
| 2.00 | 950.00 | 40.00 | 150.00 | 0.50 | 0.60 | 2.60 | 0.011 |
| 1.62 | 2500.00 | 490.00 | 280.00 | 1.80 | 0.75 | 2.40 | 0.011 |
| 1.39 | 785.00 | 290.00 | 492.00 | 1.20 | 1.20 | 2.80 | 0.011 |
| 1.33 | 110.00 | 313.00 | 420.00 | 0.77 | 1.62 | 4.00 | 0.030 |
| 1.25 | 22.00 | 105.00 | 450.00 | 0.75 | 1.32 | 3.00 | 0.350 |

22121

| | | | | | | | |
|---|---|---|---|---|---|---|---|
| 2.40 | 600.00 | 315.00 | 175.00 | 0.80 | 1.30 | 2.20 | 0.007 |
| 2.00 | 120.00 | 125.00 | 280.00 | 0.70 | 0.90 | 1.80 | 0.007 |
| 1.62 | 125.00 | 255.00 | 525.00 | 0.70 | 1.00 | 1.70 | 0.007 |
| 1.39 | 58.00 | 210.00 | 480.00 | 0.70 | 0.90 | 2.20 | 0.001 |
| 1.33 | 58.00 | 195.00 | 610.00 | 0.69 | 0.75 | 4.50 | 0.030 |
| 1.25 | 55.00 | 195.00 | 610.00 | 0.70 | 0.75 | 4.50 | 0.080 |

22122

| | | | | | | | |
|---|---|---|---|---|---|---|---|
| 2.40 | 1000.00 | 165.00 | 110.00 | 0.80 | 1.85 | 2.40 | 0.010 |
| 2.00 | 750.00 | 45.00 | 235.00 | 2.40 | 0.63 | 2.20 | 0.060 |
| 1.62 | 45.00 | 105.00 | 180.00 | 0.85 | 1.30 | 2.50 | 0.005 |
| 1.39 | 50.00 | 150.00 | 420.00 | 0.85 | 1.34 | 2.60 | 0.001 |
| 1.33 | 50.00 | 175.00 | 442.00 | 0.85 | 1.36 | 5.00 | 0.030 |

| | | | | | | | |
|---|---|---|---|---|---|---|---|
| 1.25 | 50.00 | 185.00 | 520.00 | 0.87 | 1.37 | 5.00 | 0.055 |

22123

| | | | | | | | |
|---|---|---|---|---|---|---|---|
| 2.40 | 850.00 | 115.00 | 82.00 | 0.80 | 1.60 | 3.60 | 0.011 |
| 2.00 | 220.00 | 110.00 | 115.00 | 0.75 | 1.50 | 4.50 | 0.011 |
| 1.62 | 130.00 | 132.00 | 188.00 | 0.90 | 1.30 | 3.00 | 0.001 |
| 1.39 | 125.00 | 290.00 | 455.00 | 0.60 | 1.45 | 2.80 | 0.011 |
| 1.33 | 125.00 | 335.00 | 455.00 | 0.60 | 1.45 | 2.80 | 0.011 |
| 1.25 | 19.00 | 125.00 | 455.00 | 0.66 | 1.26 | 2.80 | 0.330 |

22211

| | | | | | | | |
|---|---|---|---|---|---|---|---|
| 2.40 | 580.00 | 358.00 | 235.00 | 1.30 | 1.55 | 1.90 | 0.080 |
| 2.00 | 250.00 | 280.00 | 370.00 | 1.30 | 1.60 | 1.90 | 0.020 |
| 1.62 | 35.00 | 100.00 | 175.00 | 0.88 | 1.24 | 6.00 | 0.060 |
| 1.39 | 75.00 | 220.00 | 850.00 | 0.85 | 1.23 | 1.50 | 0.010 |
| 1.33 | 75.00 | 420.00 | 700.00 | 0.70 | 1.20 | 4.50 | 0.025 |
| 1.25 | 75.00 | 500.00 | 620.00 | 0.70 | 1.05 | 4.00 | 0.028 |

22212

| | | | | | | | |
|---|---|---|---|---|---|---|---|
| 2.40 | 950.00 | 230.00 | 130.00 | 0.80 | 1.95 | 2.50 | 0.016 |
| 2.00 | 770.00 | 40.00 | 290.00 | 2.60 | 0.58 | 2.00 | 0.016 |
| 1.62 | 650.00 | 410.00 | 475.00 | 0.65 | 1.30 | 2.50 | 0.010 |
| 1.39 | 200.00 | 250.00 | 750.00 | 1.00 | 1.10 | 3.00 | 0.010 |
| 1.33 | 200.00 | 240.00 | 660.00 | 0.95 | 0.70 | 3.40 | 0.010 |
| 1.25 | 200.00 | 330.00 | 630.00 | 0.88 | 0.66 | 3.50 | 0.016 |

22213

| | | | | | | | |
|---|---|---|---|---|---|---|---|
| 2.40 | 110.00 | 355.00 | 990.00 | 0.75 | 1.00 | 2.50 | 0.016 |
| 2.00 | 1350.00 | 160.00 | 95.00 | 0.80 | 1.50 | 3.80 | 0.014 |
| 1.62 | 1850.00 | 230.00 | 178.00 | 1.20 | 1.20 | 2.30 | 0.014 |
| 1.39 | 1450.00 | 130.00 | 290.00 | 0.80 | 0.77 | 2.00 | 0.005 |
| 1.33 | 1450.00 | 130.00 | 650.00 | 0.80 | 0.77 | 2.80 | 0.010 |
| 1.25 | 1450.00 | 130.00 | 875.00 | 0.80 | 0.77 | 4.00 | 0.016 |

22221

| | | | | | | | |
|---|---|---|---|---|---|---|---|
| 2.40 | 1450.00 | 130.00 | 1050.00 | 0.80 | 0.77 | 3.50 | 0.020 |
| 2.00 | 520.00 | 480.00 | 190.00 | 0.40 | 1.80 | 1.80 | 0.001 |
| 1.62 | 520.00 | 520.00 | 620.00 | 0.40 | 1.60 | 1.20 | 0.075 |
| 1.39 | 580.00 | 850.00 | 880.00 | 1.20 | 0.65 | 1.90 | 0.010 |
| 1.33 | 350.00 | 850.00 | 900.00 | 1.25 | 0.65 | 2.50 | 0.010 |
| 1.25 | 350.00 | 850.00 | 1020.00 | 1.28 | 0.65 | 2.80 | 0.004 |

22222

| | | | | | | | |
|---|---|---|---|---|---|---|---|
| 2.40 | 350.00 | 850.00 | 1000.00 | 1.35 | 0.65 | 5.00 | 0.010 |
| 2.00 | 1250.00 | 42.00 | 328.00 | 2.20 | 0.38 | 2.50 | 0.080 |
| 1.62 | 1250.00 | 185.00 | 620.00 | 0.95 | 0.60 | 1.85 | 0.004 |
| 1.39 | 750.00 | 250.00 | 1350.00 | 0.95 | 0.60 | 1.50 | 0.004 |

| | | | | | | | |
|---|---|---|---|---|---|---|---|
| 1.33 | 10.00 | 22.00 | 560.00 | 0.55 | 0 60 | 4.00 | 0.200 |
| 1.25 | 10.00 | 25.00 | 620.00 | 0.55 | 0.61 | 3.50 | 0.200 |

22223

| | | | | | | | |
|---|---|---|---|---|---|---|---|
| 2.40 | 1580.00 | 145.00 | 96.00 | 0.80 | 1.40 | 3.50 | 0.010 |
| 2.00 | 1100.00 | 160.00 | 156.00 | 0.80 | 1.30 | 2.60 | 0.010 |
| 1.62 | 485.00 | 200.00 | 300.00 | 0.80 | 1.30 | 2.20 | 0.010 |
| 1.39 | 485.00 | 170.00 | 620.00 | 0.80 | 1.50 | 2.80 | 0.030 |
| 1.33 | 45.00 | 175.00 | 710.00 | 0.75 | 1.50 | 2.20 | 0.010 |
| 1.25 | 45.00 | 185.00 | 650.00 | 0.75 | 1.40 | 1.65 | 0.100 |

## APPENDIX-7.5: The Predicted Parameters

PREDICTED PARAMETERS FOR THE AMC MODEL

| TEST | RHO | d50A | d50B | d50C | mA | mB | mC | Rf |
|---|---|---|---|---|---|---|---|---|
| 11111 | | | | | | | | |
| | 2.40 | 358.01 | 111.28 | 74.07 | 0.81 | 1.58 | 3.30 | 0.058 |
| | 2.00 | 225.50 | 122.65 | 108.65 | 0.81 | 1.29 | 2.87 | 0.044 |
| | 1.62 | 117.03 | 140.81 | 187.15 | 0.81 | 1.16 | 2.94 | 0.051 |
| | 1.39 | 82.17 | 151.69 | 250.88 | 0.81 | 1.17 | 3.27 | 0.070 |
| | 1.33 | 73.71 | 155.20 | 274.53 | 0.81 | 1.19 | 3.42 | 0.079 |
| | 1.25 | 59.88 | 162.15 | 326.15 | 0.81 | 1.24 | 3.79 | 0.104 |
| 11112 | | | | | | | | |
| | 2.40 | 594.03 | 111.28 | 62.09 | 0.90 | 1.90 | 3.71 | 0.058 |
| | 2.00 | 374.17 | 122.65 | 91.08 | 0.90 | 1.55 | 3.22 | 0.044 |
| | 1.62 | 194.18 | 140.81 | 156.87 | 0.90 | 1.39 | 3.30 | 0.051 |
| | 1.39 | 136.35 | 151.69 | 210.30 | 0.90 | 1.41 | 3.67 | 0.070 |
| | 1.33 | 122.31 | 155.20 | 230.12 | 0.90 | 1.43 | 3.84 | 0.079 |
| | 1.25 | 99.36 | 162.15 | 273.39 | 0.90 | 1.49 | 4.25 | 0.104 |
| 11113 | | | | | | | | |
| | 2.40 | 788.45 | 111.28 | 56.25 | 0.95 | 2.11 | 3.95 | 0.058 |
| | 2.00 | 496.63 | 122.65 | 82.52 | 0.95 | 1.72 | 3.44 | 0.044 |
| | 1.62 | 257.73 | 140.81 | 142.13 | 0.95 | 1.54 | 3.51 | 0.051 |
| | 1.39 | 180.97 | 151.69 | 190.54 | 0.95 | 1.57 | 3.92 | 0.070 |
| | 1.33 | 162.34 | 155.20 | 208.50 | 0.95 | 1.59 | 4.10 | 0.079 |
| | 1.25 | 131.88 | 162.15 | 247.70 | 0.95 | 1.65 | 4.53 | 0.104 |
| 11121 | | | | | | | | |
| | 2.40 | 358.01 | 111.28 | 74.07 | 0.81 | 1.77 | 3.30 | 0.058 |
| | 2.00 | 225.50 | 122.65 | 108.65 | 0.81 | 1.45 | 2.87 | 0.044 |
| | 1.62 | 117.03 | 140.81 | 187.15 | 0.81 | 1.29 | 2.94 | 0.051 |
| | 1.39 | 82.17 | 151.69 | 250.88 | 0.81 | 1.31 | 3.27 | 0.070 |
| | 1.33 | 73.71 | 155.20 | 274.53 | 0.81 | 1.33 | 3.42 | 0.079 |
| | 1.25 | 59.88 | 162.15 | 326.15 | 0.81 | 1.39 | 3.79 | 0.104 |
| 11122 | | | | | | | | |
| | 2.40 | 594.03 | 111.28 | 62.09 | 0.90 | 2.13 | 3.71 | 0.058 |
| | 2.00 | 374.17 | 122.65 | 91.08 | 0.90 | 1.74 | 3.22 | 0.044 |
| | 1.62 | 194.18 | 140.81 | 156.87 | 0.90 | 1.55 | 3.30 | 0.051 |
| | 1.39 | 136.35 | 151.69 | 210.30 | 0.90 | 1.58 | 3.67 | 0.070 |
| | 1.33 | 122.31 | 155.20 | 230.12 | 0.90 | 1.60 | 3.84 | 0.079 |
| | 1.25 | 99.36 | 162.15 | 273.39 | 0.90 | 1.67 | 4.25 | 0.104 |
| 11123 | | | | | | | | |
| | 2.40 | 788.45 | 111.28 | 56.25 | 0.95 | 2.36 | 3.95 | 0.058 |

| | | | | | | | |
|---|---|---|---|---|---|---|---|
| 2.00 | 496.63 | 122.65 | 82.52 | 0.95 | 1.93 | 3.44 | 0.044 |
| 1.62 | 257.73 | 140.81 | 142.13 | 0.95 | 1.72 | 3.51 | 0.051 |
| 1.39 | 180.97 | 151.69 | 190.54 | 0.95 | 1.75 | 3.92 | 0.070 |
| 1.33 | 162.34 | 155.20 | 208.50 | 0.95 | 1.78 | 4.10 | 0.079 |
| 1.25 | 131.88 | 162.15 | 247.70 | 0.95 | 1.85 | 4.53 | 0.104 |

11211

| | | | | | | | |
|---|---|---|---|---|---|---|---|
| 2.40 | 358.01 | 111.28 | 74.07 | 0.81 | 1.58 | 3.30 | 0.058 |
| 2.00 | 225.50 | 122.65 | 108.65 | 0.81 | 1.29 | 2.87 | 0.044 |
| 1.62 | 117.03 | 140.81 | 187.15 | 0.81 | 1.16 | 2.94 | 0.051 |
| 1.39 | 82.17 | 151.69 | 250.88 | 0.81 | 1.17 | 3.27 | 0.070 |
| 1.33 | 73.71 | 155.20 | 274.53 | 0.81 | 1.19 | 3.42 | 0.079 |
| 1.25 | 59.88 | 162.15 | 326.15 | 0.81 | 1.24 | 3.79 | 0.104 |

11212

| | | | | | | | |
|---|---|---|---|---|---|---|---|
| 2.40 | 594.03 | 111.28 | 62.09 | 0.90 | 1.90 | 3.71 | 0.058 |
| 2.00 | 374.17 | 122.65 | 91.08 | 0.90 | 1.55 | 3.22 | 0.044 |
| 1.62 | 194.18 | 140.81 | 156.87 | 0.90 | 1.39 | 3.30 | 0.051 |
| 1.39 | 136.35 | 151.69 | 210.30 | 0.90 | 1.41 | 3.67 | 0.070 |
| 1.33 | 122.31 | 155.20 | 230.12 | 0.90 | 1.43 | 3.84 | 0.079 |
| 1.25 | 99.36 | 162.15 | 273.39 | 0.90 | 1.49 | 4.25 | 0.104 |

11213

| | | | | | | | |
|---|---|---|---|---|---|---|---|
| 2.40 | 788.45 | 111.28 | 56.25 | 0.95 | 2.11 | 3.95 | 0.058 |
| 2.00 | 496.63 | 122.65 | 82.52 | 0.95 | 1.72 | 3.44 | 0.044 |
| 1.62 | 257.73 | 140.81 | 142.13 | 0.95 | 1.54 | 3.51 | 0.051 |
| 1.39 | 180.97 | 151.69 | 190.54 | 0.95 | 1.57 | 3.92 | 0.070 |
| 1.33 | 162.34 | 155.20 | 208.50 | 0.95 | 1.59 | 4.10 | 0.079 |
| 1.25 | 131.88 | 162.15 | 247.70 | 0.95 | 1.65 | 4.53 | 0.104 |

1122

| | | | | | | | |
|---|---|---|---|---|---|---|---|
| 2.40 | 358.01 | 111.28 | 74.07 | 0.81 | 1.77 | 3.30 | 0.058 |
| 2.00 | 225.50 | 122.65 | 108.65 | 0.81 | 1.45 | 2.87 | 0.044 |
| 1.62 | 117.03 | 140.81 | 187.15 | 0.81 | 1.29 | 2.94 | 0.051 |
| 1.39 | 82.17 | 151.69 | 250.88 | 0.81 | 1.31 | 3.27 | 0.070 |
| 1.33 | 73.71 | 155.20 | 274.53 | 0.81 | 1.33 | 3.42 | 0.079 |
| 1.25 | 59.88 | 162.15 | 326.15 | 0.81 | 1.39 | 3.79 | 0.104 |

11222

| | | | | | | | |
|---|---|---|---|---|---|---|---|
| 2.40 | 594.03 | 111.28 | 62.09 | 0.90 | 2.13 | 3.71 | 0.058 |
| 2.00 | 374.1 | 122.65 | 91.08 | 0.90 | 1.74 | 3.22 | 0.044 |
| 1.62 | 194.18 | 140.81 | 156.87 | 0.90 | 1.55 | 3.30 | 0.051 |
| 1.39 | 136.35 | 151.69 | 210.30 | 0.90 | 1.58 | 3.67 | 0.070 |
| 1.33 | 122.31 | 155.20 | 230.12 | 0.90 | 1.60 | 3.84 | 0.079 |
| 1.25 | 99.36 | 162.15 | 273.39 | 0.90 | 1.67 | 4.25 | 0.104 |

11223

| | | | | | | | |
|---|---|---|---|---|---|---|---|
| 2.40 | 788.45 | 111.28 | 56.25 | 0.95 | 2.36 | 3.95 | 0.058 |
| 2.00 | 496.63 | 122.65 | 82.52 | 0.95 | 1.93 | 3.44 | 0.044 |
| 1.62 | 257.73 | 140.81 | 142.13 | 0.95 | 1.72 | 3.51 | 0.051 |
| 1.39 | 180.97 | 151.69 | 190.54 | 0.95 | 1.75 | 3.92 | 0.070 |
| 1.33 | 162.34 | 155.20 | 208.50 | 0.95 | 1.78 | 4.10 | 0.079 |
| 1.25 | 131.88 | 162.15 | 247.70 | 0.95 | 1.85 | 4.53 | 0.104 |

12111

| | | | | | | | |
|---|---|---|---|---|---|---|---|
| 2.40 | 819.01 | 111.28 | 74.07 | 0.93 | 1.42 | 2.94 | 0.058 |
| 2.00 | 515.88 | 122.65 | 108.65 | 0.93 | 1.16 | 2.56 | 0.044 |
| 1.62 | 267.72 | 140.81 | 187.15 | 0.93 | 1.04 | 2.61 | 0.051 |
| 1.39 | 187.99 | 151.69 | 250.88 | 0.93 | 1.06 | 2.91 | 0.070 |
| 1.33 | 168.63 | 155.20 | 274.53 | 0.93 | 1.07 | 3.05 | 0.079 |
| 1.25 | 136.99 | 162.15 | 326.15 | 0.93 | 1.12 | 3.37 | 0.104 |

12112

| | | | | | | | |
|---|---|---|---|---|---|---|---|
| 2.40 | 1358.98 | 111.28 | 62.09 | 1.04 | 1.71 | 3.30 | 0.058 |
| 2.00 | 855.99 | 122.65 | 91.08 | 1.04 | 1.40 | 2.87 | 0.044 |
| 1.62 | 444.23 | 140.81 | 156.87 | 1.04 | 1.25 | 2.93 | 0.051 |
| 1.39 | 311.93 | 151.69 | 210.30 | 1.04 | 1.27 | 3.27 | 0.070 |
| 1.33 | 279.81 | 155.20 | 230.12 | 1.04 | 1.29 | 3.42 | 0.079 |
| 1.25 | 227.30 | 162.15 | 273.39 | 1.04 | 1.34 | 3.78 | 0.104 |

12113

| | | | | | | | |
|---|---|---|---|---|---|---|---|
| 2.40 | 1803.75 | 111.28 | 56.25 | 1.10 | 1.90 | 3.52 | 0.058 |
| 2.00 | 1136.14 | 122.65 | 82.52 | 1.10 | 1.55 | 3.06 | 0.044 |
| 1.62 | 589.62 | 140.81 | 142.13 | 1.10 | 1.38 | 3.13 | 0.051 |
| 1.39 | 414.02 | 151.69 | 190.54 | 1.10 | 1.41 | 3.48 | 0.070 |
| 1.33 | 371.39 | 155.20 | 208.50 | 1.10 | 1.43 | 3.65 | 0.079 |
| 1.25 | 301.69 | 162.15 | 247.70 | 1.10 | 1.49 | 4.03 | 0.104 |

12121

| | | | | | | | |
|---|---|---|---|---|---|---|---|
| 2.40 | 819.01 | 111.28 | 74.07 | 0.93 | 1.59 | 2.94 | 0.058 |
| 2.00 | 515.88 | 122.65 | 108.65 | 0.93 | 1.30 | 2.56 | 0.044 |
| 1.62 | 267.72 | 140.81 | 187.15 | 0.93 | 1.16 | 2.61 | 0.051 |
| 1.39 | 187.99 | 151.69 | 250.88 | 0.93 | 1.18 | 2.91 | 0.070 |
| 1.33 | 168.63 | 155.20 | 274.53 | 0.93 | 1.20 | 3.05 | 0.079 |
| 1.25 | 136.99 | 162.15 | 326.15 | 0.93 | 1.25 | 3.37 | 0.104 |

12122

| | | | | | | | |
|---|---|---|---|---|---|---|---|
| 2.40 | 1358.98 | 111.28 | 62.09 | 1.04 | 1.91 | 3.30 | 0.058 |
| 2.00 | 855.99 | 122.65 | 91.08 | 1.04 | 1.56 | 2.87 | 0.044 |
| 1.62 | 444.23 | 140.81 | 156.87 | 1.04 | 1.40 | 2.93 | 0.051 |
| 1.39 | 311.93 | 151.69 | 210.30 | 1.04 | 1.42 | 3.27 | 0.070 |
| 1.33 | 279.81 | 155.20 | 230.12 | 1.04 | 1.44 | 3.42 | 0.079 |
| 1.25 | 227.30 | 162.15 | 273.39 | 1.04 | 1.50 | 3.78 | 0.104 |

12123

| | | | | | | | |
|---|---|---|---|---|---|---|---|
| 2.40 | 1803.75 | 111.28 | 56.25 | 1.10 | 2.12 | 3.52 | 0.058 |
| 2.00 | 1136.14 | 122.65 | 82.52 | 1.10 | 1.73 | 3.06 | 0.044 |
| 1.62 | 589.62 | 140.81 | 142.13 | 1.10 | 1.55 | 3.13 | 0.051 |
| 1.39 | 414.02 | 151.69 | 190.54 | 1.10 | 1.58 | 3.48 | 0.070 |
| 1.33 | 371.39 | 155.20 | 208.50 | 1.10 | 1.60 | 3.65 | 0.079 |
| 1.25 | 301.69 | 162.15 | 247.70 | 1.10 | 1.66 | 4.03 | 0.104 |

12211

| | | | | | | | |
|---|---|---|---|---|---|---|---|
| 2.40 | 819.01 | 111.28 | 74.07 | 0.93 | 1.42 | 2.94 | 0.058 |
| 2.00 | 515.88 | 122.65 | 108.65 | 0.93 | 1.16 | 2.56 | 0.044 |
| 1.62 | 267.72 | 140.81 | 187.15 | 0.93 | 1.04 | 2.61 | 0.051 |
| 1.39 | 187.99 | 151.69 | 250.88 | 0.93 | 1.06 | 2.91 | 0.070 |
| 1.33 | 168.63 | 155.20 | 274.53 | 0.93 | 1.07 | 3.05 | 0.079 |
| 1.25 | 136.99 | 162.15 | 326.15 | 0.93 | 1.12 | 3.37 | 0.104 |

12212

| | | | | | | | |
|---|---|---|---|---|---|---|---|
| 2.40 | 1358.98 | 111.28 | 62.09 | 1.04 | 1.71 | 3.30 | 0.058 |
| 2.00 | 855.99 | 122.65 | 91.08 | 1.04 | 1.40 | 2.87 | 0.044 |
| 1.62 | 444.23 | 140.81 | 156.87 | 1.04 | 1.25 | 2.93 | 0.051 |
| 1.39 | 311.93 | 151.69 | 210.30 | 1.04 | 1.27 | 3.27 | 0.070 |
| 1.33 | 279.81 | 155.20 | 230.12 | 1.04 | 1.29 | 3.42 | 0.079 |
| 1.25 | 227.30 | 162.15 | 273.39 | 1.04 | 1.34 | 3.78 | 0.104 |

12213

| | | | | | | | |
|---|---|---|---|---|---|---|---|
| 2.40 | 1803.75 | 111.28 | 56.25 | 1.10 | 1.90 | 3.52 | 0.058 |
| 2.00 | 1136.14 | 122.65 | 82.52 | 1.10 | 1.55 | 3.06 | 0.044 |
| 1.62 | 589.62 | 140.81 | 142.13 | 1.10 | 1.38 | 3.13 | 0.051 |
| 1.39 | 414.02 | 151.69 | 190.54 | 1.10 | 1.41 | 3.48 | 0.070 |
| 1.33 | 371.39 | 155.20 | 208.50 | 1.10 | 1.43 | 3.65 | 0.079 |
| 1.25 | 301.69 | 162.15 | 247.70 | 1.10 | 1.49 | 4.03 | 0.104 |

12221

| | | | | | | | |
|---|---|---|---|---|---|---|---|
| 2.40 | 819.01 | 111.28 | 74.07 | 0.93 | 1.59 | 2.94 | 0.058 |
| 2.00 | 515.88 | 122.65 | 108.65 | 0.93 | 1.30 | 2.56 | 0.044 |
| 1.62 | 267.72 | 140.81 | 187.15 | 0.93 | 1.16 | 2.61 | 0.051 |
| 1.39 | 187.99 | 151.69 | 250.88 | 0.93 | 1.18 | 2.91 | 0.070 |
| 1.33 | 168.63 | 155.20 | 274.53 | 0.93 | 1.20 | 3.05 | 0.079 |
| 1.25 | 136.99 | 162.15 | 326.15 | 0.93 | 1.25 | 3.37 | 0.104 |

12222

| | | | | | | | |
|---|---|---|---|---|---|---|---|
| 2.40 | 1358.98 | 111.28 | 62.09 | 1.04 | 1.91 | 3.30 | 0.058 |
| 2.00 | 855.99 | 122.65 | 91.08 | 1.04 | 1.56 | 2.87 | 0.044 |
| 1.62 | 444.23 | 140.81 | 156.87 | 1.04 | 1.40 | 2.93 | 0.051 |
| 1.39 | 311.93 | 151.69 | 210.30 | 1.04 | 1.42 | 3.27 | 0.070 |
| 1.33 | 279.81 | 155.20 | 230.12 | 1.04 | 1.44 | 3.42 | 0.079 |
| 1.25 | 227.30 | 162.15 | 273.39 | 1.04 | 1.50 | 3.78 | 0.104 |

12223

| | | | | | | | |
|---|---|---|---|---|---|---|---|
| 2.40 | 1803.75 | 111.28 | 56.25 | 1.10 | 2.12 | 3.52 | 0.058 |
| 2.00 | 1136.14 | 122.65 | 82.52 | 1.10 | 1.73 | 3.06 | 0.044 |
| 1.62 | 589.62 | 140.81 | 142.13 | 1.10 | 1.55 | 3.13 | 0.051 |
| 1.39 | 414.02 | 151.69 | 190.54 | 1.10 | 1.58 | 3.48 | 0.070 |
| 1.33 | 371.39 | 155.20 | 208.50 | 1.10 | 1.60 | 3.65 | 0.079 |
| 1.25 | 301.69 | 162.15 | 247.70 | 1.10 | 1.66 | 4.03 | 0.104 |

21111

| | | | | | | | |
|---|---|---|---|---|---|---|---|
| 2.40 | 164.89 | 142.76 | 168.77 | 0.70 | 1.12 | 2.89 | 0.016 |
| 2.00 | 103.86 | 157.35 | 247.57 | 0.70 | 0.92 | 2.51 | 0.012 |
| 1.62 | 53.90 | 180.65 | 426.42 | 0.70 | 0.82 | 2.57 | 0.014 |
| 1.39 | 37.85 | 194.61 | 571.64 | 0.70 | 0.83 | 2.86 | 0.019 |
| 1.33 | 33.95 | 199.11 | 625.52 | 0.70 | 0.84 | 2.99 | 0.022 |
| 1.25 | 27.58 | 208.02 | 743.13 | 0.70 | 0.88 | 3.31 | 0.029 |

21112

| | | | | | | | |
|---|---|---|---|---|---|---|---|
| 2.40 | 273.60 | 142.76 | 141.47 | 0.78 | 1.35 | 3.24 | 0.016 |
| 2.00 | 172.33 | 157.35 | 207.52 | 0.78 | 1.10 | 2.82 | 0.012 |
| 1.62 | 89.44 | 180.65 | 357.43 | 0.78 | 0.98 | 2.88 | 0.014 |
| 1.39 | 62.80 | 194.61 | 479.16 | 0.78 | 1.00 | 3.21 | 0.019 |
| 1.33 | 56.33 | 199.11 | 524.32 | 0.78 | 1.01 | 3.36 | 0.022 |
| 1.25 | 45.76 | 208.02 | 622.91 | 0.78 | 1.05 | 3.71 | 0.029 |

21113

| | | | | | | | |
|---|---|---|---|---|---|---|---|
| 2.40 | 363.15 | 142.76 | 128.17 | 0.83 | 1.49 | 3.45 | 0.016 |
| 2.00 | 228.74 | 157.35 | 188.02 | 0.83 | 1.22 | 3.01 | 0.012 |
| 1.62 | 118.71 | 180.65 | 323.85 | 0.83 | 1.09 | 3.07 | 0.014 |
| 1.39 | 83.35 | 194.61 | 434.14 | 0.83 | 1.11 | 3.42 | 0.019 |
| 1.33 | 74.77 | 199.11 | 475.06 | 0.83 | 1.12 | 3.58 | 0.022 |
| 1.25 | 60.74 | 208.02 | 564.38 | 0.83 | 1.17 | 3.96 | 0.029 |

21121

| | | | | | | | |
|---|---|---|---|---|---|---|---|
| 2.40 | 164.89 | 142.76 | 168.77 | 0.70 | 1.25 | 2.89 | 0.016 |
| 2.00 | 103.86 | 157.35 | 247.57 | 0.70 | 1.02 | 2.51 | 0.012 |
| 1.62 | 53.90 | 180.65 | 426.42 | 0.70 | 0.92 | 2.57 | 0.014 |
| 1.39 | 37.85 | 194.61 | 571.64 | 0.70 | 0.93 | 2.86 | 0.019 |
| 1.33 | 33.95 | 199.11 | 625.52 | 0.70 | 0.94 | 2.99 | 0.022 |
| 1.25 | 27.58 | 208.02 | 743.13 | 0.70 | 0.98 | 3.31 | 0.029 |

21122

| | | | | | | | |
|---|---|---|---|---|---|---|---|
| 2.40 | 273.60 | 142.76 | 141.47 | 0.78 | 1.50 | 3.24 | 0.016 |
| 2.00 | 172.33 | 157.35 | 207.52 | 0.78 | 1.23 | 2.82 | 0.012 |
| 1.62 | 89.44 | 180.65 | 357.43 | 0.78 | 1.10 | 2.88 | 0.014 |
| 1.39 | 62.80 | 194.61 | 479.16 | 0.78 | 1.12 | 3.21 | 0.019 |
| 1.33 | 56.33 | 199.11 | 524.32 | 0.78 | 1.13 | 3.36 | 0.022 |
| 1.25 | 45.76 | 208.02 | 622.91 | 0.78 | 1.18 | 3.71 | 0.029 |

21123

| | | | | | | | |
|---|---|---|---|---|---|---|---|
| 2.40 | 363.15 | 142.76 | 128.17 | 0.83 | 1.67 | 3.45 | 0.016 |
| 2.00 | 228.74 | 157.35 | 188.02 | 0.83 | 1.36 | 3.01 | 0.012 |
| 1.62 | 118.71 | 180.65 | 323.85 | 0.83 | 1.22 | 3.07 | 0.014 |
| 1.39 | 83.35 | 194.61 | 434.14 | 0.83 | 1.24 | 3.42 | 0.019 |
| 1.33 | 74.77 | 199.11 | 475.06 | 0.83 | 1.26 | 3.58 | 0.022 |
| 1.25 | 60.74 | 208.02 | 564.38 | 0.83 | 1.31 | 3.96 | 0.029 |

21211

| | | | | | | | |
|---|---|---|---|---|---|---|---|
| 2.40 | 164.89 | 142.76 | 168.77 | 0.70 | 1.12 | 2.89 | 0.016 |
| 2.00 | 103.86 | 157.35 | 247.57 | 0.70 | 0.92 | 2.51 | 0.012 |
| 1.62 | 53.90 | 180.65 | 426.42 | 0.70 | 0.82 | 2.57 | 0.014 |
| 1.39 | 37.85 | 194.61 | 571.64 | 0.70 | 0.83 | 2.86 | 0.019 |
| 1.33 | 33.95 | 199.11 | 625.52 | 0.70 | 0.84 | 2.99 | 0.022 |
| 1.25 | 27.58 | 208.02 | 743.13 | 0.70 | 0.88 | 3.31 | 0.029 |

21212

| | | | | | | | |
|---|---|---|---|---|---|---|---|
| 2.40 | 273.60 | 142.76 | 141.47 | 0.78 | 1.35 | 3.24 | 0.016 |
| 2.00 | 172.33 | 157.35 | 207.52 | 0.78 | 1.10 | 2.82 | 0.012 |
| 1.62 | 89.44 | 180.65 | 357.43 | 0.78 | 0.98 | 2.88 | 0.014 |
| 1.39 | 62.80 | 194.61 | 479.16 | 0.78 | 1.00 | 3.21 | 0.019 |
| 1.33 | 56.33 | 199.11 | 524.32 | 0.78 | 1.01 | 3.36 | 0.022 |
| 1.25 | 45.76 | 208.02 | 622.91 | 0.78 | 1.05 | 3.71 | 0.029 |

21213

| | | | | | | | |
|---|---|---|---|---|---|---|---|
| 2.40 | 363.15 | 142.76 | 128.17 | 0.83 | 1.49 | 3.45 | 0.016 |
| 2.00 | 228.74 | 157.35 | 188.02 | 0.83 | 1.22 | 3.01 | 0.012 |
| 1.62 | 118.71 | 180.65 | 323.85 | 0.83 | 1.09 | 3.07 | 0.014 |
| 1.39 | 83.35 | 194.61 | 434.14 | 0.83 | 1.11 | 3.42 | 0.019 |
| 1.33 | 74.77 | 199.11 | 475.06 | 0.83 | 1.12 | 3.58 | 0.022 |
| 1.25 | 60.74 | 208.02 | 564.38 | 0.83 | 1.17 | 3.96 | 0.029 |

21221

| | | | | | | | |
|---|---|---|---|---|---|---|---|
| 2.40 | 164.89 | 142.76 | 168.77 | 0.70 | 1.25 | 2.89 | 0.016 |
| 2.00 | 103.86 | 157.35 | 247.57 | 0.70 | 1.02 | 2.51 | 0.012 |
| 1.62 | 53.90 | 180.65 | 426.42 | 0.70 | 0.92 | 2.57 | 0.014 |
| 1.39 | 37.85 | 194.61 | 571.64 | 0.70 | 0.93 | 2.86 | 0.019 |
| 1.33 | 33.95 | 199.11 | 625.52 | 0.70 | 0.94 | 2.99 | 0.022 |
| 1.25 | 27.58 | 208.02 | 743.13 | 0.70 | 0.98 | 3.31 | 0.029 |

21222

| | | | | | | | |
|---|---|---|---|---|---|---|---|
| 2.40 | 273.60 | 142.76 | 141.47 | 0.78 | 1.50 | 3.24 | 0.016 |
| 2.00 | 172.33 | 157.35 | 207.52 | 0.78 | 1.23 | 2.82 | 0.012 |
| 1.62 | 89.44 | 180.65 | 357.43 | 0.78 | 1.10 | 2.88 | 0.014 |
| 1.39 | 62.80 | 194.61 | 479.16 | 0.78 | 1.12 | 3.21 | 0.019 |
| 1.33 | 56.33 | 199.11 | 524.32 | 0.78 | 1.13 | 3.36 | 0.022 |
| 1.25 | 45.76 | 208.02 | 622.91 | 0.78 | 1.18 | 3.71 | 0.029 |

21223

| | | | | | | | |
|---|---|---|---|---|---|---|---|
| 2.40 | 363.15 | 142.76 | 128.17 | 0.83 | 1.67 | 3.45 | 0.016 |
| 2.00 | 228.74 | 157.35 | 188.02 | 0.83 | 1.36 | 3.01 | 0.012 |
| 1.62 | 118.71 | 180.65 | 323.85 | 0.83 | 1.22 | 3.07 | 0.014 |
| 1.39 | 83.35 | 194.61 | 434.14 | 0.83 | 1.24 | 3.42 | 0.019 |
| 1.33 | 74.77 | 199.11 | 475.06 | 0.83 | 1.26 | 3.58 | 0.022 |
| 1.25 | 60.74 | 208.02 | 564.38 | 0.83 | 1.31 | 3.96 | 0.029 |

22111

| | | | | | | | |
|---|---|---|---|---|---|---|---|
| 2.40 | 358.01 | 142.76 | 168.77 | 0.81 | 1.01 | 2.57 | 0.016 |
| 2.00 | 225.50 | 157.35 | 247.57 | 0.81 | 0.82 | 2.23 | 0.012 |
| 1.62 | 117.03 | 180.65 | 426.42 | 0.81 | 0.74 | 2.28 | 0.014 |
| 1.39 | 82.17 | 194.61 | 571.64 | 0.81 | 0.75 | 2.55 | 0.019 |
| 1.33 | 73.71 | 199.11 | 625.52 | 0.81 | 0.76 | 2.66 | 0.022 |
| 1.25 | 59.88 | 208.02 | 743.13 | 0.81 | 0.79 | 2.94 | 0.029 |

22112

| | | | | | | | |
|---|---|---|---|---|---|---|---|
| 2.40 | 594.03 | 142.76 | 141.47 | 0.90 | 1.21 | 2.88 | 0.016 |
| 2.00 | 374.17 | 157.35 | 207.52 | 0.90 | 0.99 | 2.51 | 0.012 |
| 1.62 | 194.18 | 180.65 | 357.43 | 0.90 | 0.88 | 2.56 | 0.014 |
| 1.39 | 136.35 | 194.61 | 479.16 | 0.90 | 0.90 | 2.86 | 0.019 |
| 1.33 | 122.31 | 199.11 | 524.32 | 0.90 | 0.91 | 2.99 | 0.022 |
| 1.25 | 99.36 | 208.02 | 622.91 | 0.90 | 0.95 | 3.30 | 0.029 |

22113

| | | | | | | | |
|---|---|---|---|---|---|---|---|
| 2.40 | 788.45 | 142.76 | 128.17 | 0.95 | 1.34 | 3.08 | 0.016 |
| 2.00 | 496.63 | 157.35 | 188.02 | 0.95 | 1.10 | 2.67 | 0.012 |
| 1.62 | 257.73 | 180.65 | 323.85 | 0.95 | 0.98 | 2.73 | 0.014 |
| 1.39 | 180.97 | 194.61 | 434.14 | 0.95 | 1.00 | 3.05 | 0.019 |
| 1.33 | 162.34 | 199.11 | 475.06 | 0.95 | 1.01 | 3.19 | 0.022 |
| 1.25 | 131.88 | 208.02 | 564.38 | 0.95 | 1.05 | 3.52 | 0.029 |

22121

| | | | | | | | |
|---|---|---|---|---|---|---|---|
| 2.40 | 358.01 | 142.76 | 168.77 | 0.81 | 1.13 | 2.57 | 0.016 |
| 2.00 | 225.50 | 157.35 | 247.57 | 0.81 | 0.92 | 2.23 | 0.012 |
| 1.62 | 117.03 | 180.65 | 426.42 | 0.81 | 0.82 | 2.28 | 0.014 |
| 1.39 | 82.17 | 194.61 | 571.64 | 0.81 | 0.84 | 2.55 | 0.019 |
| 1.33 | 73.71 | 199.11 | 625.52 | 0.81 | 0.85 | 2.66 | 0.022 |
| 1.25 | 59.88 | 208.02 | 743.13 | 0.81 | 0.88 | 2.94 | 0.029 |

22122

| | | | | | | | |
|---|---|---|---|---|---|---|---|
| 2.40 | 594.03 | 142.76 | 141.47 | 0.90 | 1.35 | 2.88 | 0.016 |
| 2.00 | 374.17 | 157.35 | 207.52 | 0.90 | 1.11 | 2.51 | 0.012 |
| 1.62 | 194.18 | 180.65 | 357.43 | 0.90 | 0.99 | 2.56 | 0.014 |
| 1.39 | 136.35 | 194.61 | 479.16 | 0.90 | 1.00 | 2.86 | 0.019 |
| 1.33 | 122.31 | 199.11 | 524.32 | 0.90 | 1.02 | 2.99 | 0.022 |

| | | | | | | | |
|---|---|---|---|---|---|---|---|
| 1.25 | 99.36 | 208.02 | 622.91 | 0.90 | 1.06 | 3.30 | 0.029 |

22123

| | | | | | | | |
|---|---|---|---|---|---|---|---|
| 2.40 | 788.45 | 142.76 | 128.17 | 0.95 | 1.50 | 3.08 | 0.016 |
| 2.00 | 496.63 | 157.35 | 188.02 | 0.95 | 1.23 | 2.67 | 0.012 |
| 1.62 | 257.73 | 180.65 | 323.85 | 0.95 | 1.10 | 2.73 | 0.014 |
| 1.39 | 180.97 | 194.61 | 434.14 | 0.95 | 1.11 | 3.05 | 0.019 |
| 1.33 | 162.34 | 199.11 | 475.06 | 0.95 | 1.13 | 3.19 | 0.022 |
| 1.25 | 131.88 | 208.02 | 564.38 | 0.95 | 1.17 | 3.52 | 0.029 |

22211

| | | | | | | | |
|---|---|---|---|---|---|---|---|
| 2.40 | 358.01 | 142.76 | 168.77 | 0.81 | 1.01 | 2.57 | 0.016 |
| 2.00 | 225.50 | 157.35 | 247.57 | 0.81 | 0.82 | 2.23 | 0.012 |
| 1.62 | 117.03 | 180.65 | 426.42 | 0.81 | 0.74 | 2.28 | 0.014 |
| 1.39 | 82.17 | 194.61 | 571.64 | 0.81 | 0.75 | 2.55 | 0.019 |
| 1.33 | 73.71 | 199.11 | 625.52 | 0.81 | 0.76 | 2.66 | 0.022 |
| 1.25 | 59.88 | 208.02 | 743.13 | 0.81 | 0.79 | 2.94 | 0.029 |

22212

| | | | | | | | |
|---|---|---|---|---|---|---|---|
| 2.40 | 594.03 | 142.76 | 141.47 | 0.90 | 1.21 | 2.88 | 0.016 |
| 2.00 | 374.17 | 157.35 | 207.52 | 0.90 | 0.99 | 2.51 | 0.012 |
| 1.62 | 194.18 | 180.65 | 357.43 | 0.90 | 0.88 | 2.56 | 0.014 |
| 1.39 | 136.35 | 194.61 | 479.16 | 0.90 | 0.90 | 2.86 | 0.019 |
| 1.33 | 122.31 | 199.11 | 524.32 | 0.90 | 0.91 | 2.99 | 0.022 |
| 1.25 | 99.36 | 208.02 | 622.91 | 0.90 | 0.95 | 3.30 | 0.029 |

22213

| | | | | | | | |
|---|---|---|---|---|---|---|---|
| 2.40 | 788.45 | 142.76 | 128.17 | 0.95 | 1.34 | 3.08 | 0.016 |
| 2.00 | 496.63 | 157.35 | 188.02 | 0.95 | 1.10 | 2.67 | 0.012 |
| 1.62 | 257.73 | 180.65 | 323.85 | 0.95 | 0.98 | 2.73 | 0.014 |
| 1.39 | 180.97 | 194.61 | 434.14 | 0.95 | 1.00 | 3.05 | 0.019 |
| 1.33 | 162.34 | 199.11 | 475.06 | 0.95 | 1.01 | 3.19 | 0.022 |
| 1.25 | 131.88 | 208.02 | 564.38 | 0.95 | 1.05 | 3.52 | 0.029 |

22221

| | | | | | | | |
|---|---|---|---|---|---|---|---|
| 2.40 | 358.01 | 142.76 | 168.77 | 0.81 | 1.13 | 2.57 | 0.016 |
| 2.00 | 225.50 | 157.35 | 247.57 | 0.81 | 0.92 | 2.23 | 0.012 |
| 1.62 | 117.03 | 180.65 | 426.42 | 0.81 | 0.82 | 2.28 | 0.014 |
| 1.39 | 82.17 | 194.61 | 571.64 | 0.81 | 0.84 | 2.55 | 0.019 |
| 1.33 | 73.71 | 199.11 | 625.52 | 0.81 | 0.85 | 2.66 | 0.022 |
| 1.25 | 59.88 | 208.02 | 743.13 | 0.81 | 0.88 | 2.94 | 0.029 |

22222

| | | | | | | | |
|---|---|---|---|---|---|---|---|
| 2.40 | 594.03 | 142.76 | 141.47 | 0.90 | 1.35 | 2.88 | 0.016 |
| 2.00 | 374.17 | 157.35 | 207.52 | 0.90 | 1.11 | 2.51 | 0.012 |
| 1.62 | 194.18 | 180.65 | 357.43 | 0.90 | 0.99 | 2.56 | 0.014 |
| 1.39 | 136.35 | 194.61 | 479.16 | 0.90 | 1.00 | 2.86 | 0.019 |

| | | | | | | | |
|---|---|---|---|---|---|---|---|
| 1.33 | 122.31 | 199.11 | 524.32 | 0.90 | 1.02 | 2.99 | 0.022 |
| 1.25 | 99.36 | 208.02 | 622.91 | 0.90 | 1.06 | 3.30 | 0.029 |

22223

| | | | | | | | |
|---|---|---|---|---|---|---|---|
| 2.40 | 788.45 | 142.76 | 128.17 | 0.95 | 1.50 | 3.08 | 0.016 |
| 2.00 | 496.63 | 157.35 | 188.02 | 0.95 | 1.23 | 2.67 | 0.012 |
| 1.62 | 257.73 | 180.65 | 323.85 | 0.95 | 1.10 | 2.73 | 0.014 |
| 1.39 | 180.97 | 194.61 | 434.14 | 0.95 | 1.11 | 3.05 | 0.019 |
| 1.33 | 162.34 | 199.11 | 475.06 | 0.95 | 1.13 | 3.19 | 0.022 |
| 1.25 | 131.88 | 208.02 | 564.38 | 0.95 | 1.17 | 3.52 | 0.029 |

APPENDIX-7.6: Predicted and Observed Ash and Yield

PREDICTED AND OBSERVED ASH AND YIELD

| TEST # | OBSERVED ASH | FITTED ASH | PREDICTED ASH | OBSERVED YIELD | FITTED YIELD | PREDICTED YIELD |
|---|---|---|---|---|---|---|
| 11111 | 19.714 | 19.582 | 17.574 | 47.320 | 46.753 | 47.315 |
| 11112 | 19.079 | 18.958 | 18.552 | 23.554 | 22.676 | 20.893 |
| 11113 | 17.062 | 16.451 | 17.106 | 16.532 | 16.645 | 15.487 |
| 11121 | 20.790 | 20.629 | 19.770 | 44.153 | 44.072 | 35.239 |
| 11122 | 16.379 | 16.252 | 19.192 | 24.880 | 24.824 | 20.030 |
| 11123 | 19.703 | 19.265 | 19.032 | 19.017 | 19.011 | 15.544 |
| 11211 | 22.350 | 22.005 | 20.481 | 50.028 | 50.487 | 42.285 |
| 11212 | 18.777 | 18.446 | 18.308 | 44.380 | 46.705 | 27.695 |
| 11213 | 19.294 | 18.599 | 19.776 | 30.144 | 30.757 | 18.859 |
| 11221 | 22.931 | 22.511 | 23.097 | 55.929 | 57.271 | 36.006 |
| 11222 | 20.198 | 20.167 | 20.498 | 37.070 | 36.629 | 23.789 |
| 11223 | 18.990 | 18.712 | 19.592 | 30.476 | 30.739 | 19.443 |
| 12111 | 19.625 | 18.916 | 18.804 | 28.142 | 28.538 | 36.818 |
| 12112 | 18.811 | 18.129 | 18.585 | 20.571 | 20.845 | 22.467 |
| 12113 | 18.002 | 17.191 | 18.333 | 14.659 | 14.529 | 18.819 |
| 12121 | 21.512 | 20.692 | 22.414 | 25.200 | 25.513 | 29.468 |
| 12122 | 19.520 | 18.917 | 20.889 | 16.987 | 17.497 | 19.644 |
| 12123 | 17.947 | 17.120 | 18.063 | 12.427 | 12.810 | 16.594 |
| 12211 | 21.210 | 20.498 | 20.146 | 32.514 | 31.904 | 35.345 |
| 12212 | 19.301 | 18.792 | 19.945 | 24.564 | 24.740 | 22.273 |
| 12213 | 18.361 | 18.004 | 18.571 | 18.598 | 18.718 | 19.329 |
| 12221 | 20.295 | 20.321 | 20.987 | 26.820 | 28.249 | 26.462 |
| 12222 | 18.504 | 18.179 | 19.455 | 20.941 | 20.651 | 18.455 |
| 12223 | 16.993 | 16.783 | 16.889 | 16.185 | 16.096 | 16.884 |
| 21111 | 26.163 | 26.173 | 26.179 | 83.449 | 83.221 | 86.807 |
| 21112 | 20.992 | 20.627 | 24.165 | 58.135 | 50.188 | 77.963 |
| 21113 | 19.023 | 18.928 | 22.169 | 41.648 | 43.401 | 66.293 |
| 21121 | 28.289 | 28.276 | 26.346 | 86.502 | 86.567 | 85.281 |
| 21122 | 23.077 | 22.797 | 23.926 | 65.866 | 66.189 | 72.123 |
| 21123 | 19.814 | 19.628 | 21.680 | 48.877 | 47.708 | 57.229 |
| 21211 | 24.869 | 24.983 | 24.811 | 83.770 | 83.765 | 88.433 |
| 21212 | 22.012 | 22.093 | 22.308 | 74.516 | 74.605 | 82.455 |
| 21213 | 19.429 | 19.274 | 21.138 | 51.787 | 52.097 | 71.599 |
| 21221 | 23.003 | 23.022 | 27.760 | 62.270 | 61.289 | 85.302 |
| 21222 | 23.985 | 23.940 | 23.462 | 74.880 | 75.136 | 75.568 |
| 21223 | 27.104 | 26.918 | 23.176 | 77.545 | 77.343 | 61.126 |
| 22111 | 23.521 | 23.588 | 24.404 | 76.694 | 76.390 | 85.133 |
| 22112 | 20.540 | 20.477 | 23.180 | 55.890 | 55.570 | 69.036 |
| 22113 | 18.067 | 17.983 | 20.933 | 31.886 | 32.248 | 50.687 |
| 22121 | 25.252 | 25.194 | 24.582 | 82.859 | 82.556 | 83.789 |
| 22122 | 19.433 | 19.099 | 21.161 | 58.862 | 57.160 | 65.808 |
| 22123 | 15.946 | 15.441 | 19.746 | 34.553 | 34.223 | 43.141 |
| 22211 | 24.429 | 24.477 | 23.354 | 85.489 | 85.588 | 86.160 |
| 22212 | 19.160 | 19.592 | 19.933 | 70.176 | 68.706 | 75.905 |
| 22213 | 18.356 | 33.865 | 20.810 | 41.553 | 43.445 | 55.820 |
| 22221 | 26.406 | 29.056 | 24.634 | 86.682 | 81.000 | 83.881 |
| 22222 | 22.797 | 29.942 | 22.240 | 70.127 | 79.481 | 67.599 |
| 22223 | 18.514 | 18.006 | 21.654 | 38.131 | 37.991 | 46.265 |